

**Determination of relationship between  
dolutegravir and trace amine profile, using  
advanced liquid chromatography tandem mass  
spectrometry analysis of various tissues**

by  
Natasha Henning

*Dissertation presented for the degree of  
Doctor of Philosophy in the Faculty of Medicine and Health  
Sciences at Stellenbosch University*

Supervisor: Prof Carine Smith  
Co-supervisor: Dr Tracy Kellermann

December 2023



## Declaration

By submitting this dissertation electronically, I declare that the entirety of the work contained therein is my own, original work, that I am the sole author thereof (save to the extent explicitly otherwise stated), that reproduction and publication thereof by Stellenbosch University will not infringe any third party rights and that I have not previously in its entirety or in part submitted it for obtaining any qualification. Declaration with signature in possession of candidate and supervisor.

Copyright © 2023 Stellenbosch University

All rights reserved

## Abstract

The immunopathogenic mechanisms of human immunodeficiency virus (HIV) are complex and require a multidimensional approach to pharmacological management. While it is known that antiretroviral therapy (ART) comprising of multi-drug treatment regimens often lead to the presentation of adverse effects, mechanisms leading to adverse effects require more elucidation. This is especially true for dolutegravir (DTG) – an integrase strand inhibitor (INSTI) – currently part of the first line treatment for HIV. Recent literature has elucidated that the neurological and gastrointestinal adverse events could be related to accumulation of DTG in these tissue compartments because of its physiochemical properties. However, few reports are available for methodology to assess DTG accumulation at tissue levels. Trace amines are biogenic amines which are endogenously produced in trace amounts in the brain, as well as in larger amounts by the gut microbiome and are known to differentially regulate inflammatory outcome. We proposed that a dysregulated trace amine profile may exacerbate the persistent inflammation associated with HIV in both neuronal and gastrointestinal tissue in response to DTG treatment.

To elucidate the potential impact of DTG administration on the trace aminergic system, a multidisciplinary approach was required. Therefore, a wistar rat model and novel liquid chromatography tandem mass spectrometry methodology was combined to accurately determine both tissue DTG and trace amine concentrations. Following this approach, data generated illustrated that DTG indeed accumulated in tissue following a chronic DTG dosing regimen which mimics human monotherapy. In addition, DTG altered the urinary and gastrointestinal trace amine profile of wistar rats.

In line with higher adverse event reporting by female patients, DTG quantification in plasma and various tissue matrices illustrated significantly higher DTG concentration in female rats when compared to males. In addition, there was a direct relationship between concentrations of DTG in plasma vs concentrations observed in muscle and liver, but not adipose tissue. Since DTG accumulated in tissue, further analytical assessments were conducted to determine potential dysregulation of the trace amine profile by DTG. Data suggest modulation of the trace amine profile by DTG administration, with confounding effect of sex.

In conclusion, this dissertation contributes to available literature aimed at elucidating potential mechanisms causing inflammation-centred adverse events following DTG treatment. Data presented illustrate the importance of including both males and females in experimental pharmacology studies. From a clinical perspective, the data presented highlight the importance of more accurate dosage adjustment for body size and/or sex, to minimize risk of over-dosing individuals with relatively smaller body size.

## Opsomming

Die immunopatogeniese meganismes van menslike immuniteitsvirus is geweldig ingewikkeld en vereis 'n multidimensionele benadering tot farmakologiese behandeling. Huidige antiretrovirale behandeling bestaan uit kombinasie terapie wat dikwels aanleiding gee tot ongewenste newe-effekte, maar die meganismes wat lei tot hierdie newe-effekte is nog onbekend, veral in die geval van dolutegravir (DTG) – 'n integrase inhibeerder - wat tans deel vorm van die eerste linie antiretrovirale middels op die mark. Die mees onlangse literatuur stel voor dat die neurologiese en die spysverterings newe-effekte veroorsaak word deur die opeenhoping van DTG in verskillende weefselkompartemente – 'n hipotese wat ondersteun word deur die middel se fisies-chemiese eienskappe. Steeds is daar bitter min literatuur beskikbaar wat metodes voorstel om DTG-opeenhoping in weefsel te ondersoek.

Spoor-amiene is biogeniese amiene wat in klein hoeveelhede in die brein vervaardig word. Die dermmikrobiom dra ook intussen by tot die vervaardiging van die spoor-amiene - in merkbaar groter hoeveelhede. Spoor-amiene word gekenmerk vir die rol wat dit speel in die modulering van 'n verskeidenheid inflammatoriese uitkomstes. Daarom het ons voorgestel dat die moonlike wanregulering van die spoor-amienegiese stelsel weens DTG toediening, potensieel mag bydra tot die voortdurende inflammasie wat met MIV geassosieer word.

Om die moontlike impak van DTG toediening aan die spoor-amienegiese stelsel te ondersoek, was 'n multidissiplinêre benadering nodig. Daarom is 'n *in vivo* wistar rot model en vloeistofchromatografie-massaspektografie metode gekombineer om die konsentrasies van DTG en verskillende spoor amine in weefsel akkuraat vas te stel. Die data wat tydens die studie gegenereer is, illustreer dat kroniese DTG behandeling - wat monoterapie in mense naboots – lei tot opeenhoping van DTG in verskillende weefsel. Verder dra die DTG by tot veranderinge in die urine en spysverteringskanaal spoor-amienprofiel van wistar rotte.

In lyn met groter voorkoms van newe-effekte in vroulike pasiënte, wys DTG bepaling in weefsels dat DTG konsentrasies beduidend hoër was in vroulike diere as in manlike diere. In lyn hiermee, was daar 'n direkte verhouding tussen DTG

plasmakonsentrasies en DTG konsentrasies in spier en lewer (maar nie vetweefsel nie). Gegewe die feit dat DTG wel in weefsel opgehoop het, is verdere analitiese ondersoek ingestel om die moontlike effek van DTG op die spoor-amienprofiel te bepaal. Modulering van die spoor-amienprofiel was inderdaad veranderd na DTG toediening, met 'n bykomende effek van geslag .

Ten slotte, hierdie proefskrif by tot ons begrip aan die verskillende meganismes wat moontlik bydrae tot die inflammasie gesentreerde newe-effekte wat volg na DTG behandeling. Huidige data lê ook klem op die feit dat beide manlike en vroulike geslagte in toekomstige studies ingesluit moet word. Vanuit 'n kliniese perspektief beklemtoon data die belangrikheid van meer akkurate aanpassings aan dosis van DTG om die risiko van oordosering (moontlik die oorsaak van die newe-effekte opgemerk) tot 'n minimum te beperk in vroue en/of persone met relatief kleiner liggaamsbou.

*“If you fail to plan, you plan to fail”*  
*Taylor Swift – Mastermind*

## Acknowledgements

Firstly, to my supervisor Prof Carine Smith, I would like to thank you for being a phenomenal and inspirational role model. Without you I would not have accomplished this milestone. You always knew exactly when I required motivation, assistance and encouragement. Thank you for always believing in me and for affording me the opportunity to be a part of your research group.

To my co-supervisor Dr Tracy Kellermann, thank you for the invaluable experiences and lessons you have taught me. Thank you for your guidance and sharing your expertise in the laboratory.

Lesha, Kelly, Janica, Yigael, Tracey and Mr Noël Markgraaff, thank you for your assistance during protocol development, sample collection and statistical analysis.

Hannes and the postgraduate office, thank you for securing financial support for me which without this would not have been possible.

Hannah, Alex, Judy, Jordan, Ruan and Karley - thank you for your constant support during my PhD journey.

Jana, thank you for all your assistance during this journey. There is no way to express my gratitude for your support. I would like to especially thank you for contributing your time during my final experiments to help me process samples. You truly are an incredibly generous and kind person.

Leon en Tana, thank you for welcoming me into your family with open arms and giving me a home away from home. You have provided endless support and advice and I will always be grateful for the role both of you played in this milestone.

Wian, thank you for being my number one supporter and teaching me about perseverance. Thank you for loving me on my worst days and for always encouraging me to remaining positive. I would not have been able to achieve this without your kind heart.

To my sister Celeste and brother Lohan, thank you for always inspiring me to work harder, to be kinder and trust myself. Your support during this journey is unforgettable.

To my dad, Frans, thank you for the opportunity to follow my passion. I am endlessly grateful for all you provided that enabled this. Thank you for investing in my future.

To my mom, Sonja, thank you for being my pillar of support over the last few years. Thank you for teaching me about good work ethic and integrity. You are the most generous and caring person I know. Thank you for inspiring me every day and for all that you sacrificed to enable this.

To every member of the Smith and Kellermann research groups, thank you all for being there no matter the crisis. Encouragement and kindness are your best assets.

## Table of Contents

<b>Declaration</b> .....	<b>ii</b>
<b>Abstract</b> .....	<b>iii</b>
<b>Opsomming</b> .....	<b>v</b>
<b>Acknowledgements</b> .....	<b>viii</b>
<b>List of figures</b> .....	<b>4</b>
<b>List of tables</b> .....	<b>7</b>
<b>List of abbreviations</b> .....	<b>9</b>
<b>Chapter 1: Introduction</b> .....	<b>13</b>
<b>Chapter 2: Literature review</b> .....	<b>15</b>
<b>2.1 Introduction</b> .....	<b>15</b>
<b>2.2 Dolutegravir</b> .....	<b>16</b>
2.2.1 Tissue distribution of dolutegravir .....	17
<b>2.3 Physiological dysregulation in HIV with/without dolutegravir</b> .....	<b>19</b>
2.3.1 Neuropathology .....	19
2.3.1.1 Neurological side effects of dolutegravir .....	21
2.3.2 Gastrointestinal symptoms and gut dysbiosis.....	23
2.3.3 Weight gain associated with dolutegravir treatment .....	25
2.3.4 Olfactory decline .....	31
<b>2.4 Trace amine system as potential (dys)regulatory role player</b> .....	<b>32</b>
2.4.1 Overview of the system .....	33
2.4.2 Formation and sources of trace amine .....	34
2.4.3. Relevance of trace amines to HIV/dolutegravir adverse profile.....	37
2.4.3.3 Relevance to gut dysbiosis .....	41
2.4.3.4 Relevance to body/fat mass changes.....	44
2.4.3.5 Sex-dependent effects of trace amines .....	45
<b>2.5 Methodological considerations</b> .....	<b>45</b>
2.5.1 Quantification of dolutegravir .....	46
2.5.2 Quantification of multiple trace amines.....	48
<b>2.6 Conclusion</b> .....	<b>52</b>
<b>2.7 Hypothesis statement</b> .....	<b>53</b>

<b>2.8 Aim and objectives</b> .....	<b>53</b>
2.8.1 Aim.....	53
2.8.2 Objectives .....	53
<b>Chapter 3: Development of liquid chromatography tandem mass spectrometry (LC-MS/MS) methods for quantification of dolutegravir in various biological matrices from wistar rats</b> .....	<b>54</b>
<b>3.1 Introduction</b> .....	<b>54</b>
<b>3.2. Materials and methods</b> .....	<b>56</b>
3.2.1 Ethical considerations and sample collection .....	56
3.2.2 Method development .....	56
3.2.3 Method parameters.....	59
<b>3.3. Results and discussion</b> .....	<b>60</b>
3.3.1 Chromatography method development .....	60
3.3.2 Extraction method development .....	61
3.3.3 Method development criteria evaluated.....	61
<b>3.4. Conclusions</b> .....	<b>70</b>
<b>Chapter 4: Dolutegravir distribution in plasma and tissue compartments after chronic administration to wistar rats</b> .....	<b>72</b>
<b>4.1 Introduction</b> .....	<b>72</b>
<b>4.2 Methods and materials</b> .....	<b>73</b>
4.2.1 Ethical consideration.....	73
4.2.2 Dolutegravir formulation and purity analysis.....	74
4.2.3 Administration of dolutegravir .....	74
4.2.4 Tissue collection and preparation .....	75
4.2.5 Dolutegravir quantification .....	76
4.2.6 Adipose tissue histology and image acquisition .....	76
4.2.7 Statistical analysis .....	77
<b>4.3 Results</b> .....	<b>77</b>
<b>4.4 Discussion</b> .....	<b>86</b>
<b>4.5 Conclusion</b> .....	<b>90</b>
<b>Chapter 5: Liquid-chromatography tandem mass spectrometry methods for the quantification of trace amines from various wistar rat matrices</b> .....	<b>92</b>
<b>5.1 Introduction</b> .....	<b>92</b>

<b>5.2 Methods and materials</b> .....	<b>95</b>
5.2.1 Ethical consideration.....	95
5.2.2 Method development.....	96
5.2.3 Method performance characterization.....	102
<b>5.3 Results and discussion</b> .....	<b>105</b>
5.3.1 Optimisation of chromatography.....	105
5.3.2 Optimisation of extraction method.....	107
5.3.3 Method performance characterization.....	109
<b>5.4 Conclusion</b> .....	<b>121</b>
<b>Chapter 6: Effect of chronic dolutegravir administration on trace amine profile</b> .....	<b>122</b>
<b>6.1 Introduction</b> .....	<b>122</b>
<b>6.2 Methods and materials</b> .....	<b>124</b>
6.2.1 Sample collection.....	124
6.2.2 Trace amine quantification.....	124
6.2.3 Statistical analysis.....	125
<b>6.3 Results</b> .....	<b>125</b>
6.3.1 Limited or low abundance of trace amines in rodent plasma and brain tissue.....	125
6.3.2 Trace amine presence in the gastrointestinal tract.....	127
6.3.3 Urinary trace amine concentrations.....	130
<b>6.4 Discussion</b> .....	<b>132</b>
<b>6.5 Conclusion</b> .....	<b>137</b>
<b>Chapter 7: Synthesis</b> .....	<b>139</b>
<b>Chapter 8: References</b> .....	<b>145</b>
<b>Addenda</b> .....	<b>179</b>
<b>Addendum A</b> .....	<b>179</b>
<b>Addendum B</b> .....	<b>180</b>
<b>Addendum C</b> .....	<b>181</b>

## List of figures

**Figure 2.1:** Formation and different sources of trace amines.

**Figure 3.1:** Chromatograms of blank extracted (A) plasma, (B) brain, (C) adipose, (D) muscle and (E) liver.

**Figure 3.2:** Representative chromatograms of the upper limit of quantification (1) in (A) plasma, (B) brain, (C) adipose (D) muscle and (E) liver.

**Figure 4.1:** Change in body mass of wistar rats over 12-week DTG administration protocol.

**Figure 4.2:** Fasting blood glucose (mmol/L) in the control and 12-week DTG administered groups.

**Figure 4.3:** Mass of (A) liver, (B) left gastrocnemius muscle, (C) left retroperitoneal adipose depot and (D) brain from males and female wistar rats after 12-week DTG administration.

**Figure 4.4:** Average DTG concentration detected in plasma following a 12-week DTG intervention. (A) Not corrected for blood volume. (B) Corrected for blood volume.

**Figure 4.5:** DTG concentration detected in (A) tip of left lateral lobe of liver (B) left gastrocnemius muscle and (C) retroperitoneal adipose depot tissue following a 12-week DTG administration.

**Figure 4.6:** Total amount of DTG detected corrected for organ mass in the (A) tip of the left lateral lobe of the liver, (B) left gastrocnemius muscle and (C) retroperitoneal adipose depot of rats following a 12-week DTG intervention size.

**Figure 4.7:** The correlation between DTG plasma concentration(ng/mL) and body mass (g) of 20-week-old wistar rats.

**Figure 4.8:** Correlation between DTG concentration (ng/g) in the (A) tip of the left lateral lobe of the liver, (B) left gastrocnemius muscle and (C) left retroperitoneal adipose depot vs plasma concentration (ng/mL) following a 12-week DTG intervention in rats.

**Figure 4.9:** (A) Correlation between adipocyte surface area ( $\mu\text{m}^2$ ) and adipose depot mass (g) Statistical analysis: Spearman's correlation. (B) The average surface area ( $\mu\text{m}^2$ ) of 50 adipocytes measured on three representative images for each animal. (C) Representative images of histological sections stained with H&E of males and females in the control and DTG groups.

**Figure 5.1:** Chemical structure and formation summary of trace amines from tryptophan, tyrosine and agmatine metabolism. Image created with Biorender.com  
Abbreviations: Tyr, tyrosine; AADC, aromatic L-amino acid decarboxylase; TYR,  $\rho$ -tyramine; DBH, dopamine- $\beta$ -hydroxylase; OCT, octopamine, PNMT, phenylethanolamine N-methyl transferase; SYN,  $\rho$ -synephrine; Arg, arginine; AGM, agmatine; PUT, putrescine; SPDS, spermidine synthase; SPD, spermidine; SMS, spermine synthase; SPM, spermine.

**Figure 5.2:** Chromatograms of (A) TYR, (B) PEA, (C) TRP, (D) SYN, (E) OCT, (F) T1AM, (G) AGM, (H) PUT, (I) CAD at the ULOQ (left) and LOQ (right). (J) PEA-d4 at 100 ng/mL and (K) PUT-d8 at 400 ng/mL.

**Supplementary figure 5.1:** Chromatograms of 400 ng/mL TYR in (A) solvent, (B) brain, (C) urine, (D) plasma and (E) gastrointestinal tissue eluting at 2.94 minutes.

**Supplementary figure 5.2:** Chromatograms of 400 ng/mL PEA in (A) solvent, (B) brain, (C) urine, (D) plasma and (E) gastrointestinal tissue eluting at 3.83 minutes.

**Supplementary figure 5.3:** Chromatograms of 400 ng/mL TRP in (A) solvent, (B) brain, (C) urine, (D) plasma and (E) gastrointestinal tissue eluting at 4.07 minutes.

**Supplementary figure 5.4:** Chromatograms of 400 ng/mL SYN in (A) solvent, (B) brain, (C) urine, (D) plasma and (E) gastrointestinal tissue eluting at 1.95 minutes.

**Supplementary figure 5.5:** Chromatograms of 400 ng/mL OCT in (A) solvent, (B) brain, (C) urine, (D) plasma and (E) gastrointestinal tissue eluting at 1.61 minutes.

**Supplementary figure 5.6:** Chromatograms of 400 ng/mL T1AM in (A) solvent, (B) brain, (C) urine, (D) plasma and (E) gastrointestinal tissue eluting at 4.91 minutes.

**Supplementary figure 5.7:** Chromatograms of 400 ng/mL AGM in (A) solvent, (B) brain, (C) urine, (D) plasma and (E) gastrointestinal tissue eluting at 3.30 minutes.

**Supplementary figure 5.8:** Chromatograms of 400 ng/mL PUT in (A) solvent, (B) brain, (C) urine, (D) plasma and (E) gastrointestinal tissue eluting at 3.26 minutes.

**Supplementary figure 5.9:** Chromatograms of 400 ng/mL CAD in (A) solvent, (B) brain, (C) urine, (D) plasma and (E) gastrointestinal tissue eluting at 3.28 minutes.

**Supplementary figure 5.10:** Chromatograms of 100 ng/mL PEA-d4 in (A) solvent, (B) brain, (C) urine, (D) plasma and (E) gastrointestinal tissue eluting at 3.81 minutes.

**Supplementary figure 5.11:** Chromatograms of 400 ng/mL PUT-d4 in (A) solvent, (B) brain, (C) urine, (D) plasma and (E) gastrointestinal tissue eluting at 3.26 minutes.

**Figure 6.1:** (A) PUT and (B) CAD concentrations (ng/g) detected in the brain.

**Figure 6.2:** Figure 6.2 (A) PEA, (B) TYR, (C) CAD (D) TRP and (E) AGM and subsequent metabolite concentrations in the different segments of gastrointestinal tract.

**Figure 6.3:** Trace amines detected in urine. (A) PEA, (B) TRP, (C) CAD, (D) TYR with subsequent metabolites and (E) AGM with subsequent metabolites.

## List of tables

**Table 2.1:** Reported neuropsychiatric adverse events for dolutegravir.

**Table 2.2:** Reported weight gain associated with dolutegravir treatment.

**Table 2.3:** Reported incidence of hyperglycaemia following dolutegravir treatment.

**Table 2.4:** Summary of previously published dolutegravir extraction methods.

**Table 2.5:** Summary of research conducted to determine trace amine concentration in mammalian biological matrices.

**Table 3.1:** Calibration range, regression, weighting and correlation coefficient of each matrix evaluated.

**Table 3.2:** Inter-run accuracy and precision of DTG standards and QCs in plasma.

**Table 3.3:** Inter-run accuracy and precision of DTG standards and QCs in brain tissue.

**Table 3.4:** Inter-run accuracy and precision of DTG standards and QCs in adipose tissue.

**Table 3.5:** Inter-run accuracy and precision of DTG standards and QCs in muscle tissue.

**Table 3.6:** Inter-run accuracy and precision of DTG standards and QCs in liver tissue.

**Table 3.7:** Average recovery and matrix effects of DTG in different biological matrices.

**Table 5.1:** Multiple reaction monitoring (MRM) conditions of each analyte.

**Table 5.2:** Calibration range, regression weighting, retention time and column used for analysis of the different trace amines.

**Table 5.3:** Inter-run accuracy and precision summary statistics of standards prepared in a solvent.

**Table 5.4:** Inter-run accuracy and precision summary statistics of QCs prepared in a solvent.

**Table 5.5:** Summary of endogenous concentrations and %accuracy for trace amine QCs prepared in different biological matrices.

**Table 5.6:** Percentage recovery of analytes from a solvent across three analytical runs.

**Table 5.7:** Percentage recovery of the internal standards in the authentic biological matrices.

**Table 5.8:** Average regression slope of QCs prepared in a solvent and QCs prepared in the authentic biological matrices.

**Table 6.1:** Summary of trace amine quantification in brain tissue.

**Table 6.2:** Summary of trace amine quantification in urine.

## List of abbreviations

%CV – percentage coefficient of variation  
3TC – lamivudine  
5-HT – serotonin  
AADC – aromatic L–amino acid decarboxylase  
ABC – abacavir  
ACN – acetonitrile  
AD – Alzheimer’s disease  
ADHD – attention deficit hyperactivity disorder  
AGM – agmatine  
ANI – asymptomatic neurocognitive impairment  
ArgDC – arginine decarboxylase  
ART – antiretroviral therapy  
BBB – blood brain barrier  
BMI – body mass index  
BSA – body surface area  
CAD – cadaverine  
CadA – lysine decarboxylase  
cAMP– Cyclic adenosine monophosphate  
cART – combination antiretroviral therapy  
CNS – central nervous system  
CREB – cAMP–response element binding protein  
CSF – cerebrospinal fluid  
DA – dopamine  
DBH – dopamine– $\beta$ –hydroxylase  
DMSO – dimethyl sulfoxide  
DRV – darunavir  
DTG – dolutegravir  
EFV – efavirenz  
EIF5A – eukaryotic initiation factor 5A  
ERK1/2 – extracellular signal–regulated kinase 1/2  
EVG – elvitegravir  
FDA – Food and Drug Administration

FDC – fixed dose combination  
FTC – emtricitabine  
GABA –  $\gamma$ -Aminobutyric acid  
GIT – gastrointestinal tract  
GPCR – G-protein coupled receptors  
HAD – HIV associated dementia  
HAND – HIV-associated neurocognitive disorder  
HED – human equivalent dose  
HEK293 – human embryonic kidney cells  
HIV – human immunodeficiency virus  
HPLC – high pressure liquid chromatography  
HT-29 – human colon adenocarcinoma cells  
I.P – intraperitoneal injection  
IBD – inflammatory bowel disease  
IL – interleukin  
IM – intramuscular injection  
INSTI – integrase strand inhibitor  
KYNA – kynurenic acid  
LC-MS/MS – Liquid chromatography tandem mass  
LLOQ – lowest limit of quantification  
LMIC – low- to middle-income countries  
LOQ – limit of quantification  
Lys – lysine  
m/z – mass-to-charge ratio  
MeOH – methanol  
MND – mild neurocognitive disorder  
MOA B – mono-amine oxidase B  
MRM – multiple reaction monitoring  
NA – noradrenaline  
NNRTI – non-nucleoside reverse-transcriptase inhibitors  
NRTI – nucleoside and nucleotide reverse  
OCT –  $\rho$ -octopamine  
p.o – oral formulation

PD – Parkinson’s disease  
PEA –  $\beta$ -phenylethylamine  
Phe – phenylalanine  
PI – protease inhibitors  
PLWH – people living with HIV  
PMN – polymorphonuclear neutrophils  
PNMT – phenylethanolamine N-methyl transferase  
PUT – putrescine  
QC – quality control  
QC H – quality control high  
QC L – quality control low  
QC M – quality control medium  
RAL – raltegravir  
RPV – rilpivirine  
RTV – ritonavir  
S/N – signal-to-noise  
SARS-CoV2 – severe acute respiratory syndrome coronavirus 2  
SD – standard deviation  
SMS – spermine synthase  
SPE – solid phase extraction  
SPM – spermine  
SPD – spermidine  
SPMS – spermidine synthase  
SS – stock solution  
SYN –  $\rho$ -synephrine  
T1AM – 3-iodothyronamine  
TAAR – trace amine associated receptors  
TAAR1 – trace amine associated receptor 1  
TAAR2 – trace amine associated receptor 2  
TAAR5 – trace amine associated receptor 5  
TAAR8 – trace amine associated receptor 8  
TAF – tenofovir alafenamide  
TCA – trichloroacetic acid

TDF – tenofovir disoproxil fumarate

TH – thyroid hormone

TNF- $\alpha$ -Tumor necrosis factor alpha

TRP – tryptamine

Trp – tryptophan

TYR –  $\rho$ -tyramine

Tyr – tyrosine

UDP-GT – Uridine 5'-diphospho-glucuronosyltransferase

UFLC-MS/MS – ultra fast liquid chromatography tandem mass spectrometry

ULOQ – upper limit of quantification

UPLC-MS/MS – Ultra-performance liquid chromatography tandem mass spectrometry

UV – ultraviolet

V – voltage

WS – working stock

## Chapter 1: Introduction

The immunopathogenic mechanisms of human immunodeficiency virus (HIV) are very complex and requires a multidimensional approach to pharmacological management. However, it is evident from the literature on antiretroviral therapy (ART) to date, that multi-drug treatment regimens often lead to the presentation of adverse effects. An in-depth understanding of the effects of various ART drugs is essential for optimising efficacy of treatment while minimising adverse outcomes.

For an ART drug to be effective, it should be able to reach its target without causing adverse effects. In order to comprehensively assess bioavailability and identify potentially vulnerable tissues, it is important to consider the distribution of ART at tissue level. To be effective, it is essential for ART to penetrate HIV reservoirs to prevent the continuous replication of the virus. A complete picture can only be gained from assessment of various biological matrices for penetration of ART into these potential viral reservoirs. Currently, dolutegravir (DTG) - an integrase strand inhibitor (INSTI) - forms part of the first line treatment for HIV. Despite its popularity, more recent literature has elucidated adverse events which could be related to accumulation of DTG in tissue compartments because of its physiochemical properties. However, few reports are available for methodology to assess DTG concentrations at tissue levels to determine DTG penetration/accumulation in tissues.

The downside of good tissue penetration is the possibility for increased adverse effects on the tissue itself. Indeed, many side effects have been reported for DTG, of which the neurological and gastrointestinal effects are most pertinent to the topic of this dissertation. In addition, high incidences of these side effects have been reported in women – suggesting that sex potentially plays a role in the frequency or severity of side effects. In terms of HIV – irrespective of whether patients are using ART – the two most common sites of inflammation are the central nervous system (CNS) and the gastrointestinal tract (GIT). Trace amines are biogenic amines which are endogenously produced in trace amounts in the brain, as well as in larger amounts by the gut microbiome, and are known to differentially regulate inflammatory outcome. We propose that a dysregulated trace amine profile may exacerbate the persistent inflammation associated with HIV in both neurological and gastrointestinal

compartments in response to DTG treatment. However, as with DTG, methodology to assess multiple trace amines in a single sample to test this notion is sparse.

This dissertation aimed to investigate the relationship between tissue DTG concentration and tissue trace amine profiles. Firstly, a review of the most pertinent literature is presented (Chapter 2), providing first an overview of the physiological dysfunction present in HIV, including a description of the relevant reported side effects of DTG. This will be followed by a discussion of the potential role of the trace aminergic system in HIV, specifically related to side effects observed in the brain and GIT and how these adverse symptoms may relate to DTG at an inflammation interface. As a large portion of the dissertation was focused on analytical pharmacology protocol development, the literature review will also include a comprehensive description of methods available for the assessment of both DTG and trace amines, pointing out challenges to address. This will be followed by a presentation of data demonstrating the successful development of complex extraction and liquid chromatography tandem mass spectrometry (LC-MS/MS) quantification protocols for DTG (Chapter 3), as well as elucidating the distribution of DTG in various tissues collected from rats administered DTG for 12 weeks (Chapter 4). Method development for the simultaneous detection of multiple trace amines using LC-MS/MS is presented in Chapter 5. Lastly, data demonstrating changes in trace amine profiles following DTG administration is presented (Chapter 6). Given the female bias in terms of adverse effects, sex was evaluated as a confounding factor throughout the dissertation.

## Chapter 2: Literature review

### 2.1 Introduction

The acquired immune deficiency syndrome caused by the human immunodeficiency virus (HIV-AIDS) was introduced in 1981 by a series of articles (Center for Disease Control, 1981a, 1981b, 1981c). Successively, the modes of transmission were identified, followed by a description of the viral agent responsible and finally, the development of a diagnostic assay (Broder and Gallo, 1984). As of 2020 an estimated 37 million (30.2 million – 45.1 million) people were living with HIV, with 1.5 million (1.0 million - 2.0 million) new infections in that year alone. At the end of June 2020, only 27.5 million people were using ART (Joint United Nations Programme on HIV/AIDS, 2021). The introduction of combination antiretroviral therapy (cART) has restored the life expectancy of people living with HIV (PLWH) to almost that of uninfected individuals (Treisman and Soudry, 2016). Currently we are in the 5<sup>th</sup> decade of the HIV pandemic and despite the advancements of HIV therapy – or perhaps rather due to the effectiveness in increasing post-infection lifespan – PLWH are still significantly burdened with increased risk for comorbidities and mortalities (Avedissian et al., 2020). The major pathophysiology of HIV is associated with the immune system, with most patients developing secondary infections and co-morbid chronic conditions. These conditions result in significantly compromised life quality in PLWH and are – at least in part – ascribed to the ART themselves. It is thus necessary to further research and develop more effective ART with reduced side effects, or to understand side effects of current ART, so that pre-emptive action may be taken to minimise adverse effects.

In terms of pharmacological management, HIV treatment evolution is essential for viral suppression, increased life expectancy and quality of life for PLWH. Advancements in HIV treatment since the turn of the century have led to a significant reduction in HIV-related morbidities and mortalities (Fantauzzi and Mezzaroma, 2014). The life cycle of HIV is categorized into five steps: (1) attachment and entry, (2) reverse transcription, (3) integration, (4) proteolytic processing and the final step, (5) release. As a result of drug resistance that frequently occurs with ART, PLWH are often prescribed multiple drugs in combination. These drugs ideally target more than one step in the virus life

cycle (Shah et al., 2016). The current ART treatments available to PLWH include the nucleoside and nucleotide reverse transcriptase (NRTI), non-nucleoside reverse-transcriptase inhibitor (NNRTI), entry inhibitors, protease inhibitors (PI) and integrase strand inhibitor (INSTI). Treatment regimens have been evolving since the introduction of PI in the mid-1990s, allowing for a triple therapy approach. The standard care of treatment for any HIV positive individual involves the combination of at least three ART drugs belonging to different classes. The introduction of INSTI by the Food and Drug Administration (FDA) in 2007, has significantly increased the efficacy of cART (Bailly and Cotelle, 2015). The first-line ART treatment regimen is currently recommended to consist of two NRTIs plus a NNRTI or INSTI (Fantauzzi and Mezzaroma, 2014; World Health Organization, 2018, 2016). A comprehensive discussion of all ART currently employed, is outside of the scope of this review. Rather, this review will focus on the INSTI, dolutegravir (DTG), which is the drug under investigation in this dissertation.

## 2.2 Dolutegravir

An INSTI targets the enzyme integrase, which is one of the three essential enzymes required for HIV replication in the host (Bailly and Cotelle, 2015). Integrase is the enzyme responsible for proviral DNA integration. Integrase catalyses two important chemical reactions, the first being 3' processing and the second the strand transfer. During 3' processing, integrase cleaves two terminal nucleotides from the 3' end of both viral DNA strands to expose a hydroxyl group. This is required for the second chemical reaction – strand transfer. During strand transfer, the viral DNA is integrated into the host cell chromatin network (Koh et al., 2013; Taha et al., 2013). DTG inhibits incorporation of proviral DNA into the host cell genome by binding to the enzyme active site and preventing the second step. This in turn prevents replication. DTG fits loosely into the binding pocket of the intasome and retains its binding ability while undergoing conformational changes. DTG is more effective when compared to other INSTIs as a result of its ability to make adjustments in the binding capacity (Hare et al., 2011). This adjustment in binding position is believed to be the reason behind DTG's high genetic barrier to resistance (Cottrell et al., 2013; NAMSAL ANRS 12313 Study Group et al., 2019). Another advantage of DTG, like other INSTI drugs, is that it uses separate metabolic pathways to other ART. In addition, it only serves as minor substrate for the cytochrome P450 system (Taha et al., 2015).

Due to these characteristics, as well as its generally good tolerability, DTG was granted FDA approval for the treatment of HIV infection in a broad patient population, in 2013 (Bailly and Cotelle, 2015; Zhang et al., 2015). More specifically, studies have indicated that DTG is well tolerated in both treatment naïve and treatment experienced HIV patient groups when used with nucleoside backbones (Castagna et al., 2014; Raffi et al., 2013; Walmsley et al., 2015). DTG has demonstrated virological suppression comparable to that of other INSTIs and superior to other recommended first-line treatments. These studies were conducted as non-inferior or superior clinical trials. DTG proved superior to first line treatments containing efavirenz (EFV) and darunavir/ritonavir (DRV/RTV) and non-inferior to treatment arms including raltegravir (RAL) (Taha et al., 2015). Moreover, DTG is currently recommended as the first line treatment for both treatment naïve and treatment experienced HIV-infected patients. (Bailly and Cotelle, 2015; Barcelo et al., 2019; World Health Organization, 2018).

### 2.2.1 Tissue distribution of dolutegravir

Returning to the specific focus of this dissertation on understanding potential tissue-specific effects of DTG, it is important to consider the distribution of the drug when evaluating potential effects of DTG in different tissues. For example, it is believed that infected CD4 T cells may enter the CNS from the periphery during early HIV infection (Sturdevant et al., 2015). Once in the CNS, HIV continues to replicate and the brain becomes a reservoir for HIV (De Almeida, 2015). Other organs/tissues suspected to act as reservoirs for HIV include the bone marrow, adipose tissue, gastrointestinal tract and genital tissues (Cory et al., 2013). As in the CNS, adipose tissue contains CD4 T cells harbouring HIV pro-viral RNA and DNA. Even though the movement of infected immune cells into adipose tissue occurs in the early events of infection, viral replication in the adipose tissue may be dependent on the type of depot, the strain of infection and the time of infection (Couturier and Lewis, 2018). The GIT is reported to be one of the first targets of HIV. It has been reported to contain the highest number of infected cells even when patients are on ART (Wong and Yukl, 2016). For effective treatment of all HIV reservoirs, it is necessary for ART to penetrate the tissue. A study evaluated the drug distribution of different ART in adipose tissue and reported only NNRTI's to be present in significant amounts, while PIs were present in relatively very

small amounts (Dupin et al., 2002). This study, however, was conducted before INSTIs were approved by the FDA.

Data on the impact of tissue penetration of DTG is only emerging now and limited tissues have been investigated in this context. For example, a relatively recent study reported DTG to penetrate adipose tissue (Couturier and Lewis, 2018). Additionally, another very recent study confirmed this finding, and reported DTG to also penetrate the digestive tract and the brain of mice, although the concentrations in the brain were significantly lower than in the other two tissues assessed. This is speculated to be due to the presence of efflux transporters and the composition of the brain tissue (Labarthe et al., 2022). Nevertheless, the ability of DTG to penetrate these tissues could contribute to its capacity for targeting persistent low-rate replication of HIV in tissue reservoirs. Clearly, more research is required in this context.

A related issue to consider is that the accumulation of DTG at multiple tissue sites could also increase risk for unwanted side effects in the longer term. In terms of safety profile, upon entry onto the market, serious adverse effect rates of around 8-11% were reported for DTG in two trials SPRING-1 (2012) and FLAMINGO (2014). However, many of these adverse effects were subsequently found to be unrelated to DTG itself (Clotet et al., 2014; Van Lunzen et al., 2012). In the early years of use, DTG was reported to have a low incidence of adverse effects, being well tolerated and exhibiting infrequent drug-drug interactions (Kandel and Walmsley, 2015). Indeed, two more early trials - SPRING-2 (2013) and SINGLE (2015) - reported a relatively high safety profile for DTG, with serious adverse events reported in <1% of patients (Raffi et al., 2013; Walmsley et al., 2015). These randomized clinical trials have indicated that DTG has lower risk than other HIV medication such as EFV and RTV. However, limitations to the safety data from these initial randomized trials include; strict inclusion/exclusion criteria, suboptimal safety reporting frequency thresholds of adverse effects, as well as the fact that original meta-analysis of key safety endpoints are seldomly published (Hill et al., 2018). These factors may have created a false optimism about the safety of DTG. In addition, these studies were only able to evaluate adverse outcome over a relatively short period, which may have limited detection of risk for chronic diseases with a somewhat longer pre-clinical (clinically asymptomatic) aetiology. Indeed, more recent reports have elucidated that adverse effects related to DTG are more frequent

than previously reported (Povar-Echeverría et al., 2021). Given the high-risk profile of most other ART in terms of co-morbidity and longer-term chronic disease risk, it is a priority to elucidate the exact nature of DTG distribution and its potential differential accumulation in tissue compartments.

In the next section, a summary of HIV pathology will be provided, with focus on effects potentially ascribed to, or exacerbated by, DTG.

## 2.3 Physiological dysregulation in HIV with/without dolutegravir

### 2.3.1 Neuropathology

HIV has a broad impact on the nervous system. Evidence has indicated a direct pathology on the brain, the spinal cord and the peripheral nerves (Clifford and Ances, 2013). HIV-induced neuropathogenesis is initiated soon after initial HIV infection, as a result of HIV invading the brain. Subsequently, the cerebrospinal fluid (CSF) becomes a reservoir for HIV copies and results in compartmentalization (Gougeon, 2016). Compartmentalization of HIV in the CNS can also result from a combination of CNS immunological characteristics, including the selective permeability of the blood-brain barrier (BBB), rapid mutation and recombination of HIV, in addition to generally poor ART penetration in the CNS (De Almeida, 2015). The effect of HIV on the CNS has been investigated but there is still great uncertainty regarding the exact mechanism(s) responsible for the symptoms observed. Due to the vulnerability of the CNS to HIV infection, the neurological implications associated with HIV infection can be vast, including neuropsychiatric symptoms, HIV myelopathy, peripheral neuropathy and decreased olfactory ability (De Almeida, 2015; Fasunla et al., 2016; Hornung et al., 1998; Watkins and Treisman, 2012). The variability in these neurological disorders suggests that multiple mechanisms and role players may contribute to the CNS dysfunction seen in HIV.

The neurological disorders and impairments associated with individuals infected with HIV have different modes of origin but are mostly related to direct HIV infection, opportunistic secondary infections and the inflammatory response by the immune system (Howlett, 2019). It has been reported that around half of HIV patients receiving treatment still present with cognitive impairment (Stern et al., 2018). Despite the

improvements in HIV therapies, neurocognitive disorders and impairment still remain prevalent among PLWH (De Almeida, 2015; Spudich and González-Scarano, 2012; Stern et al., 2018). HIV infection is associated with alterations in brain function and are referred to as HIV-associated neurocognitive disorder (HAND) (Vally, 2011). HAND in combination with several opportunistic infections and malignancies, constitute neuroAIDS. NeuroAIDS remains a large problem in the longer term management of HIV and AIDS due to the persistent low levels of HIV, inflammation and potential toxicity from ART (Clifford and Ances, 2013). HAND consists of three stages of neurocognitive impairment: asymptomatic neurocognitive impairment (ANI), mild neurocognitive disorder (MND) and the most severe form, HIV associated dementia (HAD). Following the introduction of cART, incidences of HAD have decreased but the two milder forms, ANI and MND, have increased in prevalence and remain a treatment hurdle (Clifford and Ances, 2013; Sacktor et al., 2016; Wang et al., 2020).

The clinical presentation of ANI and MND involves cortical changes such as memory impairment and executive function impairment. In contrast, HAD is reported to follow a similar pattern of cognitive dysfunction as other common neurodegenerative disorders such as Alzheimer's disease (AD) (Clifford and Ances, 2013). Of specific relevance to the current topic, neurocognitive impairment in the pre-cART era was defined by deficits in verbal fluency, motor speed and information processing speed. In contrast, in the cART era, the deficits are seen in learning and executive function domains (Heaton et al., 2011). These results suggest that neurocognitive impairment pathology may have changed after the introduction of cART (Joska et al., 2010). Due to the multifactorial nature consisting of contributions from secondary infections, the effect of ART, sustained inflammation and HIV related factors, the persistence of HAND - despite advancement in therapy - is still not well understood (Gougeon, 2016; Stern et al., 2018). Recent investigations have suggested that chronic inflammation and more specifically oxidative stress could be playing a large role in the disease pathogenesis (Buckley et al., 2021).

### 2.3.1.1 Neurological side effects of dolutegravir

While evaluating the persistence of HAND, it is important to consider the neurological implications of ART. There has been large interest in the cause of the neuropsychiatric adverse effects of DTG. Currently, the precise mechanism of neuropsychiatric adverse effects can only be speculated. After HIV exposure, the virus itself and the inflammatory response of the host are believed to jointly cause BBB dysfunction (Subra and Trautmann, 2019). The BBB is a physiological barrier that serves to maintain the microenvironment of the CNS. It presents as a functional neurovascular unit comprised of CNS endothelial cells, pericytes, neurons and astrocytes all connected by tight junction proteins (Chow and Gu, 2015). It is this close arrangement of the endothelial cells that limits molecules from paracellularly crossing the BBB. It has been suggested that viral entry into the CNS occurs due to alterations to the structure of tight junction proteins (Osborne et al., 2020). This was supported by studies illustrating increased BBB permeability after initial HIV infection (Leibrand et al., 2017; Rahimy et al., 2017). DTG has the potential to penetrate the BBB meaning it can target HIV in the CSF and thus potentially reduce the viral load. Despite this benefit, there is a possibility of drug-induced neurotoxicity associated with DTG accumulation in the CSF, even at the relatively lower concentrations that have been reported in the CSF. A recent hypothesis implicated DTG in microglial activation and neuronal apoptosis (Ma et al., 2020), which again places inflammatory dysregulation at the centre of the DTG-associated neuropathological process.

Other common neuropsychiatric adverse effects linked to DTG include insomnia, anxiety, mood alterations, psychosis, depression and sleep disturbances (Todd et al., 2017; Yombi, 2018). Several studies have indicated that numerous patients are discontinuing the use of DTG due to these adverse events experienced. Post market introduction studies reported 3-5 times higher incidences of neurological adverse events compared to the results from pivotal clinical trials (de Boer et al., 2016; Povar-Echeverría et al., 2021; Scheper et al., 2018). Most of the patients who reported these adverse events had no history of anxiety or mental health problems. It was also noted that if DTG treatment was interrupted, the symptoms returned after re-initiating (Hoffmann et al., 2017; Scheper et al., 2018). In addition, neuropsychiatric adverse effects were reported more frequently in patients using DTG than any other INSTI being investigated. This leads to speculation that the events are DTG-associated and

not necessarily an effect of the INSTI class in general. However, a change in mental health status is difficult to objectively evaluate in a clinical trial given the many confounding stressors as a result of HIV itself. Table 2.1 summarises the incidence and most reported neurological and neuropsychiatric side effects of DTG from multiple studies.

*Table 2.1: Reported neuropsychiatric adverse events for dolutegravir.*

Type of study conducted	Discontinuation rate of DTG due to adverse drug reactions	Neuropsychiatric and neurological adverse events reported and incidence (%)	Reference
Cohort study from two centres in the Netherlands	13.7%	Sleep disturbances (5.6 %) Psychological/ psychiatric symptoms, such as agitation, anxiety, depression, and emotional instability (2.5%) Neurological symptoms (1.8%)	(de Boer et al., 2016)
Retrospective analysis of data from two German HIV treatment centres	6.8 %	Overall, 5% of patients reported one or more: insomnia, poor concentration, dizziness, headaches, paraesthesia, depression.	(Hoffmann et al., 2017)
Retrospective analysis from Northern Ireland	8%	Total 25%, comprising of: Difficulty with low mood (7.1%) Anxiety (5.4%) Sleep disturbances (10.7%)	(Todd et al., 2017)
Case reports from the Netherlands	Not reported	Two male patients with no previous history of psychiatric events, presented with depression and Following cessation of DTG, symptoms resolved.	(Scheper et al., 2018)
Retrospective study from Spain	24.4%	Depression (19.1%) Anxiety (25.8%) Psychiatric disorder (3.5%) Sleep disorders (14.8%)	(Povar-Echeverría et al., 2021)

### 2.3.2 Gastrointestinal symptoms and gut dysbiosis

It has been known for many years that PLWH experience gastrointestinal symptoms not related to secondary infections (Zeitz et al., 1998). Similar to the CNS, the GIT is a major reservoir and site of HIV replication. Gastrointestinal symptomology presents across the entire GIT and symptoms experienced can range from dysphagia, nausea, vomiting and diarrhoea (Serlin and Dieterich, 2008). Early during HIV infection both inflammatory and immunological abnormalities occur in the GIT. Evidence suggests that there were particular pathologic process that occurred in the lamina propria and small intestine of PLWH (Kotler et al., 1984). Histologic studies of gut-associated lymphoid tissue from PLWH indicated significant deterioration of the GIT structure – indicated by villous atrophy – and a disproportional loss of CD4 T cells in the gut when compared to peripheral blood and lymphoid tissues (George and Asmuth, 2014; Mudd and Brenchley, 2016). These physiologic and immunological changes can lead to severe GIT symptoms drastically decreasing the quality of life of PLWH. Even though the advancements of ART have increased the life expectancy of PLWH, the frequency and severity of HIV enteropathy persists.

HIV enteropathy comprises increased GIT inflammation, diarrhoea and increased intestinal permeability (Brenchley and Douek, 2008). One of the leading gastrointestinal related causes of discomfort and even mortality, is diarrhoea. Chronic diarrhoea in PLWH can result in nutritional deficiencies, malabsorption and weight loss (Logan et al., 2016). It has been proposed that one the main causes of diarrhoea – other than opportunistic infections – is ART usage. Enteritis is typically seen in PLWH and is also associated with diarrhoea and malabsorption (Serlin and Dieterich, 2008). These symptoms are often accompanied by changes in the structure of the GIT which does not result from opportunistic infections (Brenchley and Douek, 2008). Research has indicated that intestinal damage persists in patients despite long term ART treatment and ART use does not restore the gut microbiome of PLWH (George and Asmuth, 2014; Pinto-Cardoso et al., 2018). It has been suggested that the reduction of CD4 T cells in combination with the changes in the microbial composition of the gut leads to dysbiosis and impairment of the intestinal mucosal immunity (Logan et al., 2016).

The composition of the gut microbiome has many functions, including immunologic, structural and metabolic roles which together ensure maintenance of gut barrier integrity. Studies conducted on HIV-infected patients highlighted the compositional changes that can be seen in gut microbiota – most notably, the decreased presence of commensal bacteria species such as bifidobacteria and lactobacilli and an increased number of opportunistic pathogens (Assimakopoulos et al., 2014). A significant body of literature pertaining to the impact of HIV-related gut dysbiosis on metabolic comorbidities again implicate chronic immune activation and inflammation as central role player (Funderburg et al., 2008; Marchetti et al., 2013; Sim et al., 2021).

The early events following initial HIV infection, results in rapid loss in gastrointestinal mucosal integrity which in turn causes increased permeability and translocation of microbial products into systemic circulation (Khan and Nawaz, 2016). This triggers the release of pro-inflammatory cytokines which predisposes PLWH to non-AIDS mortality and morbidity (Meyer-myklestad et al., 2021). However, the combination of microbial translocation and the disproportional loss of CD4 T cells in the gut cannot alone completely explain the broad dysfunction that exists in the gastrointestinal tract of PLWH (Mudd and Brenchley, 2016).

As a result of the link between dysbiosis and microbial translocation, it has been suggested there is a relationship between immune dysfunction and dysbiosis of gut microbiota in PLWH (Avedissian et al., 2020). The exact mechanism(s) via which the gastrointestinal dysfunction leads to metabolic complications remains a popular area of investigation. Indeed, HIV-associated inflammation driven by the alteration of the gastrointestinal barrier and microbial translocation, has directly been associated to visceral fat accumulation, dyslipidemia and insulin resistance among HIV infected individuals (Assimakopoulos et al., 2014; Kamari et al., 2019; Pedersen et al., 2013). This profile is similar to the side effects reported by patients on DTG treatment. Even though microbial translocation is a major contributor to chronic inflammation, alternative factors need to be considered due to the multifactorial nature of chronic systemic inflammation. There is still uncertainty regarding exactly how gut microbiota and the associated metabolites mechanistically influence the intestinal barrier and the consequent inflammation in HIV (Sim et al., 2021).

### *2.3.2.1 Reported gastrointestinal side effects of dolutegravir*

Gastrointestinal side effects are commonly observed in patients on ART. There could be a difference in severity of adverse effects in gastrointestinal regions due to the non-uniform expression of drug metabolizing enzymes in the GIT (Cory et al., 2013). The most notable GIT side effects ascribed to DTG in a pivotal 48 week clinical trial - the SPRING-1 safety trial - included nausea and diarrhoea (Van Lunzen et al., 2012). SPRING-2 - a 96 week follow-up of SPRING-1 - reported the same side effects, with 14% of patients experiencing nausea and 11% diarrhoea (Raffi et al., 2013). In addition, a 96-week non-inferiority study (FLAMINGO), reported the highest incidence of gastrointestinal side effects with 16% of DTG patients reporting nausea and 17% reporting diarrhoea (Clotet et al., 2014). Several studies conducted after these pivotal trials have indicated that the drug-related side effects are indeed much higher than these initial reports. The Swiss HIV Cohort Study provided data comparing DTG and RTV and reported that GIT side effects were the second most common reason for treatment modification in patients using DTG. DTG treated patients reported more GIT side effects than those using RTV (Elzi et al., 2017). The real-life effectiveness and safety of DTG was evaluated among a large cohort of treatment-experienced and naïve patients. It was reported that 22.2% of the 275 patients on DTG discontinued use due to gastrointestinal discomfort (Cid-Silva et al., 2017). Similarly, a more recent retrospective cohort study reported that GIT side effects were the most frequently noted DTG-associated side effect, with a total of 10.4% of patients reporting side effects, of which 91% were GIT related. The adverse events included nausea, vomiting, stomach ache and diarrhoea (Correa et al., 2020). From the summarised reports, it is evident that treatment with DTG is not without complications and warrants further investigation.

### *2.3.3 Weight gain associated with dolutegravir treatment*

Initially, a number of research publications suggested increased weight gain as a long-term effect in patients being treated with an INSTI (Menard et al., 2017; Taramasso et al., 2020; Venter et al., 2019). Weight gain is a well-known phenomenon for people initiating ART and was considered to be associated with patients returning to health (Eckard and McComsey, 2020). Clinical trials normally present body mass index (BMI) when reporting data. However, a BMI increase alone is not an accurate reflection of

risk associated with adipose changes. PLWH often experience adipose tissue accumulation in/around vital visceral organs or in the ectopic fat depots. This phenomenon is known as lipohypertrophy and carries an increased risk for cardiometabolic comorbidities (Eckard and McComsey, 2020). Even though the reason for the underlying weight gain is still unknown, there are some characteristics in PLWH that have been associated with more weight gain, including higher HIV-RNA, low baseline BMI, female sex, older age, certain races and lower CD4 T cell count (Eckard and McComsey, 2020; Taramasso et al., 2020). Table 2.2 summarises the weight gain observed following DTG containing ART regimens from several reports.

Table 2.2: Reported weight gain associated with dolutegravir treatment.

Type of study	ART regimen of participants in study	Weight gain	Sex distribution	Reference
Retrospective observational cohort of patients on fixed dose EFV/TDF/FTC for at least two years and then on new regimen for 18 months	Switch from EFV/TDF/FTC to INSTI or PI based regimen	After 18 months EFV/TDF/PIFTC -> 0.9 kg INSTI -> 2.9 kg PI -> 0.8 kg	85% males 15% females	(Norwood et al., 2017)
Retrospective observational cohort for patients who initiated DTG between 1 January 2014 and 30 November 2016	DTG containing	After 10 months 20% of participants had more than 10% increase from baseline 27% of participants -> 4-10%	65% males 35% females	(Menard et al., 2017)
Open-label, noninferiority, 48-week, phase 3 trial from February 2017 to May 2018 in ART naïve patients	TAF-ETC-DTG TDF-FTC-DTG TDF-FTC-EFV	After 48 weeks TAF-ETC-DTG -> 6 kg TDF-FTC-DTG -> 3 kg TDF-FTC-EFV -> 1 kg	41% males 59% females	(Venter et al., 2019).
Open-label, multicentre, randomized, phase 3 noninferiority trial	DTG TDF-3TC-EFV	After 48 weeks DTG- -> 5 kg TDF-3TC-EFV -> 3 kg	34.1% males 65.9% females	(NAMSAL ANRS 12313 Study Group et al., 2019)
Retrospective observational cohort of ART naïve initiating treatment between 1 January 2007 and 30 June	39 % PI 31% NNRTI 30% INSTI	After 18 months DTG based -> 6.0 kg EVG based -> 0.5 kg RAL based -> 3.4 kg NNRTI based -> 2.6 kg PI based -> 4.1 kg	85.5% males 14.5% females	(Bourgi et al., 2020)

Type of study	ART regimen of participants in study	Weight gain	Sex distribution	Reference
Multicentre observational study from July 2014 to December 2019. Including combination of treatment naive and experienced who switched to DTG	ABC-3TC-DTG TDF-FTC-DTG TAF-FTC-DTG 3TC – DTG RPV- DTG PI-DTG	After 24 months TDF/FTC+DTG and TAF/FTC+DTG had more than 10 % increase from baseline	74.7% males 25.3% females	(Taramasso et al., 2020)
Sub analysis of DOLBi study including patients who switched from NRTI to DTG regimen between 2015 and 2018	DTG – RPV DRV-3TC	After 12 months DTG-RPV -> 1.8 kg DRV-3TC -> 0.7 kg	61% males 39% females	(Vizcarra et al., 2020)
Retrospective observational study for patients who switched ART regimens between August 2013 and August 2018	Multiple	After 12 months 30% of all patients had >3% weight gain  The percentage of patients on INSTI regimens had statistically significant more weight gain than those not on INSTI	81% males 14% females (5% unspecified)	(Eckard and McComsey, 2020) (Mccomsey et al., 2019)

*Abbreviations: 3TC, lamivudine; ABC, abacavir; DTG, dolutegravir; DRV; darunavir; EVG, elvitegravir FTC, emtricitabine; INSTI, integrase strand inhibitor; PI, protease inhibitor; RPV, rilpivirine; TDF, tenofovir disoproxil fumarate; TAF, tenofovir alafenamide.*

### *2.3.3.1 Fixed-dose combination and the implications of weight gain on dolutegravir treatment*

Currently, DTG is administered in a fixed-dose combination (FDC) together with tenofovir disoproxil fumarate (TDF) and lamivudine (3TC) (World Health Organization, 2022). Fixed-dose combination ART was rolled out in 2013 in South Africa. This was introduced to remove three separate ART drugs to a single, fixed-dose combination tablet containing 300 mg TDF, 200 mg emtricitabine (FTC) and 600 mg EFV. This roll out was considered a significant step forward for South Africa in terms of cost-effectiveness and simplification of treatment (Clinicians Society, 2013). However, since this was implemented, the first-line regimen was changed to transition to 3TC and DTG instead of FTC and EFV (World Health Organization, 2022). Even though FDC allows for regimen simplification (reduced pill burden) and improved treatment compliance, it does not allow for easy dose adjustments. Dose adjustments are important, as a FDC could result in either overdosing or underdosing. In addition, FDC complicates identification of causal agents in case of adverse events. This is illustrated by the increased reports of weight gain during DTG treatment. Initially, evidence suggested that DTG was the ART responsible for weight gain in PLWH. However, more recently evidence has been provided suggesting that tenofovir alafenamide (TAF) potentially enhances weight gain (Venter et al., 2019; Wohl et al., 2019). A meta-analysis focussing on weight gain associated with DTG and TAF found that DTG in combination with TAF resulted in significantly higher weight gain when compared to DTG in combination with other NRTIs. It was reported that when TAF was compared to DTG, higher estimates of relative increases in weight were reported. It has been suggested that TAF and DTG may have an additive effect on weight gain, but this should be further investigated (Kanters et al., 2022). This scenario highlights how having a FDC increases the complexity in assigning an adverse event to one ART.

DTG dosage is not commonly adjusted except for when co-administered with rifampicin (X. Wang et al., 2019). However, the lipophilic nature of DTG suggests that it could accumulate in adipose tissue. If this is the case, individuals with higher adipose tissue content could be affected in two manners: 1) have increased DTG exposure in adipose tissue HIV reservoirs or 2) be exposed to greater DTG concentrations, possibly worsening adverse events. This indicates that body size should potentially be

a contributing factor when deciding on a DTG dose. Interestingly, the statistic on body size differences that males are larger than females is true for all regions across the world, except in Southern Africa where – although men are still significantly taller than females – average body mass of females generally exceeds that of men (“WorldData.info,” 2020) – this difference can largely be explained by relatively larger subcutaneous adipose stores in these females. This notion is supported by reports highlighting women of African origin reporting greater incidence of adverse events (World Health Organization, 2022).

Following these trials, a recent in depth analysis of weight gain reported in DTG trials (Shah et al., 2021) concluded that a high BMI in HIV infected individuals on ART is a risk factor for development of other comorbidities – diabetes specifically. However, it is still unknown whether INSTI, and especially DTG, accumulates in adipose tissue and/or causes physiological changes to adipose tissue metabolism (e.g. by directly affecting insulin sensitivity) (Gorwood et al., 2020). Although anecdotal clinical evidence exists, very few peer-reviewed reports in support of DTG associated hyperglycaemia exist. Limited peer reviewed reports exist and are summarised in Table 2.3 below. This contributes to existing literature that suggest a high BMI in PLWH leads to an increase risk for neurocognitive impairments and other comorbid conditions (Butt et al., 2009; Capeau et al., 2012; Norwood et al., 2017).

*Table 2.3: Reported incidence of hyperglycaemia following dolutegravir treatment.*

Case report	Presentation of patient(s)	ART regimen	Duration of treatment before onset of symptoms	Reference
1	Hyperglycaemia polyuria and polydipsia	ABC/3TC and DTG	3 weeks	(McLaughlin et al., 2018)
2	Hyperglycaemia, polyuria and polydipsia	ABC/3TC and raltegravir	4 months	(McLaughlin et al., 2018)
3	Dyslipidemia and acute diabetic ketoacidosis	ABC/ FTC and DTG	2 years	(Ntem-Mensah et al., 2019)
4	Acute diabetic ketoacidosis	ABC/ FTC and DTG	6 months	(Ntem-Mensah et al., 2019)
5	New-onset hyperglycaemia	DTG based first line therapy	4 months	(Lamorde et al., 2020)

*Abbreviations: 3TC, lamivudine; ABC, abacavir; DTG, dolutegravir; FTC, emtricitabine; RAL, raltegravir*

### 2.3.4 Olfactory decline

Similar to the recent SARS-CoV2 viral infection, several studies have reported a decline or negative impact in olfactory sensing after HIV infection (Fasunla et al., 2018; Heald et al., 1998; Mueller et al., 2002; Zucco and Ingegneri, 2004). Olfactory impairment or chemosensory dysfunction play an important role in ART adherence as patients may experience a foul smell or taste associated with their ART negatively impacting therapeutic outcome (Fasunla et al., 2016; Heald and Schiffman, 1997). PLWH often experience chemosensory decline, particularly affecting detection of odour thresholds, identification of odours and discerning tastes. This may suggest that viral infections, and in particular the persisting inflammatory response to the virus – as also widely reported on in the Covid-19 pandemic – may affect olfaction capacity. It has been suggested that the chronic inflammation associated with HIV could be related to hyposmia (Fasunla et al., 2016; Shah et al., 2005).

An additional hypothesis – or perhaps further proof of inflammatory involvement - is that HAND contributes to the declining smell and taste function in PLWH (Graham et

al., 1995). In this context, it is of interest that olfactory nerve endings are located in the olfactory mucosa at the roof of the nasal cavities. As a result of the multiple opportunistic infections (and thus repeated inflammatory episodes) that PLWH are predisposed to, these taste buds and olfactory nerve endings may thus be affected. However, limited studies have been conducted on the effect of HIV and ART on taste and olfaction. Interestingly, anosmia and respiratory tract adverse events have been reported as a side effect (albeit with low incidence) in DTG studies (de Boer et al., 2016; Miller et al., 2015; Mondri et al., 2019) and in clinical trials involving DTG (Cahn et al., 2013; Raffi et al., 2013). In terms of specific mechanisms, literature is vague.

Of particular relevance to the current dissertation, the olfaction link in HIV and DTG specifically, has led us to identify trace amines as potential role players in HIV- and DTG-associated pathology, as most of the known trace amine associated receptors are associated with olfactory tissue (more on this in the next section).

In summary, all side-effects reported for DTG suggests involvement of inflammatory dysregulation. Furthermore, given the interrelated nature of gastrointestinal health and obesity, as well as gastrointestinal health and neurological function, gut-brain signalling is most likely also dysregulated – this is supported by the reports of gut dysbiosis in PLWH. Previous work by our group, as well as the symptomatic profile seen in patients using DTG, suggest that an additional level of regulation – or dysregulation – of inflammation may be at play in PLWH. The trace aminergic signalling system has been identified as a role player at the interface of inflammation, gut health and neurological function (Berry, 2004; Pretorius and Smith, 2020). We believe that this system may offer a potential avenue for therapeutic target identification, and development of therapeutics aimed at addressing the inflammatory dysregulation occurring in HIV, but also in response to ART. I will review this system and its potential relevance in the following section.

#### 2.4 Trace amine system as potential (dys)regulatory role player

The trace aminergic system is emerging as relevant role player in many chronic diseases that are commonly diagnosed but poorly understood. Trace amine research started early in the 1970s and most of the research was centred around their relevance

to neurotransmission, given the close resemblance of trace amines to monoamine neurotransmitters. However, until relatively recently, a lack of sufficiently sensitive detection tools limited progress. More recent advances in quantification and detection techniques of small molecules have enabled more comprehensive evaluation of the relevance of trace amines to disease states. Popular research focus areas linked to trace amine involvement are neuropsychiatric, neurological and gastrointestinal disorders (Gwilt et al., 2020).

#### 2.4.1 Overview of the system

The original term trace amine was used to describe any endogenous amine with physiological concentrations below 100 ng/g tissue. However, following the detection of these “micro” amines in cerebral tissue, the term became more selective (Boulton, 1974). The original term was subsequently used to only describe compounds that were formed when a hydroxylation step in the synthesis of catecholamine and indoleamine neurotransmitters was omitted (Gainetdinov et al., 2018). Due to the (then) lack of a specific receptor targeted by trace amines and the fact that they presented indirect sympathomimetic effects, as well as lack of suitably sensitive research tools, almost all trace amine related research was concluded in the 1990's (Berry et al., 2017). However, in 2001 two independent groups identified a family of G-protein coupled receptors (GCPR) activated by trace amines such as  $\rho$ -tyramine (TYR),  $\beta$ -phenylethylamine (PEA), tryptamine (TRP) and  $\rho$ -octopamine (OCT) (Borowsky et al., 2001; Bunzow et al., 2001). These receptors have since been named trace amine associated receptors (TAAR). This name does complicate the field of trace amine research as these receptors are not activated by trace amines exclusively.

Even though this family of receptors activated by trace amines was identified, progress in the field has been very slow due to the uniqueness and challenging aspects of both trace amines and TAARs (Berry et al., 2017). While the existence of trace amines in the vertebrate brain and peripheral nervous system has been well documented, evidence of their exact functions in mammals is only now emerging. For example, it has been proposed that they are implicated in neurologic, metabolic and inflammatory function (Christian and Berry, 2018; Rutigliano et al., 2020). Trace amines are very similar to classic monoamine neurotransmitters in structure. In the CNS, trace amines

are known to have very short half-lives – similar to that of neurotransmitters – which results in only low nanomolar concentrations being present (Berry, 2004). They are categorized according to their structure, as a primary, secondary, tertiary or polyamines (Gainetdinov et al., 2018).

## 2.4.2 Formation and sources of trace amine

### 2.4.2.1 *Endogenous human production*

Most trace amines are formed by decarboxylation of amino acids by the action of aromatic L-amino acid decarboxylase (AADC) (Gainetdinov et al., 2018). Although AADC expression is predominantly reported in neuronal tissue, it has been detected in non-neuronal tissue such as the GIT, liver, kidney and the heart (Ho"nkfelt et al., 1973; Kitahama et al., 2009; Kubovcakova et al., 2004; Vieira-Coelho and Soares-da-Silva, 1993). PEA, TYR and TRP are formed by decarboxylation of L-phenylalanine, L-tyrosine and L-tryptophan respectively (Boulton and Wu, 1973, 1972) as illustrated in Figure 2.1. It has been suggested that these classic trace amines are synthesized within nigrostriatal dopaminergic neurons (Berry, 2004). OCT, another primary/classic trace amine, is thought to be synthesized from TYR - primarily in the brain and nerve tissue – by dopamine- $\beta$ -hydroxylase (DBH) within adrenergic neurons (Berry, 2004; Christian and Berry, 2018; Khan and Nawaz, 2016). Subsequently,  $\rho$ -synephrine (SYN) readily forms from methylation of OCT by phenylethanolamine N-methyl transferase (PNMT) in brain tissue (Eagles and Iqbal, 1974; Rossato et al., 2011). TYR, SYN and OCT are all considered products of tyrosine metabolism (Berry et al., 1996). Agmatine (AGM) can be formed by decarboxylation of arginine by mitochondrial enzyme arginine decarboxylase (ArgDC) (Molderings and Haenisch, 2012; Regunathan and Reis, 2008). 3-iodothyronamine (T1AM) is a thyroid hormone derivative with a PEA structure containing an additional iodine substituent (Bräunig et al., 2018). It had been suggested that it is derived from thyroid hormones through decarboxylation and extensive deionization, but currently the biosynthesis pathway remains unclear (Rutigliano et al., 2020). Furthermore, it has been reported that T1AM may not be formed by the action of AADC but rather by ornithine decarboxylase (Hoefig et al., 2015, 2012). In mammalian cells the precursor amino acid for putrescine (PUT) is L-ornithine. PUT is mainly synthesized by decarboxylation of ornithine by ornithine decarboxylase (Pegg, 2006). Likewise, PUT can also be formed by

agmatinase from AGM (Wang et al., 2014). The subsequent trace amines in the synthesis cascade are formed when PUT is converted to spermidine (SPD) by spermidine synthase (SPMS) which in turn is converted to spermine (SPM) by spermine synthase (SMS). In addition, SPM can be converted back to SPD via direct oxidation (Pegg, 2013). Another polyamine under investigation, cadaverine (CAD), is present in mammalian cells but there is currently little information regarding its synthesis in human cells. It is known that it is converted from L-lysine by lysine decarboxylase (CadA) in bacteria and plants, but the gene has not been identified in mammals. Current theory is that CAD is formed from L-lysine in mammals via the enzyme ornithine decarboxylase (Bekebrede et al., 2020).

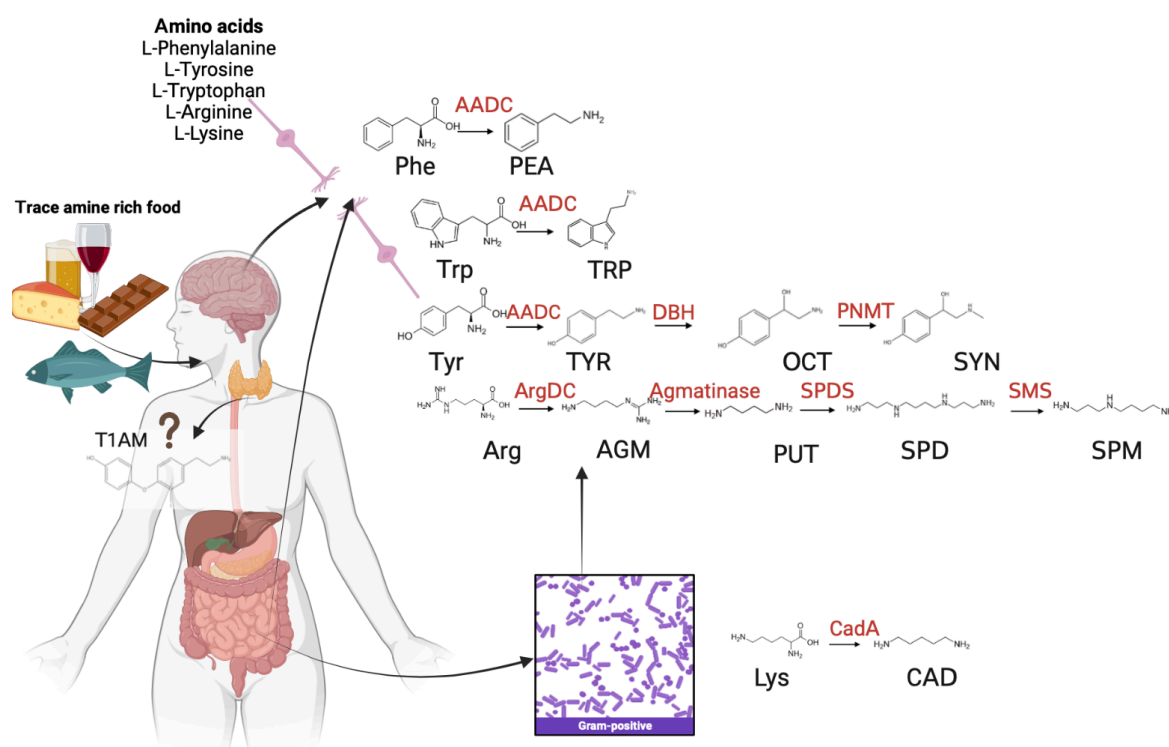


Figure 2.1: Formation and different sources of trace amines. Image created with Biorender.com.

Abbreviations: AADC, aromatic L-amino acid decarboxylase; Phe, phenylalanine; PEA,  $\beta$ -phenylethylamine; Trp, tryptophan; TRP, tryptamine; Tyr, tyrosine; TYR,  $p$ -tyramine; DBH, dopamine  $\beta$ -hydroxylase; OCT,  $p$ -octopamine; PNMT, phenylethanolamine N-methyl transferase, SYN,  $p$ -synephrine; ArgDC, arginine decarboxylase; AGM, agmatine; PUT, putrescine; SPD, spermidine; SPDS, spermidine synthase; SPM, spermine; SMS, spermine synthase; Lys, lysine; CadA, lysine decarboxylase; CAD, cadaverine; T1AM, 3-iodothyronamine.

#### 2.4.2.2 Food sources of trace amines

In addition to trace amounts of endogenous trace amines, relatively larger amounts of trace amines may be ingested from various food sources. Their presence in food is normally associated with bacterial-induced spoiled foods but also in foods produced by anaerobic microbial fermentation, such as aged cheeses, red wine, chocolate and fermented meats (Lorenzo et al., 2007; Naila et al., 2010; Shalaby, 1996). These foods are normally high in protein and as a result of the proteolytic activity during ripening there are multiple amino acid substrates for the decarboxylase enzymes (Suzzi and Gardini, 2003). The most trace amines found in food include TYR, TRP, PEA, CAD and PUT (Shalaby, 1996). PEA, TRP and TYR are found mostly found in cocoa beans, chocolate, cheese and fermented beverages and foods (Khan and Nawaz, 2016). Seafood such as molluscs, crustaceans and certain fish are rich in OCT, AGM, PEA, TRP, PUT, CAD and TYR (Gainetdinov et al., 2018). SYN is mostly consumed through citrus fruits such as grapefruits, mandarins and clementines, in addition to beverages produced from bitter orange (Stohs et al., 2020).

#### 2.4.2.3 Bacterial production of trace amines

PEA was first shown to be a product of not just bacterial composition but also part of decompositions of animal-derived products (Grandy, 2007). This evidence from these early studies elucidated that trace amines could readily be produced by microorganisms found in the microbiome of mammals and this could play an important role in the health of the host. As illustrated in Figure 2.1 it can be seen that trace amine production by prokaryotes is as a result of amino acid decarboxylases and many of them use L-amino acids as their substrates (Naila et al., 2010). Although these enzymes have been identified in species of the gram-negative *Bacillus*, *Pseudomonas* and *Photobacterium* (Morii et al., 1988), trace amines are mostly produced by gram-positive bacteria (Pugin et al., 2017). The human microbiome is mainly made up of the phyla Firmicutes and Bacteroidetes (Bekebrede et al., 2020). Many lactic acid bacteria in the genera *Lactobacillus*, *Enterococcus*, *Weissella* and *Leuconostoc* are also able to decarboxylate amino acids (Barbieri et al., 2019; Maijala and Eerola, 1993) – these bacteria are commonly found in fermented food products. It has been established that when trace amines produced by gut bacteria are present in adequate amounts, they exert different effects on the host (Gwilt et al., 2020).

In order to understand the role of trace amines in the human body, a comprehensive analysis of the production and interaction between trace amines and their receptors must be considered. Furthermore, directly relevant to the current dissertation topic, this plethora of trace amines sources complicate the clinical evaluation of potential effects of DTG in this context. Thus, in our opinion, it may be more beneficial to conduct investigations of this nature in highly standardised models, so that confounding effects of genetics, diet, microbiome, etc. may be minimised. We propose that rodent models may be a useful research tool in this context.

#### 2.4.3. Relevance of trace amines to HIV/dolutegravir adverse profile

To our knowledge, the effect of neither HIV nor DTG on a trace amine profile has been investigated in any detail. However, we provide “circumstantial evidence” for such a link, from a review of the relevant organs and systems implicated in HIV and DTG adverse outcomes.

##### 2.4.3.1. *Relevance to inflammation*

Following the identification of the archetypal trace amines such as TYR and OCT in plasma, research into their role in human physiology outside the nervous system was initiated (D’Andrea et al., 2003). Confirmation of trace amine associated receptor 1 (TAAR1) expression on leukocytes was the first indication that trace amines may have an inflammatory role (D’Andrea et al., 2003). More recent studies confirmed the original hypothesis by reporting that TAAR1 protein expression was upregulated following lymphocyte activation (Panas et al., 2012; Wasik et al., 2012). This is most likely a negative feedback mechanism, since TAAR1 activation is commonly linked with a shift towards Th2 lymphocyte predominance and antibody production, which would lead to resolution of inflammation (Babusyte et al., 2013). Similarly, trace amine associated receptor 2 (TAAR2) has been expressed in leukocytes, with mRNA detected in B-cells, monocytes, T-cells and granulocytes (Babusyte et al., 2013), although its function remains to be fully elucidated. A recent comprehensive review of trace amines and TAARs in the context of immune function summarised several time points during the inflammatory cascade where either TAARs or trace amines may play a role (Christian and Berry, 2018).

In terms of the trace amines themselves, PEA and TYR serve as chemotactic factors to attract polymorphonuclear neutrophils (PMN) during initiation of inflammation (Babusyte et al., 2013). In contrast, SYN was associated with anti-inflammatory properties in a LPS-stimulation model in macrophages, where it inhibited secretion of pro-inflammatory cytokines interleukin 6 (IL-6) and TNF- $\alpha$ , as well as nitric oxide production, which suggests lower levels of oxidative stress (Ishida et al., 2022). More indirect roles in inflammation via modulation of redox status has also been reported for other trace amines, such as the polyamines (Bekebrede et al., 2020). Briefly, polyamines – more specifically SPM – activate the eukaryotic initiation factor 5A (EIF5A) (Ivanov et al., 2018) – while being converted to hypusine. PUT and SPD indirectly affect this process as they in turn can be converted to SPM. In macrophages this hypusination of EIF5A plays a role in inducing mitochondrial genes. Depletion of PUT and the polyamines produced from PUT was indeed shown to result in a noticeable increase in pro-inflammatory macrophages, and an increase in stomach and colonic inflammation (Hardbower et al., 2017).

#### *2.4.3.2 Relevance to neurotransmission and/or neurological disorders*

Trace amines are heterogeneously distributed through the mammalian brain (Berry, 2004). Variation in concentrations of individual trace amines and combinations of trace amines have been associated with multiple neurological disorders including, schizophrenia, Parkinson's disease (PD), attention deficit hyperactivity disorder (ADHD), drug addiction, depression and recently AD. Presently there are limited published data of direct involvement of trace amines in the dysfunction associated with AD. However, there is indirect evidence supporting an association between trace amine dysregulation and AD. Currently the hypothesis surrounding trace amine involvement is centred around the relationship between trace amines and neurotransmitters and TAAR1 activation. A defective trace amine metabolism leads to lower concentrations of dopamine (DA) and serotonin (5-HT) which are detrimental during AD progression with regards to cognitive impairment. In addition, TAAR1 signalling once activated by trace amine binding, can decrease cAMP-response element binding protein (CREB) and extracellular signal-regulated kinase 1/2 (ERK1/2) and downstream signalling (Dhakal and Macreadie, 2021). This is of particular relevance to the current dissertation topic, as HAND and AD have similar

initial disease manifestations and symptomology. The overlapping symptomology suggests that there could be trace amine involvement in the HAND pathology and neurological side effects reported for DTG.

As the widest expressed trace amine receptor, expression of TAAR1 in various brain and peripheral tissue has been investigated comprehensively. TAAR1 has been shown to regulate the classic neurotransmitters that relate to many neuropsychiatric disorders (Berry et al., 2017; Efimova et al., 2022). As a result of TAAR1 localisation, there is strong evidence that it has an influence on the monoamine system (Dodd et al., 2021). For example, it has been reported that TAAR1 acts in an inhibitory manner in the brain, where it modulates catecholamine release from dopaminergic and noradrenergic fibres (D'Andrea et al., 2010). This process seems dependent on trace amines binding to TAAR1, which aids its heterodimerization with serotonin receptor 2 and dopamine receptor 2. This interaction leads to reduced cyclic adenosine monophosphate (cAMP) levels and thus decreased phosphorylation of cAMP response element binding protein and ERK1/2. This functions as a negative feedback system, reducing 5-HT and DA firing rates (Berry et al., 2017; Dhakal and Macreadie, 2021). Malfunctions in this firing/release of neurotransmitters resulting from trace amines binding to TAAR1, may lead to significant implications in the nervous system and in particular for neurocognitive function.

Various neurological disorders have been associated with dysfunctional trace amine signalling. An in-depth review surrounding trace amines and their role in pharmacology and the clinical implications was published and indicated the potential of using trace amines for innovative forms of treatments (Pei et al., 2016). Briefly, three of the classic trace amines (PEA, TRP and OCT) were shown to stimulate CNS effects. This could be due to evidence demonstrating an intimate functional relationship between trace amines and the classic monoamines (Pei et al., 2016). Even at sub micromolar concentrations trace amines have been shown to modulate classic neurotransmitters by either increasing or decreasing a cellular response to the neurotransmitters (Zucchi et al., 2006). It has been well documented that PEA, TRP and TYR can potentiate the response produced by noradrenaline (NA) and DA (Dodd et al., 2021). PEA may act as a post-synaptic neuromodulator of both DA and NA neurotransmission (Boulton, 1991), whereas TRP caused an increased response to NA, potentiated the neural

responses to DA and the inhibitory responses to 5-HT (Berry, 2004; Rutigliano et al., 2020). OCT selectively increased both the excitatory and depressant responses to NA in the rat cerebral cortex (Jones, 1982).

In addition to the neuromodulator effects of trace amines, more recent research has reported direct effects of exposure to trace amines themselves. Increased exposure of PEA may activate higher brain regions associated with fear, anxiety, defensive behaviours, and panic (Dewan, 2021; Francesconi et al., 2020). These are similar to the neuropsychiatric side effects patients using DTG have reported. Changes in trace amine concentrations have been noted in several neurological disorders. For example, increased TYR and TRP concentrations have been associated with chronic migraines and headaches (D'Andrea et al., 2017; Khan and Nawaz, 2016). It has been suggested that OCT may function as a neuromodulator, as such it has been hypothesized to be involved in PD and migraines. The exact mechanism as to how it is involved has not been identified, however a suggested hypothesis was an altered tyrosine metabolism (D'Andrea et al., 2013). Moreover, decreased concentrations of PEA, TYR and OCT have been reported in depressive disorders (Sandler et al., 1979), while in bipolar disorder there is a noted increase in urinary PEA (Karoum et al., 1982). This same increase in urinary PEA was detected in schizophrenic patients (Potkin et al., 1979). When analysing circulating concentrations of PEA in plasma, schizophrenic individuals exhibited an average level of 12.1 ng/mL vs. 4.6 ng/mL in healthy individuals (Myojin et al., 1989). A later study reported similar results for circulating PEA plasma concentrations of healthy individuals (4.9 ng/mL). Of further interest, this study also reported plasma TRP and TYR concentrations differ significantly between males and females (Mao et al., 2009) – highlighting the requirement to include both sexes in investigations of this nature. The evidence presented thus far, clearly implicate trace amines as role players in neurocognitive function. However, it is also clear that trace amine profiles and thus functional effects differ across various pathophysiological conditions. For example, in contrast to the results mentioned for schizophrenia above, in AD patients, reduced concentrations of PUT (and mildly different concentrations of its metabolites SPM and SPD) were reported when compared to healthy age-matched controls. AGM was present in human brains at concentrations between 0.50 and 0.75 ug/g tissue, while the SPM and SPD were present at much higher concentrations (30 - 90 ug/g tissue) (Liu et al., 2014). However

a different profile has been reported in PD, with lower concentrations of circulating OCT (1.80 ng/mL vs 4.30 ng/mL in healthy controls) (D'Andrea et al., 2010). A more recent study by the same group reported a statistically significant difference in TYR and PEA concentrations of healthy controls compared to a PD group. PEA concentrations were significantly lower in the PD group while TYR concentrations were significantly higher in the PD group when compared to healthy controls. This group has suggested that certain trace amines could be used as biomarkers for early PD disease detection (D'Andrea et al., 2019). Understanding how different disease states and conditions impact different trace amines concentrations is imperative for the development of therapeutic diagnostic tools. If a comprehensive panel of trace amines can be identified and accurately quantified there is potential for use of trace amines as biomarkers for various diseased states.

#### 2.4.3.3 Relevance to gut dysbiosis

As previously mentioned, the most prominent contribution to luminal trace amine concentrations is via dietary intake (in particular fermented foods) and microbiome trace amine secretion (Bekebrede et al., 2020). Dietary trace amines are absorbed in the GIT and are mostly catabolized into harmless metabolites, typically other trace amines, by oxidative deamination. On the other hand, other secondary products formed during oxidative deamination by mono-amine oxidase B (MAO B) is hydrogen peroxide and other reactive oxygen species (Grandy, 2007). Trace amines in the gut have many potential fates as *in vitro* systems have shown that they may escape the degradative effects of enzymes that degrade them so rapidly in the brain (Gwilt et al., 2020).

Research into the potential implications of trace amines on GIT health is still in its infancy. A recent study of microbial by-products and their effects on gastrointestinal health provided some evidence that trace amines could be implicated in gastrointestinal disorders (Gwilt et al., 2020). A comprehensive review discussing trace amines and their potential mechanisms of action in gastrointestinal dysfunction was recently published (Pretorius and Smith, 2020). Briefly, it is suspected that some of the trace amines may have direct cellular cytotoxicity leading to detrimental effects. Cytotoxicity (death in more than 80% of cells) was observed when 500  $\mu\text{g/mL}$  TRP

was applied to human embryonic kidney (HEK293) cells and 125 µg/mL TYR was applied to MonoMac6 human cells (Luqman et al., 2018). However, since endogenous trace amine concentrations in the gut have as yet not been elucidated, the physiological relevance of this data is unknown. In another *in vitro* study, human colon adenocarcinoma (HT-29) cells were exposed to various concentrations of PEA, TYR, TRP and AGM (Pretorius et al., 2022b). This specific cell line is an appropriate model to use for the investigation of trace amines effects on the intestine because HT-29 cells have characteristics of mature intestinal cells (Martínez-Maqueda et al., 2015). Cell viability after exposure to the trace amines was indirectly measured using metabolic activity – decreased metabolic activity indicated decreased viability. Significant loss of metabolic activity was recorded with concentrations > 200 µg/ml PEA and AGM, >25 µg/mL TYR and > 18.75 µg/mL TRP (Pretorius et al., 2022b).

Changes in trace amines present in stool samples have also been associated with gastrointestinal diseased states such as inflammatory bowel disease (IBD). PEA, CAD and PUT have all been reported to be present in significantly increased concentrations in stool samples of patients with Chron's Disease when compared to healthy controls. The specific role of these trace amines in the gut remains largely unknown. PUT and CAD are categorised as polyamines and they have been implicated in toxicity at elevated concentrations (Santoru et al., 2017). The toxicity theory seems to be related to the catabolism of the polyamines in which they form unstable and toxic products (Pegg, 2013). In addition to direct effects of trace amines, oxidative stress and inflammation can be modulated by trace amines binding to TAAR1 receptors (Pretorius and Smith, 2020).

As trace amines are endogenous TAAR ligands, changes in their concentrations present in the GIT could directly affect gut health. Archetypal trace amines, PEA and TYR have direct effects on the GIT. Both PEA and TYR have been linked to increased synthesis and release of neurotransmitters into circulation, specifically 5-HT (Xie and Miller, 2008; Yano et al., 2015). 5-HT regulates gut motility and increased concentrations can lead to increased intestinal symptoms (Kendig and Grider, 2015; Wong et al., 2019). In addition, TYR and PEA reportedly stimulate fast ileal contractions in rodents. This contractile response was independent of

sympathomimetic mechanism, indicating strong evidence for TAAR involvement (Broadley et al., 2009). These changes in gut motility and secretion of neurotransmitters may have a large effect on mucosal immune response and luminal pH which would directly affect the host (Gwilt et al., 2020). Another archetypal trace amine, TRP, is structurally similar to 5-HT and has affinity for 5-HT receptors. TRP has been demonstrated to directly interact with the gut and alter ionic flux (Bhattarai et al., 2018), suggesting a role in maintenance of luminal fluid and gastrointestinal transit. This is especially important for GIT disorders presenting with constipation (Frizzell and Hanrahan, 2012). Similarly, OCT has demonstrated a relaxant response on rat gastric fundus tissue under basal tonus conditions. When OCT was administered intraperitoneally it delayed transit of a liquid meal in the small intestine of the rats (de Oliveira et al., 2021).

The polyamines have a more direct function in intestinal barrier integrity. The native human polyamines include PUT, SPD, SPM and CAD (Sagar et al., 2021). PUT is the most ubiquitous polyamine in the colon of humans and CAD the least abundant (Bekebrede et al., 2020; Matsumoto and Benno, 2007). PUT has been demonstrated to serve as a direct energy source for rat intestinal enterocytes (Bardócz et al., 1998). Overall, PUT plays a major role in the trace aminergic system by regulating the production of other polyamines to maintain a mucosal homeostasis in the intestine of the host (Nakamura et al., 2021). Moreover, SPM and SPD - produced downstream from PUT - have multiple roles in the gut but importantly play a role in intestinal barrier integrity. This was demonstrated by the relationship between polyamines and tight junction proteins such as occludin and E-cadherin (Bekebrede et al., 2020).

When considering the gastrointestinal side effects of DTG and the presentation of gastrointestinal dysfunction of PLWH, there is significant overlap with symptomatic presentations of IBD. Considering the above-mentioned role of TAARs and trace amines directly in the immune system and inflammation, it is very plausible that a dysregulation in the trace aminergic system can contribute to the presentation of IBD and other gastrointestinal disorders/symptomology commonly reported in DTG patients. However, context-specific studies are still lacking.

#### 2.4.3.4 Relevance to body/fat mass changes

Given the risk of obesity and metabolic comorbidities associated with PLWH and patients administered DTG, trace amine involvement in metabolic disorders should be considered. There are few reports focused on trace amine involvement in metabolic disorders, but it is of significance that TAAR1 is expressed in organs and tissues involved in metabolism (Ito et al., 2009; Regard et al., 2007). Even though there are limited reports with substantial evidence, SYN is commonly included in weight-loss, slimming and meal replacement products. The main evidence for this claim of increased resting metabolic rate and lipolysis, is an early study which reported SYN to partially activate lipolysis in humans and rats. OCT was noted to be the only amine to fully stimulate lipolysis in rats (Carpéné et al., 1999). However, very little evidence has since been generated to support the claims in weight loss aid (Rossato et al., 2011). Nonetheless, SYN has been reported to increase fat oxidation rate, but not carbohydrate utilisation or energy expenditure, during exercise of moderate intensity (Gutiérrez-Hellín and Del Coso, 2016). Thyroid hormones (TH) – consisting of thyroxine and triiodothyronine - regulate energy homeostasis in adults (Rutigliano et al., 2020) and hypothyroidism is a common cause of increased body mass. The trace amine T1AM – derived from TH - however promotes an opposite, hypometabolic state and significantly decreases body temperature (Braulke et al., 2008), with consistent hyperglycaemia (Klieverik et al., 2009; Regard et al., 2007) and insulin resistance (Manni et al., 2012) reported from rodent studies. In terms of mechanisms, T1AM seems to directly inhibit insulin secretion, via effects on  $G_i$  – coupled receptors, most notably the  $\alpha_{2A}$ -adrenergic receptor (Rutigliano et al., 2018). Interestingly, TAAR1 and adrenergic receptors have similar structures (Regard et al., 2007). Furthermore, T1AM has been detected in plasma, as well as in the brain, liver and muscle (Braulke et al., 2008; Saba et al., 2010), with known affinity for TAAR1, TAAR5 and TAAR8 (Rutigliano et al., 2018; Zucchi et al., 2006) SYN and T1AM along with their affinity for TAAR1 could potentially lead to a new target for therapeutic interventions for metabolic disorders potentially exacerbated in PLWH using DTG. However, more research is required to substantiate this.

#### 2.4.3.5 Sex-dependent effects of trace amines

Recent epidemiological studies have indicated that there are key population groups accounting for the majority of new HIV infections, e.g. 25% of new HIV infections are in young females in sub-Saharan Africa, whereas women in general account for 59% of new HIV infections (Joint United Nations Programme on HIV/AIDS, 2021). In addition, according to discontinuation rates of ART there seems to be a higher rate of women discontinuing due to reported adverse events (Elzi et al., 2017; Hoffmann et al., 2017; Venter et al., 2019), suggesting that sex potentially plays a role in the incidence or severity of side effects. In this context, DTG is no exception, with discontinuation reported to be three-fold higher in women and older patients (Hoffmann et al., 2017). With regard to trace amines in plasma, statistically significant differences in reported trace amine concentrations exist between males and females (Mao et al., 2009), while oestrogen was recently shown to impact gut microbial secretome trace amine load and composition, as well as inflammatory outcome (Pretorius et al., 2022b). Taken together, this literature highlights the importance of evaluation of trace amine profile in both males and females.

From the trace amine literature, it is clear that trace amine metabolism and interaction with their various receptors are complex topics. Thus, in order to identify potential role players in any disease state, a large panel of trace amines should be evaluated simultaneously (rather than the single trace amines typically focused on in the majority of published studies) and across many tissue compartments. This will allow for informed interpretations on trace amine metabolism and inter-trace amine relationships, tissue penetration and toxicity risk, so that holistic conclusions on their relevance to disease may be attempted. Furthermore, to the best of our knowledge, trace amines have not been studied in the context of HIV or DTG, although literature on symptomology that overlaps with presentations of HIV or side effects experienced by DTG patients, certainly suggest trace amine involvement.

#### 2.5 Methodological considerations

Liquid chromatography in combination with tandem mass spectrometry (LC-MS/MS) is an important research and diagnostic tool. LC-MS/MS is highly sensitive and allows for the detection of multiple compounds at very low concentrations. Despite the ability

to detected low molecular weight analytes at low concentrations – ng/ml and pg/mL - the quality of the sample plays a large role in the ability to detect these analytes accurately. This is due to the effect of ion suppression or enhancement - a limitation of LC-MS/MS. Therefore, samples must be processed properly in order to utilise the technique effectively. Typically, LC-MS/MS uses reverse phase chromatography as this is suitable for a range of moderately polar to non-polar analytes (Want, 2018). This approach is particularly suited for the analysis of these study samples as DTG and the panel of trace amines under investigation vary vastly in hydrophobicity.

### 2.5.1 Quantification of dolutegravir

DTG concentration is frequently measured in plasma and multiple LC-MS/MS methods have been reported (Bennetto-Hood et al., 2014; Gouget et al., 2020; Grégoire et al., 2014; Penchala et al., 2016; Simiele et al., 2017; Zheng et al., 2020). Table 2.4 summarises reported methods and the limitations identified in the current reported methods. Although multiple validated LC-MS/MS methods exist in plasma, very few reports are available on methods developed for extraction and quantification of DTG from tissue (Deodhar et al., 2022; Prathipati et al., 2016).

*Table 2.4: Summary of previously published dolutegravir extraction methods.*

Matrix	Extraction technique	Sample volume required (µL)	Concentration range developed (ng/mL)	Limitations of the reported method	Reference
Human plasma	Protein precipitation followed by on-line extraction	100	25 - 2000	Low recovery (14%) under the conditions utilised	(Grégoire et al., 2014)
Human plasma	Liquid – liquid	100	10 - 4000	High level of carry-over using an acetonitrile based mobile phase	(Penchala et al., 2016)
Murine plasma and biological tissues (Liver, kidney, spleen and brain)	Solid phase extraction	100	5 - 2000	Low recovery (40.7 – 41.9%) Standards and quality control samples were not matrix matched	(Prathipati et al., 2016)
Human plasma	Protein precipitation	100	20 - 5000	Long analytical run time (18 minutes)	(Zheng et al., 2020)

Of the methods reported, insufficient information was provided regarding the method development for quantifying nano-formulated DTG from rodent muscle and liver to allow reproduction of the method employed (Deodhar et al., 2022). Similarly, another study reporting DTG distribution in multiple murine tissue sites, did not provide sufficient extraction and quantification method details. The group utilised a validated LC-MS/MS method for DTG quantification in plasma and adapted it for tissues, but did not report on the adaptations (Labarthe et al., 2022). We found only one detailed report describing method development for extracting and quantifying DTG from tissue matrices as part of a multi-analyte method from murine biological matrices (Prathipati et al., 2016). The method was developed to quantify DTG in murine tissue but did not use matrix matched standards and QCs. In addition, likely in part due to the multi-analyte approach, the recovery of DTG from murine plasma and tissues such as liver, kidney, spleen and brain was fairly low, ranging between 40.7 – 41.9% in the method reported by (Prathipati et al., 2016). This relatively low recovery of DTG suggests further method optimisation is required. Furthermore, this group reported on the method development process including DTG as part of their multi-analyte method but did not include DTG in their *in vivo* supplementation study. As a result of not including DTG in the supplementation study, the group could not evaluate the tissue distribution characteristics of DTG.

Of the reports describing DTG supplementation/intervention studies, limited information is provided with regards to the dosage of DTG administered to the rodents. The most used administration method of DTG was via oral formulation (p.o) in drinking water, intraperitoneal injection (I.P) and intramuscular injection (IM) (Deodhar et al., 2022; Labarthe et al., 2022). The dosages used in the reports were 12.6 mg/kg p.o, (Labarthe et al., 2022) 2.5 mg/kg IP (Labarthe et al., 2022) and 45 mg/kg IM (Deodhar et al., 2022). The oral formulation administration involved dissolving the DTG dose in the drinking water of the mice, however this is not ideal as DTG is sparingly soluble in water (0.095 mg/mL) (National Center for Biotechnology Information, 2023). It is therefore necessary to develop an administration technique that is cost effective and allows for easy daily administration to rodents without compromising accurate dosing.

From the reports summarised above, it can be seen that there is a lack of detailed information describing the development of a sensitive, robust LC-MS/MS method with

relatively high and consistent recoveries of DTG in tissues to determine tissue distribution into HIV reservoirs.

### 2.5.2 Quantification of multiple trace amines

Trace amine concentrations are often measured in urine and/or plasma – common matrices to investigate as plasma and urine are easily obtainable. Trace amine concentrations are being considered for their use as a clinical diagnostic tool for gastrointestinal disorders such as IBD and neurological disorders such as PD (D'Andrea et al., 2019; Maráková et al., 2020). However, the difficulty with using trace amines as biomarkers for diseased states is that trace amine load will differ from person to person – it may therefore be more useful to either express trace amine concentration as percentage of total trace amine load, or to monitor changes over time.

Matrices most frequently used for trace amine quantification is microbial media supernatants following cell cultivation, plasma, urine, faecal samples and food/beverages for quality control and toxicity screening (D'Andrea et al., 2010; Gosetti et al., 2013; Luqman et al., 2018; Maráková et al., 2020; Sagratini et al., 2012; Santoru et al., 2017). Following a comprehensive literature analysis, it can be seen that the most frequently quantified trace amines are PEA, TYR, TRP, OCT, PUT and CAD. This is probably due to PEA, TYR, TRP and OCT being classified as the archetypal trace amines and initial research focused on their role in neurological disorders. Due to PUT and CAD being present in most spoiled or contaminated food, they often serve as indicators for the quality of food (Sagratini et al., 2012). However, since trace amine research and their roles in diseased states are becoming more popular, there is a need for accurate and sensitive quantification for a large panel of these analytes.

When considering quantification of trace amines in physiological matrices from human/rats the methods become more complicated due to trace amine metabolism. As discussed earlier in this chapter (Sec. 2.4.2) trace amines are metabolised in many ways and the enzymes responsible for trace amine synthesis vary greatly. This makes quantification of trace amines very difficult, and they could degrade during the extraction process before they can be quantified in the selected matrix. In addition,

another obstacle is the number of trace amines that can be included in the panel for investigation. The varying hydrophobicity and functional groups of trace amines could cause different chromatographic behaviour. However, the greatest limitation in trace amine quantification is the fact that they are endogenous analytes in the matrices evaluated. At the moment there is no consensual guidelines to develop an analytical assay for quantification of endogenous compounds. There are three routine methods currently employed for assay validation namely, (1) using an authentic analyte in an authentic matrix, (2) using isotope-labelled internal standards as a surrogate analyte in an authentic matrix, and (3) using authentic analytes in a surrogate matrix (L. S. Wang et al., 2019). At present it would be impossible to utilise the first method as there is no manner in which to remove any of the trace amines from the authentic matrices. It would also be impractical to attempt to measure a relatively small amount added for each trace amine and extrapolate the calibration curves – moreover, introducing a possibility for significant error. The second method – using isotope-labelled internal standards – can be very costly and deuterated internal standards are not always readily available. The third method seemed most appropriate since a suitable surrogate matrix could be used. A surrogate matrix could be more complex such a synthetic matrix or something simple such as water or a buffer (L. S. Wang et al., 2019). Despite this solution it is inevitable to have matrix effects between sample in a matrix and the standards prepared in a surrogate matrix – regardless of the surrogate chosen.

Currently trace amine concentrations in the gut are inferred from faecal samples collected or from the predominant microbial species present (Luqman et al., 2018; Santoru et al., 2017). To the best of our knowledge a large panel of trace amines in the GIT has not been quantified from using biopsied gastrointestinal samples. Moreover, there is a lack of data discussing the correlation between trace amine concentrations in various matrices from an individual. This is especially important considering the recent hypothesis that trace amines may modulate connections between the gut and the brain (Gwilt et al., 2020). Even though, there is a large interest in quantification of trace amines in the brain their relatively short half-lives complicate quantitation. Table 2.5 summarises current methods utilised to determine various trace amines in mammalian biological matrices

Table 2.5: Summary of research conducted to determine trace amine concentration in mammalian biological matrices.

Matrix	Extraction protocol	Analytical technique	Analytes	Concentrations detected		Standards preparation	Limit of quantification	Limitations identified	Reference
				Males	Females				
Human serum	Derivatisation followed by online solid phase extraction	LC-MS/MS	PUT	21±7 (ng/mL)	20±10 (ng/mL)	Water	0.1 ng/mL	Required derivatization and isotopically labelled IS for each polyamine	(Magnes et al., 2014)
			SPM	10±7 (ng/mL)	12±20 (ng/mL)		Not specified		
			SPD	13±5 (ng/mL)	14±10 (ng/mL)		0.8 ng/mL		
Human urine	Protein precipitation	UFLC-MS/MS	PUT	69.0±39.7 (ng/mL)		Urine	31.3 ng/mL	Did not account for endogenous trace amines	(Liu et al., 2013)
			CAD	236±281 (ng/mL)			7.50 ng/mL		
			SPM	8.67±7.33 (ng/mL)			2.50 ng/mL		
			SPD	2.89±4.91 (ng/mL)			2.50 ng/mL	Relatively low recovery	
			AGM	9.17 x10 <sup>3</sup> ±4.66 x10 <sup>3</sup> (ng/mL)			31.25 ng/mL		
Human plasma	Protein precipitation	UFLC-MS/MS	PUT	5.28±2.70 (ng/mL)		Plasma	0.125 ng/mL	Did not account for endogenous trace amines	(Liu et al., 2013)
			CAD	2.34±0.962 (ng/mL)			0.125 ng/mL		
			SPM	8.69±7.33 (ng/mL)			0.625 ng/mL		
			SPD	0.584±0.419 (ng/mL)			0.250 ng/mL	Relatively low recovery	
			AGM	71.7±21.7 (ng/mL)			1.250 ng/mL		
Human urine	"Dilute and shoot"	HPLC-MS/MS	TYR	342 – 2480 ng/mL		Standard addition method to urine	2.5 ng/mL	Only 6/16 biogenic amines included were detected. Results very variable	(Gosetti et al., 2013)
			CAD	91.8 – 1016 ng/mL			2.6 ng/mL		
			PUT	40.2 – 658 ng/mL			2.8 ng/mL		
			SPM	2720 ng/mL			5.0 ng/mL		

Table 2.5 continued

Matrix	Extraction protocol	Analytical technique	Analytes	Concentrations detected		Standards preparation	Limit of quantification	Limitations identified	Reference
				Males	Females				
Human brain	Derivatisation using dansyl-chloride followed by liquid-liquid extraction	HPLC (SPM and SPD) LC-MS/MS (PUT and AGM)	AGM	0.45 – 0.75 µg/g tissue		Not reported	Not reported	Two separate methods – HPLC and LC-MS	(Liu et al., 2008)
			PUT	1 – 3 µg/mL tissue					
			SPM	30 - 60 µg/mL					
			SPD	50 – 100 µg/mL tissue					
Human plasma	Solid phase extraction	UPLC-MS/MS	TYR	0.418 nmol/L		Plasma	0.13 nmol/L	Did not account for endogenous trace amines	(D'Andrea et al., 2019)
			PEA	7.38 nmol/L			0.05 nmol/L		
			OCT	0.077 nmol/L			0.10 nmol/L		
			SYN	0.016 nmol/L			0.05 nmol/L		
			TRP	1.47 nmol/L			0.26 nmol/L		
Murine brain	Protein precipitation	LC-MS/MS	PUT	0.6 ng/mg tissue		Solvent	0.78 ng/mL	Only analysed polyamines	(Langner et al., 2022)
			SPM	20 ng/mg tissue			1.56 ng/mL		
			SPD	40 ng/mg tissue			0.2 ng/mL		
Rat plasma	Protein precipitation	HPLC	PEA	11.5		Solvent	5.0	Required derivatisation	(Wang et al., 2018)
			PUT	162.6			25.0		
			CAD	312.8			1.0		
			TYR	ND			10.0		
			TRP	52.7			5.0		
			SPD	273.9			5.0		
			SPM	41.5			10.0		

## 2.6 Conclusion

The major pathophysiology of HIV is associated with the immune system, with most patients developing secondary infections and co-morbid chronic conditions. These conditions result in significantly compromised life quality in PLWH and are – at least in part – ascribed to the ART themselves. From the summarised literature, it is evident that treatment with DTG is not without complications and warrants further investigation. While no studies have directly explored the implications of the trace aminergic system in HIV or DTG related side effects, it is alluded to. The fact that there is significant overlap between the symptoms of a dysfunctional trace aminergic system with reported adverse events of DTG supports this. The development of LC-MS/MS methods to quantify both DTG and trace amines in various tissues would enable investigation of the potential relationship that exists between these. As such, we suggest that DTG could alter the trace aminergic system and this could result in neurological and gastrointestinal dysfunction.

## 2.7 Hypothesis statement

Extremely limited data are available on methodology for detection of both DTG and comprehensive trace amine panels and are mostly limited to detection in serum samples. We hypothesized, firstly that current methodology for quantification of DTG and several trace amines may be further optimized to enable sensitive detection in various tissues. Secondly, we hypothesized that chronically administered DTG will show tissue specific accumulation and will correlate with tissue specific dysregulation of trace amine content. Lastly, we hypothesized that DTG effects will be influenced by sex.

## 2.8 Aim and objectives

### 2.8.1 Aim

We therefore aimed to investigate the effect of chronic (12-week) DTG treatment on tissue DTG and trace amine levels in rats to determine potential associations between DTG and individual trace amines.

### 2.8.2 Objectives

In order to achieve this aim, we formulated the following objectives:

1. Execute a 12-week DTG administration protocol in male and female wistar rats.
2. To develop a single analyte LC-MS/MS method for detection of DTG in plasma and various tissues.
3. To determine DTG distribution profile across various compartments in rodent samples.
4. To develop a multi-analyte LC-MS/MS method for detection of multiple trace amines in plasma, urine and relevant tissues.
5. To determine trace amine concentrations in these matrices.
6. To evaluate whether DTG accumulation is linked to alterations in trace amine profile.

## Chapter 3: Development of liquid chromatography tandem mass spectrometry (LC-MS/MS) methods for quantification of dolutegravir in various biological matrices from wistar rats

(This chapter has been prepared in manuscript to form and submitted to Heliyon – impact factor 3.77).

### 3.1 Introduction

DTG – an INSTI – is currently used as the first line treatment for HIV. The FDA has approved DTG for treatment of HIV in a broad patient population (Bailly and Cotellet, 2015; Zhang et al., 2015). DTG is currently recommended as a first line treatment for treatment naïve and treatment experienced HIV-infected patients (Bailly and Cotellet, 2015; Barcelo et al., 2019; World Health Organization, 2018).

For an ART drug to be effective, it should be able to reach its target without causing adverse effects. To ensure efficacy – apart from its antiviral activity - it is essential for ART to penetrate HIV reservoirs such as the brain and the gastrointestinal track (Cory et al., 2013). Penetration of reservoirs by ART is essential to prevent the continuous replication of the virus (Massanella et al., 2016). Information on the penetration of ART into HIV reservoirs will inform on risk of longer-term adverse outcomes, as well as drug efficacy at tissue level. It is therefore important to consider the distribution of ART at tissue level. A complete picture can only be gained from assessment of various biological matrices to determine penetration of ART into these potential viral reservoirs. When analysing the effect of DTG on different tissues, it is important to consider the distribution of the drug. The proven ability of DTG to penetrate tissues could contribute to its capacity for targeting persistent low-rate replication of HIV in its tissue reservoirs (Couturier and Lewis, 2018).

However, improved penetration into reservoirs and off-target tissues may predispose patients to co-morbidity risks in particular tissue compartments. In the early years of use, DTG was reported to have a low incidence of adverse effects, being well tolerated and exhibiting infrequent drug-drug interactions (Kandel and Walmsley, 2015). More recent reports have elucidated that adverse effects related to DTG are more frequent

than previously reported (Povar-Echeverría et al., 2021). This may be due (at least in part) to wider application of the drug, or more frequent prescription of DTG to patients already taking other chronic medications, but currently insufficient data preclude firm conclusions on the reasons for this. Despite the causes, given the high-risk profile of most other ART in terms of co-morbidity and longer-term chronic disease risk, it is a priority to elucidate the exact nature of DTG distribution and its potential differential accumulation in tissue compartments, as this may inform on risk profile. For example, the majority of side effects reported for DTG involve the neurological and/or gastrointestinal systems (Couturier and Lewis, 2018; Kandel and Walmsley, 2015; Povar-Echeverría et al., 2021). Thus, the ability to quantify concentrations of DTG in these tissues may provide insights into whether these tissues are most vulnerable to side-effects due to relatively low penetration of DTG into these known viral reservoirs (i.e. relatively larger viral effect), or due to high penetration of DTG, which may suggest undesired off-target effects of DTG itself.

LC-MS/MS is an important research and diagnostic tool. DTG concentration is frequently measured in plasma and multiple LC-MS/MS methods have been reported (de Boer et al., 2016; Gouget et al., 2020; Penchala et al., 2016). However, few reports are available on methods developed for extraction and quantification of DTG from tissue (Deodhar et al., 2022; Prathipati et al., 2016). Of the methods reported, insufficient information was provided regarding the method development for quantifying nano-formulated DTG from rodent muscle and liver to allow reproduction of the method employed (Deodhar et al., 2022). In addition, DTG extraction from murine plasma and tissues such as brain, spleen and kidney, has been reported (Prathipati et al., 2016). However, in this study, calibration standards and quality control samples were not matrix matched and low DTG recovery was reported, indicating that further method optimisation was likely required.

In this chapter I describe the development of a novel method to quantify DTG concentrations in wistar rat plasma, adipose, brain, muscle and liver tissue by using reverse phase liquid chromatography coupled with mass spectrometry. Importantly, the method utilises matrix matched standards and quality control samples. The method entails a combination of protein precipitation and solid phase extraction (SPE) and resulted in consistent recoveries in all matrices evaluated.

## 3.2. Materials and methods

### 3.2.1 Ethical considerations and sample collection

All animal experiments were conducted according to the guidelines and ethical standards set out by the South African National Standard (SANS: 10386:2008) for the care and use of animals for scientific purposes 10386:2008 and the Research Ethics Committee: Animal Care and Use (REC: ACU) of Stellenbosch University (ref: ACU - 2022 - 24915). Ethical approval letter attached as Addendum A. Wistar rats were euthanised by intraperitoneal injection of sodium pentobarbital. Aortic puncture was executed to collect blood in EDTA Vacutainer® (BD, Plymouth, UK) tubes. The tubes were gently inverted 10 times to ensure homogenous distribution of the anticoagulant. EDTA whole blood was centrifuged at 21°C for 10 minutes at 1 000 x *g* and subsequently the plasma layer aliquoted and frozen at -20°C until analysis. The left hemisphere of the brain, the left retroperitoneal adipose depot, the left gastrocnemius, and the tip of the left lateral lobe of the liver were excised and snap frozen in liquid nitrogen before transfer to storage at -80°C until analysis.

### 3.2.2 Method development

#### 3.2.2.1 Reagents

DTG (D528800) and its isotope-labelled internal standard, DTG-d4 (D528802), were purchased from Toronto Research Chemicals (Toronto, ON, Canada). LC-MS grade acetonitrile (ACN) and methanol (MeOH) were purchased from ROMIL Ltd. (Cambridge, UK) and formic acid from Fischer Chemicals (New Hampshire, USA). Ultrapure water was produced from a Synergy® water purification system (Merck KGaA, Darmstadt, Germany). Dimethyl sulfoxide (DMSO) was purchased from Sigma-Aldrich (Missouri, USA).

#### 3.2.2.2 Equipment

LC-MS/MS analysis was conducted on a SHIMADZU 8040 triple quadrupole-mass spectrometer (SHIMADZU, Kyoto, Japan) connected to a SHIMADZU Prominence LC system. The system consisted of a LC-20ADXR solvent delivery system, Nexera XR SIL-20AXR autosampler and CTO-20A column oven. The analytes were chromatographically resolved on an Agilent Poroshell 120 EC-C18 (3.0 x 100 mm, 2.7

$\mu\text{m}$ ) column. Data acquisition and processing was performed using LabSolutions Version 5.109 software (Shimadzu Corporation, Kyoto, Japan) and Microsoft excel version 16.

### *3.2.2.3 Chromatographic conditions*

For plasma analysis, chromatographic separation was carried out with an isocratic mobile phase consisting of water containing 0.1% formic acid (mobile phase A) and ACN containing 0.1% formic acid (mobile phase B) (40:60, v/v) at a flow rate of 0.4 mL/min. The column temperature was set at 30°C and 2  $\mu\text{L}$  of extracted plasma was injected. The autosampler temperature was set to 10°C. The needle rinse consisted of ACN containing 1% DMSO. DTG and DTG-d4 eluted at 1.80 and 1.79 minutes, respectively. For tissue sample analysis, DTG was chromatographically separated using a gradient elution profile with the same mobile phases used for the isocratic method at a flow rate of 0.4 mL/min. The gradient started at 55% mobile phase B and increased to 100% mobile phase B over 3 minutes, held at 100 % mobile phase B until 4 minutes and reduced to 55% mobile phase B until 4.50 minutes. The system was re-equilibrated at 55% mobile phase B for a total run time of 7.50 minutes. The column temperature was set at 30°C and 5  $\mu\text{L}$  of extracted adipose, muscle and liver sample were injected onto the column. For brain sample analysis, 2  $\mu\text{L}$  was injected. The autosampler temperature was set at 10°C. The needle rinse was ACN with 1% DMSO with a rinse dip time of 10 seconds. During the gradient analysis of adipose, muscle and liver, DTG and DTG-d4 eluted at 1.98 and 1.97 minutes, respectively. During brain samples analysis, DTG and DTG-d4 eluted at 2.02 and 2.01 minutes, respectively.

### *3.2.2.4 Mass spectrometry conditions*

Acquisition was set in positive electrospray ionisation mode and the following transitions for protonated products  $[\text{M}+\text{H}]^+$  were monitored:  $m/z$  DTG, 419.95  $\rightarrow$  277.05;  $m/z$  DTG-d4, 423.95  $\rightarrow$  279.00. Argon was the collision-induced dissociation gas, delivered at 230 kPa. The electrospray ionization parameters are as follows; nebulizing gas flow (3 L/min), desolvation line temperature (250°C), heating block temperature (400°C), interface voltage was 4.50 kV and drying gas flow (15 L/min).

### *3.2.2.5 Preparation of calibrators, quality controls and internal standards*

Stock solutions (SS) of DTG were prepared at 2 mg/mL in ACN. DTG-d4 internal standard SS were prepared in MeOH at 1 mg/mL. All SS were stored at -80°C. Working stocks (WS) for spiking calibration standards and quality control (QC) samples were prepared by serially diluting SS of DTG with 100% ACN. All WS were stored at -80°C. Standards and QCs were prepared on the day of extraction from frozen WS aliquots. Blank (analyte free) matrix - plasma, brain-, adipose-, muscle- and liver tissue - were collected from wistar rats not being treated with DTG. The respective organs were homogenized on the day of extraction and pooled for use in standard and QC preparations. On the day of analysis, calibration curves and QCs were prepared by spiking pooled blank matrix with working stocks not exceeding 5% (v/v) of the total volume. The plasma calibration concentrations ranged from 17.5 – 8000 ng/mL, the adipose, muscle and liver concentrations ranged from 3.05 – 3336 ng/mL and the brain calibration curved ranged from 42.1 – 3336 ng/mL. The plasma QC samples were prepared at 6400 ng/mL (QC H), 3200 ng/mL (QC M) and 50 ng/mL (QC L). The adipose, muscle and liver QC samples were prepared at 2669 ng/mL (QC H), 1345 ng/mL (QC M) and 9.00 ng/mL (QC L). The brain QC samples were prepared at 2669 ng/mL (QC H), 1345 ng/mL (QC M) 60 ng/mL (QC L). The lowest limit of quantification (LLOQ) QCs for adipose, muscle and liver were prepared at 3.05 ng/mL and for the brain at 42.1 ng/mL.

### *3.2.2.6. Sample pre-treatment*

Plasma samples were thawed on ice. A volume of 190 µL drug-free plasma was spiked with WS to generate calibration standards and QCs. For the protein precipitation, 200 µL cold ACN containing DTG-d4 at 62.5 ng/mL was added to 50 µL plasma calibration standard, QC or test sample. The samples were vortexed for 2 minutes, followed by centrifugation for 10 minutes at room temperature at 16 000 x g. The supernatant was removed and centrifuged again for 10 minutes at room temperature at 16 000 x g. The resulting supernatant was transferred to a 96-well plate and 2 µL was injected for analysis.

Brain, adipose, muscle and liver tissue were removed from -80°C, weighed, mixed 1:5 (w/v) with ACN:H<sub>2</sub>O (70:30, v/v) containing 0.2% formic acid and homogenized with a

tissue homogenizer (4 cycles, 6.95 m/s, 15 second interval with 1 minute dwell time between each cycle, Bead Ruptor Elite, OMNI International, Georgia, USA). A volume of 190  $\mu\text{L}$  tissue homogenate was individually spiked with 10  $\mu\text{L}$  working stocks for calibration standard and QC preparation. Following spiking, 700  $\mu\text{L}$  cold ACN containing 32 ng/mL DTG-d4 was added to the 200  $\mu\text{L}$  calibration standard, QC and test sample. The samples were vortexed for 2 minutes, followed by centrifugation for 10 minutes at room temperature at 16 000  $\times g$ . Thereafter, the samples were eluted through Oasis PRiME HLB sorbent wt. 60 mg 3cc cartridges (Waters™ Massachusetts, USA). The cartridges were conditioned with 1 mL ACN prior to sample loading. A volume of 700  $\mu\text{L}$  sample was loaded onto the cartridges followed by elution twice with 500  $\mu\text{L}$  MeOH containing 0.1% formic acid. The eluent was evaporated to dryness under a stream of nitrogen at 35°C and reconstituted in 350  $\mu\text{L}$  ACN. The samples were transferred to 96 well plates and 5  $\mu\text{L}$  of the adipose, muscle and liver samples was injected for analysis while 2  $\mu\text{L}$  of the brain sample was injected.

### 3.2.3 Method parameters

Considering the study was pre-clinical the methods developed did not have to be validated according to the FDA Bioanalytical Method Validation criteria. However, the criteria was used as a guidance during the method development process (Food and Drug Administration, 2022).

#### 3.2.3.1 Selectivity

Selectivity was determined by analysing three sets of blank extracted tissues (adipose, brain, muscle and liver) and plasma from untreated wistar rats. The peak area detected at the retention time of DTG in the blank samples were compared against the LLOQ (9.00 ng/mL for adipose, muscle and liver tissue, 17.5 ng/mL for plasma and 42.0 ng/mL for brain). Any observed peaks in the extracted blank sample should be less than 20% of the LLOQ.

#### 3.2.3.2 Accuracy, precision, linearity and lowest limit of quantification

Each analytical batch included calibration standards in duplicate, a blank sample (blank matrix with internal standard) and one double blank sample (only blank matrix). QCs in duplicate were included to verify the curves. Calibration curves were generated

by plotting the analyte to internal standard peak area ratio to concentration. The calibration standards were used to construct a calibration curve using a quadratic  $1/C$  or  $1/C^2$  (specified in Table 3.1 for each matrix), where  $C$  = concentration, weighed regression. The LLOQ was defined as the lowest quantified concentration at a signal-to-noise (S/N) ratio greater than 5 with an accuracy between 80 and 120%.

#### *3.2.3.3 Carryover*

Percentage carryover was determined by injecting the upper limit of quantification (ULQ) followed by two blank samples of the respective matrix. The % carryover in each blank was calculated and expressed in relation to the LLOQ. It is recommended that carryover may not exceed 20% of the LLOQ.

#### *3.2.3.4 Recovery and matrix effects*

Due to limited blank rat matrix, matrix effects and recovery were determined in each matrix in triplicate. Extraction recovery of DTG was evaluated in triplicate at low, medium, and high QC concentrations by comparing extracted analyte response (spiked pre-extraction) to analyte responses spiked into blank extracted matrix (spiked post-extraction) which is considered 100% recovery. Matrix effects for DTG were evaluated by comparison of slopes of QCs prepared in triplicate in pooled matrix for each analyte as described by (Matuszewski, 2006). The %CV of standard line slopes prepared in three different lots of matrices must be  $< 5\%$  for the method to be considered free of relative matrix effects.

#### *3.2.3.5 Application to wistar rat samples*

The method was successfully used to quantify DTG in wistar rat plasma, adipose, brain, muscle and liver following a 12-week once daily 1 mg chronic DTG treatment.

### **3.3. Results and discussion**

#### **3.3.1 Chromatography method development**

During the initial phases of method development, two different columns were evaluated for suitable chromatographic separation, including a Shimadzu Shim-pack C18 (2.1 x 100 mm, 3  $\mu$ m) and an Agilent Poroshell 120 EC-C18 (3.0 x 100 mm, 2.7

$\mu\text{m}$ ). The Agilent Poroshell 120 EC-C18 (3.0 x 100 mm, 2.7  $\mu\text{m}$ ) resulted in the best symmetrical peak shape with a satisfactory retention time.

### 3.3.2 Extraction method development

Originally, a SPE method utilising Waters Sep-Pak Vac 3cc C18 cartridges was developed according to the method previously described by Prathipati *et al.* (2016). However, this adapted method using C18 cartridges resulted in accuracy and precision values that fell outside of acceptable criteria of 85-115%. A protein precipitation using cold ACN was evaluated and resulted in acceptable recovery of DTG from plasma. However, this protein precipitation method did not yield a satisfactory recovery of DTG from muscle, brain or liver. As a result, Oasis PRiME HLB sorbent wt. 60 mg 3cc cartridges (Waters™ Massachusetts, USA) were used to further improve the quality of the samples and reduce possible matrix effects before analysis.

### 3.3.3 Method development criteria evaluated

#### 3.3.3.1 Selectivity

Blank plasma, brain, adipose, muscle and liver demonstrated suitable selectivity and minimal background interference with < 4% of the signal response of the LLOQ at the retention time of 2 minutes. Chromatograms of blank extracted matrix in comparison to the LLOQ in the respective matrices are presented in Figure 3.1.

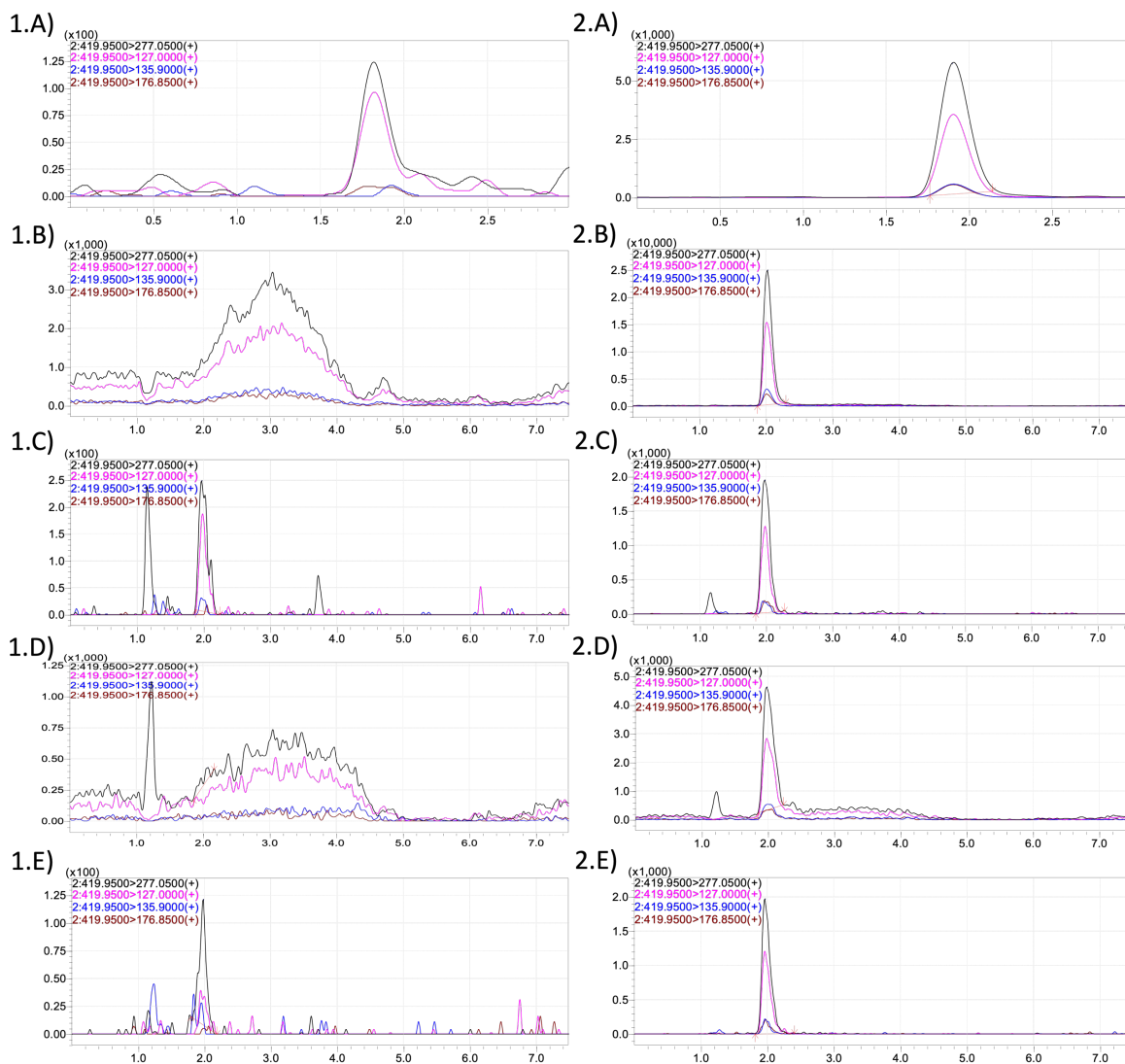


Figure 3.1: Chromatograms of (1) blank extracted and (2) the signal response of the LLOQ in (A) plasma, (B) brain, (C) adipose, (D) muscle and (E) liver. Intensity (cps) is reported on the y-axis and retention time (min) on the x-axis.

### 3.3.3.2 Accuracy, precision, linearity, and lowest limit of quantification

Calibration standards and QCs were prepared in the respective matrices. Initially, QC samples in liver were analysed against calibrators prepared in muscle homogenate. QCs prepared in liver at high and medium concentrations validated the curve with acceptable accuracies between 85 – 115%. However, the QCs prepared in liver at the low concentration fell outside of acceptable criteria. For this reason, both calibrators and QCs were prepared in liver homogenate thereafter. The calibration range, curve regression, weighting and correlation coefficient ( $r$ ) of all five matrices evaluated are presented in Table 3.1. Inter-run accuracy and precision values of the assay

calibrators and QCs fell within the acceptance criteria for all matrices evaluated and are shown in Tables 3.2 – Table 3.6.

Table 3.1: Calibration range, regression, weighting and correlation coefficient of each matrix evaluated.

Matrix	Range (ng/mL)	Regression	Weighting	r
Plasma	17.5 - 8000	Quadratic	1/C <sup>2</sup>	0.999
Brain	42.1 - 3666	Quadratic	1/C <sup>2</sup>	0.999
Adipose	3.05 - 3666	Quadratic	1/C <sup>2</sup>	0.998
Muscle	3.05 - 3666	Quadratic	1/C <sup>2</sup>	0.998
Liver	3.05 - 3666	Quadratic	1/C <sup>2</sup>	0.998

Table 3.2: Inter-run accuracy and precision of DTG standards and QCs in plasma.

Nominal conc (ng/mL)	Standard inter-assay statistics								QC inter-assay statistics		
	8000	3666	1391	580	242	101	42.1	17.5	6400	3200	50.1
Mean	8228	3375	1424	596	234	105	42.0	17.5	6524	3232	50.9
SD	248	141.2	27.4	11.4	8.58	5.22	0.895	1.04	264	33.8	2.25
%CV	3.0	4.2	1.9	1.9	3.7	5.0	2.1	5.9	4.1	1.0	4.4
% Accuracy	102.8	92.1	102.4	102.8	96.8	103.8	99.8	99.6	101.9	101.0	101.8
n	4	4	4	4	4	4	4	4	4	4	4

%CV, percentage coefficient of variation; SD, standard deviation

Table 3.3: Inter-run accuracy and precision of DTG standards and QCs in brain tissue.

		Standards inter-assay statistics					QC inter-assay statistics						
<b>Nominal conc (ng/mL)</b>		3666	1391	580	241	101	42.1			2669	1335	60.0	42.1
<b>Mean</b>		3602	1452	585	235	99.1	42.5			2924	1381	61.1	42.6
<b>SD</b>		95.3	33.2	22.1	5.08	1.05	1.68			149	56.2	1.83	0.474
<b>%CV</b>		2.6	2.3	3.8	2.2	1.1	4.0			5.1	4.1	3.0	1.1
<b>% Accuracy</b>		98.3	104.4	100.8	97.3	98.2	101			109.6	103.5	101.9	101.3
<b>n</b>		4	4	4	4	4	4			4	4	4	2

%CV, percentage coefficient of variation; SD, standard deviation

Table 3.4: Inter-run accuracy and precision of DTG standards and QCs in adipose tissue.

		Standards inter-assay statistics								QC inter-assay statistics				
<b>Nominal conc (ng/mL)</b>		3666	1391	580	242	101	42.1	17.5	7.31	3.05	2669	1335	9.00	3.05
<b>Mean</b>		3533	1489	606	245	98.8	41.5	16.9	6.93	3.14	2761	1374	8.99	3.51
<b>SD</b>		40.1	29.0	11.6	7.66	3.34	1.62	0.389	0.262	0.314	62.4	45.9	0.510	0.110
<b>%CV</b>		1.1	1.9	1.9	3.1	3.4	3.9	2.3	3.8	10.0	2.3	3.3	5.7	3.1
<b>% Accuracy</b>		96.4	107.1	104.5	101.2	97.9	98.7	96.6	94.7	102.9	103.5	103.0	99.9	115.0
<b>n</b>		4	4	4	4	4	4	4	4	4	4	4	4	2

%CV, percentage coefficient of variation; SD, standard deviation

Table 3.5: Inter-run accuracy and precision of DTG standards and QCs in muscle tissue.

Standards inter-assay statistics										QC inter-assay statistics			
<b>Nominal conc (ng/mL)</b>	3666	1391	580	242	101	42.1	17.5	7.31	3.05	2669	1335	9.00	3.05
<b>Mean</b>	3598	1426	609	246	100	40.9	16.4	7.44	3.07	2890	1390	9.12	3.33
<b>SD</b>	112	105	11.9	3.61	2.21	1.44	0.110	0.437	0.295	41.6	37.8	0.513	0.265
<b>%CV</b>	3.1	7.4	1.9	1.5	2.2	3.5	0.7	5.9	9.6	1.4	2.7	5.6	8.0
<b>% Accuracy</b>	98.1	102.5	105.1	101.8	99.3	97.2	93.8	101.9	98.9	108.3	104.1	101.3	109.3
<b>n</b>	4	4	4	4	4	4	4	4	4	4	4	4	2

%CV, percentage coefficient of variation; SD, standard deviation

Table 3.6: Inter-run accuracy and precision of DTG standards and QCs in liver tissue.

Standards inter-assay statistics										QC inter-assay statistics			
<b>Nominal conc (ng/mL)</b>	3666	1391	580	242	101	42.1	17.5	7.31	3.05	2669	1335	9.00	3.05
<b>Mean</b>	3547	1486	594	248	101	41.9	17.1	6.52	3.20	2878	1400	8.95	3.46
<b>SD</b>	77.9	35.5	10.5	3.86	0.962	1.12	0.830	0.151	0.0115	22.6	52.8	0.499	0.100
<b>%CV</b>	2.2	2.4	1.8	1.6	1.0	2.7	4.9	2.3	0.4	0.8	3.8	5.6	2.9
<b>% Accuracy</b>	96.8	106.9	102.3	102.7	100.4	99.4	97.6	89.3	103.4	107.8	104.9	99.4	113.5
<b>n</b>	4	4	4	4	4	4	4	4	3	4	4	4	2

%CV, percentage coefficient of variation; SD, standard deviation

### 3.3.3.3 Carry-over

Following development of the plasma method, significant carry-over was detected when analysing tissue samples while using the same mobile phase composition. A gradient method was developed to aid in reduction of carry-over but did not resolve it. As a result, multiple mobile phases and needle rinse solvent combinations were evaluated to reduce the carry-over. Three combinations of organic solvents were evaluated for mobile phase B 1) 0.1 % formic acid in ACN; 2) 0.1% formic acid in ACN: MeOH (1:1, v/v) and 3) 0.1 % formic acid in MeOH. The original mobile phase combination of 0.1% formic acid in ACN resulted in the least amount of carry-over but it was still present. Different needle rinse solvents were also evaluated, namely MeOH, H<sub>2</sub>O:MeOH (1:1, v/v), H<sub>2</sub>O:MeOH (60:40, v/v), MeOH:ACN (1:1) and ACN with 1% DMSO. A combination of ACN as mobile phase B and ACN with 1% DMSO as the needle rinse significantly reduced the carry-over, but not enough to meet criteria (Food and Drug Administration, 2022). To ensure the carry-over did not affect accuracies and precision of standards, blanks were introduced in-between every sample. Injecting MeOH:ACN (1:1, v/v) between tissue samples improved the carry-over to meet criteria. However, for the brain, injecting organic solvent did not diminish the carry-over. Instead, injecting blank extracted brain matrix between calibrators reduced the carry-over detected. Despite the positive effects of the blank injections, the assay LLOQ was increased from 1.27 ng/mL to 3.05 ng/mL for the adipose, muscle and liver tissue as a result of the low levels of carry-over still present. Due to the brain having the highest carry-over present, the LLOQ was increased from 1.27 ng/mL to 42.1 ng/mL. Following the measures described above, the carry-over was reduced from 76.5% to 18.7% of the LLOQ in the brain, 53.4% to 14.6% of the LLOQ in adipose and 47.2% to 13.2% of the LLOQ in the muscle. The final carry-over in the liver was 5.3% of the LLOQ following the implementation of the measures to reduce carry-over. Chromatograms of the respective blank matrices following an injection of the ULQ are presented in Figure 3.2. The most significant carry-over was associated with brain tissue, as indicated by the predominant peak detected at 2 minutes in chromatogram 2.B.

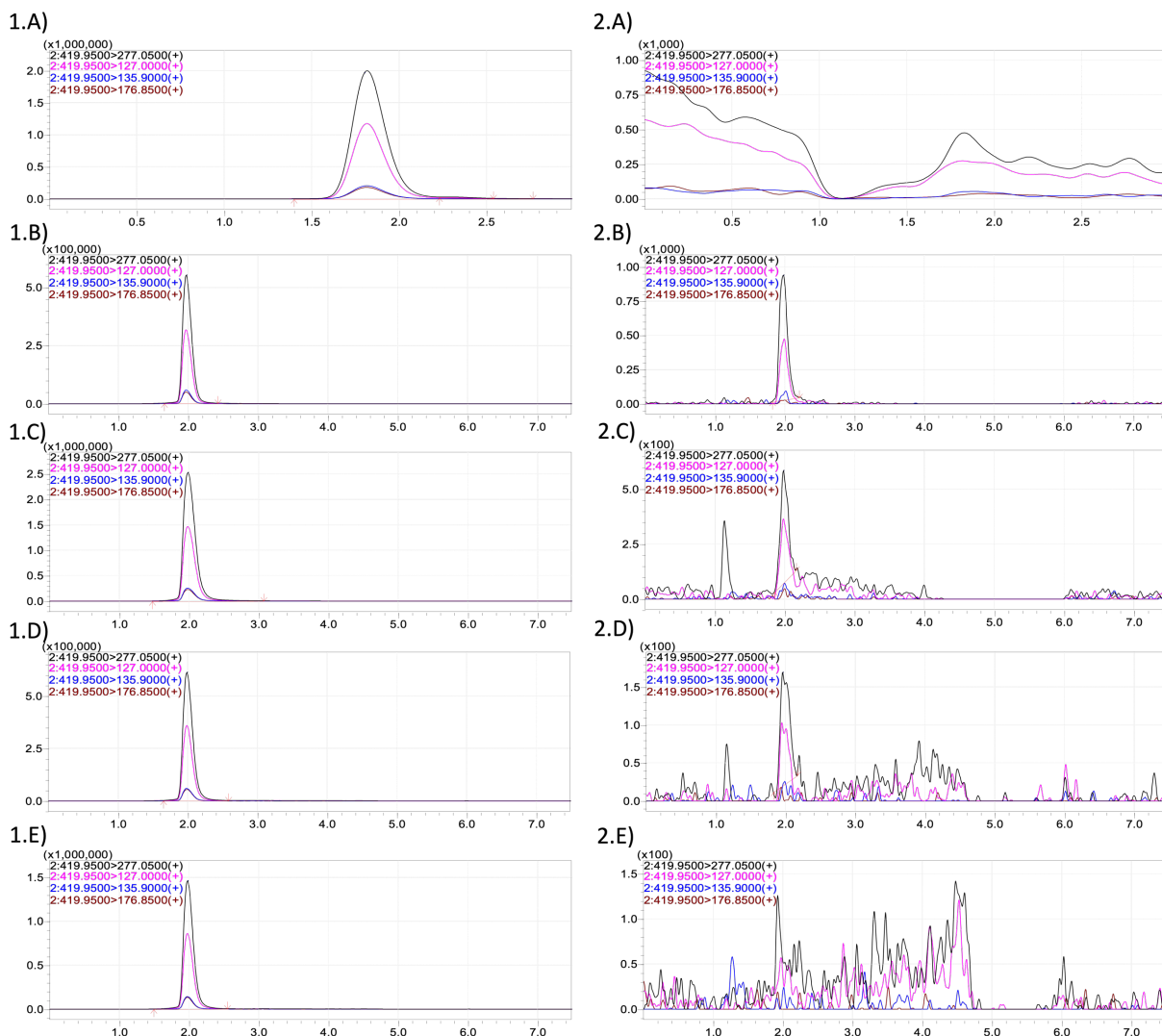


Figure 3.2: Representative chromatograms of the upper limit of quantification (1) in (A) plasma, (B) brain, (C) adipose (D) muscle and (E) liver. Representative chromatograms of a blank sample following the injection of the upper limit of quantification (2) in the respective matrices. Intensity (cps) is reported on the y-axis and retention time (min) on the x-axis.

### 3.3.3.4 Recovery and matrix effects

Initially tissue samples were extracted without the use of Oasis PRiME HLB sorbent wt. 60 mg 3cc cartridges (Waters™ Massachusetts, USA). The average recovery of DTG from brain, muscle and liver was 55.5%, 51.6% and 70.6% respectively. Following matrix effects evaluations, ion enhancement was observed at the lower concentrations in all tissue matrices investigated. After incorporation of the HLB cartridges, recoveries in the brain and adipose tissue increased but decreased in the

liver. However, the matrix effect observed in the liver was substantially reduced. The final average recovery and matrix effects observed are presented in Table 3.7.

*Table 3.7: Average recovery and matrix effects of DTG in different biological matrices.*

<b>Matrix</b>	<b>Average recovery (n=9)</b>	<b>Average recovery %CV</b>	<b>Matrix effects %CV of standard line slopes</b>
<b>Plasma</b>	91.3	7.3	0.7
<b>Brain</b>	82.5	7.3	0.5
<b>Adipose</b>	80.9	3.3	1.1
<b>Muscle</b>	76.3	9.8	1.7
<b>Liver</b>	50.6	13.0	0.4

%CV, percentage coefficient of variation

### *3.3.3.5 Application to Wistar rat samples*

The developed methods were successfully used to quantify DTG in wistar rat samples collected following a 12-week DTG treatment intervention. The DTG concentrations detected in wistar rat plasma ranged from 407 - 2143 ng/mL. The concentrations detected were similar to those detected in human patients following a 12-week drug exposure (Weidlich et al., 2020). DTG concentrations ranged between 3.60 - 12.4 ng/mL, 3.40 - 20.1 ng/mL and 6.29 - 22.4 ng/mL in adipose, muscle and liver homogenate respectively. The tissue DTG concentration obtained during LC-MS/MS analysis (ng/mL) were normalised by tissue weight in g per mL homogenising solvent (Ocque et al., 2017). Therefore, the ranges detected were between 18.0 – 62.0 ng/g, 17.0 – 100.5 ng/g and 31.5 – 112 ng/g for adipose, muscle and liver tissue respectively. Although no DTG was not detected in the brain, we acknowledge that the range developed may not have been sufficiently sensitive to detect the low concentrations of DTG expected in the brain – a limitation to the method.

### *3.3.3.6 Method innovation*

As discussed in the introduction, several LC-MS/MS methods are available for quantification of DTG from plasma. However, we found only one detailed report describing method development for extracting and quantifying DTG from tissue matrices as part of a multi-analyte method from murine biological matrices (Prathipati

et al., 2016). These authors reported the quantification of DTG in murine tissue but did not use matrix matched standards and QCs. Our current study investigated this possibility however, QC samples prepared in liver did not validate the standards prepared in muscle. It was therefore decided to matrix match all standards and QCs for each tissue investigated. Likely in part due to the multi-analyte approach by (Prathipati et al., 2016), recovery of DTG from murine plasma and tissues such as liver, kidney, spleen and brain was fairly low, ranging between 40.7 – 41.9%. In our current study, we were able to optimise protocols to achieve improved recoveries of 91.3%, 82.5%, 80.9%, 76.3% and 50.6% in plasma, brain, adipose, muscle and liver respectively. Despite these authors including DTG in the extraction method development, there was no application of the DTG method to pre-clinical samples, therefore they could not determine the suitability of their method to tissue samples (Prathipati et al., 2016). In comparison our current study aimed to expand on the knowledge available to evaluate the applicability of a developed extraction and LC-MS/MS method to pre-clinical wistar rat samples following DTG administration. Given we developed methods to quantify tissue and plasma DTG concentrations, it allows for the investigation of the relationship between different compartments.

### 3.4. Conclusions

A sensitive and robust LC-MS/MS method has been developed for the accurate quantification of DTG in rat plasma and tissues at physiologically relevant concentrations. Although recovery of DTG from brain tissue improved on than that reported in other published methods, the protocol is not yet sufficiently sensitive to detect physiological concentrations of DTG in rodent brain tissue. The method described is time efficient, robust, and accurate, with consistent recoveries. In addition, this chapter also describes the increased carry-over observed from tissue in comparison to plasma and describes solutions for overcoming this problem. Furthermore, I also provide evidence for the importance of matrix-matched calibration standards and QCs, which has been a limitation to previous methods describing DTG quantitation in tissue. The DTG concentrations detected in plasma and tissues fell within the concentration ranges developed, 17.5 – 8000 ng/mL in plasma and 15.3 – 18330 ng/g in tissues. Finally, these developed methods can aid in the determination

of tissue penetration, drug accumulation and potential tissue vulnerability in biological matrices following DTG exposure. This concept will be explored further in chapter 4.

## Chapter 4: Dolutegravir distribution in plasma and tissue compartments after chronic administration to wistar rats

### 4.1 Introduction

DTG, which is commonly administered as a compounded drug – together with tenofovir and lamivudine (World Health Organization, 2022) – was originally reported to result in fewer adverse effects. However, more recently, its adverse effect risk profile seems to have changed for the worse (Povar-Echeverría et al., 2021). Several side effects – most with an inflammatory character – have been reported for DTG-containing ART regimens, especially in female patients. The tissues that seem to be affected with highest prevalence are the gastrointestinal tract and the brain (Couturier and Lewis, 2018; Elzi et al., 2017; Hoffmann and Llibre, 2019). However, since DTG is not administered as monotherapy, it is difficult to assign its relative contribution to these side-effects without assessing its effects in isolation. Given the relatively inability of low- to middle-income countries (LMIC) to carry the additional cost of management of chronic side-effects, research in this context is a priority. We hypothesised that plasma and tissue distribution of DTG may provide insight into potential sex- or tissue-specific risk for adverse outcome in patients.

For an ART drug to be effective, it should be able to reach its target without causing adverse effects. Plasma vs tissue levels of DTG may indicate the ability of the ART to penetrate HIV tissue reservoirs and thus prevent the continuous replication of the virus. A complete picture can only be gained from assessment of various biological matrices for penetration of ART into these potential viral reservoirs, which includes the gut, adipose and the brain (Cory et al., 2013).

In terms of risk profile, the distribution or potential accumulation profile of DTG at multiple tissue sites could provide information on tissues most at risk for side effects in the longer term. Integrase strand inhibitors have been linked to higher risk for immune reconstitution inflammatory syndrome (Wijting et al., 2019). In addition, DTG in particular has been linked to increased pro-inflammatory signalling by pre-adipocytes (Domingo et al., 2022) as well as activation of neutrophils (Theron et al.,

2022) Importantly, these interactions were observed at non-cytotoxic concentrations attainable within a therapeutic setting by using a 50 mg DTG dose (Theron et al., 2022). This unfortunately increases the risk of adverse and/or chronic complications, should DTG accumulate in tissue. Given these facts, as well as the known high-risk profile of most other ART in terms of co-morbidity and longer-term chronic disease risk, it is a priority to elucidate the exact nature of DTG distribution and its potential differential accumulation in tissue compartments.

The methods developed and described in chapter 3 were used to quantify DTG in different rat matrices to determine distribution and potential sex- or tissue-specific relative accumulation of DTG following a 12-week DTG administration.

## 4.2 Methods and materials

### 4.2.1 Ethical consideration

All animal experiments were conducted according to the guidelines and ethical standards set out by the South African National Standard (SANS: 10386:2008) for the care and use of animals for scientific purposes 10386:2008 and the Research Ethics Committee: Animal Care and Use (REC: ACU) of Stellenbosch University (ref: ACU-2021-22035).

Wistar rats were obtained from and housed in the Stellenbosch University Animal Facility under normal husbandry conditions. Briefly, a 12-hour light-dark cycle (lights on at 7am) applied and animals were housed in groups of 4 in standard rat cages, in a temperature and humidity-controlled room ( $23 \pm 1^\circ\text{C}$ , 40 – 60 % humidity). Autoclaved water and standard rat chow were provided *ab libitum*. Nesting materials and housing tubes were supplied for enrichment. Starting at seven weeks old, the 12 female and 12 male rats (average body mass  $185 \pm 26.6$  g) were matched according to body mass and divided into four groups; a female control group (who received placebo jelly cubes), a female intervention group (who received DTG infused jelly cubes), a male control group (who received placebo jelly cubes) and a male intervention group (who received DTG infused jelly cubes). Rats were allowed to acclimatise to cage grouping, handling and experimental procedures for one week before initiation of the DTG intervention.

#### 4.2.2 Dolutegravir formulation and purity analysis

The DTG used for the intervention study was extracted from (50 mg) Olegra<sup>®</sup> dolutegravir sodium tablets (Aurobindo Pharma, South Africa). A simple liquid-liquid extraction protocol was used for the extraction. Briefly, two tablets were crushed and ground to a fine powder with a glass mortar and pestle and transferred to a 50 mL centrifuge tube. 10 mL ultrapure water (Synergy, Merck) was added to the tablets, the mixture vortexed for 2 minutes and sonicated for 10 minutes. A volume of 30 mL ethyl acetate (ROMIL Ltd., Cambridge, UK) was added to the mixture and vortexed for 2 minutes, followed by 10 minutes of sonication. The mixture was centrifuged at 2000 x g for 10 minutes before the supernatant was transferred to pre-weighed borosilicate glass tubes and evaporated to dryness under vacuum utilising the Genevac miVac Duo Sample Concentrator at 30°C. The extracted DTG powder residue remaining in the borosilicate glass tubes was weighed, transferred to glass vials, and stored at 4°C in a desiccator until use.

The purity of the extracted DTG was determined by high pressure liquid chromatography (HPLC) analysis. A 10 µg/mL stock solution in acetonitrile (ACN) (ROMIL Ltd., Cambridge, UK) was prepared using the extracted DTG. The analysis was performed on an Agilent Technologies 1100 Series system (California, US) consisting of Agilent 1260 Infinity binary pumps coupled to an Agilent Series 1100 autosampler, column compartment and variable wavelength detector. UV detection was set at 256 nm and a Venusil C18 column (4.6 x 150 mm, 5µm particle size) column was used for separation. Mobile phase A was ultrapure water (Synergy, Merck) containing 0.1% formic acid (Fischer Chemicals, New Hampshire, USA) and mobile phase B consisted of ACN containing 0.1% formic acid at a flow rate of 0.5 mL/min. The run was performed in isocratic mode (65% mobile phase B over 7 minutes) with DTG eluting at 4.85 minutes. Data acquisition and analysis was performed using OpenLab CDS Chemstation edition.

#### 4.2.3 Administration of dolutegravir

A human equivalent dose (HED) for rats was calculated based on average body mass and average body surface area (BSA) according to previous methods (Nair and Jacob, 2016; Reagan-Shaw et al., 2008) with some adaptations to the formula:

$$HED (mg / kg) = Animal\ dose (mg / kg) \times \frac{Animal\ K_m}{Human\ K_m}$$

The  $K_m$  factor is determined by dividing the body mass (kg) by BSA ( $m^2$ ). The equation was adapted by adjusting the average human body mass from 60 kg to 70 kg (U.S Department of Health and Human Services et al., 2019) and the average human BSA from 1.60  $m^2$  to 1.73  $m^2$  (Pai, 2012). In addition, the average rat mass was adjusted to the average body mass of 5 month-old wistar rats (0.219 kg) and average BSA of 0.036  $m^2$  (Gouma et al., 2012). Using the respective mass and BSA a HED dose of 4.7 mg/kg was determined. The intervention groups were therefore administered 1 mg daily (instead of dose continuously adjusted for body mass) to more closely mimic the standard practise of administration of a 50 mg daily DTG dose in human patients weighing more than 35 kg (Republic of South Africa National Department of Health, 2020). The final dose of DTG was administered 24 hours prior to killing and endpoint sample collection.

Chronic DTG administration was achieved by daily jelly cube administration for a period of 12 weeks, starting at the age of 8 weeks. Jelly cubes were prepared daily by mixing 810 mg unflavoured gelatine with 16 g of Moir's raspberry jelly powder in 30 mL boiling water. Once the jelly mixture was dissolved it was transferred to a 1  $cm^3$  silicon mould. The placebo blocks were prepared by using drug-free jelly. The intervention blocks were prepared by aliquoting 400  $\mu$ L jelly into the mould, followed by the 1 mg extracted DTG and then another 400  $\mu$ L jelly to ensure the DTG was covered entirely. The jelly cubes were left to set at 4°C for at least two hours. One entire jelly block was hand fed directly to each rat to ensure that the full dose was consumed. The animals were accustomed to placebo jelly blocks for one week before intervention initiation and consumed all jelly blocks (without wasting) within a period of approximately 1 minute.

#### 4.2.4 Tissue collection and preparation

General wellness was assessed daily, and body mass biweekly. One week prior to experimental endpoint, blood glucose was measured by tail-vein needle prick and a

Contour® Plus Blood Glucose Monitoring System (Bayer, Germany). At the end of the 12-week intervention, rats were killed by intraperitoneal injection of sodium pentobarbital overdose (200 mg/kg). Aortic puncture was executed and blood anticoagulated in EDTA Vacutainer® (BD-Plymouth, UK) tubes. EDTA whole blood was centrifuged at 21°C for 10 minutes at 1 000 x g and subsequently the plasma layer aliquoted and frozen at - 20°C until analysis.

The left hemisphere of the brain, the left retroperitoneal adipose depot, the tip of the left lateral lobe of the liver, and the left gastrocnemius muscle were excised and immediately snap frozen in liquid nitrogen. The tissue samples were then stored at - 80°C until analysis.

#### 4.2.5 Dolutegravir quantification

The DTG concentration in the various tissues and plasma was detected using the LC-MS/MS method described in chapter 3.

#### 4.2.6 Adipose tissue histology and image acquisition

The right retroperitoneal adipose depot was excised, coated in tissue freezing media and snap frozen in liquid nitrogen. Prior to imaging the adipose tissue was removed from the tissue freezing media and thawed for one day in 4% buffered paraformaldehyde. This facilitated fixing of the tissue before processing. The adipose tissue was processed and wax impregnated using an automated tissue processor (Leica HistoCore Pearl, Leica Biosystems Nussloch GmbH, Germany), before being embedded in paraffin wax (Leica HistoCore Arcadia H, Leica Biosystems Nussloch GmbH, Germany). Subsequently, the tissue was sectioned at 5 µm on a rotary microtome (Leica RM2125 RTS). Adipose tissue sections were deparaffinized in xylene and rehydrated in decreasing ethanol concentrations before being stained using haemoloxylin and eosin (H&E). Finally, slides were mounted in mounting media (DPX, 06522, Sigma- Aldrich, USA) and fitted with coverslips for viewing. All histological slides were viewed using an inverted microscope (Nikon eclipse Ti2, Japan) mounted with a camera (LWD 0.52 Nikon, Japan). Image processing was done on Nikon Instrument Software (NIS- Elements D 5.30.02 64-bit) on a desktop computer (Dell, USA) running Windows 7 (Microsoft, USA). Three representative images of each

section were captured at 10x magnification with an additional 10x magnification on the eye piece (resulting in a x100 magnification).

Following images acquisition, the images were analysed using Image J software (version 1.49). The 100  $\mu\text{m}^2$  scale bar was measured using the straight-line tool and the measurement was imported to the “set-scale function” allowing cell area to be recorded in  $\mu\text{m}$ . The border of 50 adipocytes (50 cells is a representative of the population) was traced using the polygon selection tool to measure and record cell area of each of the three representative images.

This section of the data was acquired and analysed by another MSc student in the research group who work on the same wistar rat model. This data was included in the current chapter as the data had interpretive value which supported the observations from my data.

#### 4.2.7 Statistical analysis

Data was obtained from instrument software (LabSolutions version 5.109) and analysed using Microsoft excel version 16.54 and GraphPad Prism 9.4.1 software. Data is presented as the mean  $\pm$  the standard deviation (SD). Outliers were determined using ROUT (Q=1%). Distribution of data was assessed using Shapiro-Wilk normality test. Statistical analyses of end-point measurements included 2-way ANOVA with Tukey’s multiple comparison test. DTG concentration in the plasma and tissues detected between males and females was analysed using an unpaired *t* test. Linear relationships were determined using Pearson’s correlation or Spearman’s correlation (*r*) depending on distribution of data.

### 4.3 Results

Male rats exhibited significantly higher body mass ( $p < 0.0001$ ) than females, irrespective of DTG intervention, at the end of the protocol, with no apparent effect of DTG (Figure 4.1). Fasting blood glucose was similar and within the normal range for fasting blood glucose of wistar rats ( $3.95 \pm 1.31$  mmol/L) (Wang et al., 2010) for all experimental groups (Figure 4.2).

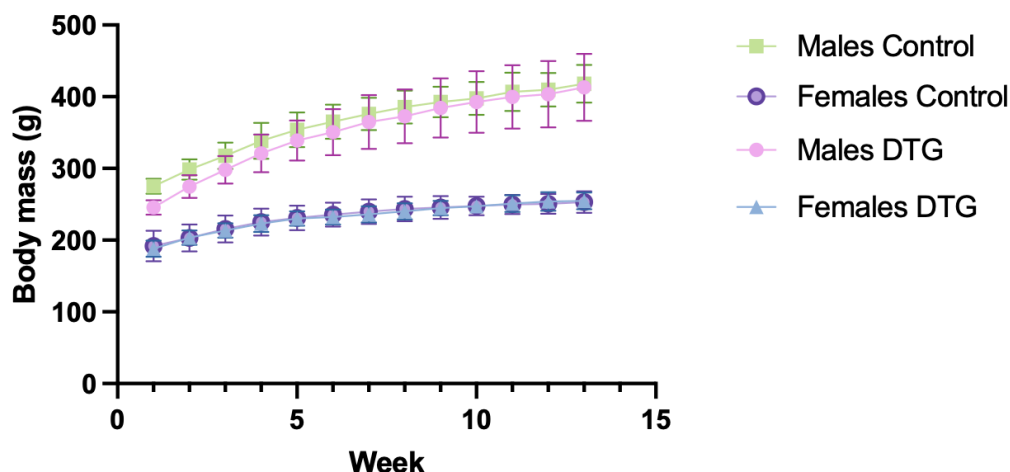


Figure 4.1: Change in body mass of wistar rats over 12-week DTG administration protocol. Data is expressed as mean  $\pm$  SD.  $n=6$  per group. Statistical analysis: 2-way ANOVA with Tukey's multiple comparison test.

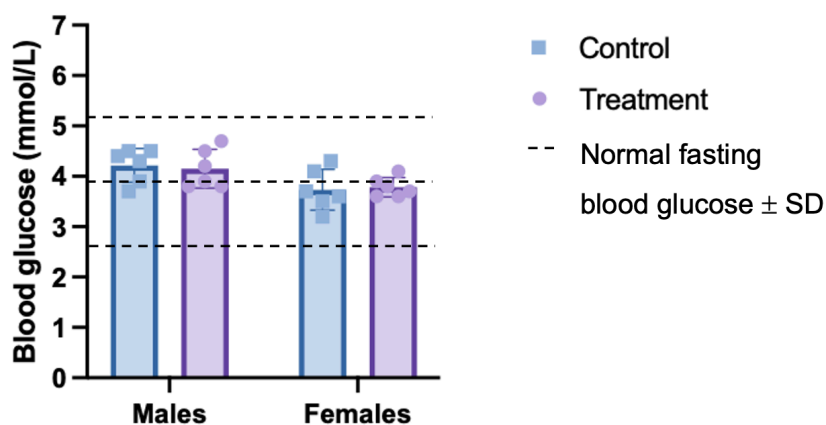


Figure 4.2: Fasting blood glucose (mmol/L) in the control and 12-week DTG administered groups. Data are expressed as mean  $\pm$  SD,  $n=6$  per group. Statistical analysis: 2-way ANOVA with Tukey's multiple comparison test. Dotted lines represents the normal range for fasting blood glucose in rats  $3.95 \pm 1.31$  mmol/L (Wang et al., 2010).

In line with the larger body mass in males, organ masses were also larger in males, but with no significant effect of DTG (Figure 4.3).

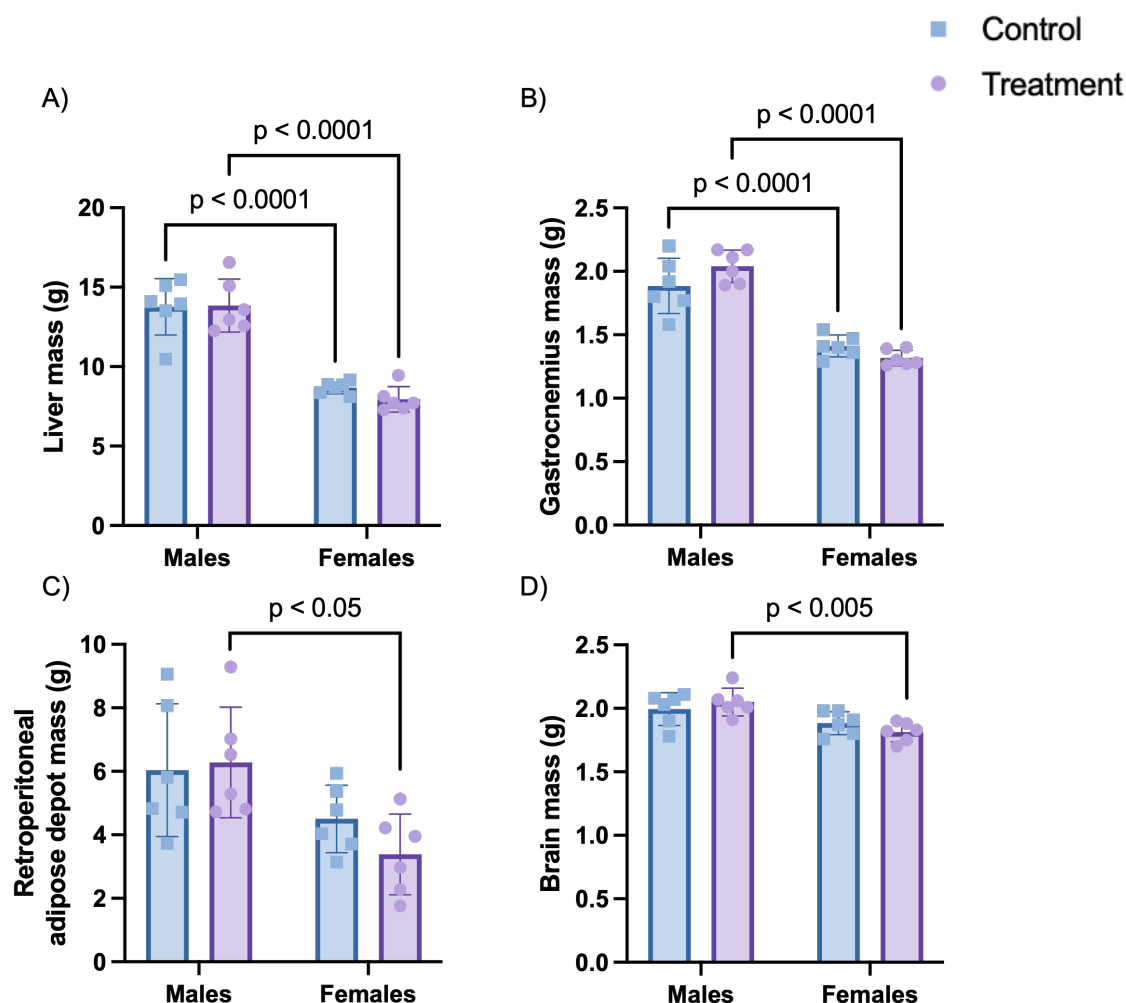


Figure 4.3: Mass of (A) liver, (B) left gastrocnemius muscle, (C) left retroperitoneal adipose depot and (D) brain from males and female wistar rats after 12-week DTG administration. Data are expressed as mean  $\pm$  SD,  $n=6$ . Statistical analysis: 2-way ANOVA with Tukey's multiple comparison test

In terms of DTG distribution, DTG-administered female rats exhibited significantly higher plasma DTG concentration vs males, that was corrected by adjustment for calculated total blood volume (Figure 4.4).

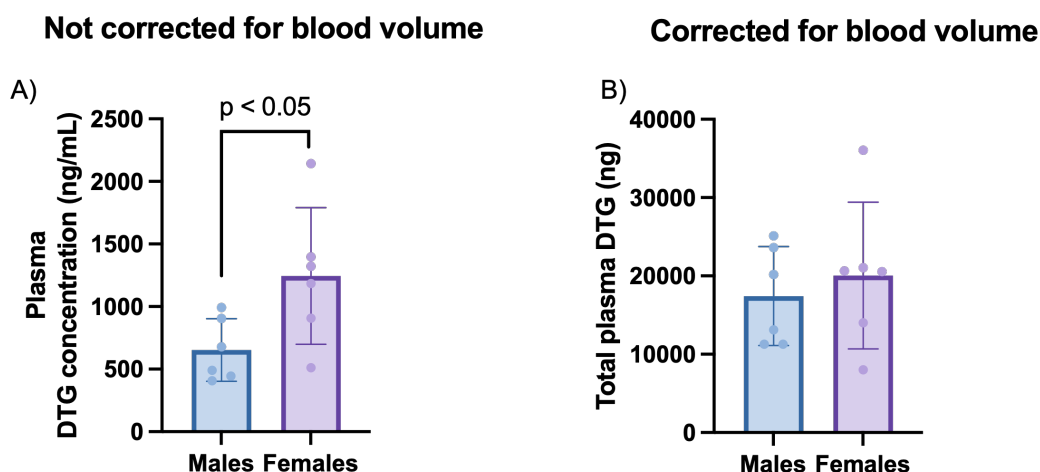


Figure 4.4. Average DTG concentration detected in plasma following a 12-week DTG intervention. (A) Not corrected for blood volume. (B) Corrected for blood volume. Data are expressed as mean  $\pm$  SD,  $n=6$ . Statistical analysis: unpaired  $t$  test.

Turning attention to tissue levels of DTG, the highest concentration of DTG was detected in the liver (Figure 4.5A). Concentrations in adipose and muscle tissue were in a range similar to each other (Figure 4.5 B, C), but approximately 50% lower than those in liver, while no DTG was detected in the brain. In addition, in all tissues with detectable concentrations of DTG, average concentrations were higher in female than male rats, although this difference only reached statistical significance for muscle tissue, where data were less variable. Similar to findings in plasma, correction of tissue DTG concentrations for total organ mass, also abolished this difference (Figure 4.6).

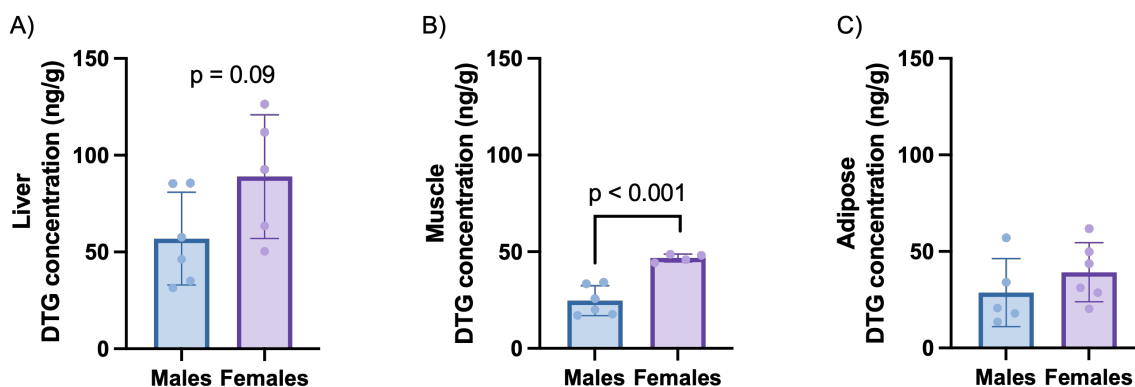


Figure 4.5: DTG concentration detected in (A) tip of left lateral lobe of liver (B) left gastrocnemius muscle and (C) retroperitoneal adipose depot tissue following a 12-week DTG administration. Data are expressed as mean  $\pm$  SD. Statistical analysis: unpaired  $t$  test.

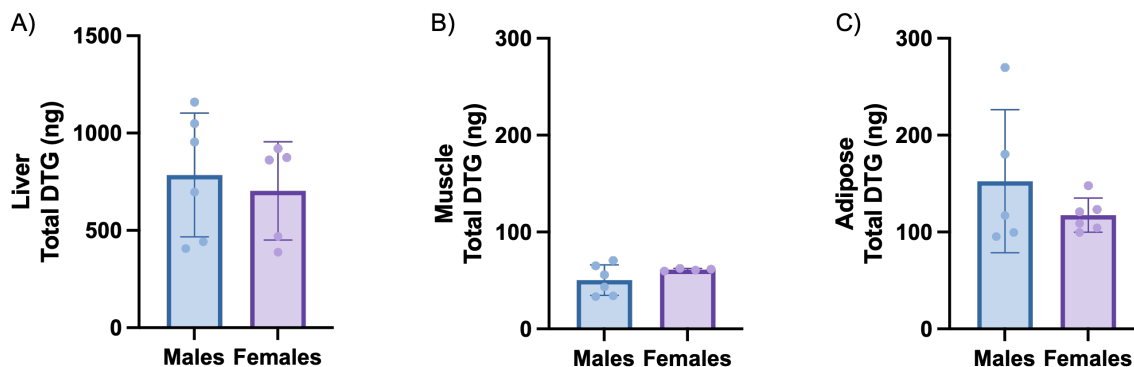


Figure 4.6: Total amount of DTG detected corrected for organ mass in the (A) tip of the left lateral lobe of the liver, (B) left gastrocnemius muscle and (C) retroperitoneal adipose depot of rats following a 12-week DTG intervention size. Data are expressed as mean  $\pm$  SD. Statistical analysis: unpaired *t* test.

Correlation analyses shed further light on the relationship between body/organ mass and DTG levels measured. Given the relatively low statistical power for correlations in a sex-specific manner, we opted not to perform such correlations. However, correlation data is presented in a manner distinguishing between males (indicated in blue on graphs) and females (in purple).

When considering both sex groups together, lower body mass is correlated with higher plasma concentrations of DTG (Figure 4.7). However, qualitative assessment of the sex groups independently of each other on the same graph, suggest that at least in the female group, there is no correlation between body mass and plasma DTG concentration.

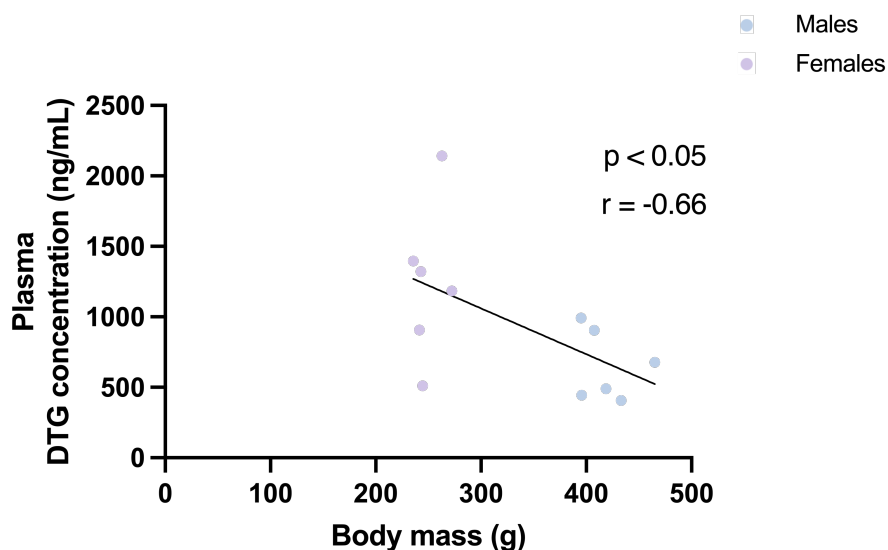


Figure 4.7: The correlation between DTG plasma concentration (ng/mL) and body mass (g) of 20-week-old wistar rats. Statistical analysis: Spearman's correlation.

When considering tissue DTG concentrations however, clear positive correlations existed between plasma DTG vs both liver and muscle, but not adipose DTG levels (Figure 4.8 A, B, C). These data suggest that plasma DTG concentration cannot serve as proxy for events at the level of adipose tissue but may correspond closely to changes in DTG in some other body compartments. Of further interest, in muscle and liver tissue the correlation patterns seem similar for males and females. However, in adipose tissue, while a similar positive correlation as that seen in muscle and liver seems evident in females at least qualitatively, no such correlation pattern was observed in males.

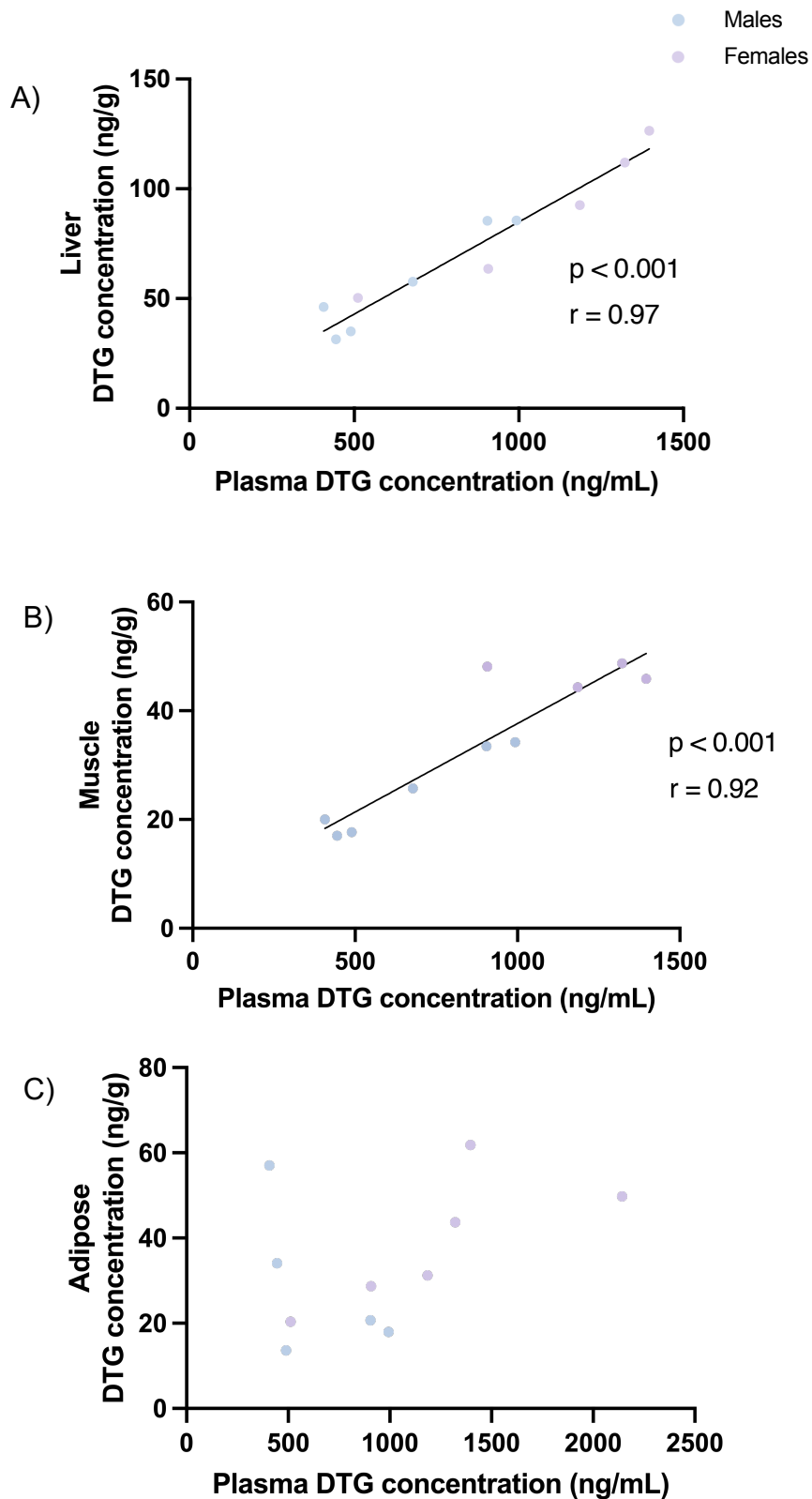


Figure 4.8: Correlation between DTG concentration (ng/g) in the (A) tip of the left lateral lobe of the liver, (B) left gastrocnemius muscle and (C) left retroperitoneal adipose depot vs plasma concentration (ng/mL) following a 12-week DTG intervention in rats. Statistical analysis: Pearson's correlation.

When considering adipocyte surface area, there is a clear positive relationship with adipose depot mass (Figure. 4.9 A). The adipocytes for both males and females in the control group are relatively the same size (Figure 4.9 B). However, in the DTG group females have smaller adipocytes than males. Moreover, looking at the histological differences between the control and DTG groups, the males and females in the control group had greater adipocyte size for the same size depot masses when compared to the DTG group (Figure 4.9 C).

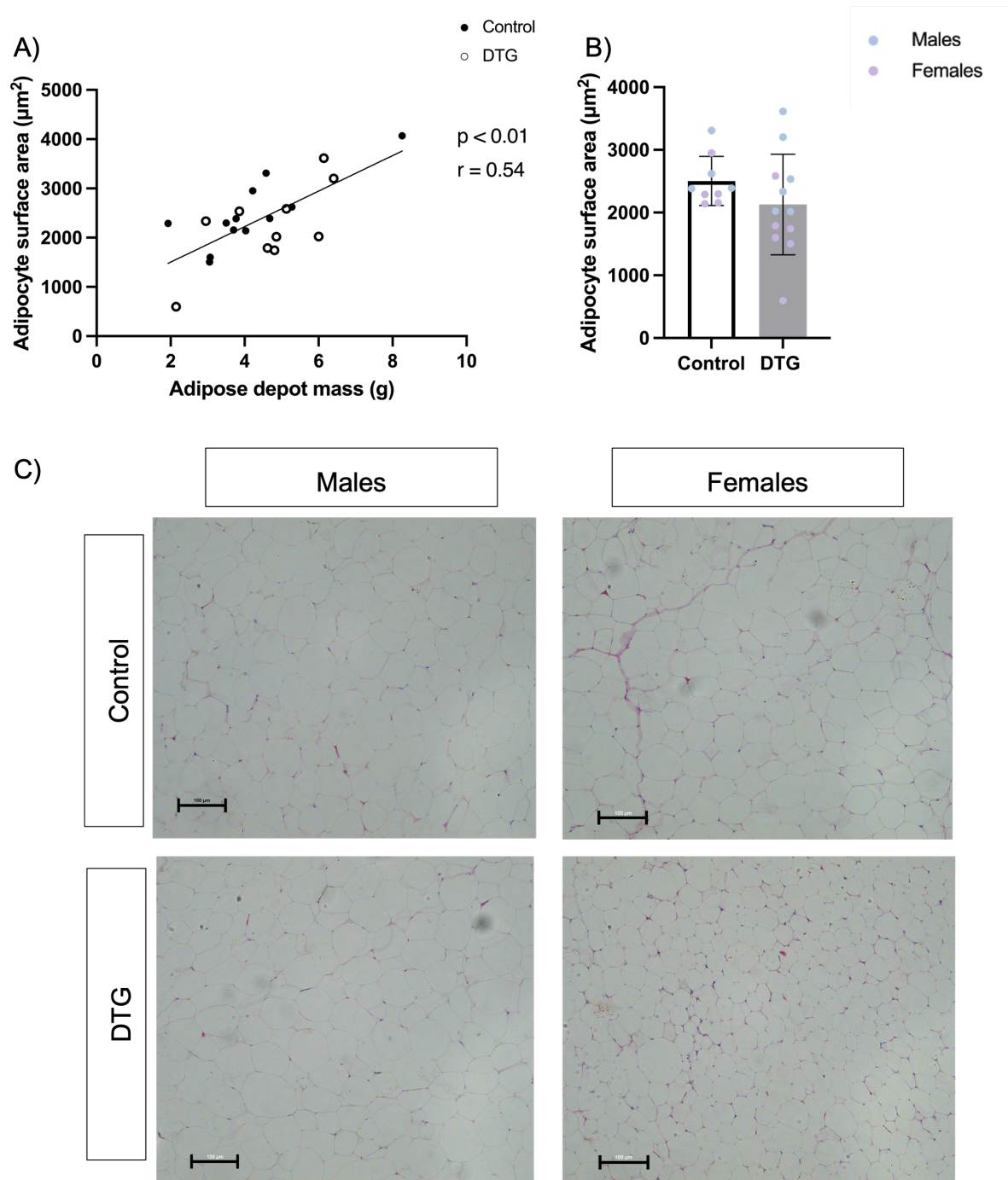


Figure 4.9: (A) Correlation between adipocyte surface area ( $\mu\text{m}^2$ ) and adipose depot mass (g) Statistical analysis: Spearman's correlation. (B) The average surface area ( $\mu\text{m}^2$ ) of 50 adipocytes measured on three representative images for each animal. Statistical analysis: unpaired t test. Data are presented as mean  $\pm$  SD. (C) Representative images of histological sections stained with H&E of males and females in the control and DTG groups.

## 4.4 Discussion

The current study reports plasma and tissue concentrations of DTG after chronic administration in male and female rats. It is important to focus attention on the fact that the plasma DTG concentrations achieved in this study closely corresponded to DTG levels reported in humans (Weidlich et al., 2020). This suggests that an accurate, physiologically relevant dosing strategy was employed in the rodent study, which validates interpretations made from this pre-clinical model.

Analysis of the data presented here elucidated three key findings. Firstly, chronic DTG administration in rodents - following a dosing strategy aligning with current clinical practise – resulted in a significantly higher concentration of DTG in plasma, liver and muscle (but not adipose) of female wistar rats than males, which was negated when corrected for total blood volume or organ mass. Secondly, plasma DTG concentration was closely correlated with DTG concentrations in the liver and muscle tissue of both males and females, but not in adipose tissue. Thirdly, DTG was not detected in brain tissue, suggesting either absence or concentrations below the detection threshold of the method employed.

Current practise in the clinical environment in terms of DTG prescription, is a single dose administered daily to all patients with a body mass equal to or higher than 35 kg (Republic of South Africa National Department of Health, 2020). At first glance, the significantly higher plasma and tissue levels of DTG observed in female rats in the current study seem to suggest a sex difference in DTG pharmacodynamics. However, when the plasma and tissue concentrations were corrected for total blood volume and total organ mass respectively, these differences were abolished, suggesting that body size, rather than sex, may be the major determining factor at play. Indeed, correlation analysis indicated a significant, inverse correlation between plasma DTG and body mass. The fact that male rats weighed significantly more than female rats (approximately 60% more in the current study), achieved a larger effect size than what is likely possible to achieve in human cohorts, demonstrating the benefit of pre-clinical studies in pharmacovigilance research. Furthermore, this model allowed for elucidation of similar trends at tissue level. Thus, although current study design did not allow for calculation of volume of distribution, the consistent trend of higher DTG

in smaller body size may suggest that individuals of smaller stature may be exposed to relatively greater DTG concentrations both in circulation and at tissue level, when administered the same dose as individuals with relatively larger body size, irrespective of sex. This also means that a relative “overdose” in smaller bodies may increase risk of adverse effects.

In support of this notion, women generally have a smaller blood volume than men (Sharma and Sharma, 2022), and currently world data supports the assumption that in general, men weigh more than women and are taller than women in the same population (“WorldData.info,” 2020). This interpretation of current data is in line with a number of more recent studies reporting that women and older individuals (i.e. those with relatively smaller stature) seem to experience higher incidences of side effects and discontinue DTG treatment (Elzi et al., 2017; Hoffmann et al., 2017; Venter et al., 2019). This was seldom reported in initial and/or earlier clinical trials including DTG, but may have gone unnoticed due to the fact that women frequently comprised less than 25% of study participants in earlier studies (Bourgi et al., 2020; Eckard and McComsey, 2020; Taramasso et al., 2020) The fact that weight and BMI are often reported as averages of the study cohort and not by sex, excludes many studies from contributing to wider evaluation of this possibility. Nevertheless, current data suggest that dosing strategy of DTG should be revisited to account for smaller body size.

Interestingly, the statistic on body size differences between males and females is true for all regions across the world, except in Southern Africa , where - although men are still significantly taller than females - average body mass of females generally exceeds that of men (“WorldData.info,” 2020) – this difference can largely be explained by relatively larger subcutaneous adipose stores in these females. The fact that DTG levels in adipose tissue seemed to deviate from other compartments in terms of its relationship to body size in the current study, may have specific significance in this population in particular, although a number of factors may have contributed to the outcome.

Firstly, pathological expansion of adipose tissue can lead to excessive lipid accumulation and in turn an immune/inflammatory response (Theron et al., 2022), which has been shown to be exacerbated by DTG (Domingo et al., 2022). Females

are considered to have greater subcutaneous adiposity than males, while males tend to accumulate adipose tissue in the visceral compartment in the abdominal region, (Gavin and Bessesen, 2020). In the current study, relative “dysregulation” of DTG distribution was observed in a visceral adipose depot. Generally, an increased visceral adiposity is linked to metabolic dysregulation – which is commonly reported after ART use (Ergin et al., 2020). Adipose tissue expands by means of hypertrophy (increase in size of adipocytes) or hyperplasia (increase in number of adipocytes). Male adipose depots accretion occurs mostly due to hypertrophy and females depots by hyperplasia (Lee and Fried, 2017). The balance between the two states plays a large role in final lipid storage homeostasis and metabolic health (Harvey et al., 2020; Ibáñez et al., 2018). Pathological expansion of adipose tissue can lead to an excessive lipid accumulation which elicits an immune/inflammatory response (Theron et al., 2022). These processes are largely dependent on sex hormones and metabolic state. In terms of sex hormones, it has been shown that testosterone has a more consistent effect on adipocyte development than oestrogen (Gavin and Bessesen, 2020). The effect of oestrogen on the depot relies largely on the number of oestrogen receptors and this will vary in each adipose depot (Newell-Fugate, 2017). Females are considered to have greater adiposity than males but despite this, males tend to accumulate adipose tissue in the abdominal region, in the visceral compartment (Gavin and Bessesen, 2020).

This is indeed the picture observed on histological visualisation of the visceral adipose depot in the current study. Adipose tissue ultrastructure could be dependent on the different stages/phases of hypertrophy and hyperplasia based on the metabolic state of the individual rats. Since the significant difference in tissue mass was only seen between males and female in the treatment group it does suggest that DTG may exacerbate the effects. Current data suggests that the DTG group has decreased adipocyte surface area for the same mass of tissue when compared to the control group. This possibly indicates tissue expansion solely by hyperplasia. Even though tissue expansion by hyperplasia is considered metabolically healthier, this has negative implications for the homeostatic control of adipose tissue expansion. Too many small fat cells i.e. cells only expanding via hyperplasia are also considered dysfunctional if not being able to expand in size (hypertrophy). This would impact smaller individuals negatively by resulting in impaired lipid storage functions and

energy metabolism (Stenkula and Erlanson-Albertsson, 2018). Impairment in adipose tissue functioning could have great implications on cellular turnover of DTG, especially if an equivalent dose is given to a smaller individual with reduced cellular function to metabolise the drug.

Another consideration is the fact that DTG is highly protein bound (Taha et al., 2015). In plasma, DTG is 99% bound to plasma proteins, mainly albumin and to a lesser extent alpha-1-acid-glycoprotein (AGP) (Metsu et al., 2018). Both albumin and AGP are also produced in adipose tissue (Ruiz, 2021; Sirico et al., 2012), as well as other proteins that make up the extracellular matrix (ECM) such as proteoglycans, fibrous tissues, as well as regulatory proteins such as adipocyte fatty acid binding protein, C-reactive protein, adiponectin and leptin (Hu et al., 2016). Dysfunction in the expression of these proteins and the ECM have been linked to increased adiposity and metabolic syndrome (Hu et al., 2016; Khera et al., 2009) - two conditions that have been associated with DTG treatment (Hu et al., 2016; Khera et al., 2009; McLaughlin et al., 2018; Taramasso et al., 2020). Thus, the lack of correlation between DTG levels in adipose vs plasma, may suggest that the 12-week administration of DTG could have dysregulated the adipose protein profile, and thus DTG binding in this tissue. This would suggest that adipose tissue could be more vulnerable to an inflammatory outcome in response to DTG. Although human females are known to have a higher adipose protein content than males (Delaney and Santosa, 2022; Khera et al., 2009) male rodents accumulate significantly more adipose depots than females of a similar age (Maric et al., 2022). Thus, although no sex-differences in adipose DTG levels was observed in the current study, a rodent model may not be the ideal model for adipose-related studies on sex differences in this context. Proteomics analysis of adipose protein profile in humans treated with DTG may shed more light on this possibility.

In terms of tissue penetration, current data confirms good tissue penetration of DTG, with the exception of brain tissue. DTG is mainly metabolized in the liver by hepatic glucuronidation by UDP-glucuronosyltransferase (Kandel and Walmsley, 2015). It was therefore expected that more DTG would be detected in the primary site of elimination, as was indeed the case. This result is similar to another recent report on rodent liver DTG concentrations following administration of a similar dose (Deodhar et al., 2022).

The fact that adipose tissue exhibited a similar DTG content to muscle tissue, suggests that high tissue adipose content is not a limiting factor for DTG penetration into brain tissue. Reports on DTG penetration into brain tissue are variable. Relatively low levels of DTG (5 ng/g tissue) have been reported in murine brain tissue previously (Labarthe et al., 2022) in conjunction with plasma DTG levels very similar to those in the current study. This could suggest that the method employed for detection in the current study was not able to detect these low levels, as the limit of detection was  $\approx$  200 ng/g for brain tissue homogenate (Chapter 3). However, in contrast, another study in male wistar rats administered 45 mg/kg (in nano formulation) DTG via intra-muscular injection and no DTG was detected in the brain, using an LC-MS method with a 25 ng/g limit of detection (Deodhar et al., 2022). Collectively, despite potential limitations in detection methods, these studies indicate that DTG is unlikely to readily penetrate the blood-brain barrier in the absence of viral infection. However, the effects of HIV-infection on BBB permeability to DTG remains to be investigated.

Finally, current data suggest that in the absence of HIV infection and other ART, DTG does not seem to contribute to weight gain or dysregulation of glucose. These data correspond to the more recent literature in which it is proposed that DTG alone is not responsible for weight gain. Evidence has been provided suggesting that tenofovir alafenamide (TAF) potentially enhances weight gain. It has been suggested that TAF and DTG may have an additive effect on weight gain, but this should be further investigated (Kanters et al., 2022).

#### 4.5 Conclusion

Current data suggest that DTG on its own does not contribute to weight gain or glucose dysregulation. However, data also suggest a specific vulnerability of adipose tissue to DTG, which warrants further elucidation. Importantly, data suggest that body size may be a major risk factor determining adverse effect outcome, with a potential added sex effect in the context of adipose tissue sensitivity to DTG. We recommend that dosing strategy is revised to allow administration of DTG in a manner more closely adjusted for body mass. Considering that DTG did accumulate in tissue, more human trials including both males and females, are warranted to fully elucidate potential dysregulation at tissue level by DTG.



## Chapter 5: Liquid-chromatography tandem mass spectrometry methods for the quantification of trace amines from various wistar rat matrices

### 5.1 Introduction

The trace aminergic system and trace amines are emerging as relevant role players in many chronic diseases that are commonly diagnosed, but poorly understood. Trace amines are biogenic amines which are endogenously produced - but can also be ingested by intake of trace amine-rich foods (Broadley, 2010). Trace amine research was initiated early in the 1970s and most of the research was centred around its relevance to neurotransmission. This was presumably given the close resemblance of trace amines to monoamine neurotransmitters. However, until relatively recently, a lack of sufficiently sensitive detection tools limited progress in the field. More recent advances in quantification and detection techniques of small molecules have enabled more comprehensive evaluation of the relevance of trace amines to disease states. Popular research focus areas linked to trace amine involvement are neuropsychiatric, neurological and gastrointestinal disorders (Christian and Berry, 2018; Gwilt et al., 2020; Rutigliano et al., 2018).

Progress in the field has been slow due to the uniqueness and challenging aspects of both trace amines and their associated receptors – TAAR (Berry et al., 2017). While the existence of trace amines in the vertebrate brain and peripheral nervous system has been well documented, evidence of their exact functions in mammals is only now emerging. For example, it has been proposed that they are implicated in neurologic, metabolic and inflammatory function (Christian and Berry, 2018; Gwilt et al., 2020; Rutigliano et al., 2018). Understanding how different disease states and conditions impact different trace amines is imperative for the development of therapeutic diagnostic tools. If a comprehensive panel of trace amines can be identified and accurately quantified there is potential for trace amines to serve as biomarkers for various diseased states.

There are limited analytical methods reporting the quantification of both polar and non-polar trace amines in a single method – possibly due to their varying degrees of hydrophobicity. Most methods either analyse non-polar trace amines or polar amines individually. Most trace amines are formed by decarboxylation of amino acids by the action of aromatic L-amino acid decarboxylase (Gainetdinov et al., 2018). The trace amines formed from the decarboxylation of L-tryptophan, L-tyrosine and L-arginine via AADC enzymes are of particular relevance to the analytical method reported in this chapter. L-tryptophan is decarboxylated to form TRP via tryptophane decarboxylase. In addition, L-tyrosine is decarboxylated to form TYR which is subsequently thought to form OCT by dopamine- $\beta$ -hydroxylase (Berry, 2004; Christian and Berry, 2018; Khan and Nawaz, 2016). SYN readily forms from methylation of OCT by phenylethanolamine N-methyl transferase (Eagles and Iqbal, 1974; Rossato et al., 2011). TYR, SYN and OCT are considered products of tyrosine metabolism. Dysregulation in this synthesis pathway has been linked to Parkinson's disease, migraine and other neurological disorders (D'Andrea et al., 2013). Another trace amine synthesis cascade relevant to the analytical method in this chapter is the decarboxylation of L-arginine leading to the formation of polyamines. AGM can be formed by decarboxylation of arginine by the mitochondrial enzyme arginine decarboxylase (Molderings and Haenisch, 2012; Regunathan and Reis, 2008). AGM is further metabolised to form PUT via agmatinase (Wang et al., 2014). The subsequent trace amines in the synthesis cascade are formed when PUT is converted to a triamine, SPD, by spermidine synthase (SPDS) which in turn is converted to SPM by spermine synthase (SMS). In addition, SPM can be converted back to SPD via direct oxidation (Pegg, 2013). These synthesis cascades are represented in Figure 5.1. It would be extremely beneficial to investigate trace amines simultaneously instead of individually, as well as across multiple synthesis cascades to determine potential relationships between trace amines in different matrices.

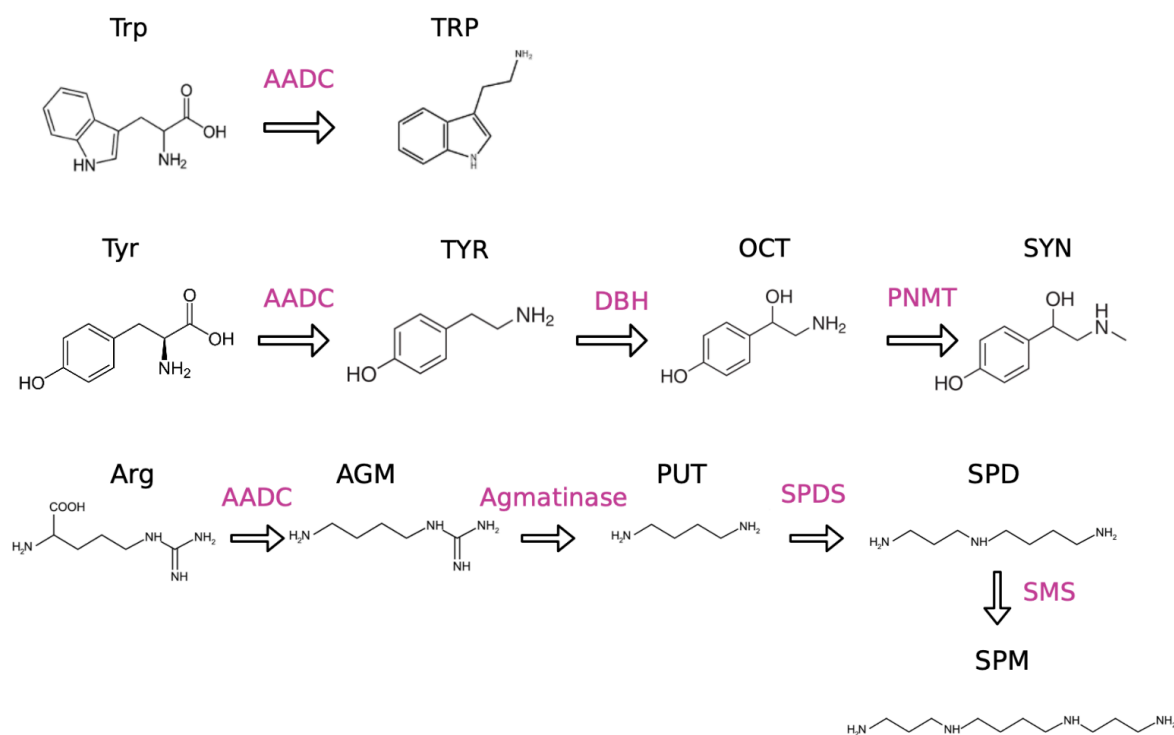


Figure 5.1: Chemical structure and formation summary of trace amines from tryptophan, tyrosine and arginine metabolism. Image created with Biorender.com

Abbreviations: Tyr, tyrosine; AADC, aromatic L-amino acid decarboxylase; TYR, p-tyramine; DBH, dopamine-β-hydroxylase; OCT, octopamine, PNMT, phenylethanolamine N-methyl transferase; SYN, p-syneprhine; Arg, arginine; AGM, agmatine; PUT, putrescine; SPDS, spermidine synthase; SPD, spermidine; SMS, spermine synthase; SPM, spermine.

Matrices most frequently used for trace amine quantification are microbial media supernatants following cell cultivation, plasma, urine, faecal samples and food/beverages for quality control and toxicity screening (D'Andrea et al., 2010; Gosetti et al., 2013; Luqman et al., 2018; Maráková et al., 2020; Sagratini et al., 2012; Santoru et al., 2017). The most commonly quantified trace amines include TYR, PEA, TRP, OCT, PUT, CAD, SPD and SPM. This is probably due to PEA, TYR, TRP and OCT being classified as the archetypal trace amines and initial research focused on their role in neurological disorders. Due to PUT, CAD, SPM and SPD being present in most spoiled or contaminated food, they often serve as indicators for the quality of food (Sagratini et al., 2012). Moreover, trace amines are often measured in urine and/or plasma – common matrices to investigate as they are easily obtainable in a clinical setting. This is particularly relevant as trace amine concentrations are being considered for their use as a clinical diagnostic tool for gastrointestinal disorders such

as IBD and neurological disorders such as PD (D'Andrea et al., 2019; Maráková et al., 2020). Since trace amines and their roles in diseased states are becoming more popular areas of research, there is a need for accurate and sensitive quantification for a large panel of these analytes.

LC-MS/MS is a highly sensitive research tool which enables simultaneous quantification of analytes. However, considering that trace amines are endogenous analytes, the conventional method development process needs to be adjusted to allow for interfering endogenous concentrations which would affect accurate and reliable quantification. In addition to this, the trace amines in this panel vary in hydrophobicity, and this would have implications on the chromatographic behaviour. Albeit a number of analytical methods have been developed for combinations of the trace amines included in our panel, many of them require derivatization and are limited to plasma and urine, often requiring large sample volumes greater than 500  $\mu\text{L}$  (D'Andrea et al., 2019; Gosetti et al., 2013; Mao et al., 2009; Maráková et al., 2020). Of those methods developed for tissue, they are mostly applicable to food products such as fish and plant tissue (Sagrati et al., 2012). The most used extraction techniques involve protein precipitations, and this would not be suitable for the tissue types being investigated in this study.

This chapter describes the development of a robust and sensitive extraction method for the simultaneous detection and quantification of nine trace amines. It was particularly important that the methods were developed in such a way that they could be applicable to multiple biological matrices including, urine, plasma, brain and gastrointestinal tissue and only require a small volume of sample. Below is a description of the development of a novel solid phase extraction and LC-MS/MS methods that can be used to quantify trace amines at physiologically relevant concentrations.

## 5.2 Methods and materials

### 5.2.1 Ethical consideration

Ethical approval for collection of wistar rat matrices have been described above in section 3.2.1. In addition, urine was extracted directly from the bladder and stored at

-20°C until analysis. The left hemisphere of the brain, the duodenum, jejunum and ileum were excised and snap frozen in liquid nitrogen. The tissue samples were stored at -80°C until analysis.

## 5.2.2 Method development

### 5.2.2.1 Reagents

Tyramine Hydrochloride (T898493), Phenethylamine (P321335), Tryptamine (T894600), rac-Synephrine (S920000), rac Octopamine Hydrochloride (O239750), Cadaverine (C058000), 1,4-Diaminobutane (Putrescine) (D416025), 3-Iodothyronamine Hydrochloride (I720500) and the internal standards, Phenethylamine-d4 (P321336) and 1,4-Butane-1,1,2,2,3,3,4,4-d8-diamine-d8 (Putrescine-d8) (D416027) were purchased from Toronto Research Chemicals (Toronto, ON, Canada). Agmatine sulfate salt (A7127), Spermidine (49761), Spermine (S3256), trichloroacetic acid (TCA) and LC-MS grade ammonium formate was purchased from Merck KGaA (Darmstadt, Germany). LC-MS grade ACN and MeOH were purchased from ROMIL Ltd. (Cambridge, UK). Formic acid and acetic acid were purchased from Fischer Chemicals (New Hampshire, USA). Ammonium acetate was purchased from Labchem (Johannesburg, South Africa). Ultrapure water was produced from a Synergy® water purification system (Merck KGaA, Darmstadt, Germany).

### 5.2.2.2 Equipment

LC-MS/MS analysis was conducted on a SHIMADZU 8040 triple quadrupole-mass spectrometer (SHIMADZU, Kyoto, Japan) connected to a SHIMADZU Prominence LC system (Kyoto, Japan). The system consisted of a LC-20ADXR solvent delivery system, Nexera XR SIL-20AXR autosampler and CTO-20A column oven. The analytes were chromatographically resolved on an Agilent Poroshell 120 EC-C18 (3.0 x 100 mm, 2.7 µm) and an Agilent ZORBAX Eclipse XDB-C8 (4.6 x 150 mm, 5 µm).

### 5.2.2.3. Chromatographic conditions

Two different chromatographic methods were developed due to varying polarities of the analytes under investigation.

#### *Method 1:*

Mobile phase A composition was 5 mM ammonium formate and 0.1 % formic acid in ultrapure water (Synergy, Merck) while mobile phase B consisted of 5 mM ammonium formate and 0.1 % formic acid in MeOH:H<sub>2</sub>O (95:5, v/v). The mobile phase solutions were filtered through 0.45 µm membranes and degassed by ultrasonication before use. Chromatographic separation was carried out using a gradient elution program and an Agilent Poroshell 120 EC-C18 (3.0 x 100 mm, 2.7 µm) with a flow rate of 0.4 mL/min. The gradient started at 5% mobile phase B held for 0.5 minutes, mobile phase B was increased to 95% until 4 minutes and held at 95% until 5 minutes, reduced to 5% mobile phase B until 6 minutes and re-equilibrated at 5% mobile phase B for 3 minutes giving a total run time of 9 minutes. The column temperature was set at 30°C and 10 µL of extracted sample was injected onto the column. The autosampler temperature was set at 15°C. The needle rinse was H<sub>2</sub>O:MeOH (20:80, v/v).

#### *Method 2:*

Mobile phase A composition was 5 mM ammonium formate and 0.1 % formic acid in ultrapure water (Synergy, Merck) while mobile phase B consisted of 5 mM ammonium formate and 0.1 % formic acid in ACN:H<sub>2</sub>O (95:5, v/v). The mobile phase solutions were filtered through 0.45 µm membranes and degassed by ultrasonication before use. Chromatographic separation was carried out using a gradient elution program and an Agilent ZORBAX Eclipse XDB-C8 (4.6 x 150 mm, 5 µm) with a flow rate of 0.4 mL/min. The gradient started at 30% mobile phase B and was increased to 95% mobile phase B over 3 minutes, held at 95% until 5.5 minutes, reduced to 30% mobile phase B until 6.5 minutes and re-equilibrated for 3 minutes giving a total run time of 9.5 minutes. The column temperature was set at 30°C and 10 µL of extracted sample was injected onto the column. The autosampler temperature was set at 15°C. The needle rinse was H<sub>2</sub>O:MeOH (20:80, v/v).

#### *5.2.2.4 Mass spectrometry conditions*

Each analyte was infused into the mass spectrometer and tuned for its mass transitions. A multiple reaction monitoring (MRM) event was created for each analyte containing several transitions. One transition was used for quantification and a second transition for confirmation. The MRM events were combined for the final method. The

highest sensitivity for all analytes and internal standards were achieved in positive ionization mode. As a result, the acquisition was set in positive electrospray ionisation mode. Argon was the collision-induced dissociation gas, delivered at 230 kPa. The electrospray ionization parameters are as follows: nebulizing gas flow (3 L/min), desolvation line temperature (250°C), heating block temperature (400°C), interface voltage was 4.50 kV, interface current was 11.10  $\mu$ A and drying gas flow (15 L/min). The mass spectrometer parameters such as Q1 pre bias (V), collision energy (CE) and Q3 pre bias (V) are listed in Table 5.1.

Table 5.1: Multiple reaction monitoring (MRM) conditions of each analyte.

Analyte	Precursor ion (m/z)	Product ions (m/z)	Q1 Pre bias (V)	CE	Q3 pre bias (V)
TYR	138.10	77.000 (Q)	23.0	13.0	21.0
		91.000	10.0	28.0	28.0
PEA	122.10	105.05 (Q)	22.0	14.0	19.0
		77.000	21.0	29.0	30.0
TRP	161.10	144.10 (Q)	27.0	13.0	26.0
		117.05	11.0	27.0	22.0
SYN	168.10	150.100 (Q)	18.0	12.0	28.0
		91.050	19.0	23.0	16.0
OCT	153.90	91.000 (Q)	16.0	21.0	16.0
		136.05	16.0	13.0	23.0
T1AM	355.80	212.05 (Q)	16.0	19.0	13.0
		195.000	16.0	26.0	19.0
SPD	146.25	72.200 (Q)	10.0	16.0	27.0
		112.15	14.0	15.0	22.0
SPM	203.30	112.15 (Q)	13.0	18.0	19.0
		84.15	13.0	32.0	30.0
AGM	130.95	72.050 (Q)	14.0	15.0	27.0
		59.950	14.0	14.0	22.0
PUT	89.000	72.150 (Q)	19.0	13.0	27.0
		55.050	19.0	22.0	21.0
CAD	103.30	86.100 (Q)	15.0	13.0	29.0
		69.050	14.0	27.0	25.0
PEA-d4	126.20	109.05 (Q)	21.0	15.0	19.0
		79.100	22.0	28.0	29.0
PUT-d8	97.150	80.100 (Q)	15.0	13.0	29.0
		61.850	14.0	27.0	25.0

Abbreviations: m/z, mass-to-charge ratio; V, voltage; Q, quantifier ion

### 5.2.2.5 Preparation of stock solutions and internal standards

According to analyte stability and solubility, each trace amine was dissolved in an appropriate solvent. The most appropriate solvent was chosen based on recommendation from the certificate of analysis. Stock solutions of 1mg/mL were prepared by dissolving TYR, PEA, TRP, SYN, OCT, T1AM, PUT and CAD in MeOH. Stock solutions of 1 mg/mL AGM, SPD and SPM were prepared by dissolving the reference standard in H<sub>2</sub>O. Two separate stock solutions of each analyte were prepared and used for preparation of calibration standards and QCs. The stock solutions were further diluted to working solutions of 10 µg/mL. The first working stock solution was prepared by spiking 10 µg/mL of each trace amine solution into MeOH:H<sub>2</sub>O (1:1, v/v) to prepare a pooled working stock solution containing all the trace amines. The rest of the working stock solutions for calibration standards were prepared by serial dilution with MeOH:H<sub>2</sub>O (1:1, v/v). Three QC concentrations were prepared for all trace amines. The QC H and QC M were prepared at 800 ng/mL and 400 ng/mL respectively for all trace amines. The QC L was prepared at a concentration within 3 x of the limit of quantification (LOQ) of each trace amine (Table 5.4). Aliquots of all working solutions were stored at -80°C. Calibration curves were prepared on the day of extraction from frozen working stock solutions. The calibration standards were prepared by spiking a blank solvent with the trace amine working stocks not exceeding 5% (v/v) of the final volume. For the quantification of trace amines in urine and plasma, the standards were prepared in water. Standards were prepared using ACN:H<sub>2</sub>O (70:30, v/v) with 0.2% formic acid for the analysis of trace amines from brain and gastrointestinal tissue. The calibration curves prepared ranged from 1.98 – 1000 ng/mL but specific ranges for each analyte are summarised in Table 5.2. Internal standard stock solutions were prepared at 1 mg/mL by dissolving PEA-d<sub>4</sub> and PUT-d<sub>8</sub> in MeOH. An internal standard working solution was prepared in MeOH containing concentrations of 1.6 µg/mL PUT-d<sub>8</sub> and 0.4 µg/mL PEA-d<sub>4</sub>.

### 5.2.2.6 Sample preparation in different matrices

#### 5.2.2.6.1 Preparation of urine and plasma samples

Urine and plasma samples were removed from -20°C and thawed on ice. A volume of 50 µL 10% w/v TCA solution was added to 250 µL plasma and urine. The samples

were vortexed for 30 seconds and centrifuged at 16 000 x *g* for 10 minutes at room temperature.

For the standards and QCs, 50  $\mu\text{L}$  10% w/v TCA solution was added to 250  $\mu\text{L}$  aliquots ultrapure water (Synergy, Merck), and vortexed for 30 seconds followed by centrifugation at 16 000 x *g* for 10 minutes at room temperature.

#### 5.2.2.6.2 Preparation of brain and gut samples

Brain and gastrointestinal tissue samples were removed from  $-80^{\circ}\text{C}$ , weighed, mixed 1:5 (w/v) with ACN:H<sub>2</sub>O (70:30, v/v) with 0.2% formic acid and homogenized with a tissue homogenizer (2 cycles, 6.95 m/s, 15 second interval with 1 min dwell time on ice between each cycle, Bead Ruptor Elite, OMNI International, Georgia, USA). A volume of 300  $\mu\text{L}$  of homogenate was evaporated under vacuum using the Genevac miVac Duo Sample Concentrator at  $40^{\circ}\text{C}$  for 45 minutes. Following evaporation, the samples were reconstituted with ultrapure water (Synergy, Merck) to 300  $\mu\text{L}$  and centrifuged at 1000 x *g* for 3 minutes at room temperature to ensure there was no particulate in the supernatant.

For the standards and QCs, 300  $\mu\text{L}$  aliquots of the homogenising solvent - ACN:H<sub>2</sub>O (70:30, v/v) with 0.2% formic acid was evaporated under vacuum using the Genevac miVac Duo Sample Concentrator at  $40^{\circ}\text{C}$  for 45 minutes. Following evaporation, the samples were reconstituted with ultrapure water (Synergy, Merck) to 300  $\mu\text{L}$  and centrifuged at 1000 x *g* for 3 minutes at room temperature.

#### 5.2.2.7 Sample extraction

A SPE protocol was developed by using a method previously published with minor modifications (Pretorius et al., 2022a). The original method was modified by increasing the amount of internal standard spiked from 10  $\mu\text{L}$  to 50  $\mu\text{L}$  and introducing sample preparation before solid phase extraction to ensure sample suitability. The SPE protocol included the Supel-clean™ LC-WCX SPE cartridges with 100 mg bed wt. and 1 cc barrel. Briefly, the cartridges were conditioned with 1 mL MeOH followed by two 1 mL equilibration steps with 50 mM ammonium acetate pH 5.2. Samples were buffered with 50 mM ammonium acetate pH 5.2 (200  $\mu\text{L}$  sample: 800  $\mu\text{L}$  buffer) and

individually spiked with 50  $\mu\text{L}$  IS working stock (PEA-d4 at 0.4 ng/mL and PUT-d8 at 1.6  $\mu\text{g/mL}$ ). Following sample loading, the cartridges were washed with 1 mL 5% MeOH in  $\text{H}_2\text{O}$ , 1 mL 10% MeOH in  $\text{H}_2\text{O}$  and 1 mL 20% MeOH in  $\text{H}_2\text{O}$ . Analytes were eluted using ACN with 5% formic acid. The eluent was evaporated to dryness under vacuum utilising the Genevac miVac Duo Sample Concentrator at 40°C. Samples were reconstituted in 200  $\mu\text{L}$  MeOH: $\text{H}_2\text{O}$  with 0.1% formic acid, vortexed vigorously and transferred to 96-well plates.

### 5.2.3 Method performance characterization

#### 5.2.3.1 Selectivity

The selectivity was assessed for endogenous analytes and internal standards. There should be no interference at the retention time for each analyte. Since standards were prepared in a solvent, there should be no change in retention time when samples in authentic matrix were analysed.

#### 5.2.3.2 Linearity, accuracy and precision

Due to the trace amines being endogenous compounds, calibration standards were prepared in solvent. Each analytical batch included calibration standards in duplicate, a blank sample (blank solvent with internal standard) and one double blank sample (only blank solvent). QCs prepared in the respective solvent were included to validate the curves. Precision was calculated as the %CV within a single run and accuracy as the percentage deviation between the nominal and observed concentrations. Due to this assay being used for pre-clinical samples it was possible to have less stringent acceptance criteria than for methods with clinical application. Therefore, acceptance criteria for calibrators and QCs were an accuracy of between 80 – 120% and %CV  $\leq$  20. At least 50% of standards at each calibration concentration had to pass and 75% of the standards in a batch had to pass. The LOQ was defined as the lowest quantified concentration at a signal-to-noise (S/N) ratio greater than 5 with an accuracy between 80 and 120%. Calibration curves were generated by plotting the peak area ratio of analyte to internal standard versus analyte concentration. The calibration standards were used to construct a calibration curve using a quadratic  $1/C$  or  $1/C^2$ , where  $C$  = concentration, weighed regression (Table 5.2).

Table 5.2: Calibration range, regression weighting, retention time and column used for analysis of the different trace amines in all matrices.

Analyte	Calibration range (ng/mL)	Quadratic regression weighting	Retention time (min)	Column used for analysis
TYR	3.91 – 1000	1/C <sup>2</sup>	2.94	Poroshell
PEA	1.95 – 1000	1/C <sup>2</sup>	3.83	
TRP	1.95 – 1000	1/C <sup>2</sup>	4.07	
SYN	3.91 – 1000	1/C <sup>2</sup>	1.95	
OCT	7.81 – 1000	1/C	1.61	
T1AM	7.81 – 1000	1/C	4.91	
AGM	3.91 – 1000	1/C	3.30	Zorbax
PUT	31.3 – 1000	1/C <sup>2</sup>	3.26	
CAD	7.81 – 1000	1/C <sup>2</sup>	3.28	

### 5.2.3.3 Carry-over

Percentage carry-over was determined by injecting the upper limit of quantification (ULOQ) followed by two blank samples of the respective solvent. The % carry-over into each blank was calculated and expressed in relation to the LOQ. It is currently recommended that carry-over may not exceed 20% of the LOQ (Food and Drug Administration, 2022).

### 5.2.3.4 Recovery

Extraction recovery of each trace amine was evaluated across three different analytical batches in triplicate at QC H, QC M and QC L concentrations by comparing extracted analyte response (spiked pre-extraction) to analyte responses spiked into blank solvent (spiked post-extraction) which is considered 100% recovery. Recovery of the two internal standards was assessed in each matrix in triplicate at one concentration (100 ng/mL for PEA-d4 and 400 ng/mL for PUT-d8) by comparing extracted analyte response (spiked pre-extraction) to analyte responses (spiked post extraction) into blank matrix which is considered 100% recovery. Recovery was assessed in every run with samples to ensure the recovery was sufficient and consistent (%CV < 20).

#### 5.2.3.5 Differences between QCs in solvent and QCs in matrix

QCs in duplicate were prepared in urine, plasma, brain and gut tissue. QC samples in brain and gut were prepared by homogenizing the tissue in 1:5 (w/v) with ACN:H<sub>2</sub>O (70:30, v/v) containing 0.2% formic acid with a tissue homogenizer (2 cycles, 6.95 m/s, 15 second interval with 1 min dwell time on ice between each cycle, Bead Ruptor Elite, OMNI International, Georgia, USA). The homogenates were pooled together and spiked with a known concentration of analyte at high, medium and low concentrations. The urine and plasma samples were also pooled from three different wistar rats. These QC samples were used to evaluate the endogenous concentrations of trace amines present in each matrix. In addition, the samples were prepared to determine if the QCs in the relevant matrix validated the curves prepared in solvent. The difference between standards prepared in solvent and QCs prepared in actual matrix was determined by comparing the regression slope of QCs prepared in solvent and in actual matrix. The average response of the analytes from the two different regression slopes were compared using a *t test* (Rodríguez-Palazón et al., 2023). To accept that there are no differences between the solvent and actual matrix, there should be no significant difference between the two regression slopes.

#### 5.2.3.6 Method applicability

The developed methods were applied to wistar rat plasma, urine, brain and gastrointestinal tissue samples to quantify trace amines present in the respective matrices. The tissue analyte concentrations obtained during LC-MS/MS analysis (ng/mL) were normalised by tissue weight in g per mL homogenising solvent (Ocque et al., 2017).

#### 5.2.4 Data analysis

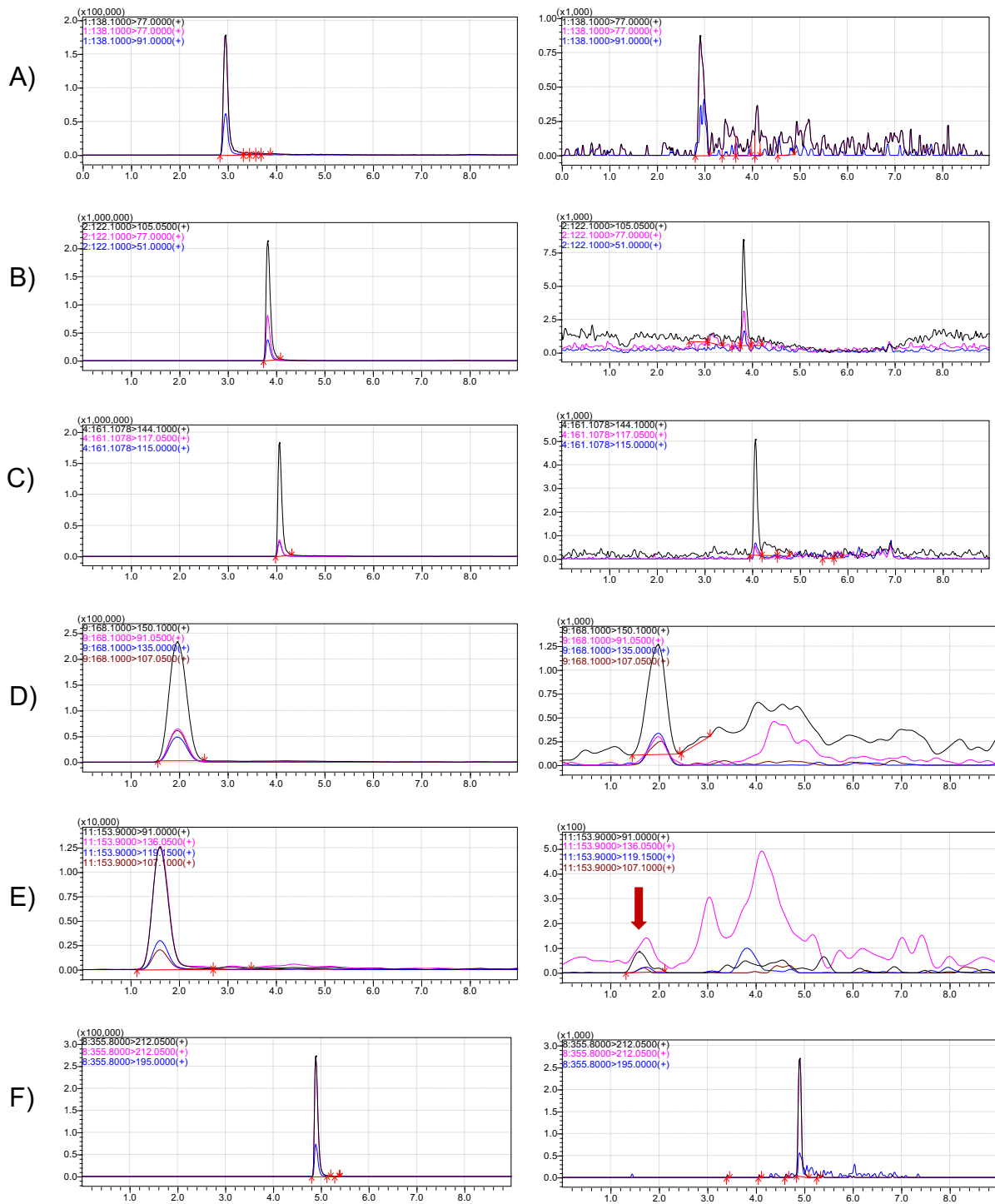
Data acquisition and processing was performed using LabSolutions version 5.109 (Shimadzu Corporation, Kyoto, Japan). Microsoft excel version 16.54 was used to calculate the means, standard deviation and %CV. GraphPad Prism 9.4.1 software was used to determine the distribution of data using Shapiro-Wilk normality test. Differences between regression slopes was determined by using a *t-test*. A *p* value < 0.05 was considered statistically significant. The concentrations of CAD in urine and CAD and PUT in the gastrointestinal tissue were found to be higher than the ULOQ

for most of the collected samples and therefore their concentrations were determined based on extrapolation of the standard curves prepared. Data collected for SPD was semi-quantitative. Data for SPM was exploratory and based on the detection of a relatively large peak area for the specific MRM event created.

## 5.3 Results and discussion

### 5.3.1 Optimisation of chromatography

Separation of the different trace amines was investigated with three different columns: a Shim-pack Velox Biphenyl (2.1 x 100 mm, 2.7  $\mu\text{m}$ ), an Agilent Poroshell 120 EC-C18 and an Agilent ZORBAX Eclipse XDB-C8 (4.6 x 150 mm, 5  $\mu\text{m}$ ). The Shim-pack Velox Biphenyl resulted in poor retention with many analytes eluting well before 1 minute. The Agilent Poroshell 120 EC-C18 in combination with an acidified MeOH mobile phase improved retention of most analytes but not AGM, PUT, CAD, SPD and SPM. For this reason, a second method was created using an Agilent ZORBAX Eclipse XDB-C8 (4.6 x 150 mm, 5  $\mu\text{m}$ ) to allow investigation of these trace amines. ACN with the addition of 5 mM ammonium formate and 0.1% formic acid resulted in sharp, symmetrical peaks on the C-8 column. SPD and SPM had improved retention on the C-8 column but had poor peak symmetry and shape with the ACN mobile phase containing additives. For this reason, they were analysed on the Poroshell, despite their retention time of approximately 1 minute. For this reason, data obtained from SPD and SPM was exploratory. Chromatograms of the analytes at the ULOQ and LOQ, as well as the internal standards, are presented in Figure 5.2.



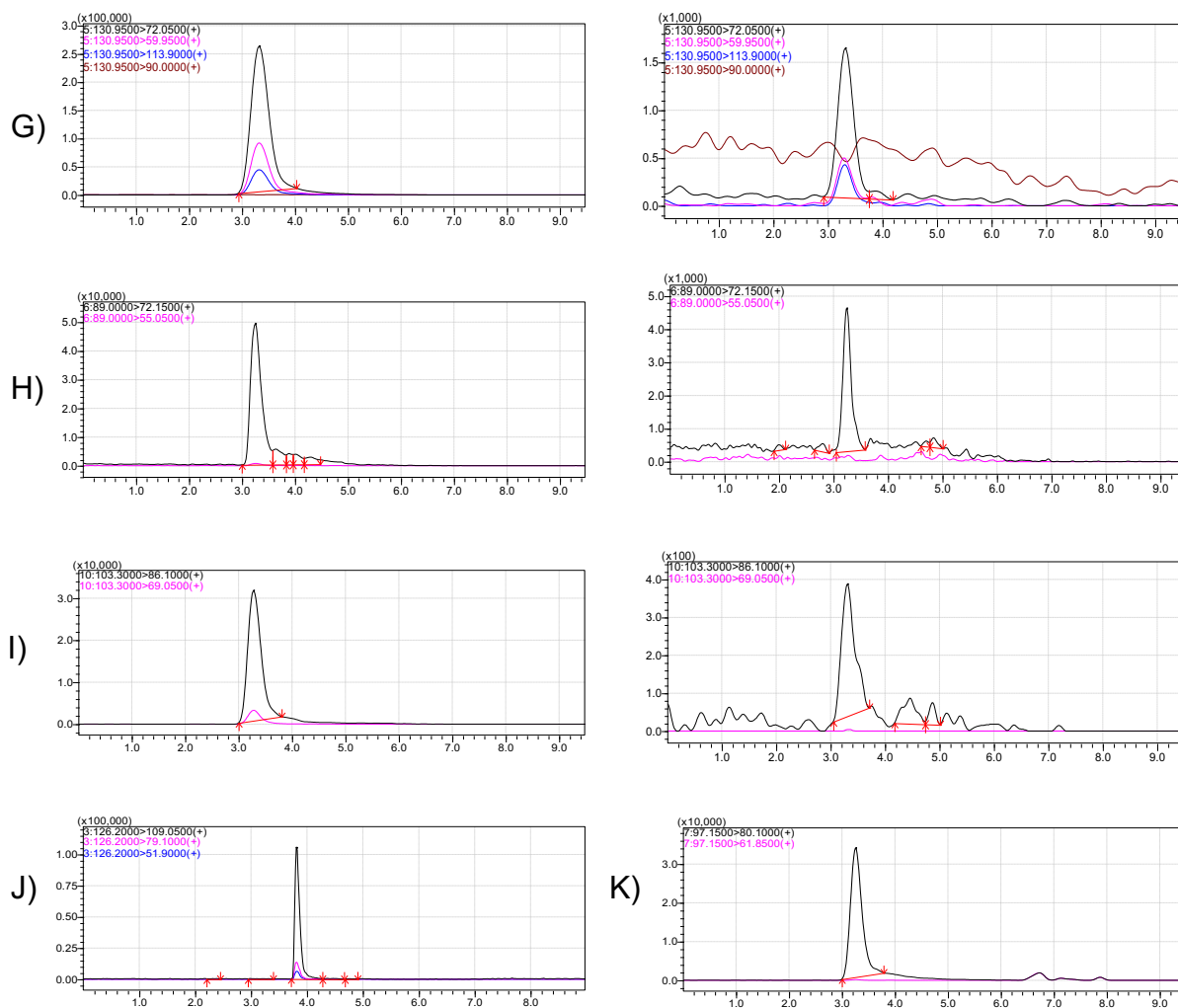


Figure 5.2: Chromatograms of (A) TYR, (B) PEA, (C) TRP, (D) SYN, (E) OCT, (F) T1AM, (G) AGM, (H) PUT, (I) CAD at the ULOQ (left) and LOQ (right). (J) PEA-d4 at 100 ng/mL and (K) PUT-d8 at 400 ng/mL. Intensity (cps) is reported on the y-axis and retention time (min) on the x-axis.

### 5.3.2 Optimisation of extraction method

A SPE protocol was developed by adapting a previously method reported by D'Andrea *et al.* (2019). Method development initially started in bacterial and yeast conditioned supernatants as there were overlapping interests in the research group. Supleclean LC-WCX sorbent wt. 30 mg 1 cc cartridges were used for initial method development. Briefly, the cartridges were conditioned with 1 mL MeOH, equilibrated with 1 mL 50 mM ammonium acetate at pH 5, samples were buffered 1:1 with 500  $\mu$ L 50 mM ammonium acetate containing 100 ng/mL PEA-d4 and washed with 25% MeOH in H<sub>2</sub>O. Analytes were eluted with 5% formic acid in ACN. Following analysis, it was determined that further sample clean-up was necessary. In addition, the internal

standard was spiked individually into samples instead of being included in the 50 mM ammonium formate buffer. The amount of sample being loaded was reduced from 500  $\mu$ L to a ratio of 1:4 (1 part sample: 4 parts buffer) and the bed wt. of the cartridges was increased to 100 mg. Additional washing steps of 1 mL 5% MeOH and 1 mL 10% MeOH in H<sub>2</sub>O was included. The formic acid in the elution solvent was reduced to 2% from 5%. Following re-evaluation of the adjusted method, it was noted that AGM and PUT were not recovered from the sample. Further investigation revealed that a lower pH is required for analyte elution from the sorbent and the change from 5% formic acid to 2% formic acid resulted in AGM and PUT being retained on the sorbent. Finally, a method including three washing steps and two elution steps was developed. This extraction method was applied to analyses of samples from a collaborative study (Pretorius et al., 2022a, 2022b). Following these publications, the method was expanded to include T1AM, OCT, SYN, CAD, SPD and SPM.

Due to the nature of the matrices under investigation for this thesis (plasma, urine, brain- and gastrointestinal tissue), additional sample preparation was required. The existing method described above was evaluated in urine and proved sufficient with recoveries above 60% with no prior sample treatment. However, since the tissue matrices were homogenized in organic solvent, the supernatant was not suitable for the current SPE method without risking breakthrough of the analytes. The tissue samples were homogenized in this manner as all analytes (including DTG from chapter 3 and 4) were soluble in the chosen homogenate solvent and some matrices overlapped with DTG analysis. In addition, plasma would not pass through the sorbent without causing a blockage. For this reason, a simple protein precipitation using MeOH:ACN (90:10, v/v) was developed for plasma and tissue samples. This method proved effective in extracting trace amines from solvent, but it was not suitable for extracting the trace amines from actual matrix. In addition, PEA-d4 extracted poorly and recovery was inconsistent. Since PEA-d4 was the internal standard which compensated for most of the trace amines, it was essential that it had a consistent recovery. Following further investigations, it was determined that urine and plasma could be precipitated with 10% (w/v) TCA solution before SPE analysis to remove particulate that could cause blockages on the cartridges. In addition, following homogenisation in ACN:H<sub>2</sub>O (70:30, v/v) with 0.2% formic acid, the organic

supernatant could be evaporated and the samples reconstituted in water to prevent breakthrough of analytes during sample loading on the SPE cartridges. During this time the laboratory acquired a nitrogen generator and instead of evaporating the samples to dryness in the Genevac miVac Duo Sample Concentrator under a vacuum, samples were evaporated under a gentle stream of nitrogen at 40°C. However, subsequent experiments resulted in inconsistent recoveries of AGM and PUT and the internal standard PEA-d4. In addition, the 5% formic acid included in the elution step resulted in the sample pH being out of the working range of the columns being used during LC-MS/MS analysis. A series of experiments revealed that drying under nitrogen concentrated AGM and PUT and degraded PEA and PEA-d4, possibly due to their volatility. Once the original protocol using the Genevac miVac Duo Sample Concentrator was reinstated, the anomalies were no longer observed.

### 5.3.3 Method performance characterization

#### 5.3.3.1 Selectivity

The retention time of each analyte and internal standard in plasma, urine, brain- and gut homogenate was the same as the reference standard in the solvent. Chromatograms of QC M spiked into solvent, brain, urine and gastrointestinal tissue are depicted in addendum C (Supplementary Figure 5.1 – Figure 5.11) and demonstrate that the retention times did not change between the different matrices and the solvents.

#### 5.3.3.2 Linearity, accuracy, and precision

The intra-run data collected for each analyte from three analytical batches were combined to determine the inter-run assay accuracy and precision for the standards prepared in solvents for each analyte (Table 5.3). The same data was collected for the QCs from three analytical batches (Table 5.4). To determine if the QCs in the authentic matrix validated the curves prepared in solvents, a standard addition method was adopted. Pooled blank matrix was analysed in triplicate to determine an average endogenous concentration of the different trace amines present. This average concentration obtained was subtracted from the observed concentration to determine the %accuracy (Table 5.5).

QCs prepared at high, medium and low in brain tissue validated the curves prepared in solvent for all the trace amines except for OCT and CAD. CAD had accuracies > 120% and OCT accuracies < 80%.

In general, the endogenous concentrations of trace amines present in urine skewed the QC L accuracies and they rarely validated the curves prepared in solvents. Despite this, the QC H and QC M for PEA and TRP validated the curves prepared in a solvent. All QCs prepared in urine for T1AM validated the curves prepared in a solvent. Endogenous concentrations of CAD and PUT were too high in the urine to determine if the QCs in the authentic matrix validated the curves as the endogenous and spiked concentrations combined fell outside the calibration range.

In comparison to urine, all QCs for TYR, PEA, TRP and SYN prepared in plasma validated the curves prepared in a solvent. The QC H and M for PUT and CAD validated the curves while endogenous concentrations present at QC L skewed the accuracies as they were very high, even after subtracting endogenous concentrations present. QCs in plasma prepared for OCT, AGM and T1AM did not validate the curves at any concentrations.

Likewise, high endogenous concentrations skewed the accuracies at QC L for most analytes in the QCs prepared in gastrointestinal tissue. The QC H and M prepared in gastrointestinal tissue validated the solvent curves for TYR, PEA, TRP, SYN, T1AM and AGM. None of the QCs prepared for OCT in gastrointestinal tissue validated the curves. As with urine, the endogenous concentrations of CAD and PUT were too high to determine if the QCs validated the curve. As a result of inconsistency between the different QC concentrations, no correction factor was applied when analysing the predicted concentrations of trace amines in the samples and data were analysed on face value (these results are presented in chapter 6).

Table 5.3: Inter-run accuracy and precision summary statistics of standards prepared in a solvent.

Analyte	Nominal concentration (ng/mL)	1000	500	250	125	62.5	31.3	15.6	7.81	3.91	1.95	Correlation coefficient (r)
<b>TYR</b>	%Accuracy	95.6	107.3	108.8	99.0	103.3	86.4	95.6	103.0	99.4		>0.996
	%CV	3.7	3.5	3.7	6.0	6.8	5.3	12.4	10.7	3.7		
	n	6	6	6	6	6	6	6	6	5	5	
<b>PEA</b>	%Accuracy	98.2	104.0	102.2	95.7	100.1	96.3	95.8	99.1	103.0	102.1	>0.999
	%CV	12.3	7.7	7.3	8.3	8.2	6.1	5.6	8.9	7.3	5.4	
	n	6	6	6	6	6	6	6	6	6	6	
<b>TRP</b>	%Accuracy	97.0	103.4	107.6	101.4	101.1	95.7	97.9	94.2	99.7	104.7	>0.995
	%CV	9.6	7.1	5.3	9.1	12.1	9.8	10.7	8.9	12.5	8.9	
	n	6	6	6	6	6	6	6	6	6	5	
<b>SYN</b>	%Accuracy	97.7	104.9	103.7	96.3	101.2	90.4	97.5	97.1	107.2		>0.995
	%CV	7.4	5.7	5.8	4.6	7.5	8.6	9.8	11.4	8.1		
	n	6	6	6	6	6	6	6	5	6	5	
<b>OCT</b>	%Accuracy	99.4	102.3	100.8	93.5	97.1	95.1	99.5	104.7			>0.998
	%CV	9.1	6.3	7.6	8.9	10.5	12.0	13.6	8.9			
	n	6	5	6	5	6	6	5	5			
<b>T1AM</b>	%Accuracy	100.3	97.1	105.2	97.0	99.7	101.5	95.0	99.9			>0.999
	%CV	5.7	9.4	3.5	7.7	10.6	6.2	6.5	11.3			
	n	6	6	5	6	5	5	4	5			

%CV, % coefficient of variation

Table 5.3 continued.

Analyte	Nominal concentration (ng/mL)	1000	500	250	125	62.5	31.3	15.6	7.81	3.91	1.95	Correlation coefficient (r)
<b>AGM</b>	%Accuracy	101.4	95.2	100.4	106.3	103.8	102.4	99.7	89.1	99.0		>0.998
	%CV	9.9	12.7	11.4	12.2	10.8	6.4	12.0	5.7	10.4		
	n	6	6	5	5	6	6	4	4	4		
<b>PUT</b>	%Accuracy	98.7	102.4	99.5	101.5	102.7	94.1					>0.996
	%CV	5.5	5.3	2.0	2.8	9.2	12.1					
	n	6	6	6	6	6	5					
<b>CAD</b>	%Accuracy	99.0	104.3	98.0	92.6	94.8	102.4	100.4	106.4			>0.995
	%CV	7.8	4.6	3.8	8.2	7.1	11.2	11.4	11.1			
	n	5	6	6	6	5	5	4	5			

%CV, % coefficient of variation

Table 5.4: Inter-run accuracy and precision summary statistics of QCs prepared in a solvent.

Analyte	Nominal concentration (ng/mL)	Mean observed concentration (ng/mL)	n	%Accuracy	%CV
TYR	5.00	5.40	8	107.9	13.6
	400	398	9	99.4	6.7
	800	775	9	96.8	5.0
PEA	2.50	2.44	9	97.6	5.7
	400	378	9	94.4	5.7
	800	765	9	95.6	6.4
TRP	2.50	2.32	9	93.0	9.3
	400	373	9	93.1	9.4
	800	741	9	92.6	6.8
SYN	10.0	10.6	9	105.8	7.0
	400	415	9	103.6	9.6
	800	833	9	104.2	3.4
OCT	10.0	10.2	8	102.0	13.0
	400	388	9	97.0	6.4
	800	787	9	98.4	9.3
T1AM	10.0	9.79	9	97.9	9.9
	400	363	9	90.8	9.5
	800	705	9	88.1	8.6
AGM	5.00/*40.0	4.90/*45.5	8	97.9/*110.0	12.0/*7.7
	400	395	9	98.7	11.5
	800	806	9	100.8	8.2
PUT	40.0	36.9	9	92.3	6.0
	400	403	9	100.8	4.0
	800	813	9	101.6	4.7
CAD	10.0	11.4	7	114.0	17.0
	400	356	9	89.0	5.5
	800	777	9	97.1	6.0

\* a higher QC L of 40 ng/mL was used in the tissue analysis than the QC L of 5 ng/mL in plasma and urine analysis

%CV, % coefficient of variation

Table 5.5: Summary of endogenous concentrations and %accuracy for trace amine QCs prepared in different biological matrices.

Analyte	Brain tissue			Urine		Plasma		Gastrointestinal tissue	
	Nominal spiked concentration (ng/mL)	Observed concentration (ng/ml)	%Accuracy after subtracting endogenous	Observed concentration (ng/ml)	%Accuracy after subtracting endogenous	Observed concentration (ng/ml)	%Accuracy after subtracting endogenous	Observed concentration (ng/ml)	%Accuracy after subtracting endogenous
TYR	*Endogenous	<3.91		86.9		1.70		48.2	
	5.00	5.58	111.7	134	-	7.11	108.3	43.5	
	400	422	105.4	419	83.0	378	94.1	504	114.0
	800	917	114.6	529	55.2	725	90.4	877	103.6
PEA	*Endogenous	<1.98		35.2		<1.98		15.3	
	2.50	2.62	104.8	29.4	-	3.21	88.6	15.9	
	400	349	87.3	403	92.0	384	95.6	448	108.1
	800	715	89.4	692	82.2	778	97.2	818	100.4
TRP	*Endogenous	<1.98		20.2		<1.98		16.4	
	2.50	2.81	112.4	21.6	55.4	2.36	94.2	15.8	
	400	367	91.8	437	104.3	370	92.6	466	112.5
	800	710	88.8	698	84.7	696	87.0	841	103.0
SYN	*Endogenous	<3.91		18.9		<3.91		<3.91	
	10.0	11.9	119.2	13.5		10.1	101.1	11.7	117.1
	400	400	100.0	195	44.1	401	100.2	442	110.4
	800	942	117.7	300	35.2	758	94.8	890	111.2

\*endogenous concentrations were determined by pooling matrix (n=3).

The grey shaded block indicates the endogenous concentration detected was higher than the observed concentration resulting in a negative accuracy.

- endogenous concentrations in the pooled blank resulted in the observed concentration being > than nominal spiked concentration.

Table 5.5 continued.

Analyte	Brain tissue			Urine		Plasma		Gastrointestinal tissue	
	Nominal spiked concentration (ng/mL)	Observed concentration (ng/ml)	%Accuracy after subtracting endogenous	Observed concentration (ng/ml)	%Accuracy after subtracting endogenous	Observed concentration (ng/ml)	%Accuracy after subtracting endogenous	Observed concentration (ng/ml)	%Accuracy after subtracting endogenous
<b>OCT</b>	*Endogenous	<7.81		<7.81		<7.81		<7.81	
	10.0	6.06	60.6	5.96	59.6	7.79	77.9	7.57	75.7
	400	270	67.6	75.2	18.8	242	60.6	230	57.5
	800	680	85.0	167	20.9	501	62.6	558	69.8
<b>T1AM</b>	*Endogenous	<7.81		<7.81		<7.81		<7.81	
	10.0	8.99	89.9	8.43	84.3	4.36	43.6	12.0	119.8
	400	368	91.9	443	110.8	184	46.1	469	117.1
	800	751	93.8	670	83.8	527	65.9	905	113.1
<b>AGM</b>	*Endogenous	<3.91		32.6		<3.91		84.2	
	40.0/5.0	33.8	84.5	38.6	119.0	6.31	-	147	-
	400	339	84.8	181	37.0	499	-	507	105.7
	800	645	80.7	332	37.4	1168	-	789	88.1
<b>PUT</b>	*Endogenous	56.8		-		43.2		-	-
	400	451	98.4	-	-	483	109.8	-	-
	800	867	101.3	-	-	891	105.9	-	-

\*endogenous concentrations were determined by pooling matrix (n=3).

The grey shaded block indicates the endogenous concentration detected was higher than the observed concentration resulting in a negative accuracy.

- endogenous concentrations in the pooled blank resulted in the observed concentration being > than nominal spiked concentration.

Table 5.5 continued.

Analyte	Brain tissue			Urine		Plasma		Gastrointestinal tissue	
	Nominal spiked concentration (ng/mL)	Observed concentration (ng/ml)	%Accuracy after subtracting endogenous	Observed concentration (ng/ml)	%Accuracy after subtracting endogenous	Observed concentration (ng/ml)	%Accuracy after subtracting endogenous	Observed concentration (ng/ml)	%Accuracy after subtracting endogenous
CAD	*Endogenous	13.4		1047		12.5		709	
	400	582	142.0	-	-	417	101.2	-	-
	800	1071	133.8	-	-	742	91.1	-	-

\*endogenous concentrations were determined by pooling matrix (n=3).

The grey shaded block indicates the endogenous concentration detected was higher than the observed concentration resulting in a negative accuracy.

- endogenous concentrations in the pooled blank resulted in the observed concentration being > than nominal spiked concentration.

### 5.3.3.3 Carry-over

Carry-over was mitigated by investigating different needle rinse solvents to reduce the %carry-over between samples. Different ratios of MeOH:H<sub>2</sub>O water were evaluated to determine which ratio was efficient in reducing carry-over. MeOH:H<sub>2</sub>O (80:20; v/v) mitigated carry-over sufficiently to meet criteria (Food and Drug Administration, 2022). The %carry-over present after injecting the ULOQ was not more than 20% of the LOQ.

### 5.3.3.4 Recovery of trace amines

Recovery of the analytes was variable between runs during method development (%CVs of 15-20). It was also noted that recovery differed for some analytes depending on how the QCs were prepared – either in water with 10% w/v TCA as for the plasma and urine samples or in the homogenising solvent as for the brain and gastrointestinal samples. For this reason, recovery was evaluated in every run to ensure consistent results for that specific analytical batch. Recoveries were considered consistent with a %CV of 20. Although a %CV of 20 is not ideal, it was acceptable for this purpose. It is suspected that the higher %CV resulted from the samples being individually spiked onto the SPE cartridges.

Table 5.6: Percentage recovery of analytes from a solvent across three analytical runs.

Analyte	%Recovery during brain analysis (%CV)	%Recovery during plasma analysis (%CV)	%Recovery during gastrointestinal analysis (%CV)
TYR	117.0 (14.7)	66.2 (4.4)	75.4 (13.4)
PEA	121.7 (1.2)	101.2 (10.6)	96.5 (5.0)
TRP	112.4 (2.5)	84.1 (7.2)	85.2 (9.0)
SYN	113.1 (9.5)	73.6 (3.8)	78.9 (1.6)
OCT	112.5 (2.1)	62.1 (16.8)	79.3 (19.3)
T1AM	113.1 (12.6)	83.4 (15.3)	82.7 (2.0)
AGM	*105.4 (10.5)	*66.4 (6.8)	76.9 (7.0)
PUT	69.2 (19.4)	62.9 (16.3)	71.9 (9.6)
CAD	80.0 (8.2)	109.6 (5.4)	89.8 (11.3)

\*%Recovery calculated only using the average recovery at QC H and QC M as the average recovery at QC L was inconsistent (%CV > 35%).

Table 5.7: Percentage recovery of the internal standards in the authentic biological matrices.

Internal standard	%Recovery from brain tissue (%CV) (n=3)	%Recovery from urine (%CV) (n=3)	%Recovery from plasma (%CV) (n=3)	%Recovery from gastrointestinal tissue (%CV) (n=3)
PEA-d4	67.2 (6.6)	71.8 (6.6)	81.4 (0.4)	90.1 (1.0)
PUT-d8	54.1(8.9)	73.0 (8.6)	46.0 (3.2)	77.1 (2.2)

Recovery of the internal standards was determined in each of the authentic biological matrices to ensure extraction was consistent. The recovery of the internal standard in the biological matrices had to be consistent as any inconsistency would indicate a change in the detector's response to the different matrices. In addition, the internal standard had to compensate for any changes between the standards in a solvent and the QCs in authentic matrix. The consistent recovery of both internal standards in all matrices evaluated suggested that the LC-MS/MS methods developed had good sensitivity and reproducibility, therefore compensating for variability in all the analytes from the different matrices. This implied that the methods could be used to quantify analyte concentrations in the different biological samples successfully.

#### 5.3.3.5 Differences between QCs in a solvent and QCs in actual matrix

The QCs prepared in a solvent and the QCs prepared in the authentic biological matrices were used to plot a regression line. The regression slopes prepared in the solvent and matrices were compared using a *t* test to determine if they were statistically different (Table 5.8). However, this method to determine differences between the QCs prepared in solvent and QCs in matrix was limited by the need to use pooled matrix from different rats and QCs in authentic matrix only being analysed in duplicate. The two regression slopes were significantly different if they had a  $p < 0.05$ . The average regression slopes of urine and plasma were both compared to the same average regression slope in solvent as these two matrices were analysed in the same analytical batch. It is suspected that the differences between the regression slopes are as a result of the endogenous concentrations of trace amines present skewing the regression, especially at low concentrations. This is supported by the fact that when the slopes were significantly different between the solvent and the authentic

matrix, the QCs in the matrix often did not validate at QC L. This illustrates how important it is to look at these two data sets together (Table 5.5 and Table 5.8).

Table 5.8: Average regression slope of QCs prepared in a solvent and QCs prepared in the authentic biological matrices.

Analyte	Average regression slope in solvent (n=3)	Average regression slope in brain (n=2)	Average regression slope in solvent (n=3)	Average regression slope in urine (n=2)	Average regression slope in plasma (n=2)	Average regression slope in solvent (n=3)	Average regression slope in gastrointestinal tissue (n=2)
TYR	0.00191	<b>*0.00238</b>	0.00178	<b>*0.000751</b>	0.00176	0.00199	0.00244
PEA	0.0186	0.0189	0.0223	<b>*0.0158</b>	<b>*0.0210</b>	0.0211	0.0212
TRP	0.0128	0.0136	0.0160	0.0127	0.0135	0,0154	<b>*0.0178</b>
SYN	0.00912	<b>*0.0104</b>	0.00958	<b>*0.00281</b>	0.00856	0.00900	0.0102
OCT	0.000469	<b>*0.000364</b>	0.000347	<b>*0.0000641</b>	<b>*0.000229</b>	0.000369	0.000304
T1AM	0.00166	<b>*0.00191</b>	0.00182	0.00145	<b>*0.00118</b>	0.00186	<b>*0.00237</b>
AGM	0.0136	<b>*0.00942</b>	0.00786	<b>*0.00289</b>	0.00862	0.00777	0.00635
PUT	0.00163	0.00151	0.00123	-	0.00105	-	-
CAD	0.00127	<b>*0.00202</b>	0.000803	-	0.000758	-	-

- could not determine regression slope due to endogenous concentrations present being too high to plot a regression line

\* Indicates that the regression slope prepared in the authentic biological matrix differed significantly from the regression slope in solvent

## 5.4 Conclusion

Sensitive and specific LC-MS/MS methods have been developed to quantify TYR, PEA, TRP, SYN, OCT, T1AM, AGM, PUT and CAD in urine, plasma, brain and gastrointestinal tissue. Despite the different hydrophobicities of the trace amines, reverse phased chromatography coupled with acidic mobile phases resulted in sufficient retention times for nine compounds without the need for derivatization. This however, did require two different LC-MS/MS methods. Despite this, the methods are suitable for both polar and non-polar analytes and potentially allow for incorporation of more trace amines. The extraction method developed is suitable for aqueous and solid tissue matrices. Even though the extraction method utilizes SPE that requires extensive sample clean-up, the LC-MS/MS methods developed have relatively short run times. Method performance was assessed in terms of selectivity, linearity and recovery and was fit for intended purposes.

A limitation of the methods developed were that standards had to be prepared in solvent and as a result many of the QCs in the authentic matrix did not validate the standard curves. Another limitation of the method was that OCT and T1AM were not detected in any of the samples, potentially as a result of the method not being sensitive enough to detect very low endogenous concentrations. However, this could be overcome by using a more sensitive MS instrument. Future work could include increasing the concentration range to accurately quantify PUT and CAD or diluting samples so that they fall within the calibration range. This was unfortunately not possible in the current study as a result of the limited volume of sample collected from a wistar rat. In addition, the recovery of SPD and SPM could be optimised to enable accurate quantitation instead of semi-quantitative analysis.

Considering the implications of a dysregulated trace aminergic system in neurological and gastrointestinal disorders and the overlap these symptoms have with DTG adverse effects we hypothesized that DTG could alter the trace amine profile. For this reason, the methods developed in this chapter needed to be sensitive enough to quantify trace amines in different wistar rat matrices. This would enable the determination of changes to the trace aminergic system following DTG administration.

## Chapter 6: Effect of chronic dolutegravir administration on trace amine profile

### 6.1 Introduction

Despite the popularity of dolutegravir (DTG) as a first line treatment for HIV/AIDS, more recent literature has reported adverse events which could be related to accumulation of DTG in tissue compartments. In chapter 4, rodents chronically administered DTG indeed exhibited accumulation of DTG in muscle, liver and adipose tissue. Although we were unable to detect DTG in brain tissue of DTG-administered rats, this was likely due to insufficient sensitivity of the instrument used, as DTG has been reported to have the capacity to cross the blood brain-barrier and contribute to HIV-related neuropathology (Huang et al., 2023). Due to the small organ sizes, DTG levels were not assessed in the GIT. However, since DTG has previously been demonstrated to have highest distribution to the GIT (Labarthe et al., 2022), there is little doubt that all tissues – including the GIT and CNS – are potentially vulnerable to adverse effects of DTG. In terms of HIV – irrespective of whether the patients are using ART - the two most common sites of inflammation, and thus longer-term adverse outcome, are the CNS and GIT.

The effect of HIV on the CNS has been investigated for many years but there is still great uncertainty regarding the exact mechanism(s) responsible for the symptoms observed. Due to the vulnerability of the CNS to HIV infection, the neurological implications associated with HIV infection can be vast, including neuropsychiatric symptoms, HIV myelopathy, peripheral neuropathy and decreased olfactory ability (De Almeida, 2015; Fasunla et al., 2016; Hornung et al., 1998; Watkins and Treisman, 2012). The variability in these neurological disorders suggests that multiple mechanisms and role players may contribute to the CNS dysfunction seen in HIV. It has been reported that around half of PLWH receiving treatment still present with cognitive impairment (Stern et al., 2018). Despite the improvements in HIV therapies, neurocognitive disorders and impairment still remain prevalent among PLWH (De Almeida, 2015; Spudich and González-Scarano, 2012; Stern et al., 2018). HIV infection is associated with alterations in brain function referred to as HIV-associated

neurocognitive disorder (HAND) (Vally, 2011). HAND is reported to follow a similar pattern of cognitive dysfunction as other common neurodegenerative disorders such as AD (Clifford and Ances, 2013).

Similar to the CNS, the GIT is a major reservoir and site of HIV replication, with many PLWH experiencing gastrointestinal symptoms not related to secondary infections (Zeitz et al., 1998). Gastrointestinal symptomology presents across the entire GIT and symptoms experienced can range from dysphagia, nausea, vomiting and diarrhoea (Serlin and Dieterich, 2008). Physiological and immunological changes to the GIT during HIV infection can lead to severe GIT symptoms which drastically decrease quality of life for PLWH. Similar to HAND, even though the advancements of ART have increased the life expectancy of PLWH, the frequency and severity of HIV enteropathy persists. HIV enteropathy comprises increased GIT inflammation, diarrhoea and increased intestinal permeability (Brenchley and Douek, 2008). Many of these have been linked to microbial imbalances and changes to the composition of the gut microbiome (Avedissian et al., 2020).

Given the GIT and CNS as systems centrally affected in HIV- and ARV-associated adverse outcome, modulated trace amine signalling was identified as potential source of dysregulation in this context. As already introduced in the literature review chapter, trace amines are biogenic amines which are endogenously produced in trace amounts in the brain, as well as in larger amounts by the gut microbiome and are known to differentially regulate inflammatory outcome. Many of the trace amines under investigation in this dissertation have been linked to AD, neurocognitive disorders including neuropsychiatric symptomology (D'Andrea et al., 2013; Dewan, 2021; Dhakal and Macreadie, 2021; Pei et al., 2016; Sandler et al., 1979) These overlap with the neurological adverse events reported by PLWH after treatment with DTG. This literature suggests that trace amines might be implicated in the presentation of HAND and neurological adverse events of DTG. In contrast, research into the potential role of trace amines on GIT health is still relatively sparse, although our group and others has recently illustrated roles for different trace amines in the context of irritable bowel syndrome (Pretorius and Smith, 2023, 2022, 2020) and other GIT disorders (Gwilt et al., 2020). Some of this work also suggested oestrogen to affect the trace amine secretion profile of gut commensals and probiotic microbes (Pretorius et al., 2022b),

which is in line with women reporting relatively more adverse effects of DTG (Elzi et al., 2017; Hoffmann et al., 2017; Venter et al., 2019). A very recent report of dysregulated trace amine profile – implicating tryptophan metabolism and increased levels of phenylethylamine and polyamines – in stool samples from HIV patients (Zhang et al., 2023) aligns with our theory of a role for trace amines in DTG-associated adverse outcome, but specific evidence is lacking. A recent study of microbial by-products and their effects on gastrointestinal health provided some evidence that trace amines could be implicated in gastrointestinal disorders (Gwilt et al., 2020).

We propose that DTG administration could dysregulate the trace amine profile not only in the GIT and CNS, but also in other tissue compartments. Given the potential confounder presented by dietary trace amine ingestion in human studies, the use of a rodent model, where dietary intake is standardised across experimental groups, is particularly useful in establishing whether DTG may dysregulate trace amine distribution. Thus, we evaluated the concentration of a panel of trace amines across different tissues in control vs DTG-administered rats.

## 6.2 Methods and materials

### 6.2.1 Sample collection

Plasma collection was described above in section 4.2.4. Urine was drawn from the bladder and frozen at  $-20^{\circ}\text{C}$  until analysis. The left hemisphere of the brain, the duodenum (1 cm from the stomach), the jejunum (15 cm from the stomach) and the ileum (1 cm back from the caecum) were excised and immediately snap frozen in liquid nitrogen. The tissue samples were then stored at  $-80^{\circ}\text{C}$  until analysis. On the day of analysis, the entire hemisphere of the brain was homogenised in sections, which were then pooled again to produce the sample for analysis for each rat.

### 6.2.2 Trace amine quantification

The trace amine concentrations in urine, plasma, brain and gastrointestinal tissue were detected using LC-MS/MS methods described in detail in chapter 5. CAD and PUT concentrations in the urine, duodenum and jejunum fell above the upper limit of quantification (5000 ng/g tissue) for most of the collected samples. Their concentrations should be considered as semi quantitative as they were determined by

extrapolation of the standard curve. SPD concentrations in all matrices were semi-quantitative. SPM presence in a matrix was interpreted by the presence of a relatively large peak area for the specific MRM event.

### 6.2.3 Statistical analysis

Data was obtained from instrument software (LabSolutions version 5.109) and analysed using Microsoft excel version 16.54 and GraphPad Prism 9.4.1 software. Data is presented as the mean  $\pm$  the standard deviation (SD). Distribution of data was assessed using the Shapiro-Wilk normality test. Statistical analyses included 2-way ANOVA with Tukey's multiple comparison test and Mann-Whitney U test for ileal trace amine concentrations. A p-value of  $<0.05$  was considered statistically significant.

## 6.3 Results

### 6.3.1 Limited or low abundance of trace amines in rodent plasma and brain tissue

The concentrations and type of trace amines detected were largely dependent on the matrix under investigation. In plasma, despite the high sensitivity of the method employed, only trace amounts of TYR and TRP were detected at concentrations just below the level of quantification (3.91 ng/mL and 1.95 ng/mL respectively). TYR and TRP concentrations in rodents have seldomly been reported (Han et al., 2019; Wang et al., 2018), therefore reference concentrations could not be obtained. Despite previous studies not detecting TYR or TRP, we detected TYR and TRP, but the concentrations observed were just below the limit of quantification. Plasma PUT concentrations ranged between 50.0 – 100 ng/mL. These concentration detected were similar to those previously reported in rodents (Wang et al., 2018). SPD concentrations were inferred semi-quantitatively and were  $< 2000$  ng/mL. SPD and SPM concentrations have been reported in plasma at approximately 270 ng/mL and 40 ng/mL respectively (Wang et al., 2018). The other trace amines included in the panel were not detected in plasma despite high sensitivity of the method developed (Limits of quantification: PEA= 1.95 ng/mL, AGM, and SYN = 3.91 ng/mL and T1AM, CAD and OCT = 7.81 ng/mL). Given these low concentrations, these data were excluded from statistical analysis. As a result of the few trace amines detection in plasma, it has limited interpretive value.

Of the panel selected for analysis, only three trace amines (SPM, PUT and CAD) were detected in the brain (Table 6.1). PUT concentration was significantly higher in male than female wistar rats (ANOVA main effect,  $p < 0.01$ ) (Figure 6.1 A), but no effect of DTG was evident for either PUT or CAD (Figure 6.1). SPD concentrations by far exceeded the upper limit of detection.

*Table 6.1: Trace amine concentrations in rodent brain tissue.*

Trace amine	Lower limit of quantification (ng/g)	Concentration range detected (ng/g)
TYR	19.6	N.D
PEA	9.75	N.D
TRP	9.75	N.D
SYN	19.6	N.D
OCT	39.1	N.D
T1AM	39.1	N.D
AGM	19.6	N.D
PUT	156	301 - 621
CAD	39.1	46.5 - 141
SPD	2000	>2000

Abbreviations: N.D, not detected (< limit of quantification).

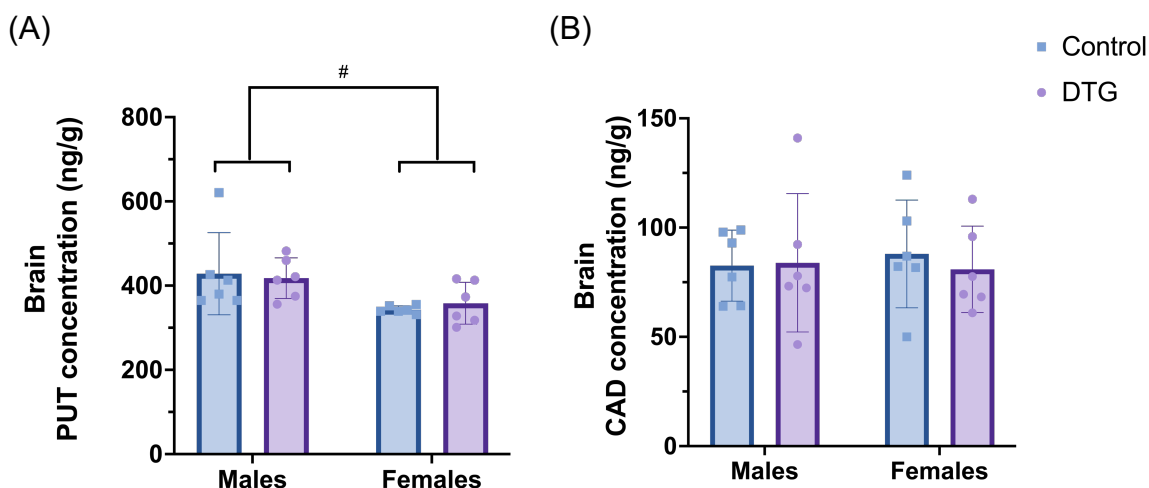
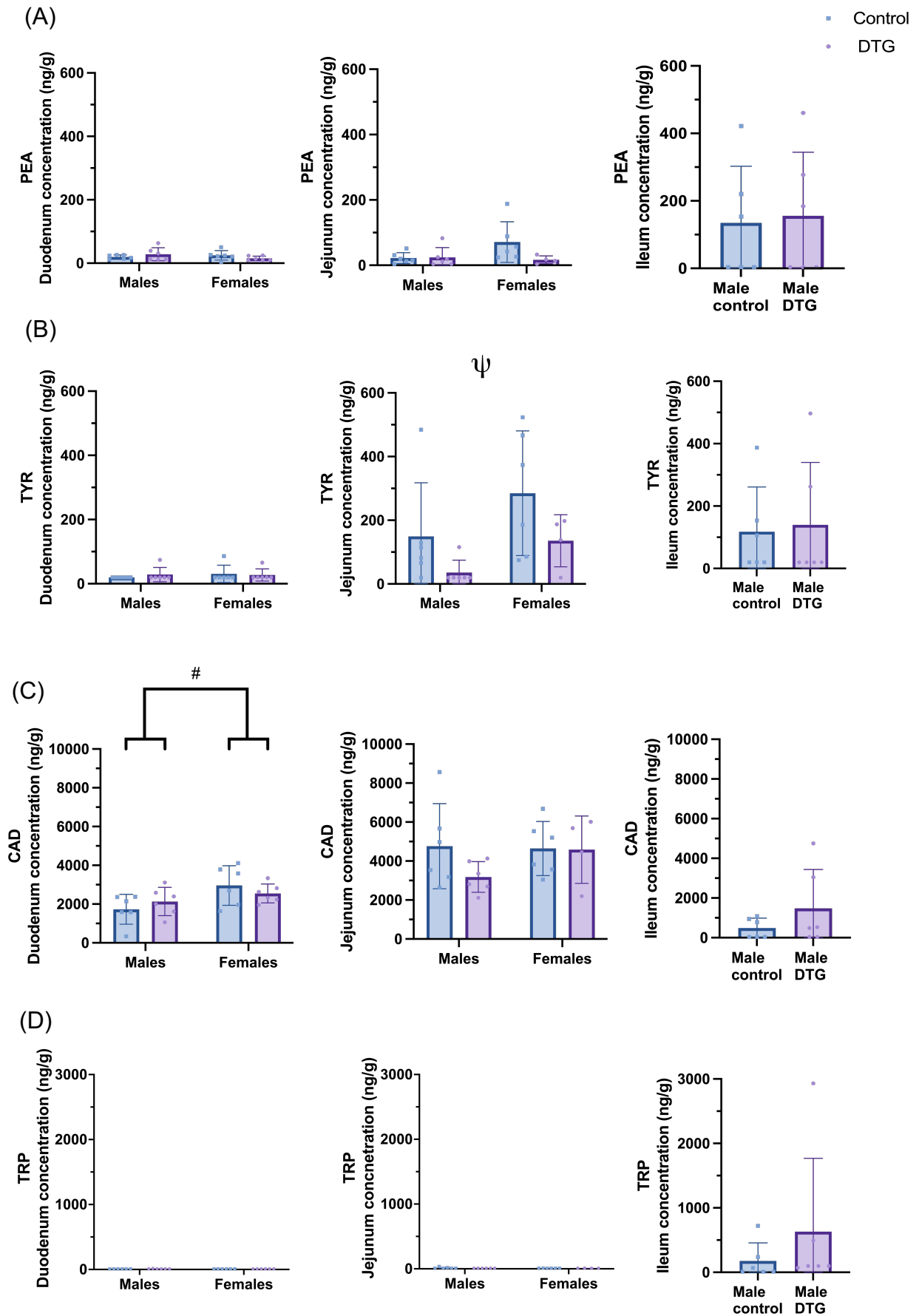


Figure 6.1: (A) PUT and (B) CAD concentrations (ng/g) detected in the brain. Statistical analysis: 2-way ANOVA with Tukey's multiple comparison test. Data are presented as mean  $\pm$  SD,  $n=6$ . # = ANOVA main effect of sex ( $p<0.05$ ).

### 6.3.2 Trace amine presence in the gastrointestinal tract

The highest concentrations of trace amines were detected in the different segments of the small intestines (Figure 6.2), with trace amine concentrations differing significantly between the segments of gut (ANOVA main effect,  $p<0.05$ ). The relatively large inter-individual variability between the concentrations detected could be due to the presence of varying amounts of fecal matter present in the gastrointestinal tissue sample, as GIT samples were not rinsed on collection. The presence of live microbes in fecal matter would allow for continual trace amine secretion until the samples are frozen. Only two trace amines (OCT and T1AM) were not detected in gastrointestinal tissue.

Female rats exhibited a general tendency for higher trace amines levels than male rats, with significantly higher duodenal CAD, PUT and AGM, as well as jejunal AGM concentrations ( $p < 0.05$  for all). Furthermore, jejunal TYR concentrations were significantly higher ( $p < 0.05$ ) in control rats when compared to rats administered DTG.



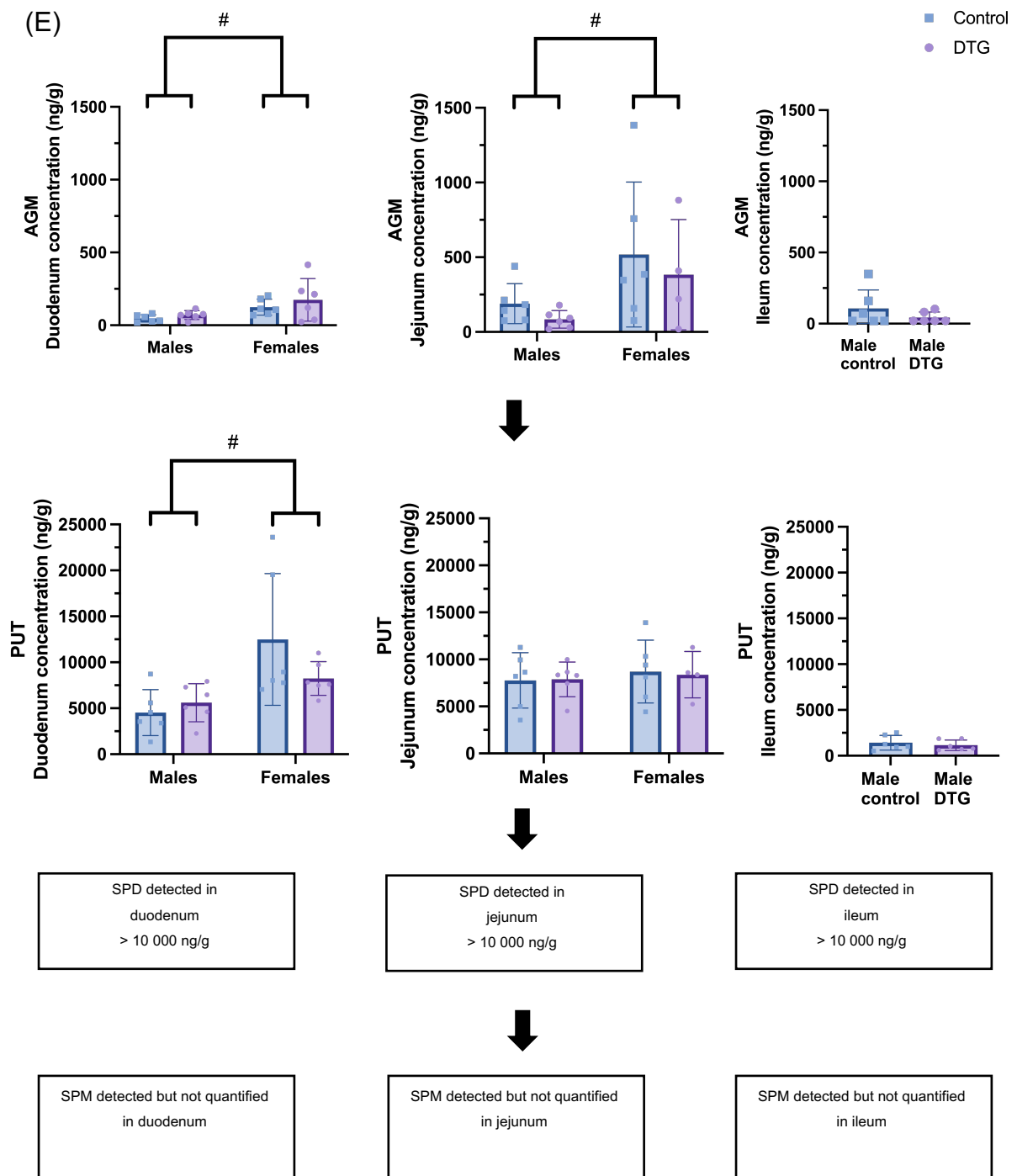


Figure 6.2 (A) PEA, (B) TYR, (C) CAD (D) TRP and (E) AGM and subsequent metabolite concentrations in the different segments of gastrointestinal tract. Data are presented as mean  $\pm$  SD,  $n$  = minimum of 3. Statistical analysis: 2-way ANOVA with Tukey's multiple comparison test on the duodenum and jejunum and Mann Whitney or  $t$  test for the ileum # = ANOVA main effect of sex ( $p < 0.05$ ).  $\psi$  = ANOVA main effect of DTG administration ( $p < 0.05$ ).

### 6.3.3 Urinary trace amine concentrations

The concentration ranges of trace amines detected in the urine are represented in Table 6.2.

*Table 6.2: Summary of trace amine quantification in urine.*

Trace amine	Limit of quantification (ng/mL)	Concentration range detected (ng/mL)
TYR	3.91	66.4 – 1000
PEA	1.95	17.7 – 515
TRP	1.95	2.81 – 85.0
SYN	3.91	16.9 – 89.6
OCT	7.81	N.D
T1AM	7.81	N.D
AGM	3.91	29.1 - 214
PUT	31.25	>1000
CAD	7.81	>1000
SPD	2000	>2000

Figure 6.3 illustrates the effects of sex and DTG on urinary trace amine levels. TRP concentrations were significantly higher in females than males (main ANOVA effect  $p < 0.05$ ) and SYN concentrations were significantly decreased in DTG-administered groups (main ANOVA effect  $p < 0.05$ ). Similar decreases in response to DTG were observed for several other trace amines assessed, but these did not reach statistical significance. OCT and T1AM were not detected in the urine samples. However, OCT is seldomly detected in urine as a result of its rapid metabolism (Hengstmann et al., 1974) and if present ranges reported for OCT have been between 1 – 5 ng/mL (Stohs, 2015) - which explains why OCT was not detected in the current study.

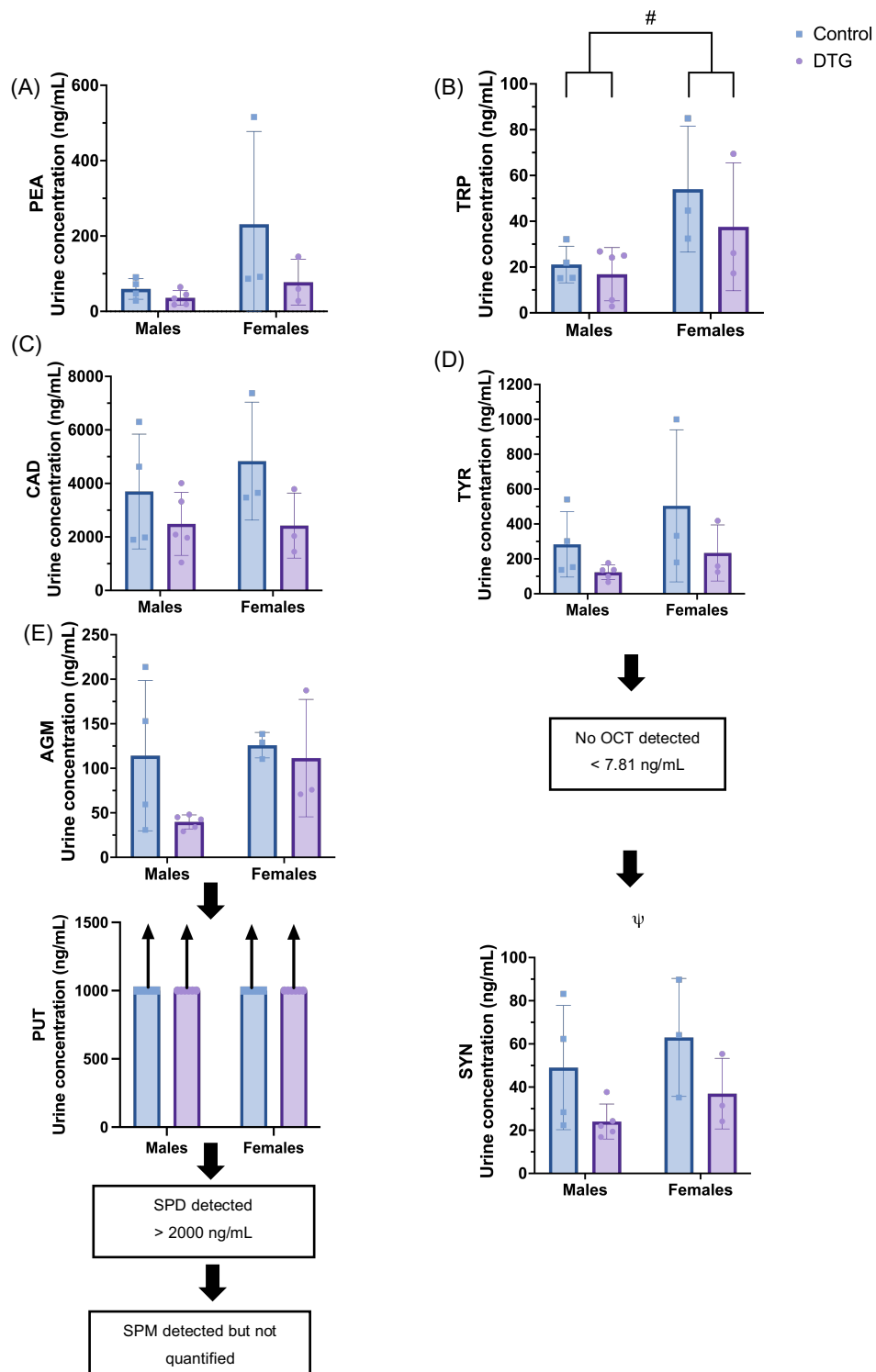


Figure 6.3: Trace amines detected in urine. (A) PEA, (B) TRP, (C) CAD, (D) TYR with subsequent metabolites and (E) AGM with subsequent metabolites. Data are presented as mean  $\pm$  SD,  $n$  = minimum of 3. Statistical analysis: 2-way ANOVA with Tukey's multiple comparison test. # = ANOVA main effect for sex ( $p < 0.05$ ).  $\psi$  = ANOVA main effect of DTG administration ( $p < 0.05$ ).

## 6.4 Discussion

Although the use of rodents on a standardized diet negates confounding effects of dietary trace amines, which is a strength of the current study design, a limitation to data interpretation is the species differences in microbiome composition between rodents and humans. Thus, we refrained here from discussing the absolute concentrations of trace amines detected, instead focusing on the relative abundance of trace amines within specific synthetic pathways. In addition, the relevance of sex- or DTG-associated differences observed for specific trace amines, as the mechanisms involved, are most likely highly conserved across species.

Current data presents novel findings on the effect of sex and DTG administration on the trace amine profile of wistar rats, which may, at least in part, inform on the possible mechanisms at play in a dysregulated trace amine system. Firstly, current data illustrates that polyamines differ significantly between males and females in various matrices. Secondly, the trace amine profile seemed relatively resistant to modulation by DTG, although DTG did have effects on a limited number of trace amines that may have significance. In line with this, we will discuss the findings most relevant to ART-associated adverse events, as well as those trace amines that exhibited sex or DTG dependence in more detail below.

Decreased and increased levels of the same polyamines can result in uniquely different pathologies (Nakanishi and Cleveland, 2021). Given this fact, it is very difficult to assign a specific symptom or characteristic to altered concentration or relative abundance of any specific trace amine. In addition, trace amine concentrations will vary in distinctive compartments, presumably as a result of the different microbial colonies in that compartment and/or the relative abundance of substrate and vital enzymatic catalysts. The absence of certain trace amines from a specific matrix is not necessarily due to degradation during extraction, since most trace amines were detected in at least one of the matrices under investigation. The only potential exception here may be the brain tissue, in which trace amines are known to degrade rapidly (Grandy, 2007). However, since we had additional measures in place to prevent degradation, by working at cold temperatures/ on ice and at an acidic pH to inactivate metabolizing enzymes, poor sample quality is unlikely to be the reason for

failure to detect trace amines. Furthermore, the quantification of various trace amines across multiple compartments with significant sex and DTG differences indicates the validity of the model.

The polyamines (AGM, CAD, PUT, SPD and SPM) were the trace amines most abundantly detected across matrices. Anti-inflammatory responses have been reported as a result of increased production of these polyamines in the gastrointestinal tract and brain (Grosheva et al., 2020; Nakamura et al., 2021; Sharma et al., 2018). AGM - a precursor of PUT - has been demonstrated to attenuate mucosal damage. Interestingly, it was demonstrated that the protective effects decline at higher concentrations (Zádori et al., 2014). This is supported by evidence that AGM's neuroprotective, anti-apoptotic, anti-inflammatory and anti-oxidant properties were only observed at low concentrations (Song et al., 2014; Xu et al., 2017). Of particular relevance to this study, the metabolites produced downstream from AGM metabolism - PUT, SPM and SPD - were consistently detected at higher concentrations than AGM. This potentially suggests that tight regulation of AGM concentrations (to prevent accumulation) could promote metabolite (PUT, SPD and SPM) formation. This notion is supported by previous data from our group, which links disruption of tight junction protein expression and distribution profile to accumulation of AGM in (HT-29) human gut epithelial cells (Pretorius et al., 2022b). Metabolites of AGM (PUT, SPD and SPM) have been demonstrated to accelerate epithelial cell renewal and increase the abundance of anti-inflammatory macrophages (Nakamura et al., 2021). Limited and contradictory data on basal concentration ranges of polyamines in various rat matrices, meant the concentrations detected in this study could not be contextualized. Nonetheless, increased concentrations of these polyamines detected in female rats could be a mechanism by which to mitigate inflammation and oxidative stress. However, the physiological implications of current data are inconclusive and more parameters would need to be assessed in future work. This could not be assessed in the current study as sample volume limitations did not allow for further assessments.

Polyamine concentrations have been reported to be under tight homeostatic control - especially in the brain (Inoue et al., 2013; Makletsova et al., 2022; Murray-Stewart et al., 2018). This tight homeostatic control of CAD and PUT in the brain and the lack of perturbation by DTG is a positive indication that DTG administration possibly does not

contribute to the predisposition of neurological disorders associated with polyamine dysregulation in the brain.  $\gamma$ -Aminobutyric acid (GABA) is the major inhibitory neurotransmitter in the central nervous system (CNS) and a dynamic balance is essential for neuronal functioning (Roy et al., 2018). PUT is a precursor required for the production of GABA via monoamine oxidase B and diamine oxidase (Kovács et al., 2022). Interestingly, higher concentrations of GABA have been detected in females than males in both humans and rodents (Cosgrove et al., 2007; Frankfurt et al., 1984). This could indicate that a greater amount of PUT is converted to GABA, thus explaining why males had a greater concentration of PUT than females. However, a second explanation is that the production of SPD and SPM from PUT metabolism (Makletsova et al., 2022) may have been relatively higher in females. Unfortunately, given the high levels of SPD and SPM, it was not possible to assess sex differences in the levels of these two polyamines. Thus, it would be relevant to elucidate whether PUT concentrations are lower in females due to a higher conversion of PUT to SPM and SPD, or PUT to GABA, or both. This hypothesis would need to be further explored by isolating and quantitating more role players in this pathway from different brain regions to confirm this relationship.

SPD and SPM synthesis cascade has been reported to inhibit cytokine release and inhibit production of reactive oxygen species (Madeo et al., 2018). A dysregulation in the formation of SPD and SPM have both been associated in the pathogenesis of neurological disorders (Ghosh et al., 2020). It has been reported that dysregulation resulting in decreased polyamine concentrations are involved in the pathogenesis of PD (Lewandowski et al., 2010). Supporting this, are reports that increased SPD in an *in-vivo* rotenone-induced PD model reduced proinflammatory cytokines such as TNF- $\alpha$  and IL-1 $\beta$  and inhibited microglial activation (Sharma et al., 2018). These characteristics would suggest that these two polyamines could have neuroprotective effects in the brain, as well as beneficial effects in terms of oxidative stress and inflammation, given the well-known link between these two mechanisms. Conversely, it has been speculated that decreased concentrations of SPD could have major implications in the regulation of mitochondrial metabolism in the brain and this could lead to neurodegeneration and neuroinflammation (Connell et al., 2022; Misrani et al., 2021; Simpson and Oliver, 2020) However, due to poor recovery of SPD and SPM in

the current multi-analyte analytical protocol for trace amine determination – which was necessary due to the extremely limited sample size obtained from rats - we could not accurately determine the response of SPM and SPD to either sex or DTG. A follow up study using an improved extraction method with consistent recoveries of SPD and SPM is required to inform on this unavoidable limitation in the current study.

Sex effects were not as prominent in the archetypal trace amines in any of the matrices investigated. Despite this, there were significantly higher urine concentrations of TRP in female than male rats. This observation supports our earlier report of *Lactobacilli* monocultures producing more TRP in the presence of oestrogen (Pretorius et al., 2022a). Moreover, it has been reported that the female urinary microbiome is dominated by the *Lactobacilli* genus (Brubaker and Wolfe, 2017). This could potentially explain the sex difference seen with greater TRP concentrations in females. Interestingly, in another study it was demonstrated that bacterially derived TRP in female mice resulted in increased mucus production which had a positive effect of preventing barrier disruption (Bhattarai et al., 2020). Despite detecting TRP in male ileac tissue, the smaller size of ileac tissue mass excised from females meant ileac TRP concentrations could not be determined. In addition, due to the low concentrations of TRP in the duodenum and jejunum the effect of DTG could not be determined in either of these sections. However, given the beneficial effects of TRP, it is a positive outcome that DTG does not seem to disrupt TRP production in either males or females.

Turning attention to observed DTG effects, clear and consistent treatment effects were observed in both urine and GIT tissues. Generally, trace amine concentrations seemed lower in the DTG group when compared to the control group, although only reaching statistical significance for TYR and SYN. This trend was most notable in the trace amines detected in urine formed via the AADC enzymes. Interestingly, it has been reported that AADC activity increases along the small intestine with the greatest activity in the jejunum (Schultz, 1991). Some of the trace amines formed by AADC enzymes include TYR, PEA, TRP, AGM and CAD. Considering that this trend is seen in all AADC-dependent trace amines assessed in the urine and jejunum, it is possible that DTG inhibits or decreases the activity of the AADC enzyme. Of relevance to the HIV context, a reduction in AADC activity has been reported in the non-HIV literature

to be linked to neurological symptoms such as behavioral disorders, mood disturbances, insomnia and gastrointestinal symptoms (Gostner et al., 2015), all of which are adverse events ascribed to DTG use (de Boer et al., 2016; Hoffmann et al., 2017). Furthermore, given the central role of AADC in cellular redox status (Meiser et al., 2013) which is also dysregulated in HIV, the possibility of DTG-induced reduction of AADC function should be further elucidated in purpose designed studies.

In line with this, decarboxylation of L-tyrosine via AADC forms TYR (Boulton and Wu, 1973, 1972). TYR can subsequently undergo hydroxylation via dopamine- $\beta$ -hydroxylase to form OCT (Berry, 2004; Christian and Berry, 2018; Khan and Nawaz, 2016). Furthermore, OCT serves as a precursor for SYN which readily forms from the methylation of OCT by PNMT (Eagles and Iqbal, 1974; Rossato et al., 2011). SYN was the only trace amine in urine which was significantly lower in the DTG administered group vs controls. Since SYN is the last metabolite in the tyrosine metabolic pathway in our panel, this possibly indicates a tyrosine dysregulation. Under the assumption that DTG does affect AADC enzyme activity, there would be high likelihood of noticeable dysregulation in the tyrosine metabolic pathway. This supports our interpretation of a dysfunction in tyrosine metabolism from DTG administration.

In addition to TYR, AADC enzyme activity is also involved in the kynurenine pathway in the metabolism of tryptophan. Similarly to tyrosine forming TYR, tryptophan undergoes decarboxylation via AADC to form TRP (Gainetdinov et al., 2018). Dysregulation in either of these amino acid metabolic pathways have negative implications for neurotransmitter formation (Gostner et al., 2015). Decreased AADC activity can result in decreased DA production from TYR and reduced 5-HT from TRP. In addition, decreased AADC activity would result in increased concentrations of intermediate metabolites in other pathways considering metabolism is directed away from trace amine formation. For example, if metabolism of tryptophan is directed away from TRP formation, the additional tryptophan can be converted to kynurenine and subsequently kynurenic acid (KYNA) (Fukuwatari, 2020). Interestingly, increased KYNA concentrations have been reported to reversibly reduce extracellular DA and GABA to less than 50% of baseline concentrations (Beggiato et al., 2014; Rassoulpour et al., 2005). Reduction in GABA and DA have been demonstrated to result in

depression, generalized anxiety disorder and panic disorder (de Leon and Tadi, 2023). Many patients using DTG have experienced neuropsychiatric side effects which commonly result from decreased GABA and DA (de Boer et al., 2016; Hoffmann et al., 2017; Povar-Echeverría et al., 2021; Todd et al., 2017). Considering that PLWH using DTG typically present with neuropsychiatric symptoms such as anxiety and depression (both associated with decreased neurotransmitter levels (de Leon and Tadi, 2023; Fettiplace et al., 2017)), this supports our current hypothesis of decreased trace amine formation by DTG-associated reduction in AADC activity. These mechanisms could possibly explain the long-term complications seen in HIV patients on ART and warrants further investigation.

In summary, we have illustrated that a dysfunction in the flux of specific trace amine synthesis pathways (e.g. TYR-OCT-SYN) following DTG administration, can have a negative impact on concentrations of downstream metabolites. This disturbed metabolism can negatively impact neuropsychimmunological signaling and thus contribute to the already vulnerable (patho)physiology seen in HIV-associated neuropsychiatric symptoms (Gostner et al., 2015). We hypothesize that this could be due to modulation of AADC enzyme activity by DTG. However, further analysis into more analytes involved in this mechanism of action is required. We have further illustrated that the trace aminergic system – specifically the concentrations of polyamines panel – are dependent on both sex and DTG administration.

## 6.5 Conclusion

Taken together, current data presented expands on the available literature by illustrating concentrations of various trace amines in different wistar rats biological matrices. In addition, we demonstrated statistically significant differences in trace amines profiles between male and female wistar rats. Furthermore, current data suggests that DTG may directly result in decreased concentrations of trace amines, potentially by decreasing activity of AADC. Contextualization of current data with HIV- and general inflammation literature, suggest that altered trace amine signaling potentially contribute to the development of neuropsychiatric and gastrointestinal adverse events associated with DTG administration. These data warrant further

investigations into potential trace amine mechanisms in this context, as well as translation from a rodent model into human patients.

## Chapter 7: Synthesis

HIV/AIDS is still a global health crisis. Most new infections are in LMIC and most of these are in women and young girls (Joint United Nations Programme on HIV/AIDS, 2021). It is well known that HIV itself has a broad impact on the nervous system and GIT. Despite the improvements in HIV therapies, neurocognitive and gastrointestinal disorders still remain prevalent among PLWH (De Almeida, 2015; George and Asmuth, 2014; Pinto-Cardoso et al., 2018; Spudich and González-Scarano, 2012; Stern et al., 2018), suggesting that exacerbation of these disorders can – at least in part – be ascribed to the ART themselves. Adverse effects associated with ART treatment are negatively impacting the quality of life of PLWH. Specifically, females have been reported to be more susceptible to develop adverse events associated with ART (Geretti et al., 2017). Seeing that these individuals are already predisposed for comorbidities and mortalities, adverse events resulting from treatment only add to their burden of disease. It is therefore necessary to understand the side effects of ART and potentially elucidate the mechanism behind DTG associated side effects. However, I acknowledge the limitation of investigating the potential side effects of DTG without the confounding factors associated with HIV infection.

To the best of our knowledge, the role of a dysregulated trace aminergic system has not been investigated in the context of HIV/DTG. As previously mentioned in the formal hypothesis statement, investigation into the ability of DTG to modulate the trace aminergic system was warranted.

Considering these unknowns, the novelty of this dissertation is evidenced by the following main findings which contributed significantly to current knowledge about DTG and trace amines. Firstly, I have demonstrated that DTG does indeed accumulate in multiple tissue compartments following chronic administration of a human equivalent dose of DTG in wistar rats (Chapter 4). Secondly, I demonstrated that chronic administration of DTG altered the trace amine profile in urine and the gastrointestinal tract (Chapter 6). Moreover, sex played an important role, with females exhibiting generally higher polyamine concentrations than male wistar rats. Despite differences in microbiome composition between rodents and humans, the differences observed for sex- or DTG-associated changes in the trace amines, remain relevant as

the mechanisms involved in formation and degradation of trace amines are most likely conserved across species.

In terms of methodology, determination of DTG accumulation across various compartments, required a sensitive LC-MS/MS method. Even though methods for extraction of DTG from plasma have been developed, I expanded on the available literature to include multiple tissue matrices. Due to the lack of published, detailed methods describing DTG extraction from tissue matrices, I developed a novel extraction method combining protein precipitation and hydrophilic-lipophilic balanced (HLB) cartridges (Chapter 3). These methods were evaluated in terms of selectivity for DTG, linearity, recovery and matrix effects. During method development, I encountered several analytical hurdles and thus describe the increased carry-over observed from tissue in comparison to plasma and discuss solutions for mitigating this problem. In addition, I also provide evidence for the importance of matrix-matched calibration standards and QCs, which has been a limitation to previous methods describing DTG quantitation in tissue. Furthermore, I used these developed methods to determine relationships between DTG concentration in different compartments (Chapter 4). I have indicated that plasma concentration of DTG is directly correlated to liver and muscle concentrations, but not adipose. Currently I propose that the lack of correlation between DTG levels in adipose vs plasma may suggest that the 12-week administration of DTG dysregulated the adipose protein profile, and thus DTG binding in this tissue. This would suggest that adipose tissue could be more vulnerable to an inflammatory outcome in response to DTG. However, further data will be required to determine this hypothesis. Although no sex-differences in adipose DTG levels was observed in the current study, I acknowledge that a rodent model may not be the ideal model for adipose-related studies on sex differences in this context. This is due to human females having a higher percentage body fat accumulation than human males and in rats the males exhibit this higher percentage body fat accumulation. Moreover, it was demonstrated that the consistent trend of higher DTG in smaller body size may suggest that individuals of smaller stature may be exposed to relatively greater DTG concentrations both in circulation and at tissue level, when administered the same dose as individuals with relatively larger body size, irrespective of sex. While DTG is commonly administered as a FDC, these findings have indicated primary risks that can be ascribed to DTG itself – which is not possible when using multi-drug treatment

protocols. In addition, the data generated may aid in providing evidence for DTG dose adjustments based on body mass.

To further our understating of the dysregulation caused by DTG – specifically inflammatory related dysregulation – I proposed that adverse events may be caused by DTG modulation of the trace aminergic system. In order to determine this, I had to develop an LC-MS/MS method that was sensitive enough to detect trace concentrations of multiple trace amines. However, developing an analytical method to quantify endogenous analytes did have several complex aspects. Firstly, the limitations of sample size obtained from rats required a single extraction method and multi-analyte determination protocol. Secondly, due to the endogenous presence of trace amines in the matrix, calibration standards had to be prepared in solvent instead of authentic matrix. For this reason, potential matrix effects could also not be evaluated in the traditional manner. Despite these limitations, I successfully developed two separate chromatographic methods and one SPE method to quantify a panel of nine trace amines. The calibration ranges developed were in line with a previously reported method but also improved on other available methods (Langner et al., 2022; Wang et al., 2018). Continuing onto my final trace amine component of the study, I used the collected rodent samples, and the LC-MS/MS methods developed (Chapter 5) to determine the effects of chronic DTG administration on the trace amine profile in various compartments (Chapter 6). The main findings of this study included the demonstration that DTG administration altered the urinary and gastrointestinal trace amine profile. We demonstrated that DTG decreased trace amine concentrations – specifically trace amines formed by AADC enzymes activity. This suggests that DTG may be inhibiting trace amine synthesis. Moreover, sex differences were illustrated - specifically that higher polyamine concentrations were detected in females. Considering the role these polyamines play in inflammatory responses it warrants further investigation.

Taken together, these data support my stated hypothesis. Firstly, in terms of the first hypothesis, current results demonstrated sensitive methods developed to enable quantitation of trace amounts of both DTG and trace amines in various matrices. Furthermore, our *in vivo* DTG administration protocol in wistar rats demonstrated that

following chronic administration DTG does accumulate in various tissues. In addition, DTG did alter the trace amine content in specific compartments.

With regard to future perspectives, some main areas of interest have emerged from the current studies. Firstly, we illustrated a lack of LC-MS/MS methods for quantifying DTG in tissue matrices following an *in vivo* study. Even though I describe the development of a robust extraction and LC-MS/MS method for DTG quantification in tissue (chapter 3), the method was not validated according to FDA guidelines, as the study was pre-clinical in nature. However, I suggest that when translating this protocol for human sample the methods developed should be validated according to FDA or European Medicine Agency (EMA) bioanalytical method validation guidelines. In addition, determine if human tissue samples cross-validate these animal tissue samples as this would reduce the need for human matrix collection if a human study were to follow.

Secondly, considering the fact that male rats weighed significantly more than female rats (approximately 60% more in the current study), we probably achieved a larger effect size than what is likely possible to achieve in human cohorts (Chapter 4). Therefore, I suggest that the implications of body mass differences in DTG treatment should be investigated in human populations in future work. This would illustrate if body weight does impact pharmacokinetic parameters and if dose adjustments should be considered (Geretti et al., 2017). Furthermore, relevant to the dysregulation we demonstrated in rat adipose tissue (Chapter 4), I suggest that parallel analysis of subcutaneous and visceral adipose DTG levels is required before the significance of the current result can be fully interpreted in terms of risk for adverse outcome. In addition, I suggest that the mechanism of action behind the lack of correlation between DTG levels in adipose vs plasma, could be a dysregulated adipose protein profile. Due to the lack of sex-differences in adipose DTG levels, the current study suggests a rodent model may not be ideal for adipose-related studies on sex differences in this context. Proteomics analysis of adipose protein profile in humans treated with DTG may shed more light on this possibility. It would be interesting if future studies could evaluate the effect of DTG on the protein profile on adipose tissue to determine if adipose tissue could be more vulnerable to an inflammatory outcome in response to DTG.

Thirdly, given the lack of consensual guidelines for developing an analytical method quantifying endogenous analytes and the observed difference between quality control samples in solvent and those in authentic matrix (Chapter 5), I suggest future trace amine work should be conducted in a surrogate matrix. The surrogate matrix could be prepared by diluting the authentic matrix to the extent that the endogenous concentrations of trace amines would not affect the accuracies, but matrix constituents are still present. In addition, we suggest working with larger animal model to increase the sample size/volume collected per individual so that a full calibration curve and set of quality control samples could be prepared in the matrix obtained from one individual. This would enable determining average endogenous concentrations present and using a standard addition method to calculate accuracies of standards. Moreover, I suggest that the extraction method be revised to allow accurate quantification of both SPD and SPM. As illustrated in Chapter 2, these polyamines have been extracted before and their inclusion in the panel would be very beneficial, however due to lack of sample and the cost of additional equipment required we could not achieve this.

Finally, given the reported anti-inflammatory effects of polyamine in the brain and GIT (Grosheva et al., 2020; Nakamura et al., 2021; Sharma et al., 2018) I suggest future studies investigate inflammatory and redox markers in conjunction with AGM, PUT, SPD and SPM concentrations following DTG administration. This may shed light on the direct effects on the inflammatory response associated with a dysregulated trace amine panel following DTG administration. In addition, I suggest that inhibition of AADC by DTG may be the possible mechanism of action for the decreased concentrations of trace amines observed (Chapter 6). I recommend that the effect of DTG (and potentially other ARTs) on AADC enzyme activity should be assessed in purpose designed protocols. If such studies indeed confirm this interpretation, trace amine deficiencies as a result of DTG can potentially be corrected therapeutically by exogenous supplementation. Although trace amine supplementation was beyond the scope of this dissertation, the therapeutic intervention of exogenous trace amines warrants further investigation in future studies.

In conclusion, current data suggest a link between DTG treatment and dysregulated trace amine profile, which aligns with neurological and gastrointestinal disorders

prevalent in PLWH and using DTG. This dissertation furthers our understating of DTG accumulation in tissue and the difference between DTG distribution in various tissues, as well as highlights the importance of body size and the implications on circulating concentrations of DTG. It highlights previously unknown interactions between DTG and the trace aminergic system. While current findings demonstrated these effects in rodents, the novelty and importance of findings reported, warrants translation of this work into a human population.

## Chapter 8: References

- Assimakopoulos, S.F., Dimitropoulou, D., Marangos, M., Gogos, C.A., 2014. Intestinal barrier dysfunction in HIV infection : pathophysiology , clinical implications and potential therapies. *Infection* 42, 951–959. <https://doi.org/10.1007/s15010-014-0666-5>
- Avedissian, S.N., Dyavar, S.R., Fox, H.S., Fletcher, C. V, 2020. Pharmacologic approaches to HIV-associated neurocognitive disorders. *Curr. Opin. Pharmacol.* 54, 102–108. <https://doi.org/10.1016/j.coph.2020.09.003>
- Babusyte, A., Kotthoff, M., Fiedler, J., Krautwurst, D., 2013. Biogenic amines activate blood leukocytes via trace amine-associated receptors TAAR1 and TAAR2. *J. Leukoc. Biol.* 93, 387–394. <https://doi.org/10.1189/jlb.0912433>
- Bailly, F., Cotelle, P., 2015. The preclinical discovery and development of dolutegravir for the treatment of HIV. *Expert Opin. Drug Discov.* 10, 1243–1253. <https://doi.org/10.1517/17460441.2015.1064896>
- Barbieri, F., Montanari, C., Gardini, F., Tabanelli, G., 2019. Biogenic amine production by lactic acid bacteria: A review. *Foods* 8, 1–27. <https://doi.org/10.3390/foods8010017>
- Barcelo, C., Aouri, M., Courlet, P., Guidi, M., Braun, Dominique L., Günthard, Huldrych F., Pisco, R.J., Cavassini, Matthias, Buclin, T., Decosterd, L.A., Csajka, C., Anagnostopoulos, A., Battegay, M., Bernasconi, E., Böni, J., Braun, D. L., Bucher, H.C., Calmy, A., Cavassini, M., Ciuffi, A., Dollenmaier, G., Egger, M., Elzi, L., Fehr, J., Fellay, J., Furrer, H., Fux, C.A., Günthard, H. F., Haerry, D., Hasse, B., Hirsch, H.H., Hoffmann, M., Hösli, I., Huber, M., Kahlert, C.R., Kaiser, L., Keiser, O., Klimkait, T., Kouyos, R.D., Kovari, H., Ledergerber, B., Martinetti, G., Martinez de Tejada, B., Marzolini, C., Metzner, K.J., Müller, N., Nicca, D., Paioni, P., Pantaleo, G., Perreau, M., Rauch, A., Rudin, C., Scherrer, A.U., Schmid, P., Speck, R., Stöckle, M., Tarr, P., Trkola, A., Vernazza, P., Wandeler, G., Weber, R., Yerly, S., 2019. Population pharmacokinetics of dolutegravir: influence of drug–drug interactions in a real-life setting. *J. Antimicrob. Chemother.* 74, 2690–2697. <https://doi.org/10.1093/jac/dkz217>
- Bardócz, S., Grant, G., Brown, D.S., Pusztai, A., 1998. Putrescine as a source of instant energy in the small intestine of the rat. *Gut* 42, 24–28. <https://doi.org/10.1136/gut.42.1.24>

- Beggiato, S., Tanganelli, S., Fuxe, K., Antonelli, T., Schwarcz, R., Ferraro, L., 2014. Endogenous kynurenic acid regulates extracellular GABA levels in the rat prefrontal cortex. *Neuropharmacology* 82, 11–18. <https://doi.org/10.1016/j.neuropharm.2014.02.019>
- Bekebrede, A.F., Keijer, J., Gerrits, W.J.J., Boer, V.C.J. de, 2020. The Molecular and Physiological Effects of Protein-Derived Polyamines in the Intestine. *Nutrients* 12, 197. <https://doi.org/10.3390/nu12010197>
- Bennetto-Hood, C., Tabolt, G., Savina, P., Acosta, E.P., 2014. A sensitive HPLC-MS/MS method for the determination of dolutegravir in human plasma. *J. Chromatogr. B Anal. Technol. Biomed. Life Sci.* 945–946, 225–232. <https://doi.org/10.1016/j.jchromb.2013.11.054>
- Berry, M.D., 2004. Mammalian central nervous system trace amines. Pharmacologic amphetamines, physiologic neuromodulators. *J. Neurochem.* 90, 257–271. <https://doi.org/10.1111/j.1471-4159.2004.02501.x>
- Berry, M.D., Gainetdinov, R.R., Hoener, M.C., Shahid, M., 2017. Pharmacology of human trace amine-associated receptors: Therapeutic opportunities and challenges. *Pharmacol. Ther.* 180, 161–180. <https://doi.org/10.1016/j.pharmthera.2017.07.002>
- Berry, M.D., Juorio, A. V., Li, X.M., Boulton, A.A., 1996. Aromatic L-amino acid decarboxylase: A neglected and misunderstood enzyme. *Neurochem. Res.* 21, 1075–1087. <https://doi.org/10.1007/BF02532418>
- Bhattarai, Y., Jie, S., Linden, D.R., Ghatak, S., Mars, R.A.T., Williams, B.B., Pu, M., Sonnenburg, J.L., Fischbach, M.A., Farrugia, G., Sha, L., Kashyap, P.C., 2020. Bacterially Derived Tryptamine Increases Mucus Release by Activating a Host Receptor in a Mouse Model of Inflammatory Bowel Disease. *iScience* 23, 101798. <https://doi.org/10.1016/j.isci.2020.101798>
- Bhattarai, Y., Williams, B.B., Battaglioli, E.J., Whitaker, W.R., Till, L., Grover, M., Linden, D.R., Akiba, Y., Kandimalla, K.K., Zachos, N.C., Kaunitz, J.D., Sonnenburg, J.L., Fischbach, M.A., Farrugia, G., Kashyap, P.C., 2018. Gut Microbiota-Produced Tryptamine Activates an Epithelial G-Protein-Coupled Receptor to Increase Colonic Secretion. *Cell Host Microbe* 23, 775-785.e5. <https://doi.org/10.1016/j.chom.2018.05.004>
- Borowsky, B., Adham, N., Jones, K.A., Raddatz, R., Artymyshyn, R., Ogozalek, K.L., Durkin, M.M., Lakhani, P.P., Bonini, J.A., Pathirana, S., Boyle, N., Pu, X.,

- Kouranova, E., Lichtblau, H., Ochoa, F.Y., Branchek, T.A., Gerald, C., 2001. Trace amines: Identification of a family of mammalian G protein-coupled receptors. *Proc. Natl. Acad. Sci. U. S. A.* 98, 8966–8971. <https://doi.org/10.1073/pnas.151105198>
- Boulton, A.A., 1991. Phenylethylaminergic modulation of catecholaminergic neurotransmission. *Prog. Neuro-Psychopharmacology Biol. Psychiatry* 15, 139–156. [https://doi.org/10.1016/0278-5846\(91\)90076-D](https://doi.org/10.1016/0278-5846(91)90076-D)
- Boulton, A.A., 1974. Amines and Theories in Psychiatry. *Lancet* 304, 52–53. [https://doi.org/10.1016/S0140-6736\(74\)91390-7](https://doi.org/10.1016/S0140-6736(74)91390-7)
- Boulton, A.A., Wu, P.H., 1973. Biosynthesis of Cerebral Phenolic Amines. II. In Vivo Regional Formation of p -Tyramine and Octopamine from Tyrosine and Dopamine. *Can. J. Biochem.* 51, 428–435. <https://doi.org/10.1139/o73-050>
- Boulton, A.A., Wu, P.H., 1972. Biosynthesis of Cerebral Phenolic Amines. I. In Vivo Formation of p -Tyramine, Octopamine, and Synephrine. *Can. J. Biochem.* 50, 261–267. <https://doi.org/10.1139/o72-037>
- Bourgi, K., Rebeiro, P.F., Turner, M., Castilho, J.L., Hulgan, T., Raffanti, S.P., Koethe, J.R., Sterling, T.R., 2020. Greater Weight Gain in Treatment-naive Persons Starting Dolutegravir-based Antiretroviral Therapy. *Clin. Infect. Dis.* 70, 1267–1274. <https://doi.org/10.1093/cid/ciz407>
- Braulke, L.J., Klingenspor, M., DeBarber, A., Tobias, S.C., Grandy, D.K., Scanlan, T.S., Heldmaier, G., 2008. 3-Iodothyronamine: A novel hormone controlling the balance between glucose and lipid utilisation. *J. Comp. Physiol. B Biochem. Syst. Environ. Physiol.* 178, 167–177. <https://doi.org/10.1007/s00360-007-0208-x>
- Bräunig, J., Dinter, J., Höfig, C.S., Paisdzior, S., Szczepek, M., Scheerer, P., Rosowski, M., Mittag, J., Kleinau, G., Biebermann, H., 2018. The trace amine-associated receptor 1 agonist 3-iodothyronamine induces biased signaling at the serotonin 1b receptor. *Front. Pharmacol.* 9, 1–11. <https://doi.org/10.3389/fphar.2018.00222>
- Brenchley, J.M., Douek, D.C., 2008. HIV infection and the gastrointestinal immune system. *Mucosal Immunol.* 1, 23–30. <https://doi.org/10.1038/mi.2007.1>
- Broadley, K.J., 2010. The vascular effects of trace amines and amphetamines. *Pharmacol. Ther.* 125, 363–375. <https://doi.org/10.1016/j.pharmthera.2009.11.005>

- Broadley, K.J., Akhtar Anwar, M., Herbert, A.A., Fehler, M., Jones, E.M., Davies, W.E., Kidd, E.J., Ford, W.R., 2009. Effects of dietary amines on the gut and its vasculature. *Br. J. Nutr.* 101, 1645–1652.  
<https://doi.org/10.1017/S0007114508123431>
- Broder, S., Gallo, R.C., 1984. A Pathogenic Retrovirus (HTLV-III) Linked to AIDS. *N. Engl. J. Med.* 311, 1292–1297. <https://doi.org/10.1056/NEJM198411153112006>
- Brubaker, L., Wolfe, A.J., 2017. The Female Urinary Microbiota/Microbiome: Clinical and Research Implications. *Rambam Maimonides Med. J.* 8, e0015.  
<https://doi.org/10.5041/RMMJ.10292>
- Buckley, S., Byrnes, S., Cochrane, C., Roche, M., Estes, J.D., Selemidis, S., Angelovich, T.A., Churchill, M.J., 2021. The role of oxidative stress in HIV-associated neurocognitive disorders. *Brain, Behav. Immun. - Heal.* 13, 100235.  
<https://doi.org/10.1016/j.bbih.2021.100235>
- Bunzow, J.R., Sonders, M.S., Arttamangkul, S., Harrison, L.M., Zhang, G., Quigley, D.I., Darland, T., Suchland, K.L., Pasumamula, S., Kennedy, J.L., Olson, S.B., Magenis, R.E., Amara, S.G., Grandy, D.K., 2001. Amphetamine, 3,4-Methylenedioxymethamphetamine, Lysergic Acid Diethylamide, and Metabolites of the Catecholamine Neurotransmitters Are Agonists of a Rat Trace Amine Receptor. *Mol. Pharmacol.* 60, 1181–1188.  
<https://doi.org/10.1124/mol.60.6.1181>
- Butt, A.A., McGinnis, K., Rodriguez-Barradas, M.C., Crystal, S., Simberkoff, M., Goetz, M.B., Leaf, D., Justice, A.C., 2009. HIV infection and the risk of diabetes mellitus. *Aids* 23, 1227–1234. <https://doi.org/10.1097/QAD.0b013e32832bd7af>
- Cahn, P., Pozniak, A.L., Mingrone, H., Shuldyakov, A., Brites, C., Andrade-Villanueva, J.F., Richmond, G., Buendia, C.B., Fourie, J., Ramgopal, M., Hagins, D., Felizarta, F., Madruga, J., Reuter, T., Newman, T., Small, C.B., Lombaard, J., Grinsztejn, B., Dorey, D., Underwood, M., Griffith, S., Min, S., 2013. Dolutegravir versus raltegravir in antiretroviral-experienced, integrase-inhibitor-naïve adults with HIV: Week 48 results from the randomised, double-blind, non-inferiority SAILING study. *Lancet* 382, 700–708.  
[https://doi.org/10.1016/S0140-6736\(13\)61221-0](https://doi.org/10.1016/S0140-6736(13)61221-0)
- Capeau, J., Bouteloup, V., Katlama, C., Bastard, J.P., Guiyedi, V., Salmon-Ceron, D., Protopopescu, C., Leport, C., Raffi, F., Chêne, G., 2012. Ten-year diabetes incidence in 1046 HIV-infected patients started on a combination antiretroviral

- treatment. *Aids* 26, 303–314. <https://doi.org/10.1097/QAD.0b013e32834e8776>
- Carpéné, C., Galitzky, J., Fontana, E., Atgié, C., Lafontan, M., Berlan, M., 1999. Selective activation of  $\beta$ 3-adrenoceptors by octopamine: Comparative studies in mammalian fat cells. *Naunyn. Schmiedeberg's Arch. Pharmacol.* 359, 310–321. <https://doi.org/10.1007/PL00005357>
- Castagna, A., Maggiolo, F., Penco, G., Wright, D., Mills, A., Grossberg, R., Molina, J.M., Chas, J., Durant, J., Moreno, S., Doroana, M., Ait-Khaled, M., Huang, J., Min, S., Song, I., Vavro, C., Nichols, G., Yeo, J.M., 2014. Dolutegravir in antiretroviral-experienced patients with raltegravir- and/or elvitegravir-resistant HIV-1: 24-week results of the phase III VIKING-3 study. *J. Infect. Dis.* 210, 354–362. <https://doi.org/10.1093/infdis/jiu051>
- Center for Disease Control, 1981a. Pneumocystis Pneumonia --- Los Angeles. *Morb. Mortal. Wkly. Rep.* 30.
- Center for Disease Control, 1981b. Kaposi's Sarcoma and Pneumocystis Pneumonia Among Homosexual Men —New York City and California. *Morb. Mortal. Wkly. Rep.* 30, 305–308.
- Center for Disease Control, 1981c. Follow-Up on Kaposi's Sarcoma and Pneumocystis Pneumonia. *Morb. Mortal. Wkly. Rep.* 30, 409–420.
- Chow, B.W., Gu, C., 2015. The Molecular Constituents of the Blood-Brain Barrier. *Trends Neurosci.* 38, 598–608. <https://doi.org/10.1016/j.tins.2015.08.003>
- Christian, S.L., Berry, M.D., 2018. Trace Amine-Associated Receptors as Novel Therapeutic Targets for Immunomodulatory Disorders. *Front. Pharmacol.* 9. <https://doi.org/10.3389/fphar.2018.00680>
- Cid-Silva, P., Llibre, J.M., Fernández-Bargiela, N., Margusino-Framiñán, L., Balboa-Barreiro, V., Pernas-Souto, B., Martín-Herranz, I., Castro-Iglesias, Á., Poveda, E., 2017. Clinical Experience with the Integrase Inhibitors Dolutegravir and Elvitegravir in HIV-infected Patients: Efficacy, Safety and Tolerance. *Basic Clin. Pharmacol. Toxicol.* 121, 442–446. <https://doi.org/10.1111/bcpt.12828>
- Clifford, D.B., Ances, B.M., 2013. HIV-associated neurocognitive disorder. *Lancet Infect. Dis.* 13, 976–986. [https://doi.org/10.1016/S1473-3099\(13\)70269-X](https://doi.org/10.1016/S1473-3099(13)70269-X)
- Clinicians Society, S.H., 2013. Fixed-dose combination for adults accessing antiretroviral therapy. *South. Afr. J. HIV Med.* 14. <https://doi.org/10.7196/sajhivmed.913>
- Clotet, B., Feinberg, J., Van Lunzen, J., Khuong-Josses, M.A., Antinori, A., Dumitru,

- I., Pokrovskiy, V., Fehr, J., Ortiz, R., Saag, M., Harris, J., Brennan, C., Fujiwara, T., Min, S., 2014. Once-daily dolutegravir versus darunavir plus ritonavir in antiretroviral-naive adults with HIV-1 infection (FLAMINGO): 48 week results from the randomised open-label phase 3b study. *Lancet* 383, 2222–2231. [https://doi.org/10.1016/S0140-6736\(14\)60084-2](https://doi.org/10.1016/S0140-6736(14)60084-2)
- Connell, E., Le Gall, G., Pontifex, M.G., Sami, S., Cryan, J.F., Clarke, G., Müller, M., Vauzour, D., 2022. Microbial-derived metabolites as a risk factor of age-related cognitive decline and dementia. *Mol. Neurodegener.* 17, 1–26. <https://doi.org/10.1186/s13024-022-00548-6>
- Correa, A., Monteiro, P., Calixto, F., d’Arc Lyra Batista, J., de Alencar Ximenes, R.A., Montarroyos, U.R., 2020. Dolutegravir: Virologic response and tolerability of initial antiretroviral regimens for adults living with HIV. *PLoS One* 15, 1–10. <https://doi.org/10.1371/journal.pone.0238052>
- Cory, T.J., Schacker, T.W., Stevenson, M., Fletcher, C. V., 2013. Overcoming pharmacologic sanctuaries. *Curr. Opin. HIV AIDS* 8, 190–195. <https://doi.org/10.1097/COH.0b013e32835fc68a>
- Cosgrove, K.P., Mazure, C.M., Staley, J.K., 2007. Evolving Knowledge of Sex Differences in Brain Structure, Function, and Chemistry. *Biol. Psychiatry* 62, 847–855. <https://doi.org/10.1016/j.biopsych.2007.03.001>
- Cottrell, M.L., Hadzic, T., Kashuba, A.D.M., 2013. Clinical pharmacokinetic, pharmacodynamic and drug-interaction profile of the integrase inhibitor dolutegravir. *Clin. Pharmacokinet.* 52, 981–994. <https://doi.org/10.1007/s40262-013-0093-2>
- Couturier, J., Lewis, D.E., 2018. HIV Persistence in Adipose Tissue Reservoirs. *Curr. HIV/AIDS Rep.* 15, 60–71. <https://doi.org/10.1007/s11904-018-0378-z>
- D’Andrea, G., Bussone, G., Di Fiore, P., Perini, F., Gucciardi, A., Bolner, A., Aguggia, M., Saracco, G., Galloni, E., Giordano, G., Leon, A., 2017. Pathogenesis of chronic cluster headache and bouts: role of tryptamine, arginine metabolism and  $\alpha$ 1-agonists. *Neurol. Sci.* 38, 37–43. <https://doi.org/10.1007/s10072-017-2862-4>
- D’Andrea, G., D’Amico, D., Bussone, G., Bolner, A., Aguggia, M., Saracco, M.G., Galloni, E., De Riva, V., Colavito, D., Leon, A., Rosteghin, V., Perini, F., 2013. The role of tyrosine metabolism in the pathogenesis of chronic migraine. *Cephalalgia* 33, 932–937. <https://doi.org/10.1177/0333102413480755>

- D'Andrea, G., Nordera, G., Pizzolato, G., Bolner, A., Colavito, D., Flaibani, R., Leon, A., 2010. Trace amine metabolism in Parkinson's disease: Low circulating levels of octopamine in early disease stages. *Neurosci. Lett.* 469, 348–351.  
<https://doi.org/10.1016/j.neulet.2009.12.025>
- D'Andrea, G., Pizzolato, G., Gucciardi, A., Stocchero, M., Giordano, G., Baraldi, E., Leon, A., 2019. Different Circulating Trace Amine Profiles in De Novo and Treated Parkinson's Disease Patients. *Sci. Rep.* 9, 1–11.  
<https://doi.org/10.1038/s41598-019-42535-w>
- D'Andrea, G., Terrazzino, S., Fortin, D., Farruggio, A., Rinaldi, L., Leon, A., 2003. HPLC electrochemical detection of trace amines in human plasma and platelets and expression of mRNA transcripts of trace amine receptors in circulating leukocytes. *Neurosci. Lett.* 346, 89–92. [https://doi.org/10.1016/S0304-3940\(03\)00573-1](https://doi.org/10.1016/S0304-3940(03)00573-1)
- De Almeida, S.M., 2015. Cerebrospinal fluid analysis in the HIV infection and compartmentalization of HIV in the central nervous system. *Arq. Neuropsiquiatr.* 73, 624–629. <https://doi.org/10.1590/0004-282X20150071>
- de Boer, M.G.J., Van Den Berk, G.E.L., Van Holten, N., Oryszczyn, J.E., Dorama, W., Ait Moha, D., Brinkman, K., 2016. Intolerance of dolutegravir-containing combination antiretroviral therapy regimens in real-life clinical practice. *Aids* 30, 2831–2834. <https://doi.org/10.1097/QAD.0000000000001279>
- de Leon, A.S., Tadi, P., 2023. *Biochemistry, Gamma Aminobutyric Acid*, [Updated 2. ed. Treasure Island (FL).
- de Oliveira, D.M.N., Oliveira-Silva, C.A., Pinheiro, C.G., de Carvalho, E.F., Gadelha, K.K.L., Lima-Silva, K., Cavalcante, A.K.M., Belém, M. de O., Paula, S.M., dos Santos, A.A., Magalhães, P.J.C., 2021. Differential effects of  $\beta$ -methylphenylethylamine and octopamine on contractile parameters of the rat gastrointestinal tract. *Eur. J. Pharmacol.* 908, 174339.  
<https://doi.org/10.1016/j.ejphar.2021.174339>
- Delaney, K.Z., Santosa, S., 2022. Sex differences in regional adipose tissue depots pose different threats for the development of Type 2 diabetes in males and females. *Obes. Rev.* 23. <https://doi.org/10.1111/obr.13393>
- Deodhar, S., Sillman, B., Bade, A.N., Avedissian, S.N., Podany, A.T., McMillan, J.E.M., Gautam, N., Hanson, B., Dyavar Shetty, B.L., Szlachetka, A., Johnston, M., Thurman, M., Munt, D.J., Dash, A.K., Markovic, M., Dahan, A., Alnouti, Y.,

- Yazdi, A., Kevadiya, B.D., Byrareddy, S.N., Cohen, S.M., Edagwa, B., Gendelman, H.E., 2022. Transformation of dolutegravir into an ultra-long-acting parenteral prodrug formulation. *Nat. Commun.* 13. <https://doi.org/10.1038/s41467-022-30902-7>
- Dewan, A., 2021. Olfactory signaling via trace amine-associated receptors. *Cell Tissue Res.* 383, 395–407. <https://doi.org/10.1007/s00441-020-03331-5>
- Dhakal, S., Macreadie, I., 2021. Potential contributions of trace amines in Alzheimer's disease and therapeutic prospects. *Neural Regen. Res.* 16, 1394–1396. <https://doi.org/10.4103/1673-5374.300985>
- Dodd, S., F. Carvalho, A., Puri, B.K., Maes, M., Bortolaschi, C.C., Morris, G., Berk, M., 2021. Trace Amine-Associated Receptor 1 (TAAR1): A new drug target for psychiatry? *Neurosci. Biobehav. Rev.* 120, 537–541. <https://doi.org/10.1016/j.neubiorev.2020.09.028>
- Domingo, P., Quesada-López, T., Villarroya, J., Cairó, M., Gutierrez, M.D.M., Mateo, M.G., Mur, I., Corbacho, N., Domingo, J.C., Villarroya, F., Giralt, M., 2022. Differential effects of dolutegravir, bictegravir and raltegravir in adipokines and inflammation markers on human adipocytes. *Life Sci.* 308. <https://doi.org/10.1016/j.lfs.2022.120948>
- Dupin, N., Buffet, M., Marcelin, A.G., Lamotte, C., Gorin, I., Ait-Arkoub, Z., Tréluyer, J.M., Bui, P., Calvez, V., Peytavin, G., 2002. HIV and antiretroviral drug distribution in plasma and fat tissue of HIV-infected patients with lipodystrophy. *Aids* 16, 2419–2424. <https://doi.org/10.1097/00002030-200212060-00006>
- Eagles, P.A.M., Iqbal, M., 1974. The properties of phenylethanolamine N-methyl transferase from brain tissue. *Brain Res.* 80, 177–180. [https://doi.org/10.1016/0006-8993\(74\)90739-2](https://doi.org/10.1016/0006-8993(74)90739-2)
- Eckard, A.R., McComsey, G.A., 2020. Weight gain and integrase inhibitors. *Curr. Opin. Infect. Dis.* 33, 10–19. <https://doi.org/10.1097/QCO.0000000000000616>
- Efimova, E. V., Katolikova, N. V., Kanov, E. V., Gainetdinov, R.R., 2022. Trace amine-associated receptors at the cross-road between innate olfaction of amines, emotions, and adult neurogenesis. *Neural Regen. Res.* 17, 1257–1258. <https://doi.org/10.4103/1673-5374.327338>
- Elzi, Luigia, Erb, S., Furrer, Hansjakob, Cavassini, Matthias, Calmy, Alexandra, Vernazza, Pietro, Günthard, H., Bernasconi, Enos, Battegay, Manuel, Aubert, V., Battegay, M., Bernasconi, E., Böni, J., Braun, D.L., Bucher, H.C., Calmy, A.,

- Cavassini, M., Ciuffi, A., Dollenmaier, G., Egger, M., Elzi, L., Fehr, J., Fellay, J., Furrer, H., Fux, C.A., Günthard, H.F., Haerry, D., Hasse, B., Hirsch, H.H., Hoffmann, M., Hösli, I., Kahlert, C., Kaiser, L., Keiser, O., Klimkait, T., Kouyos, R.D., Kovari, H., Ledergerber, B., Martinetti, G., Martinez De Tejada, B., Marzolini, C., Metzner, K.J., Müller, N., Nicca, D., Pantaleo, G., Paioni, P., Rauch, A., Rudin, C., Scherrer, A.U., Schmid, P., Speck, R., Stöckle, M., Tarr, P., Trkola, A., Vernazza, P., Wandeler, G., Weber, R., Yerly, S., 2017. Adverse events of raltegravir and dolutegravir. *Aids* 31, 1853–1858. <https://doi.org/10.1097/QAD.0000000000001590>
- Ergin, H.E., Inga, E.E., Maung, T.Z., Javed, M., Khan, S., 2020. HIV, Antiretroviral Therapy and Metabolic Alterations: A Review. *Cureus* 12. <https://doi.org/10.7759/cureus.8059>
- Fantauzzi, A., Mezzaroma, I., 2014. Dolutegravir: Clinical efficacy and role in HIV therapy. *Ther. Adv. Chronic Dis.* 5, 164–177. <https://doi.org/10.1177/2040622314530461>
- Fasunla, A.J., Daniel, A., Nwankwo, U., Kutji, K.M., Nwaorgu, O.G., Akinyinka, O.O., 2016. Evaluation of olfactory and gustatory function of HIV infected women. *AIDS Res. Treat.* 2016. <https://doi.org/10.1155/2016/2045383>
- Fasunla, A.J., Nwankwo, U., Adebayo, A.M., Nwaorgu, O.G., 2018. Association between Sex, CD4 Cell Counts, Antiretroviral Medications, and Olfactory and Gustatory Functions of HIV-Infected Adults. *Otolaryngol. - Head Neck Surg. (United States)* 158, 90–99. <https://doi.org/10.1177/0194599817733664>
- Fettiplace, A., Stainsby, C., Winston, A., Givens, N., Puccini, S., Vannappagari, V., Hsu, R., Fusco, J., Quercia, R., Aboud, M., Curtis, L., 2017. Psychiatric Symptoms in Patients Receiving Dolutegravir. *JAIDS J. Acquir. Immune Defic. Syndr.* 74, 423–431. <https://doi.org/10.1097/QAI.0000000000001269>
- Food and Drug Administration, 2022. M10 Bioanalytical Method Validation and Study Sample Analysis, Center for Drug Evaluation and Research Center for Biologics Evaluation and Research.
- Francesconi, J.A., Macaroy, C., Sawant, S., Hamrick, H., Wahab, S., Klein, I., McGann, J.P., 2020. Sexually dimorphic behavioral and neural responses to a predator scent. *Behav. Brain Res.* 382, 112467. <https://doi.org/10.1016/j.bbr.2020.112467>
- Frankfurt, M., Fuchs, E., Wuttke, W., 1984. Sex differences in  $\gamma$ -aminobutyric acid

- and glutamate concentrations in discrete rat brain nuclei. *Neurosci. Lett.* 50, 245–250. [https://doi.org/10.1016/0304-3940\(84\)90493-2](https://doi.org/10.1016/0304-3940(84)90493-2)
- Frizzell, R.A., Hanrahan, J.W., 2012. Physiology of Epithelial Chloride and Fluid Secretion. *Cold Spring Harb. Perspect. Med.* 2, a009563–a009563. <https://doi.org/10.1101/cshperspect.a009563>
- Fukuwatari, T., 2020. Possibility of amino acid treatment to prevent the psychiatric disorders via modulation of the production of tryptophan metabolite kynurenic acid. *Nutrients* 12. <https://doi.org/10.3390/nu12051403>
- Funderburg, N., Luciano, A.A., Jiang, W., Rodriguez, B., Sieg, S.F., Michael, M., 2008. Toll-Like Receptor Ligands Induce Human T Cell Activation and Death , a Model for HIV Pathogenesis 3, 1–7. <https://doi.org/10.1371/journal.pone.0001915>
- Gainetdinov, R.R., Hoener, M.C., Berry, M.D., 2018. Trace amines and their receptors. *Pharmacol. Rev.* 70, 549–620. <https://doi.org/10.1124/pr.117.015305>
- Gavin, K.M., Bessesen, D.H., 2020. Sex Differences in Adipose Tissue Function. *Endocrinol. Metab. Clin. North Am.* 49, 215–228. <https://doi.org/10.1016/j.ecl.2020.02.008>
- George, M.D., Asmuth, D.M., 2014. Mucosal immunity in HIV infection. *Curr. Opin. Infect. Dis.* 27, 275–281. <https://doi.org/10.1097/QCO.0000000000000059>
- Geretti, A.M., Loutfy, M., D’Arminio Monforte, A., Latysheva, I., Pérez Elías, M.J., Rymer, J., Boffito, M., 2017. Out of focus: tailoring the cascade of care to the needs of women living with HIV. *HIV Med.* 18, 3–17. <https://doi.org/10.1111/hiv.12533>
- Ghosh, I., Sankhe, R., Mudgal, J., Arora, D., Nampoothiri, M., 2020. Spermidine, an autophagy inducer, as a therapeutic strategy in neurological disorders. *Neuropeptides* 83, 102083. <https://doi.org/10.1016/j.npep.2020.102083>
- Gorwood, J., Bourgeois, C., Pourcher, V., Pourcher, G., Charlotte, F., Mantecon, M., Rose, C., Morichon, R., Atlan, M., Le Grand, R., Desjardins, D., Katlama, C., Fève, B., Lambotte, O., Capeau, J., Béréziat, V., Lagathu, C., 2020. The integrase inhibitors dolutegravir and raltegravir exert proadipogenic and profibrotic effects and induce insulin resistance in human/simian adipose tissue and human adipocytes. *Clin. Infect. Dis.* 71, E549–E560. <https://doi.org/10.1093/cid/ciaa259>
- Gosetti, F., Mazzucco, E., Gennaro, M.C., Marengo, E., 2013. Simultaneous

- determination of sixteen underivatized biogenic amines in human urine by HPLC-MS/MS. *Anal. Bioanal. Chem.* 405, 907–916.  
<https://doi.org/10.1007/s00216-012-6269-z>
- Gostner, J.M., Becker, K., Kurz, K., Fuchs, D., 2015. Disturbed Amino Acid Metabolism in HIV: Association with Neuropsychiatric Symptoms. *Front. Psychiatry* 6. <https://doi.org/10.3389/fpsy.2015.00097>
- Gougeon, M.-L., 2016. Alarmins and central nervous system inflammation in HIV-associated neurological disorders. *J. Intern. Med.* 281, 433–447.  
<https://doi.org/10.1111/joim.12570>
- Gouget, H., Noé, G., Barrail-Tran, A., Furlan, V., 2020. UPLC–MS/MS method for the simultaneous quantification of bicitgravir and 13 others antiretroviral drugs plus cobicistat and ritonavir boosters in human plasma. *J. Pharm. Biomed. Anal.* 181, 113057. <https://doi.org/10.1016/j.jpba.2019.113057>
- Gouma, E., Simos, Y., Verginadis, I., Lykoudis, E., Evangelou, A., Karkabounas, S., 2012. A simple procedure for estimation of total body surface area and determination of a new value of Meeh's constant in rats. *Lab. Anim.* 46, 40–45.  
<https://doi.org/10.1258/la.2011.011021>
- Graham, C.S., Graham, B.G., Bartlett, J.A., Heald, A.E., Schiffman, S.S., 1995. Taste and smell losses in HIV infected patients. *Physiol. Behav.* 58, 287–293.  
[https://doi.org/10.1016/0031-9384\(95\)00049-O](https://doi.org/10.1016/0031-9384(95)00049-O)
- Grandy, D.K., 2007. Trace amine-associated receptor 1—Family archetype or iconoclast? *Pharmacol. Ther.* 116, 355–390.  
<https://doi.org/10.1016/j.pharmthera.2007.06.007>
- Grégoire, M., Deslandes, G., Renaud, C., Bouquié, R., Allavena, C., Raffi, F., Jolliet, P., Dailly, E., 2014. A liquid chromatography-tandem mass spectrometry assay for quantification of rilpivirine and dolutegravir in human plasma. *J. Chromatogr. B Anal. Technol. Biomed. Life Sci.* 971, 1–9.  
<https://doi.org/10.1016/j.jchromb.2014.09.006>
- Grosheva, I., Zheng, D., Levy, M., Polansky, O., Lichtenstein, A., Golani, O., Dori-Bachash, M., Moresi, C., Shapiro, H., Del Mare-Roumani, S., Valdes-Mas, R., He, Y., Karbi, H., Chen, M., Harmelin, A., Straussman, R., Yissachar, N., Elinav, E., Geiger, B., 2020. High-Throughput Screen Identifies Host and Microbiota Regulators of Intestinal Barrier Function. *Gastroenterology* 159, 1807–1823.  
<https://doi.org/10.1053/j.gastro.2020.07.003>

- Gutiérrez-Hellín, J., Del Coso, J., 2016. Acute p-syneprine ingestion increases fat oxidation rate during exercise. *Br. J. Clin. Pharmacol.* 362–368.  
<https://doi.org/10.1111/bcp.12952>
- Gwilt, K.B., González, D.P., Olliffe, N., Oller, H., Hoffing, R., Puzan, M., El Aidy, S., Miller, G.M., 2020. Actions of Trace Amines in the Brain-Gut-Microbiome Axis via Trace Amine-Associated Receptor-1 (TAAR1). *Cell. Mol. Neurobiol.* 40, 191–201. <https://doi.org/10.1007/s10571-019-00772-7>
- Han, X.M., Qin, Y.J., Zhu, Y., Zhang, X.L., Wang, N.X., Rang, Y., Zhai, X.J., Lu, Y.N., 2019. Development of an underivatized LC-MS/MS method for quantitation of 14 neurotransmitters in rat hippocampus, plasma and urine: Application to CUMS induced depression rats. *J. Pharm. Biomed. Anal.* 174, 683–695.  
<https://doi.org/10.1016/j.jpba.2019.06.043>
- Hardbower, D.M., Asim, M., Luis, P.B., Singh, K., Barry, D.P., Yang, C., Steeves, M.A., Cleveland, J.L., Schneider, C., Piazuelo, M.B., Gobert, A.P., Wilson, K.T., 2017. Ornithine decarboxylase regulates M1 macrophage activation and mucosal inflammation via histone modifications. *Proc. Natl. Acad. Sci. U. S. A.* 114, E751–E760. <https://doi.org/10.1073/pnas.1614958114>
- Hare, S., Smith, S.J., Métifiot, M., Jaxa-Chamiec, A., Pommier, Y., Hughes, S.H., Cherepanov, P., 2011. Structural and functional analyses of the second-generation integrase strand transfer inhibitor dolutegravir (S/GSK1349572). *Mol. Pharmacol.* 80, 565–572. <https://doi.org/10.1124/mol.111.073189>
- Harvey, I., Boudreau, A., Stephens, J.M., 2020. Adipose tissue in health and disease: Adipose Tissue in Health and Disease. *Open Biol.* 10.  
<https://doi.org/10.1098/rsob.200291>
- Heald, A.E., Pieper, C.F., Schiffman, S.S., 1998. Taste and smell complaints in HIV-infected patients. *Aids* 12, 1667–1674. <https://doi.org/10.1097/00002030-199813000-00015>
- Heald, A.E., Schiffman, S.S., 1997. Taste and smell. Neglected senses that contribute to the malnutrition of AIDS. *N. C. Med. J.* 58, 100–4.
- Heaton, R.K., Franklin, D.R., Ellis, R.J., McCutchan, J.A., Letendre, S.L., LeBlanc, S., Corkran, S.H., Duarte, N.A., Clifford, D.B., Woods, S.P., Collier, A.C., Marra, C.M., Morgello, S., Rivera Mindt, M., Taylor, M.J., Marcotte, T.D., Atkinson, J.H., Wolfson, T., Gelman, B.B., McArthur, J.C., Simpson, D.M., Abramson, I., Gamst, A., Fennema-Notestine, C., Jernigan, T.L., Wong, J., Grant, I., 2011.

- HIV-associated neurocognitive disorders before and during the era of combination antiretroviral therapy: Differences in rates, nature, and predictors. *J. Neurovirol.* 17, 3–16. <https://doi.org/10.1007/s13365-010-0006-1>
- Hengstmann, J.H., Konen, W., Konen, C., Eichelbaum, M., Dengler, H.J., 1974. The physiological disposition of p-octopamine in man. *Naunyn. Schmiedebergs. Arch. Pharmacol.* 283, 93–106. <https://doi.org/10.1007/BF00500148>
- Hill, A.M., Mitchell, N., Hughes, S., Pozniak, A.L., 2018. Risks of cardiovascular or central nervous system adverse events and immune reconstitution inflammatory syndrome, for dolutegravir versus other antiretrovirals: Meta-analysis of randomized trials. *Curr. Opin. HIV AIDS* 13, 102–111. <https://doi.org/10.1097/COH.0000000000000445>
- Hoökfelt, T., Fuxe, K., Goldstein, M., 1973. Immunohistochemical localization of aromatic L-amino acid decarboxylase (DOPA decarboxylase) in central dopamine and 5-hydroxytryptamine nerve cell bodies of the rat. *Brain Res.* 53, 175–180. [https://doi.org/10.1016/0006-8993\(73\)90776-2](https://doi.org/10.1016/0006-8993(73)90776-2)
- Hoefig, C.S., Renko, K., Piehl, S., Scanlan, T.S., Bertoldi, M., Opladen, T., Hoffmann, G.F., Klein, J., Blankenstein, O., Schweizer, U., Köhrle, J., 2012. Does the aromatic l-amino acid decarboxylase contribute to thyronamine biosynthesis? *Mol. Cell. Endocrinol.* 349, 195–201. <https://doi.org/10.1016/j.mce.2011.10.024>
- Hoefig, C.S., Wuensch, T., Rijntjes, E., Lehmpful, I., Daniel, H., Schweizer, U., Mittag, J., Köhrle, J., 2015. Biosynthesis of 3-iodothyronamine from T4 in murine intestinal tissue. *Endocrinology* 156, 4356–4364. <https://doi.org/10.1210/en.2014-1499>
- Hoffmann, C., Llibre, J.M., 2019. Neuropsychiatric adverse events with dolutegravir and other integrase strand transfer inhibitors. *AIDS Rev.* 21, 4–10. <https://doi.org/10.24875/AIDSRev.19000023>
- Hoffmann, C., Welz, T., Sabranski, M., Kolb, M., Wolf, E., Stellbrink, H.-J., Wyen, C., 2017. Higher rates of neuropsychiatric adverse events leading to dolutegravir discontinuation in women and older patients. *HIV Med.* 18, 56–63. <https://doi.org/10.1111/hiv.12468>
- Hornung, D.E., Kurtz, D.B., Bradshaw, C.B., Seipel, D.M., Kent, P.F., Blair, D.C., Emko, P., 1998. The olfactory loss that accompanies an HIV infection. *Physiol. Behav.* 64, 549–556. [https://doi.org/10.1016/S0031-9384\(98\)00112-7](https://doi.org/10.1016/S0031-9384(98)00112-7)

- Howlett, W.P., 2019. Neurological disorders in HIV in Africa: a review William P Howlett 1. Department of Internal Medicine, Kilimanjaro Christian Medical Centre, Moshi, Tanzania. 2. Center for International Health, University of Bergen, Norway. *Afr. Health Sci.* 19, 1953–1977.
- Hu, X., Ma, X., Pan, X., Luo, Y., Xu, Y., Xiong, Q., Bao, Y., Jia, W., 2016. Association of androgen with gender difference in serum adipocyte fatty acid binding protein levels. *Sci. Rep.* 6, 1–8. <https://doi.org/10.1038/srep27762>
- Huang, C., Hoque, T., Bendayan, R., 2023. Antiretroviral drugs efavirenz, dolutegravir and bictegravir dysregulate blood-brain barrier integrity and function. *Front. Pharmacol.* 14, 1–16. <https://doi.org/10.3389/fphar.2023.1118580>
- Ibáñez, C.A., Vázquez-Martínez, M., León-Contreras, J.C., Reyes-Castro, L.A., Rodríguez-González, G.L., Bautista, C.J., Nathanielsz, P.W., Zambrano, E., 2018. Different statistical approaches to characterization of adipocyte size in offspring of obese rats: Effects of maternal or offspring exercise intervention. *Front. Physiol.* 9, 1–13. <https://doi.org/10.3389/fphys.2018.01571>
- Inoue, K., Tsutsui, H., Akatsu, H., Hashizume, Y., Matsukawa, N., Yamamoto, T., Toyo'oka, T., 2013. Metabolic profiling of Alzheimer's disease brains. *Sci. Rep.* 3, 2364. <https://doi.org/10.1038/srep02364>
- Ishida, M., Takekuni, C., Nishi, K., Sugahara, T., 2022. p-Syneprine suppresses inflammatory responses in lipopolysaccharide-stimulated RAW264.7 cells and alleviates systemic inflammatory response syndrome in mice. *Food Funct.* 13, 5229–5239. <https://doi.org/10.1039/d2fo00299j>
- Ito, J., Ito, M., Nambu, H., Fujikawa, T., Tanaka, K., Iwaasa, H., Tokita, S., 2009. Anatomical and histological profiling of orphan G-protein-coupled receptor expression in gastrointestinal tract of C57BL/6J mice. *Cell Tissue Res.* 338, 257–269. <https://doi.org/10.1007/s00441-009-0859-x>
- Ivanov, I.P., Shin, B., Loughran, G., Tzani, I., Young-Baird, S.K., Cao, C., Atkins, J.F., Dever, T.E., 2018. Polyamine Control of Translation Elongation Regulates Start Site Selection on Antizyme Inhibitor mRNA via Ribosome Queuing. *Mol. Cell* 70, 254-264.e6. <https://doi.org/10.1016/j.molcel.2018.03.015>
- Joint United Nations Programme on HIV/AIDS, 2021. UNAIDS data 2021. Geneva.
- Jones, R.S.G., 1982. Noradrenaline-octopamine interactions on cortical neurones in the rat. *Eur. J. Pharmacol.* 77, 159–162. [158](https://doi.org/10.1016/0014-</a></p></div><div data-bbox=)

2999(82)90012-7

- Joska, J.A., Gouse, H., Paul, R.H., Stein, D.J., Flisher, A.J., 2010. Does highly active antiretroviral therapy improve neurocognitive function? A systematic review. *J. Neurovirol.* 16, 101–114. <https://doi.org/10.3109/13550281003682513>
- Kamari, V. El, Moser, C., Hileman, C.O., Currier, J.S., Brown, T.T., Johnston, L., Hunt, P.W., Mccomsey, G.A., 2019. Lower Pretreatment Gut Integrity Is Independently Associated With Fat Gain on Antiretroviral Therapy. *Clin. Infect. Dis.* 68, 1349–1401. <https://doi.org/10.1093/cid/ciy716>
- Kandel, C.E., Walmsley, S.L., 2015. Dolutegravir – A review of the pharmacology, efficacy, and safety in the treatment of HIV. *Drug Des. Devel. Ther.* 9, 3547–3555. <https://doi.org/10.2147/DDDT.S84850>
- Kanters, S., Renaud, F., Rangaraj, A., Zhang, K., Limbrick-Oldfield, E., Hughes, M., Ford, N., Vitoria, M., 2022. Evidence synthesis evaluating body weight gain among people treating HIV with antiretroviral therapy - a systematic literature review and network meta-analysis. *eClinicalMedicine* 48, 1–12. <https://doi.org/10.1016/j.eclinm.2022.101412>
- Karoum, F., Linnoila, M., Potter, W.Z., Chuang, L.W., Goodwin, F.K., Wyatt, R.J., 1982. Fluctuating high urinary phenylethylamine excretion rates in some bipolar affective disorder patients. *Psychiatry Res.* 6, 215–222. [https://doi.org/10.1016/0165-1781\(82\)90009-9](https://doi.org/10.1016/0165-1781(82)90009-9)
- Kendig, D.M., Grider, J.R., 2015. Serotonin and colonic motility. *Neurogastroenterol. Motil.* 27, 899–905. <https://doi.org/10.1111/nmo.12617>
- Khan, M. zahid, Nawaz, W., 2016. The emerging roles of human trace amines and human trace amine-associated receptors (hTAARs) in central nervous system. *Biomed. Pharmacother.* 83, 439–449. <https://doi.org/10.1016/j.biopha.2016.07.002>
- Khera, A., Vega, G.L., Das, S.R., Ayers, C., McGuire, D.K., Grundy, S.M., De Lemos, J.A., 2009. Sex differences in the relationship between c-reactive protein and body fat. *J. Clin. Endocrinol. Metab.* 94, 3251–3258. <https://doi.org/10.1210/jc.2008-2406>
- Kitahama, K., Ikemoto, K., Jouvet, A., Araneda, S., Nagatsu, I., Raynaud, B., Nishimura, A., Nishi, K., Niwa, S. ichi, 2009. Aromatic l-amino acid decarboxylase-immunoreactive structures in human midbrain, pons, and medulla. *J. Chem. Neuroanat.* 38, 130–140.

- <https://doi.org/10.1016/j.jchemneu.2009.06.010>
- Klieverik, L.P., Foppen, E., Ackermans, M.T., Serlie, M.J., Sauerwein, H.P., Scanlan, T.S., Grandy, D.K., Fliers, E., Kalsbeek, A., 2009. Central effects of thyronamines on glucose metabolism in rats. *J. Endocrinol.* 201, 377–386. <https://doi.org/10.1677/JOE-09-0043>
- Koh, Y., Wu, X., Ferris, A.L., Matreyek, K.A., Smith, S.J., Lee, K., KewalRamani, V.N., Hughes, S.H., Engelman, A., 2013. Differential Effects of Human Immunodeficiency Virus Type 1 Capsid and Cellular Factors Nucleoporin 153 and LEDGF/p75 on the Efficiency and Specificity of Viral DNA Integration. *J. Virol.* 87, 648–658. <https://doi.org/10.1128/jvi.01148-12>
- Kotler, D.P., Gaetz, H.P., Lange, M., Klein, E.B., Holt, P.R., 1984. Enteropathy associated with the acquired immunodeficiency syndrome. *Ann. Intern. Med.* 101, 421–8. <https://doi.org/10.7326/0003-4819-101-4-421>
- Kovács, Z., Skatchkov, S.N., Veh, R.W., Szabó, Z., Németh, K., Szabó, P.T., Kardos, J., Héja, L., 2022. Critical Role of Astrocytic Polyamine and GABA Metabolism in Epileptogenesis. *Front. Cell. Neurosci.* 15, 1–15. <https://doi.org/10.3389/fncel.2021.787319>
- Kubovcakova, L., Krizanova, O., Kvetnansky, R., 2004. Identification of the aromatic L-amino acid decarboxylase gene expression in various mice tissues and its modulation by immobilization stress in stellate ganglia. *Neuroscience* 126, 375–380. <https://doi.org/10.1016/j.neuroscience.2004.04.005>
- Labarthe, L., Gelé, T., Gouget, H., Benzemrane, M., Calvez, P. Le, Legrand, N., Lambotte, O., Grand, R. Le, Bourgeois, C., Barrail-tran, A., Paris-saclay, U., Paris-saclay, U., Bicêtre, H., Kremlin-bicêtre, L., 2022. Pharmacokinetics and tissue distribution of tenofovir , emtricitabine and dolutegravir in mice 1–8.
- Lamorde, M., Atwiine, M., Owarwo, N.C., Ddungu, A., Laker, E.O., Mubiru, F., Kiragga, A., Lwanga, I.B., Castelnovo, B., 2020. Dolutegravir-associated hyperglycaemia in patients with HIV. *Lancet HIV* 7, e461–e462. [https://doi.org/10.1016/S2352-3018\(20\)30042-4](https://doi.org/10.1016/S2352-3018(20)30042-4)
- Langner, M., Mateska, I., Bechmann, N., Wielockx, B., Chavakis, T., Alexaki, V.I., Peitzsch, M., 2022. Liquid chromatography-tandem mass spectrometry based quantification of arginine metabolites including polyamines in different sample matrices. *J. Chromatogr. A* 1671, 463021. <https://doi.org/10.1016/j.chroma.2022.463021>

- Lee, M.J., Fried, S.K., 2017. Sex-dependent depot differences in adipose tissue development and function; Role of sex steroids. *J. Obes. Metab. Syndr.* 26, 172–180. <https://doi.org/10.7570/jomes.2017.26.3.172>
- Leibrand, C.R., Paris, J.J., Ghandour, M.S., Knapp, P.E., Kim, W.K., Hauser, K.F., McRae, M.P., 2017. HIV-1 Tat disrupts blood-brain barrier integrity and increases phagocytic perivascular macrophages and microglia in the dorsal striatum of transgenic mice. *Neurosci. Lett.* 640, 136–143. <https://doi.org/10.1016/j.neulet.2016.12.073>
- Lewandowski, N.M., Ju, S., Verbitsky, M., Ross, B., Geddie, M.L., Rockenstein, E., Adame, A., Muhammad, A., Vonsattel, J.P., Ringe, D., Cote, L., Lindquist, S., Masliah, E., Petsko, G.A., Marder, K., Clark, L.N., Small, S.A., 2010. Polyamine pathway contributes to the pathogenesis of Parkinson disease. *Proc. Natl. Acad. Sci. U. S. A.* 107, 16970–16975. <https://doi.org/10.1073/pnas.1011751107>
- Liu, P., Fleete, M.S., Jing, Y., Collie, N.D., Curtis, M.A., Waldvogel, H.J., Faull, R.L.M., Abraham, W.C., Zhang, H., 2014. Altered arginine metabolism in Alzheimer's disease brains. *Neurobiol. Aging* 35, 1992–2003. <https://doi.org/10.1016/j.neurobiolaging.2014.03.013>
- Liu, P., Gupta, N., Jing, Y., Zhang, H., 2008. Age-related changes in polyamines in memory-associated brain structures in rats. *Neuroscience* 155, 789–796. <https://doi.org/10.1016/j.neuroscience.2008.06.033>
- Liu, R., Li, Q., Ma, R., Lin, X., Xu, H., Bi, K., 2013. Determination of polyamine metabolome in plasma and urine by ultrahigh performance liquid chromatography-tandem mass spectrometry method: Application to identify potential markers for human hepatic cancer. *Anal. Chim. Acta* 791, 36–45. <https://doi.org/10.1016/j.aca.2013.06.044>
- Logan, C., Beadsworth, M.B.J., Beeching, N.J., 2016. HIV and diarrhoea: What is new? *Curr. Opin. Infect. Dis.* 29, 486–494. <https://doi.org/10.1097/QCO.0000000000000305>
- Lorenzo, J.M., Martínez, S., Franco, I., Carballo, J., 2007. Biogenic amine content during the manufacture of dry-cured lacón, a Spanish traditional meat product: Effect of some additives. *Meat Sci.* 77, 287–293. <https://doi.org/10.1016/j.meatsci.2007.03.020>
- Luqman, A., Nega, M., Nguyen, M.T., Ebner, P., Götz, F., 2018. SadA-Expressing Staphylococci in the Human Gut Show Increased Cell Adherence and

- Internalization. *Cell Rep.* 22, 535–545.  
<https://doi.org/10.1016/j.celrep.2017.12.058>
- Ma, Q., Schifitto, G., Venuto, C., Ocque, A., Dewhurst, S., Morse, G.D., Aalinkeel, R., Schwartz, S.A., Mahajan, S.D., 2020. Effect of Dolutegravir and Sertraline on the Blood Brain Barrier (BBB). *J. Neuroimmune Pharmacol.* 15, 7–9.  
<https://doi.org/10.1007/s11481-020-09904-z>
- Madeo, F., Eisenberg, T., Pietrocola, F., Kroemer, G., 2018. Spermidine in health and disease. *Science (80-. )*. 359. <https://doi.org/10.1126/science.aan2788>
- Magnes, C., Fauland, A., Gander, E., Narath, S., Ratzner, M., Eisenberg, T., Madeo, F., Pieber, T., Sinner, F., 2014. Polyamines in biological samples: rapid and robust quantification by solid-phase extraction online-coupled to liquid chromatography-tandem mass spectrometry. *J. Chromatogr. A* 1331, 44–51.  
<https://doi.org/10.1016/j.chroma.2013.12.061>
- Maijala, R., Eerola, S., 1993. Contaminant lactic acid bacteria of dry sausages produce histamine and tyramine. *Meat Sci.* 35, 387–395.  
[https://doi.org/10.1016/0309-1740\(93\)90043-H](https://doi.org/10.1016/0309-1740(93)90043-H)
- Makletsova, M.G., Rikhireva, G.T., Kirichenko, E.Y., Trinitatsky, I.Y., Vakulenko, M.Y., Ermakov, A.M., 2022. The Role of Polyamines in the Mechanisms of Cognitive Impairment. *Neurochem. J.* 16, 283–294.  
<https://doi.org/10.1134/S1819712422030059>
- Manni, M.E., De Siena, G., Saba, A., Marchini, M., Dicembrini, I., Bigagli, E., Cinci, L., Lodovici, M., Chiellini, G., Zucchi, R., Raimondi, L., 2012. 3-Iodothyronamine: A modulator of the hypothalamus-pancreas-thyroid axes in mice. *Br. J. Pharmacol.* 166, 650–658. <https://doi.org/10.1111/j.1476-5381.2011.01823.x>
- Mao, H. ming, Chen, B. guan, Qian, X. ming, Liu, Z., 2009. Simultaneous determination of twelve biogenic amines in serum by high performance liquid chromatography. *Microchem. J.* 91, 176–180.  
<https://doi.org/10.1016/j.microc.2008.10.005>
- Maráková, K., Piešťanský, J., Zelinková, Z., Mikuš, P., 2020. Simultaneous determination of twelve biogenic amines in human urine as potential biomarkers of inflammatory bowel diseases by capillary electrophoresis – tandem mass spectrometry. *J. Pharm. Biomed. Anal.* 186.  
<https://doi.org/10.1016/j.jpba.2020.113294>
- Marchetti, G., Tincati, C., Silvestri, G., 2013. Microbial Translocation in the

- Pathogenesis of HIV Infection and. *Clin. Microbiol. Rev.* 26, 2–18.  
<https://doi.org/10.1128/CMR.00050-12>
- Maric, I., Krieger, J.P., van der Velden, P., Borchers, S., Asker, M., Vujcic, M., Wernstedt Asterholm, I., Skibicka, K.P., 2022. Sex and Species Differences in the Development of Diet-Induced Obesity and Metabolic Disturbances in Rodents. *Front. Nutr.* 9, 1–14. <https://doi.org/10.3389/fnut.2022.828522>
- Martínez-Maqueda, D., Miralles, B., Recio, I., 2015. HT29 Cell Line, in: *The Impact of Food Bioactives on Health*. Springer International Publishing, Cham, pp. 113–124. [https://doi.org/10.1007/978-3-319-16104-4\\_11](https://doi.org/10.1007/978-3-319-16104-4_11)
- Massanella, M., Fromentin, R., Chomont, N., 2016. Residual inflammation and viral reservoirs. *Curr. Opin. HIV AIDS* 11, 234–241.  
<https://doi.org/10.1097/COH.0000000000000230>
- Matsumoto, M., Benno, Y., 2007. The relationship between microbiota and polyamine concentration in the human intestine: A pilot study. *Microbiol. Immunol.* 51, 25–35. <https://doi.org/10.1111/j.1348-0421.2007.tb03887.x>
- Matuszewski, B.K., 2006. Standard line slopes as a measure of a relative matrix effect in quantitative HPLC-MS bioanalysis. *J. Chromatogr. B Anal. Technol. Biomed. Life Sci.* 830, 293–300. <https://doi.org/10.1016/j.jchromb.2005.11.009>
- Mccomsey, G.A., Eron, J.J., Santiago, S., Mounzer, K., Moyle, G., Vanig, T., Sax, P.E., Althoff, K.N., Milligan, S., Haubrich, R., Elion, R.A., Carolina, N., Hill, C., Resource, C., Fight, P., Hospital, W., 2019. Weight Gain During Treatment Among 3 , 468 Treatment-Experienced Adults with HIV. *Conf. Retroviruses Opportunistic Infect.* 974.
- McLaughlin, M., Walsh, S., Galvin, S., 2018. Dolutegravir-induced hyperglycaemia in a patient living with HIV. *J. Antimicrob. Chemother.* 73, 258–260.  
<https://doi.org/10.1093/jac/dkx365>
- Meiser, J., Weindl, D., Hiller, K., 2013. Complexity of dopamine metabolism. *Cell Commun. Signal.* 11, 1–18. <https://doi.org/10.1186/1478-811X-11-34>
- Menard, A., Meddeb, L., Tissot-Dupont, H., Ravaux, I., Dhiver, C., Mokhtari, S., Tomei, C., Brouqui, P., Colson, P., Stein, A., 2017. Dolutegravir and weight gain: An unexpected bothering side effect? *Aids* 31, 1499–1500.  
<https://doi.org/10.1097/QAD.0000000000001495>
- Metsu, D., Lanot, T., Fraissinet, F., Picot, M., Concordet, D., Cabrol, M., Dubois-Galopin, F., Chatelut, E., Delobel, P., Gandia, P., 2018. Determination of

dolutegravir's unbound fraction in human plasma using validated equilibrium dialysis and LC-MS/MS methods. *Clin. Chim. Acta* 479, 56–65.

<https://doi.org/10.1016/j.cca.2017.12.034>

Meyer-myklestad, M.H., Medhus, A.W., Lorvik, K.B., Seljeflot, I., Hansen, S.H., Holm, K., Stiksrud, B., Trøseid, M., Hov, J.R., Kvale, D., Dyrholm-riise, A.M., Kummen, M., Reikvam, D.H., 2021. Human Immunodeficiency Virus – Infected Immunological Nonresponders Have Colon-Restricted Gut Mucosal Immune Dysfunction. *J. Infect. Dis.* XX, 1–14. <https://doi.org/10.1093/infdis/jiaa714>

Miller, M.M., Liedtke, M.D., Lockhart, S.M., Chris Rathbun, R., 2015. The role of dolutegravir in the management of HIV infection. *Infect. Drug Resist.* 8, 19–29. <https://doi.org/10.2147/IDR.S58706>

Misrani, A., Tabassum, S., Yang, L., 2021. Mitochondrial Dysfunction and Oxidative Stress in Alzheimer's Disease. *Front. Aging Neurosci.* 13, 1–20.

<https://doi.org/10.3389/fnagi.2021.617588>

Molderings, G.J., Haenisch, B., 2012. Agmatine (decarboxylated l-arginine): Physiological role and therapeutic potential. *Pharmacol. Ther.* 133, 351–365. <https://doi.org/10.1016/j.pharmthera.2011.12.005>

Mondi, A., Cozzi-Lepri, A., Tavelli, A., Rusconi, S., Vichi, F., Ceccherini-Silberstein, F., Calcagno, A., De Luca, A., Maggiolo, F., Marchetti, G., Antinori, A., d'Arminio Monforte, A., Andreoni, M., Castagna, A., Castelli, F., Cauda, R., Di Perri, G., Galli, M., Iardino, R., Ippolito, G., azzarin, A., Rezza, G., von Schloesser, F., Viale, P., Girardi, E., Lo Caputo, S., Mussini, C., Puoti, M., Perno, C.F., Balotta, C., Bandera, A., Bonora, S., Borderi, M., Capetti, A., Capobianchi, M.R., Cicalini, S., Cingolani, A., Cinque, P., Di Biagio, A., Gianotti, N., Gori, A., Guaraldi, G., Lapadula, G., Lichtner, M., Madeddu, G., Monno, L., Nozza, S., Quiros Roldan, E., Rossotti, R., Santoro, M.M., aracino, A., Sarmati, L., Fanti, I., Lorenzini, P., Rodano', A., Macchia, M., Carletti, F., Carrara, S., Di Caro, A., Graziano, S., Petrone, F., Prota, G., Quartu, S., Truffa, S., Giacometti, I.A., Costantini, A., Barocci, V., Angarano, G., Fabrizio, C., Suardi, C., i, V., Verucchi, G., Castelnuovo, F., Minardi, C., Menzaghi, B., Abeli, C., Cacopardo, B., Celesia, B., Vecchiet, J., Falasca, K., Pan, A., Lorenzotti, S., Sighinolfi, L., Segala, D., Blanc, P., Cassola, G., Viscoli, C., lessandrini, A., Bobbio, N., Mazzarello, G., Pozzetto, I., Bonfanti, P., Molteni, C., Chiodera, A., Milini, P., Nunnari, G., Pellicanò, G., Rizzardini, G., Bai, F., Moioli, M.C., Piolini, R.,

- Ridolfo, A.L., Salpietro, S., Tincati, C., Puzzolante, C., Migliorino, C., Sangiovanni, V., Borgia, G., Esposito, V., Di Martino, F., Gentile, I., Maddaloni, L., Cattelan, A.M., Marinello, S., Cascio, A., Colomba, C., Baldelli, F., Schiaroli, E., Parruti, G., Sozio, F., Magnani, G., Ursitti, M.A., Cristaudo, A., Vullo, V., Acinapura, R., Baldin, G., Capozzi, M., Rivano Capparucia, M., Iaiani, G., atini, A., Mastroso, I., Plazzi, M.M., Savinelli, S., Vergori, A., Cecchetto, M., Viviani, F., Bagella, P., Rossetti, B., Fontana Del Vecchio, R., Francisci, D., Di Giuli, C., Caramello, P., Orofino, G.C., Sciandra, M., Bassetti, M., ondero, A., Pellizzer, G., Manfrin, V., Starnini, G., alungo, A., 2019. Effectiveness of dolutegravir-based regimens as either first-line or switch antiretroviral therapy: data from the Icona cohort. *J. Int. AIDS Soc.* 22, 1–10. <https://doi.org/10.1002/jia2.25227>
- Morii, H., Cann, D.C., Taylor, L.Y., 1988. Histamine Formation by Luminous Bacteria in Mackerel Stored at Low Temperatures. *Nippon Suisan Gakkaishi (Japanese Ed.* 54, 299–305. <https://doi.org/10.2331/suisan.54.299>
- Mudd, J.C., Brenchley, J.M., 2016. Gut Mucosal Barrier Dysfunction , Microbial Dysbiosis , and Their Role in HIV-1 Disease Progression 214. <https://doi.org/10.1093/infdis/jiw258>
- Mueller, C., Temmel, A.F.P., Quint, C., Rieger, A., Hummel, T., 2002. Olfactory Function in HIV-positive Subjects 67–71.
- Murray-Stewart, T., Dunworth, M., Foley, J., Schwartz, C., Casero, R., 2018. Polyamine Homeostasis in Snyder-Robinson Syndrome. *Med. Sci.* 6, 112. <https://doi.org/10.3390/medsci6040112>
- Myojin, T., Taga, C., Tsuji, M., 1989. Concentrations of  $\beta$ -Phenylethylamine in Plasma and Platelets of Schizophrenics. *Psychiatry Clin. Neurosci.* 43, 171–176. <https://doi.org/10.1111/j.1440-1819.1989.tb02566.x>
- Naila, A., Flint, S., Fletcher, G., Bremer, P., Meerdink, G., 2010. Control of biogenic amines in food - existing and emerging approaches. *J. Food Sci.* 75. <https://doi.org/10.1111/j.1750-3841.2010.01774.x>
- Nair, A., Jacob, S., 2016. A simple practice guide for dose conversion between animals and human. *J. Basic Clin. Pharm.* 7, 27. <https://doi.org/10.4103/0976-0105.177703>
- Nakamura, A., Kurihara, S., Takahashi, D., Ohashi, W., Nakamura, Y., Kimura, S., Onuki, M., Kume, A., Sasazawa, Y., Furusawa, Y., Obata, Y., Fukuda, S., Saiki, S., Matsumoto, M., Hase, K., 2021. Symbiotic polyamine metabolism regulates

- epithelial proliferation and macrophage differentiation in the colon. *Nat. Commun.* 12, 1–14. <https://doi.org/10.1038/s41467-021-22212-1>
- Nakanishi, S., Cleveland, J.L., 2021. Polyamine Homeostasis in Development and Disease. *Med. Sci.* 9, 28. <https://doi.org/10.3390/medsci9020028>
- NAMSAL ANRS 12313 Study Group, Kouanfack, C., Mpoudi-Etame, M., Omgba Bassega, P., Eymard- Duvernay, S., Leroy, S., Boyer, S., Peeters, M., Calmy, A., Delaporte, E., 2019. Dolutegravir-Based or Low-Dose Efavirenz-Based Regimen for the Treatment of HIV-1. *N. Engl. J. Med.* 381, 816–826. <https://doi.org/10.1056/NEJMoa1904340>
- National Center for Biotechnology Information, 2023. PubChem Annotation Record for Dolutegravir, Source: Hazardous Substances Data Bank (HSDB). [WWW Document]. URL <https://pubchem.ncbi.nlm.nih.gov>. (accessed 4.20.23).
- Newell-Fugate, A.E., 2017. The role of sex steroids in white adipose tissue adipocyte function. *Reproduction* 153, R133–R149. <https://doi.org/10.1530/REP-16-0417>
- Norwood, J., Turner, M., Bofill, C., Rebeiro, P., Shepherd, B., Bebawy, S., Hulgan, T., Raffanti, S., Haas, D.W., Sterling, T.R., Koethe, J.R., 2017. Brief Report: Weight Gain in Persons With HIV Switched From Efavirenz-Based to Integrase Strand Transfer Inhibitor-Based Regimens. *JAIDS J. Acquir. Immune Defic. Syndr.* 76, 527–531. <https://doi.org/10.1097/QAI.0000000000001525>
- Ntem-Mensah, A.D., Millman, N., Jakharia, N., Theppote, A., Toeque, M.-G., Riedel, D.J., 2019. 345. Acute Onset Diabetic Ketoacidosis/Hyperosmolar Hyperglycemic State in Patients Taking Integrase Strand Transfer Inhibitors. *Open Forum Infect. Dis.* 6, S183–S184. <https://doi.org/10.1093/ofid/ofz360.418>
- Ocque, A.J., Hagler, C.E., DiFrancesco, R., Morse, G.D., Talal, A.H., 2017. Ultra-performance liquid chromatography tandem mass spectrometry for determination of Direct Acting Antiviral drugs in human liver fine needle aspirates. *J. Chromatogr. B. Analyt. Technol. Biomed. Life Sci.* 1052, 103–109. <https://doi.org/10.1016/j.jchromb.2017.03.020>
- Osborne, O., Peyravian, N., Nair, M., Daunert, S., Toborek, M., 2020. The Paradox of HIV Blood–Brain Barrier Penetrance and Antiretroviral Drug Delivery Deficiencies. *Trends Neurosci.* 43, 695–708. <https://doi.org/10.1016/j.tins.2020.06.007>
- Pai, M.P., 2012. Drug dosing based on weight and body surface area: Mathematical assumptions and limitations in obese adults. *Pharmacotherapy* 32, 856–868.

<https://doi.org/10.1002/j.1875-9114.2012.01108.x>

- Panas, M.W., Xie, Z., Panas, H.N., Hoener, M.C., Vallender, E.J., Miller, G.M., 2012. Trace amine associated receptor 1 signaling in activated lymphocytes. *J. Neuroimmune Pharmacol.* 7, 866–876. <https://doi.org/10.1007/s11481-011-9321-4>
- Pedersen, K.K., Pedersen, M., Trøseid, M., Gaardbo, J.C., Lund, T.T., Thomsen, C., Gerstoft, J., Kvale, D., Nielsen, S.D., 2013. Microbial Translocation in HIV Infection Is Associated With Dyslipidemia , Insulin Resistance , and Risk of Myocardial Infarction. *J. Acquir. Immune Defic. Syndr.* 64, 425–433.
- Pegg, A.E., 2013. Toxicity of polyamines and their metabolic products. *Chem. Res. Toxicol.* 26, 1782–1800. <https://doi.org/10.1021/tx400316s>
- Pegg, A.E., 2006. Regulation of ornithine decarboxylase. *J. Biol. Chem.* 281, 14529–14532. <https://doi.org/10.1074/jbc.R500031200>
- Pei, Y., Asif-Malik, A., Canales, J.J., 2016. Trace amines and the trace amine-associated receptor 1: Pharmacology, neurochemistry, and clinical implications. *Front. Neurosci.* 10, 1–17. <https://doi.org/10.3389/fnins.2016.00148>
- Penchala, S.D., Fawcett, S., Else, L., Egan, D., Amara, A., Elliot, E., Challenger, E., Back, D., Boffito, M., Khoo, S., 2016. The development and application of a novel LC-MS/MS method for the measurement of Dolutegravir, Elvitegravir and Cobicistat in human plasma. *J. Chromatogr. B Anal. Technol. Biomed. Life Sci.* 1027, 174–180. <https://doi.org/10.1016/j.jchromb.2016.05.040>
- Pinto-Cardoso, S., Klatt, N.R., Reyes-Terán, G., 2018. Impact of antiretroviral drugs on the microbiome: Unknown answers to important questions. *Curr. Opin. HIV AIDS* 13, 53–60. <https://doi.org/10.1097/COH.0000000000000428>
- Potkin, S.G., Karoum, F., Chuang, L.-W., Cannon-Spoor, H.E., Phillips, I., Wyatt, R.J., 1979. Phenylethylamine in Paranoid Chronic Schizophrenia. *Science* (80-). 206, 470–471. <https://doi.org/10.1126/science.504988>
- Povar-Echeverría, M., Comet-Bernad, M., Gasso-Sánchez, A., Ger-Buil, A., Navarro-Aznarez, H., Martínez-Álvarez, R., Arazo-Garcés, P., 2021. Neuropsychiatric adverse effects of dolutegravir in real-life clinical practice. *Enfermedades Infecc. y Microbiol. Clin. (English ed.)* 39, 78–82. <https://doi.org/10.1016/j.eimce.2020.02.009>
- Prathipati, P.K., Mandal, S., Destache, C.J., 2016. Simultaneous quantification of tenofovir, emtricitabine, rilpivirine, elvitegravir and dolutegravir in mouse

- biological matrices by LC–MS/MS and its application to a pharmacokinetic study. *J. Pharm. Biomed. Anal.* 129, 473–481.  
<https://doi.org/10.1016/j.jpba.2016.07.040>
- Pretorius, L., Smith, C., 2023. Tyramine-induced gastrointestinal dysregulation is attenuated via estradiol associated mechanisms in a zebrafish larval model. *Toxicol. Appl. Pharmacol.* 461, 116399.  
<https://doi.org/10.1016/j.taap.2023.116399>
- Pretorius, L., Smith, C., 2022. *Aspalathus linearis* (Rooibos) and Agmatine May Act Synergistically to Beneficially Modulate Intestinal Tight Junction Integrity and Inflammatory Profile. *Pharmaceuticals* 15, 1097.  
<https://doi.org/10.3390/ph15091097>
- Pretorius, L., Smith, C., 2020. The trace aminergic system: A gender-sensitive therapeutic target for IBS? *J. Biomed. Sci.* 27, 1–19.  
<https://doi.org/10.1186/s12929-020-00688-1>
- Pretorius, L., Van Staden, A., Kellermann, T., Henning, N., Smith, C., 2022a. Rooibos (*Aspalathus linearis*) alters secretome trace amine profile of probiotic and commensal microbes in vitro. *J. Ethnopharmacol.* 297, 115548.  
<https://doi.org/10.1016/j.jep.2022.115548>
- Pretorius, L., Van Staden, A., Van der Merwe, J.J., Henning, N., Smith, C., 2022b. Alterations to microbial secretome by estrogen may contribute to sex bias in irritable bowel syndrome. *Inflammopharmacology* 30, 267–281.  
<https://doi.org/10.1007/s10787-021-00906-8>
- Pugin, B., Barcik, W., Westermann, P., Heider, A., Wawrzyniak, M., Hellings, P., Akdis, C.A., O'Mahony, L., 2017. A wide diversity of bacteria from the human gut produces and degrades biogenic amines. *Microb. Ecol. Health Dis.* 28, 1353881. <https://doi.org/10.1080/16512235.2017.1353881>
- Raffi, F., Rachlis, A., Stellbrink, H.J., Hardy, W.D., Torti, C., Orkin, C., Bloch, M., Podzamczar, D., Pokrovsky, V., Pulido, F., Almond, S., Margolis, D., Brennan, C., Min, S., 2013. Once-daily dolutegravir versus raltegravir in antiretroviral-naive adults with HIV-1 infection: 48 week results from the randomised, double-blind, non-inferiority SPRING-2 study. *Lancet* 381, 735–743.  
[https://doi.org/10.1016/S0140-6736\(12\)61853-4](https://doi.org/10.1016/S0140-6736(12)61853-4)
- Rahimy, E., Li, F.Y., Hagberg, L., Fuchs, D., Robertson, K., Meyerhoff, D.J., Zetterberg, H., Price, R.W., Gisslén, M., Spudich, S., 2017. Blood-brain barrier

- disruption is initiated during primary HIV infection and not rapidly altered by antiretroviral therapy. *J. Infect. Dis.* 215, 1132–1140.  
<https://doi.org/10.1093/infdis/jix013>
- Rassoulpour, A., Wu, H.Q., Ferre, S., Schwarcz, R., 2005. Nanomolar concentrations of kynurenic acid reduce extracellular dopamine levels in the striatum. *J. Neurochem.* 93, 762–765. <https://doi.org/10.1111/j.1471-4159.2005.03134.x>
- Reagan-Shaw, S., Nihal, M., Ahmad, N., 2008. Dose translation from animal to human studies revisited. *FASEB J.* 22, 659–661. <https://doi.org/10.1096/fj.07-9574lsf>
- Regard, J.B., Kataoka, H., Cano, D.A., Camerer, E., Yin, L., Zheng, Y.W., Scanlan, T.S., Hebrok, M., Coughlin, S.R., 2007. Probing cell type-specific functions of Gi in vivo identifies GPCR regulators of insulin secretion. *J. Clin. Invest.* 117, 4034–4043. <https://doi.org/10.1172/JCI32994>
- Regunathan, S., Reis, D.J., 2008. Characterization of Arginine Decarboxylase in Rat Brain and Liver. *J. Neurochem.* 74, 2201–2208. <https://doi.org/10.1046/j.1471-4159.2000.0742201.x>
- Republic of South Africa National Department of Health, 2020. 2019 ART Clinical Guidelines.
- Rodríguez-Palazón, M.C., Arroyo-Manzanares, N., Campillo, N., Viñas, P., 2023. Monitoring of Biogenic Amines in Human Urine Using Dispersive Liquid–Liquid Microextraction and Liquid Chromatography with High-Resolution Mass Spectrometry. *Separations* 10. <https://doi.org/10.3390/separations10040232>
- Rossato, L.G., Costa, V.M., Limberger, R.P., Bastos, M. de L., Remião, F., 2011. Synephrine: From trace concentrations to massive consumption in weight-loss. *Food Chem. Toxicol.* 49, 8–16. <https://doi.org/10.1016/j.fct.2010.11.007>
- Roy, U., Stute, L., Höfling, C., Hartlage-Rübsamen, M., Matysik, J., Roßner, S., Alia, A., 2018. Sex- and age-specific modulation of brain GABA levels in a mouse model of Alzheimer’s disease. *Neurobiol. Aging* 62, 168–179.  
<https://doi.org/10.1016/j.neurobiolaging.2017.10.015>
- Ruiz, M., 2021. Into the Labyrinth of the Lipocalin  $\alpha$ 1-Acid Glycoprotein. *Front. Physiol.* 12, 1–10. <https://doi.org/10.3389/fphys.2021.686251>
- Rutigliano, G., Accorroni, A., Zucchi, R., 2018. The case for TAAR1 as a modulator of central nervous system function. *Front. Pharmacol.* 8, 1–18.

- <https://doi.org/10.3389/fphar.2017.00987>
- Rutigliano, G., Bandini, L., Sestito, S., Chiellini, G., 2020. 3-iodothyronamine and derivatives: New allies against metabolic syndrome? *Int. J. Mol. Sci.* 21. <https://doi.org/10.3390/ijms21062005>
- Saba, A., Chiellini, G., Frascarelli, S., Marchini, M., Ghelardoni, S., Raffaelli, A., Tonacchera, M., Vitti, P., Scanlan, T.S., Zucchi, R., 2010. Tissue distribution and cardiac metabolism of 3-iodothyronamine. *Endocrinology* 151, 5063–5073. <https://doi.org/10.1210/en.2010-0491>
- Sacktor, N., Skolasky, R.L., Seaberg, E., Munro, C., Becker, J.T., Martin, E., Ragin, A., Levine, A., Miller, E., 2016. Prevalence of HIV-associated neurocognitive disorders in the Multicenter AIDS Cohort Study. *Neurology* 86, 334–340. <https://doi.org/10.1212/WNL.0000000000002277>
- Sagar, N.A., Tarafdar, S., Agarwal, S., Tarafdar, A., Sharma, S., 2021. Polyamines: Functions, Metabolism, and Role in Human Disease Management. *Med. Sci.* 9, 44. <https://doi.org/10.3390/medsci9020044>
- Sagrati, G., Fernández-Franzón, M., De Berardinis, F., Font, G., Vittori, S., Mañes, J., 2012. Simultaneous determination of eight underivatized biogenic amines in fish by solid phase extraction and liquid chromatography-tandem mass spectrometry. *Food Chem.* 132, 537–543. <https://doi.org/10.1016/j.foodchem.2011.10.054>
- Sandler, M., Ruthven, C.R.J., Goodwin, B.L., Reynolds, G.P., Rao, V.A.R., Coppen, A., 1979. Deficient production of tyramine and octopamine in cases of depression. *Nature*. <https://doi.org/10.1038/278357a0>
- Santorù, M.L., Piras, C., Murgia, A., Palmas, V., Camboni, T., Liggi, S., Ibba, I., Lai, M.A., Orrù, S., Blois, S., Loizedda, A.L., Griffin, J.L., Usai, P., Caboni, P., Atzori, L., Manzin, A., 2017. Cross sectional evaluation of the gut-microbiome metabolome axis in an Italian cohort of IBD patients. *Sci. Rep.* 7, 1–14. <https://doi.org/10.1038/s41598-017-10034-5>
- Scheper, H., van Holten, N., Hovens, J.G.F.M., de Boer, M.G.J., 2018. Severe depression as a neuropsychiatric side effect induced by dolutegravir. *HIV Med.* 19, e58–e59. <https://doi.org/10.1111/hiv.12538>
- Schultz, E., 1991. Catechol-O-methyltransferase and aromatic L-amino acid decarboxylase activities in human gastrointestinal tissues. *Life Sci.* 49, 721–725. [https://doi.org/10.1016/0024-3205\(91\)90104-J](https://doi.org/10.1016/0024-3205(91)90104-J)

- Serlin, M.H., Dieterich, D., 2008. Gastrointestinal Disorders in HIV. *Glob. HIV/AIDS Med.* 251–260. <https://doi.org/10.1016/B978-1-4160-2882-6.50027-7>
- Shah, A., Gangwani, M.R., Chaudhari, N.S., Glazyrin, A., Bhat, H.K., Kumar, A., 2016. Neurotoxicity in the Post-HAART Era: Caution for the Antiretroviral Therapeutics. *Neurotox. Res.* 30, 677–697. <https://doi.org/10.1007/s12640-016-9646-0>
- Shah, A.R., Hairston, J.A., Tami, T.A., 2005. Sinusitis in HIV: Microbiology and therapy. *Curr. Infect. Dis. Rep.* 7, 165–169. <https://doi.org/10.1007/s11908-005-0029-6>
- Shah, S., Hindley, L., Hill, A., 2021. Are New Antiretroviral Treatments Increasing the Risk of Weight Gain? *Drugs* 81, 299–315. <https://doi.org/10.1007/s40265-020-01457-y>
- Shalaby, A.R., 1996. Significance of biogenic amines to food safety and human health. *Food Res. Int.* 29, 675–690. [https://doi.org/10.1016/S0963-9969\(96\)00066-X](https://doi.org/10.1016/S0963-9969(96)00066-X)
- Sharma, R., Sharma, S., 2022. Physiology, Blood Volume, StatPearls [Internet]. StatPearls, Treasure Island.
- Sharma, S., Kumar, P., Deshmukh, R., 2018. Neuroprotective potential of spermidine against rotenone induced Parkinson's disease in rats. *Neurochem. Int.* 116, 104–111. <https://doi.org/10.1016/j.neuint.2018.02.010>
- Sim, J.H., Mukerji, S.S., Russo, S.C., Lo, J., 2021. Gastrointestinal Dysfunction and HIV Comorbidities. *Curr. HIV/AIDS Rep.* 18, 57–62. <https://doi.org/10.1007/s11904-020-00537-8>
- Simiele, M., Ariaudo, A., De Nicolò, A., Favata, F., Ferrante, M., Carcieri, C., Bonora, S., Di Perri, G., D'Avolio, A., 2017. UPLC–MS/MS method for the simultaneous quantification of three new antiretroviral drugs, dolutegravir, elvitegravir and rilpivirine, and other thirteen antiretroviral agents plus cobicistat and ritonavir boosters in human plasma. *J. Pharm. Biomed. Anal.* 138, 223–230. <https://doi.org/10.1016/j.jpba.2017.02.002>
- Simpson, D.S.A., Oliver, P.L., 2020. Ros generation in microglia: Understanding oxidative stress and inflammation in neurodegenerative disease. *Antioxidants* 9, 1–27. <https://doi.org/10.3390/antiox9080743>
- Sirico, M.L., Guida, B., Procino, A., Pota, A., Sodo, M., Grandaliano, G., Simone, S., Pertosa, G., Riccio, E., Memoli, B., 2012. Human Mature Adipocytes Express

- Albumin and This Expression Is Not Regulated by Inflammation. *Mediators Inflamm.* 2012, 1–8. <https://doi.org/10.1155/2012/236796>
- Song, J., Hur, B.E., Bokara, K.K., Yang, W., Cho, H.J., Park, K.A., Lee, W.T., Lee, K.M., Lee, J.E., 2014. Agmatine improves cognitive dysfunction and prevents cell death in a streptozotocin-induced Alzheimer rat model. *Yonsei Med. J.* 55, 689–699. <https://doi.org/10.3349/ymj.2014.55.3.689>
- Spudich, S., González-Scarano, F., 2012. HIV-1-related central nervous system disease: Current issues in pathogenesis, diagnosis, and treatment. *Cold Spring Harb. Perspect. Med.* 2, 1–17. <https://doi.org/10.1101/cshperspect.a007120>
- Stenkula, K.G., Erlanson-Albertsson, C., 2018. Adipose cell size: importance in health and disease. *Am. J. Physiol. Integr. Comp. Physiol.* 315, R284–R295. <https://doi.org/10.1152/ajpregu.00257.2017>
- Stern, A.L., Lee, R.N., Panvelker, N., Li, J., Harowitz, J., Jordan-Sciutto, K.L., Akay-Espinoza, C., 2018. Differential Effects of Antiretroviral Drugs on Neurons In Vitro: Roles for Oxidative Stress and Integrated Stress Response. *J. Neuroimmune Pharmacol.* 13, 64–76. <https://doi.org/10.1007/s11481-017-9761-6>
- Stohs, S.J., 2015. Physiological functions and pharmacological and toxicological effects of p-octopamine. *Drug Chem. Toxicol.* 38, 106–112. <https://doi.org/10.3109/01480545.2014.900069>
- Stohs, S.J., Shara, M., Ray, S.D., 2020. p-Syneprine, ephedrine, p-octopamine and m-syneprine: Comparative mechanistic, physiological and pharmacological properties. *Phyther. Res.* 34, 1838–1846. <https://doi.org/10.1002/ptr.6649>
- Sturdevant, C.B., Joseph, S.B., Schnell, G., Price, R.W., Swanstrom, R., Spudich, S., 2015. Compartmentalized Replication of R5 T Cell-Tropic HIV-1 in the Central Nervous System Early in the Course of Infection. *PLoS Pathog.* 11, 1–24. <https://doi.org/10.1371/journal.ppat.1004720>
- Subra, C., Trautmann, L., 2019. Role of T Lymphocytes in HIV Neuropathogenesis. *Curr. HIV/AIDS Rep.* 16, 236–243. <https://doi.org/10.1007/s11904-019-00445-6>
- Suzzi, G., Gardini, F., 2003. Biogenic amines in dry fermented sausages: A review. *Int. J. Food Microbiol.* 88, 41–54. [https://doi.org/10.1016/S0168-1605\(03\)00080-1](https://doi.org/10.1016/S0168-1605(03)00080-1)
- Taha, H., Das, A., Das, S., 2015. Clinical effectiveness of dolutegravir in the treatment of HIV/AIDS. *Infect. Drug Resist.* 8, 339–352.

<https://doi.org/10.2147/IDR.S68396>

Taha, H., Morgan, J., Das, A., Das, S., 2013. Parenteral patent drug S/GSK1265744 has the potential to be an effective agent in pre-exposure prophylaxis against HIV infection. *Recent Pat. Antiinfect. Drug Discov.* 8, 213–218.

Taramasso, L., Bonfanti, P., Ricci, E., Orofino, G., Squillace, N., Menzaghi, B., De Socio, G.V., Madeddu, G., Pellicanò, G.F., Pagnucco, L., Celesia, B.M., Calza, L., Conti, F., Martinelli, C.V., Valsecchi, L., Cascio, A., Bolla, C., Maggi, P., Vichi, F., Dentonell, C., Angioni, G., Mastroianni, A., Falasca, K., Cenderello, G., Di Biagio, A., 2020. Factors associated with weight gain in people treated with dolutegravir. *Open Forum Infect. Dis.* 7, 1–8.

<https://doi.org/10.1093/ofid/ofaa195>

Theron, A.J., Anderson, R., Madzime, M., Rossouw, T.M., Steel, H.C., Meyer, P.W.A., Cholo, M.C., Kwofie, L.L.I., Feldman, C., Tintinger, G.R., 2022. Pro-Inflammatory Interactions of Dolutegravir with Human Neutrophils in an In Vitro Study. *Molecules* 27. <https://doi.org/10.3390/molecules27249057>

Todd, S.E.J., Rafferty, P., Walker, E., Hunter, M., Dinsmore, W.W., Donnelly, C.M., McCarty, E.J., Quah, S.P., Emerson, C.R., 2017. Early clinical experience of dolutegravir in an HIV cohort in a larger teaching hospital. *Int. J. STD AIDS* 28, 1074–1081. <https://doi.org/10.1177/0956462416688127>

Treisman, G.J., Soudry, O., 2016. Neuropsychiatric Effects of HIV Antiviral Medications. *Drug Saf.* 39, 945–957. <https://doi.org/10.1007/s40264-016-0440-y>  
U.S Department of Health and Human Services, Food and Drug Administration, Center for Drug Evaluation and Research (CDER), Center for Biologics Evaluation and Research (CBER), Oncology Center of Excellence (OCE), 2019. Considerations for the Inclusion of Adolescent Patients in Adult Oncology Clinical Trials Guidance for Industry.

Vally, Z., 2011. HIV-associated neurocognitive disorders. *South African J. Psychiatry* 17, 98–102. <https://doi.org/10.4102/sajpsy psychiatry.v17i4.294>

Van Lunzen, J., Maggiolo, F., Arribas, J.R., Rakhmanova, A., Yeni, P., Young, B., Rockstroh, J.K., Almond, S., Song, I., Brothers, C., Min, S., 2012. Once daily dolutegravir (S/GSK1349572) in combination therapy in antiretroviral-naive adults with HIV: Planned interim 48 week results from SPRING-1, a dose-ranging, randomised, phase 2b trial. *Lancet Infect. Dis.* 12, 111–118. [https://doi.org/10.1016/S1473-3099\(11\)70290-0](https://doi.org/10.1016/S1473-3099(11)70290-0)

- Venter, W.D.F., Moorhouse, M., Sokhela, S., Fairlie, L., Mashabane, N., Masenya, M., Serenata, C., Akpomiemie, G., Qavi, A., Chandiwana, N., Norris, S., Chersich, M., Clayden, P., Abrams, E., Arulappan, N., Vos, A., McCann, K., Simmons, B., Hill, A., 2019. Dolutegravir plus Two Different Prodrugs of Tenofovir to Treat HIV. *N. Engl. J. Med.* 381, 803–815.  
<https://doi.org/10.1056/NEJMoa1902824>
- Vieira-Coelho, M., Soares-da-Silva, P., 1993. Dopamine formation, from its immediate precursor 3,4-dihydroxyphenylalanine, along the rat digestive tract. *Fundam. Clin. Pharmacol.* 7, 235–243. <https://doi.org/10.1111/j.1472-8206.1993.tb00237.x>
- Vizcarra, P., Vivancos, M.J., Pérez-Elías, M.J., Moreno, A., Casado, J.L., 2020. Weight gain in people living with HIV switched to dual therapy: Changes in body fat mass. *Aids* 34, 155–157. <https://doi.org/10.1097/QAD.0000000000002421>
- Walmsley, S., Baumgarten, A., Berenguer, J., Felizarta, F., Florence, E., Khuong-Josses, M.A., Kilby, J.M., Lutz, T., Podzamczar, D., Portilla, J., Roth, N., Wong, D., Granier, C., Wynne, B., Pappa, K., 2015. Dolutegravir plus abacavir/lamivudine for the treatment of HIV-1 infection in antiretroviral therapy-naive patients: Week 96 and week 144 results from the SINGLE randomized clinical trial. *J. Acquir. Immune Defic. Syndr.* 70, 515–519.  
<https://doi.org/10.1097/QAI.0000000000000790>
- Wang, L.S., Zhang, M. Di, Tao, X., Zhou, Y.F., Liu, X.M., Pan, R. Le, Liao, Y.H., Chang, Q., 2019. LC-MS/MS-based quantification of tryptophan metabolites and neurotransmitters in the serum and brain of mice. *J. Chromatogr. B Anal. Technol. Biomed. Life Sci.* 1112, 24–32.  
<https://doi.org/10.1016/j.jchromb.2019.02.021>
- Wang, X., Cerrone, M., Ferretti, F., Castrillo, N., Maartens, G., McClure, M., Boffito, M., 2019. Pharmacokinetics of dolutegravir 100 mg once daily with rifampicin. *Int. J. Antimicrob. Agents* 54, 202–206.  
<https://doi.org/10.1016/j.ijantimicag.2019.04.009>
- Wang, X., Liang, Y., Wang, Y., Fan, M., Sun, Y., Liu, J., Zhang, N., 2018. Simultaneous determination of 10 kinds of biogenic amines in rat plasma using high-performance liquid chromatography coupled with fluorescence detection. *Biomed. Chromatogr.* 32, e4211. <https://doi.org/10.1002/bmc.4211>
- Wang, X., Ying, W., Dunlap, K.A., Lin, G., Satterfield, M.C., Burghardt, R.C., Wu, G.,

- Bazer, F.W., 2014. Arginine decarboxylase and agmatinase: An alternative pathway for de novo biosynthesis of polyamines for development of mammalian conceptuses. *Biol. Reprod.* 90, 1–15.  
<https://doi.org/10.1095/biolreprod.113.114637>
- Wang, Y., Liu, M., Lu, Q., Farrell, M., Lappin, J.M., Shi, J., Lu, L., Bao, Y., 2020. Global prevalence and burden of HIV-associated neurocognitive disorder. *Neurology* 95, e2610–e2621. <https://doi.org/10.1212/WNL.00000000000010752>
- Wang, Z., Yang, Y., Xiang, X., Zhu, Y., Men, J., He, M., 2010. [Estimation of the normal range of blood glucose in rats]. *Wei Sheng Yan Jiu* 39, 133–7, 142.
- Want, E.J., 2018. LC-MS Untargeted Analysis, in: *Metabolic Profiling: Methods and Protocols*. pp. 99–116. [https://doi.org/10.1007/978-1-4939-7643-0\\_7](https://doi.org/10.1007/978-1-4939-7643-0_7)
- Wasik, A.M., Millan, M.J., Scanlan, T., Barnes, N.M., Gordon, J., 2012. Evidence for functional trace amine associated receptor-1 in normal and malignant B cells. *Leuk. Res.* 36, 245–249. <https://doi.org/10.1016/j.leukres.2011.10.002>
- Watkins, C.C., Treisman, G.J., 2012. Neuropsychiatric complications of aging with HIV. *J. Neurovirol.* 18, 277–290. <https://doi.org/10.1007/s13365-012-0108-z>
- Weidlich, S., Boesecke, C., Schneider, J., Klinker, H.H.F., Zink, A., Balogh, A., Wolf, E., Bidner, H., Spinner, C.D., Spinner, C.D., Jensen, B., Lutz, T., Spornraft-Ragaller, P., Hans Jürgen, S., Hower, M., Bohr, U., Obst, W., Krznaric, I., Sprinzl, M., Audebert, F., Kuemmerle, T., Scholten, S., Hillenbrand, H., Cordes, C., Knechten, H., Kuhlmann, B., Jessen, H., Beck, P., Fätkenheuer, G., Klinker, H.H.F., Rockstroh, J.K., Esser, S., Stephan, C., Degen, O., Bellmunt-Zschäpe, A., Khaykin, P., Brockmeyer, N., Stoehr, A., Spinner, C.D., Jensen, B., Lutz, T., Spornraft-Ragaller, P., Hans Jürgen, S., Hower, M., Bohr, U., Obst, W., Krznaric, I., Sprinzl, M., Audebert, F., Kuemmerle, T., Scholten, S., Hillenbrand, H., Cordes, C., Knechten, H., Kuhlmann, B., Jessen, H., Beck, P., Fätkenheuer, G., Klinker, H.H.F., Rockstroh, J.K., Esser, S., Stephan, C., Degen, O., Bellmunt-Zschäpe, A., Khaykin, P., Brockmeyer, N., Stoehr, A., 2020. Adequate plasma levels of dolutegravir in combination with ritonavir-boosted darunavir: a pharmacokinetic subgroup analysis of the DUALIS study. *J. Antimicrob. Chemother.* 75, 3082–3084. <https://doi.org/10.1093/jac/dkaa234>
- Wijting, I.E.A., Wit, F.W.N.M., Rokx, C., Leyten, E.M.S., Lowe, S.H., Brinkman, K., Bierman, W.F.W., van Kasteren, M.E.E., Postma, A.M., Bloemen, V.C.M., Bouchtoubi, G., Hoepelman, A.I.M., van der Ende, M.E., Reiss, P., Rijnders,

- B.J.A., 2019. Immune reconstitution inflammatory syndrome in HIV infected late presenters starting integrase inhibitor containing antiretroviral therapy. *EClinicalMedicine* 17. <https://doi.org/10.1016/j.eclinm.2019.11.003>
- Wohl, D.A., Yazdanpanah, Y., Baumgarten, A., Clarke, A., Thompson, M.A., Brinson, C., Hagins, D., Ramgopal, M.N., Antinori, A., Wei, X., Acosta, R., Collins, S.E., Brainard, D., Martin, H., 2019. Bictegravir combined with emtricitabine and tenofovir alafenamide versus dolutegravir, abacavir, and lamivudine for initial treatment of HIV-1 infection: week 96 results from a randomised, double-blind, multicentre, phase 3, non-inferiority trial. *Lancet HIV* 6, e355–e363. [https://doi.org/10.1016/S2352-3018\(19\)30077-3](https://doi.org/10.1016/S2352-3018(19)30077-3)
- Wong, H.L.X., Qin, H. yan, Tsang, S.W., Zuo, X., Che, S., Chow, C.F.W., Li, X., Xiao, H. tao, Zhao, L., Huang, T., Lin, C.Y., Kwan, H.Y., Yang, T., Longo, F.M., Lyu, A., Bian, Z. xiang, 2019. Early life stress disrupts intestinal homeostasis via NGF-TrkA signaling. *Nat. Commun.* 10. <https://doi.org/10.1038/s41467-019-09744-3>
- Wong, J.K., Yukl, S.A., 2016. Tissue reservoirs of HIV. *Curr. Opin. HIV AIDS* 11, 362–370. <https://doi.org/10.1097/COH.0000000000000293>
- World Health Organization, 2022. Update on the transition to dolutegravir-based antiretroviral therapy: report of a WHO meeting, 29–30 March 2022. Geneva, Switzerland.
- World Health Organization, 2018. Updated recommendations on first-line and second-line antiretroviral regimens and post-exposure prophylaxis and recommendations on early infant diagnosis of HIV: interim guidelines. Supplement to the 2016 consolidated guidelines on the use of antiretrovir. Geneva.
- World Health Organization, 2016. The use of antiretroviral drugs for treating and preventing HIV infection.
- WorldData.info [WWW Document], 2020. URL <https://www.worlddata.info/average-bodyheight.php> (accessed 4.2.23).
- Xie, Z., Miller, G.M., 2008.  $\beta$ -phenylethylamine alters monoamine transporter function via trace amine-associated receptor 1: Implication for modulatory roles of trace amines in brain. *J. Pharmacol. Exp. Ther.* 325, 617–628. <https://doi.org/10.1124/jpet.107.134247>
- Xu, W., Gao, L., Li, T., Shao, A., Zhang, J., 2017. Neuroprotective Role of Agmatine

- in Neurological Diseases. *Curr. Neuropharmacol.* 16, 1296–1305.  
<https://doi.org/10.2174/1570159x15666170808120633>
- Yano, J.M., Yu, K., Donaldson, G.P., Shastri, G.G., Ann, P., Ma, L., Nagler, C.R., Ismagilov, R.F., Mazmanian, S.K., Hsiao, E.Y., 2015. Indigenous bacteria from the gut microbiota regulate host serotonin biosynthesis. *Cell* 161, 264–276.  
<https://doi.org/10.1016/j.cell.2015.02.047>
- Yombi, J.C., 2018. Dolutegravir Neuropsychiatric Adverse Events: Specific Drug Effect or Class Effect. *AIDS Rev.* 20, 14–26.  
<https://doi.org/10.24875/AIDSRev.M17000013>
- Zádori, Z.S., Tóth, V.E., Fehér, Á., Philipp, K., Németh, J., Gyires, K., 2014. Evidence for the gastric cytoprotective effect of centrally injected agmatine. *Brain Res. Bull.* 108, 51–59. <https://doi.org/10.1016/j.brainresbull.2014.07.008>
- Zeitz, M., Ullrich, R., Schneider, T., Kewenig, S., Hohloch, K., Riecken, E.O., 1998. HIV/SIV Enteropathy. *Ann. N. Y. Acad. Sci.* 859, 139–148.  
<https://doi.org/10.1111/j.1749-6632.1998.tb11118.x>
- Zhang, J., Hayes, S., Sadler, B.M., Minto, I., Brandt, J., Piscitelli, S., Min, S., Song, I.H., 2015. Population pharmacokinetics of dolutegravir in HIV-infected treatment-naive patients. *Br. J. Clin. Pharmacol.* 80, 502–514.  
<https://doi.org/10.1111/bcp.12639>
- Zhang, Y., Xie, Z., Zhou, J., Li, Y., Ning, C., Su, Qisi, Ye, L., Ai, S., Lai, J., Pan, P., Liu, N., Liao, Y., Su, Qijian, Li, Z., Liang, H., Cui, P., Huang, J., 2023. The altered metabolites contributed by dysbiosis of gut microbiota are associated with microbial translocation and immune activation during HIV infection. *Front. Immunol.* 13, 1–14. <https://doi.org/10.3389/fimmu.2022.1020822>
- Zheng, Y., Aboura, R., Boujaafar, S., Lui, G., Hirt, D., Bouazza, N., Foissac, F., Treluyer, J.M., Benaboud, S., Gana, I., 2020. HPLC-MS/MS method for the simultaneous quantification of dolutegravir, elvitegravir, rilpivirine, darunavir, ritonavir, raltegravir and raltegravir- $\beta$ -D-glucuronide in human plasma. *J. Pharm. Biomed. Anal.* 182. <https://doi.org/10.1016/j.jpba.2020.113119>
- Zucchi, R., Chiellini, G., Scanlan, T.S., Grandy, D.K., 2006. Trace amine-associated receptors and their ligands. *Br. J. Pharmacol.* 149, 967–978.  
<https://doi.org/10.1038/sj.bjp.0706948>
- Zucco, G.M., Ingegneri, G., 2004. Olfactory deficits in HIV-infected patients with and without AIDS dementia complex. *Physiol. Behav.* 80, 669–674.

<https://doi.org/10.1016/j.physbeh.2003.12.001>

# Addenda

## Addendum A



### REC: Animal Care and Use

#### Approval Letter: Use of animal tissue or animals not covered by the SANS: 10386:2008

12 April 2022

**PI:** Miss N Henning

**REC: ACU Reference #:** ACU-2022-24915

**Title:** The impact of chronic dolutegravir treatment on tissue trace amine distribution

Dear Miss N Henning

Your Animal Tissue Use - Notification with reference number ACU-2022-24915, was reviewed by the Research Ethics Committee: Animal Care and Use via committee review procedures and was approved.

Please note that this clearance is valid for a period of five years. A new application must be submitted when the source of the material changes.

**Approval Period:** 12 April 2022 - 11 April 2027

**Applicants are reminded that they are expected to comply with accepted standards for the use of animals in research and teaching as reflected in the South African National Standards 10386: 2008. The SANS 10386: 2008 document is available on the Division for Research Developments website [www.sun.ac.za/research](http://www.sun.ac.za/research).**

Please remember to use your REC: ACU reference number: # ACU-2022-24915 on any documents or correspondence with the REC: ACU concerning your research protocol.

If you have any questions or need further help, please contact the REC: ACU office at 021 808 9003.

Visit the Division for Research Developments website [www.sun.ac.za/research](http://www.sun.ac.za/research) for documentation on REC: ACU policy and procedures.

Sincerely,

Mr Winston Beukes

Coordinator: Research Ethics (Animal Care and Use)

## Addendum B



UNIVERSITEIT  
STELLENBOSCH  
UNIVERSITY

### Approved with Stipulations

24/06/2021

**PI:** Dr KS Petersen-Ross

**REC: ACU Reference #:** ACU-2021-22035

**Title:** Obesity; a confounder in Dolutegravir treatment?

Dear Dr KS Petersen-Ross

Your response to modifications, with reference number #ACU-2021-22035 was reviewed by the Research Ethics Committee: Animal Care and Use via committee review procedures and was approved on condition that the following stipulations are clarified:

1. A long list of side effects and adverse clinical effects to the drug that will be given is provided; however, the pain and distress category is given as C. Will the animals not require treatment or intervention if they develop these symptoms?
2. Rats will be housed 4 per cage and be given jelly blocks for the drug administration. How will you ensure that each rat get the same amount of drugs?

**Applicants are reminded that they are expected to comply with accepted standards for the use of animals in research and teaching as reflected in the South African National Standards 10386: 2008. The SANS 10386: 2008 document is available on the Division for Research Developments website [www.sun.ac.za/research](http://www.sun.ac.za/research).**

**As provided for in the Veterinary and Para-Veterinary Professions Act, 1982. It is the principal investigator's responsibility to ensure that all study participants are registered with or have been authorised by the South African Veterinary Council (SAVC) to perform the procedures on animals, or will be performing the procedures under the direct and continuous supervision of a SAVC-registered veterinary professional or SAVC-registered para-veterinary professional, who are acting within the scope of practice for their profession.**

Please remember to use your REC: ACU reference number: # ACU-2021-22035 on any documents or correspondence with the REC: ACU concerning your research protocol.

If you have any questions or need further help, please contact the REC: ACU office at 021 808 9003.

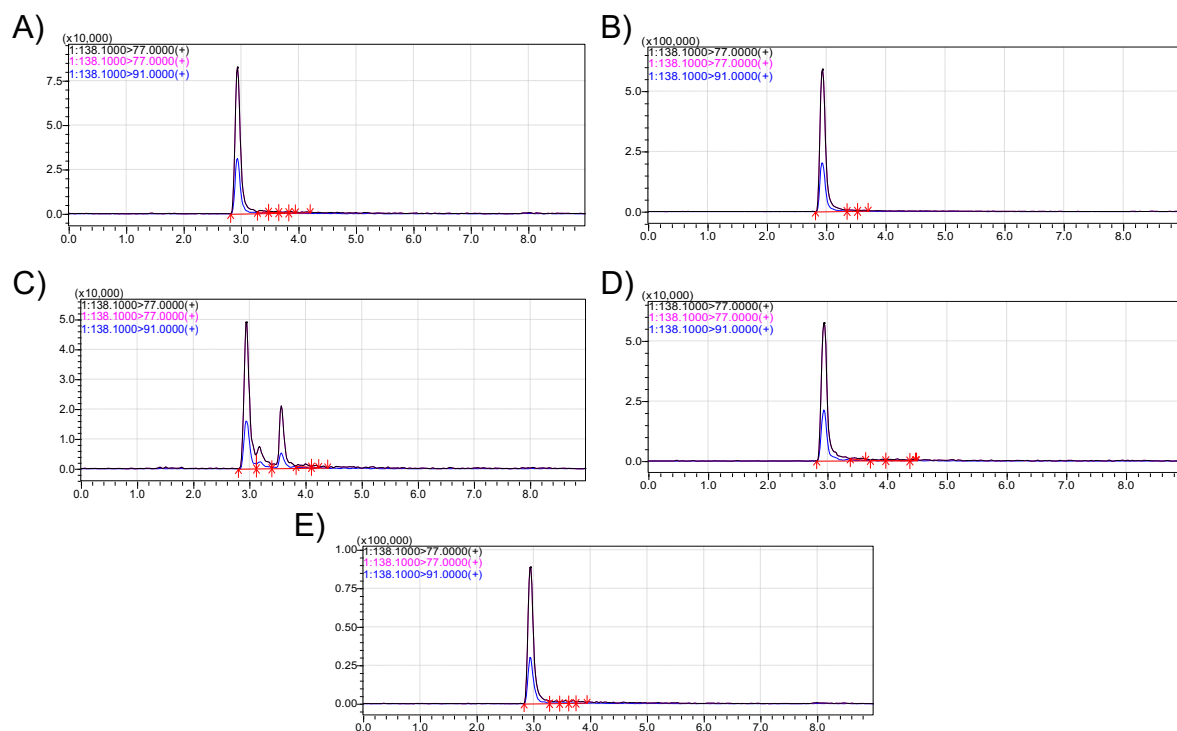
Visit the Division for Research Developments website [www.sun.ac.za/research](http://www.sun.ac.za/research) for documentation on REC: ACU policy and procedures.

Sincerely,

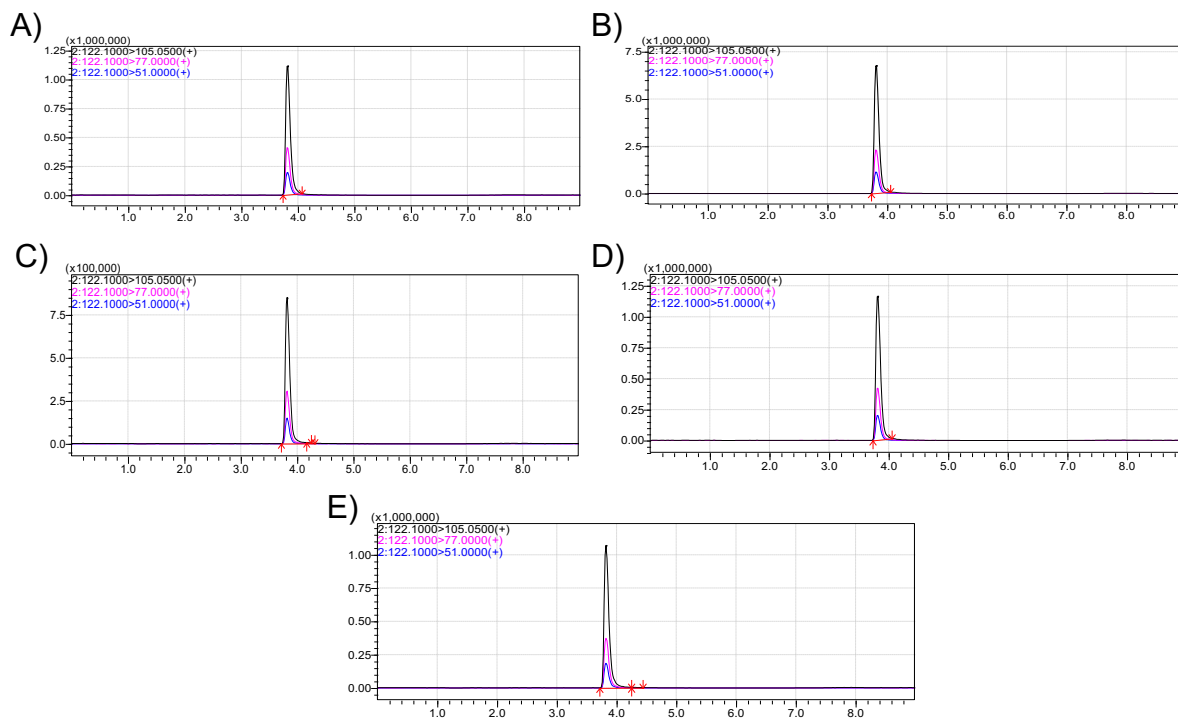
Mr Winston Beukes

Coordinator: Research Ethics (Animal Care and Use)

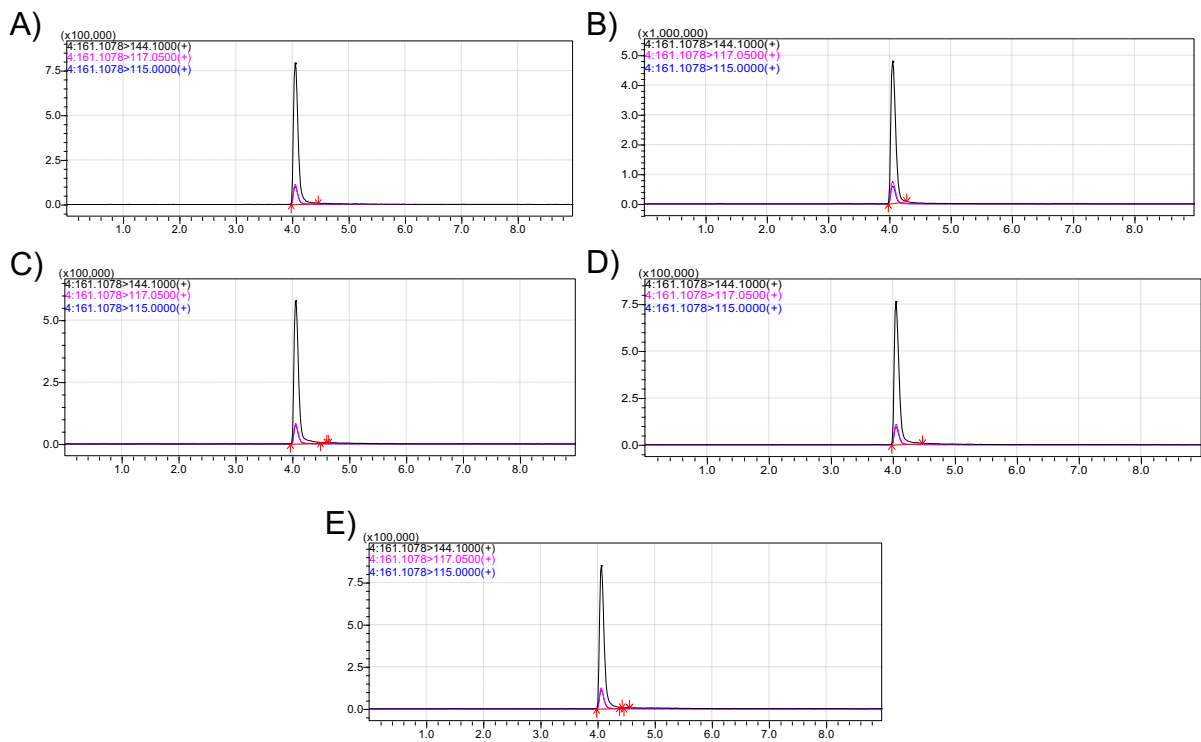
## Addendum C



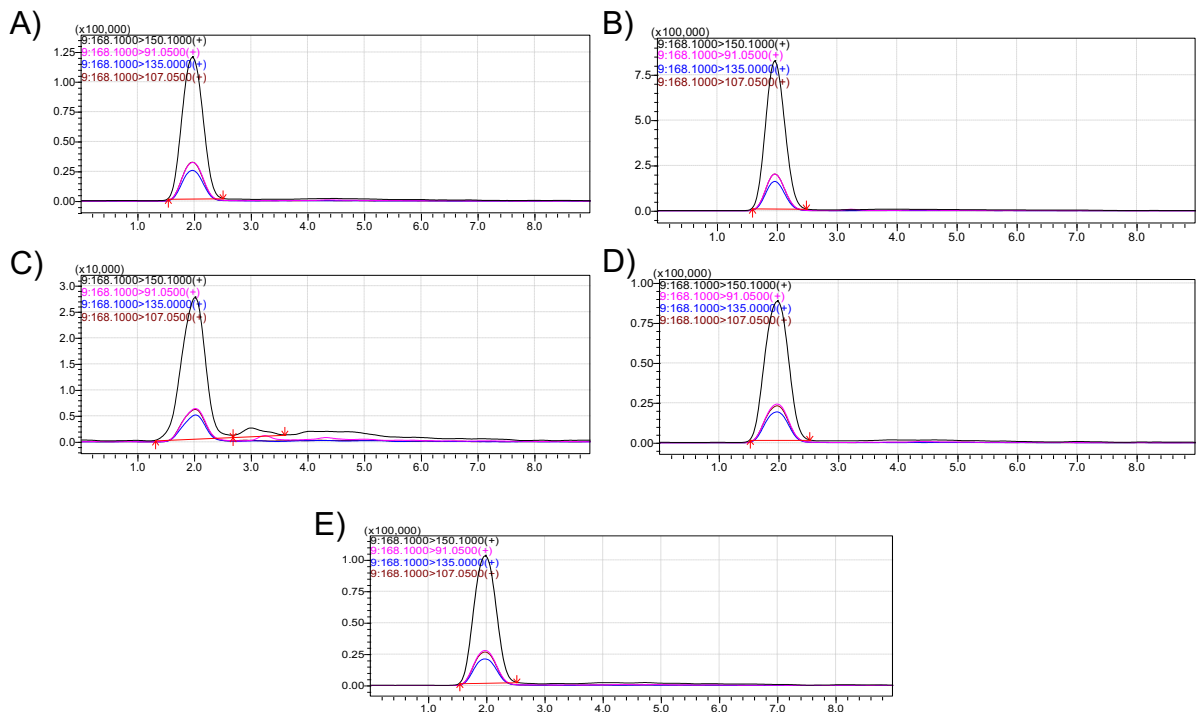
Supplementary figure 5.1: Chromatograms of 400 ng/mL TYR in (A) solvent, (B) brain, (C) urine, (D) plasma and (E) gastrointestinal tissue eluting at 2.94 minutes. Intensity (cps) is reported on the y-axis and retention time (min) on the x-axis.



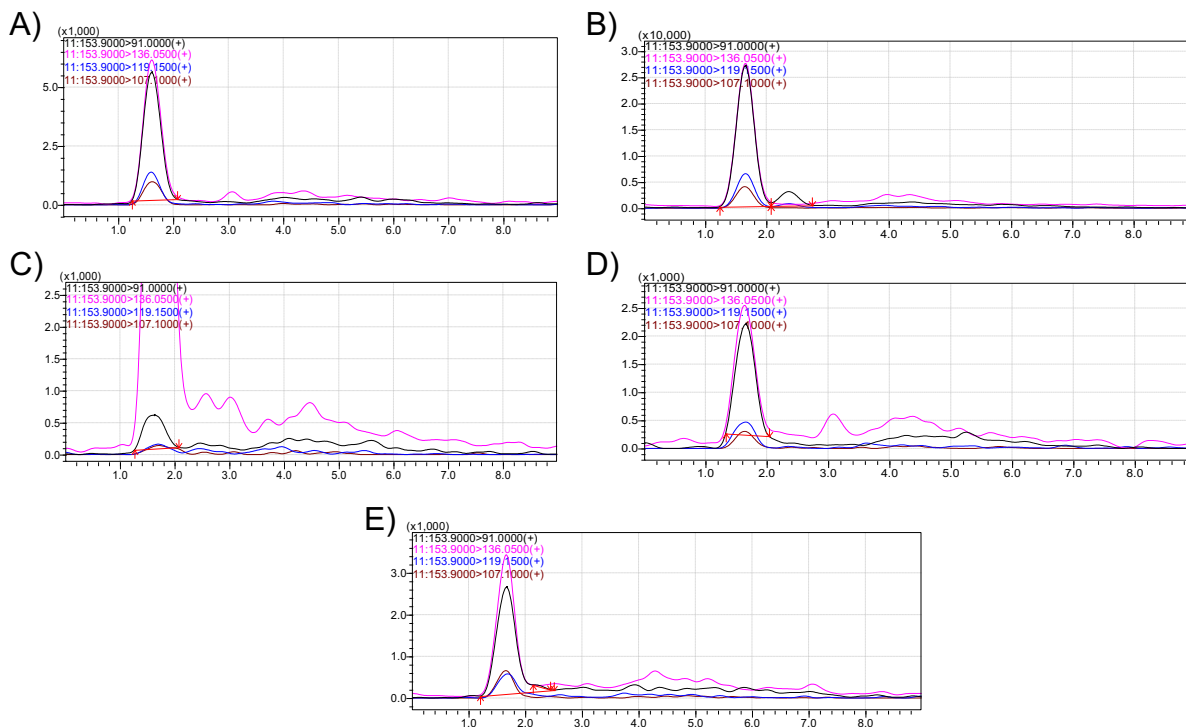
Supplementary figure 5.2: Chromatograms of 400 ng/mL PEA in (A) solvent, (B) brain, (C) urine, (D) plasma and (E) gastrointestinal tissue eluting at 3.83 minutes. Intensity (cps) is reported on the y-axis and retention time (min) on the x-axis.



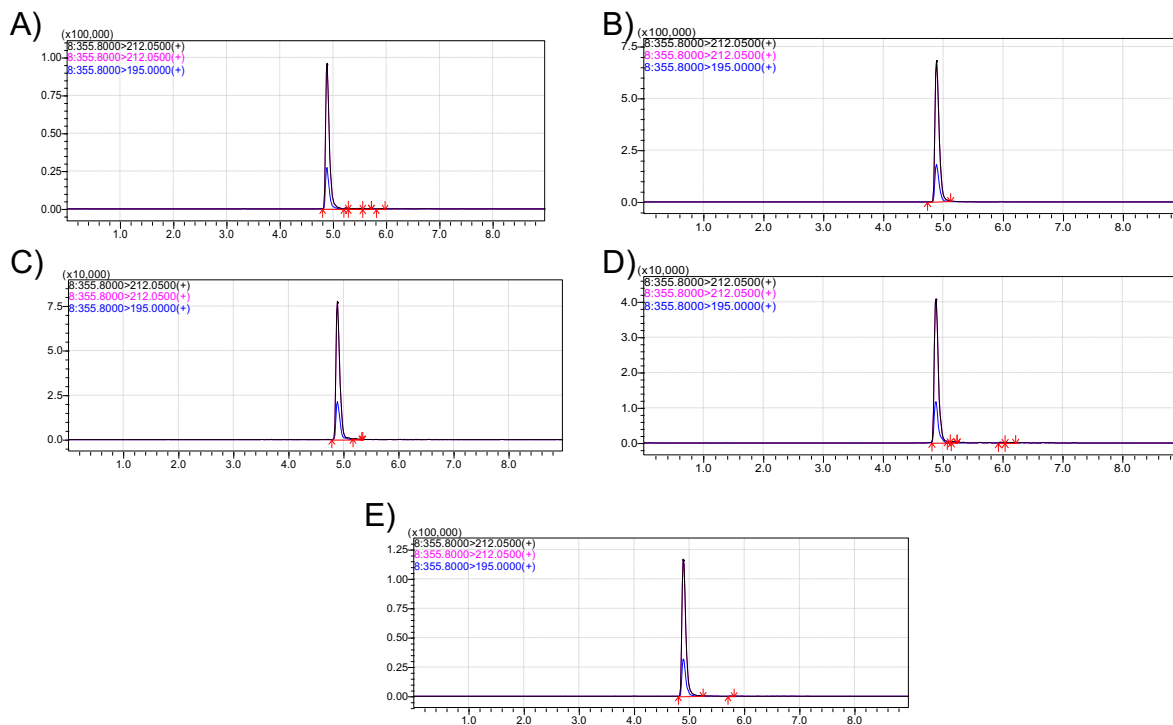
Supplementary figure 5.3: Chromatograms of 400 ng/mL TRP in (A) solvent, (B) brain, (C) urine, (D) plasma and (E) gastrointestinal tissue eluting at 4.07 minutes. Intensity (cps) is reported on the y-axis and retention time (min) on the x-axis.



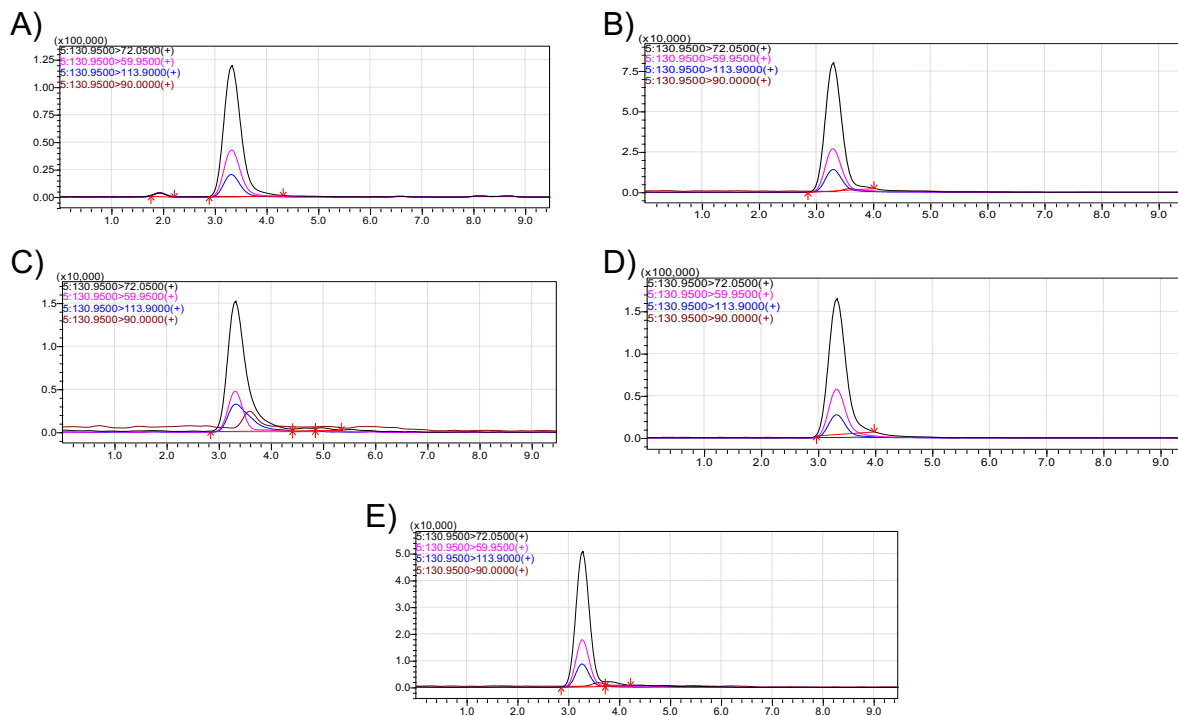
Supplementary figure 5.4: Chromatograms of 400 ng/mL SYN in (A) solvent, (B) brain, (C) urine, (D) plasma and (E) gastrointestinal tissue eluting at 1.95 minutes. Intensity (cps) is reported on the y-axis and retention time (min) on the x-axis.



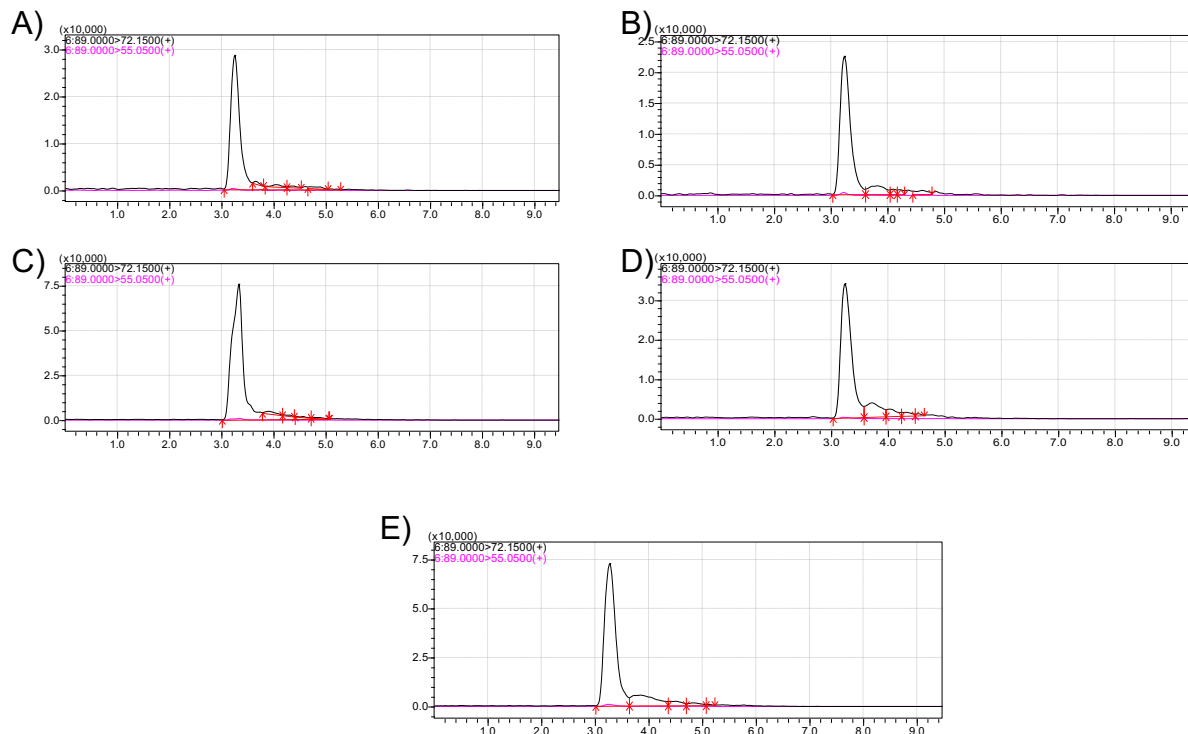
Supplementary figure 5.5: Chromatograms of 400 ng/mL OCT in (A) solvent, (B) brain, (C) urine, (D) plasma and (E) gastrointestinal tissue eluting at 1.61 minutes. Intensity (cps) is reported on the y-axis and retention time (min) on the x-axis.



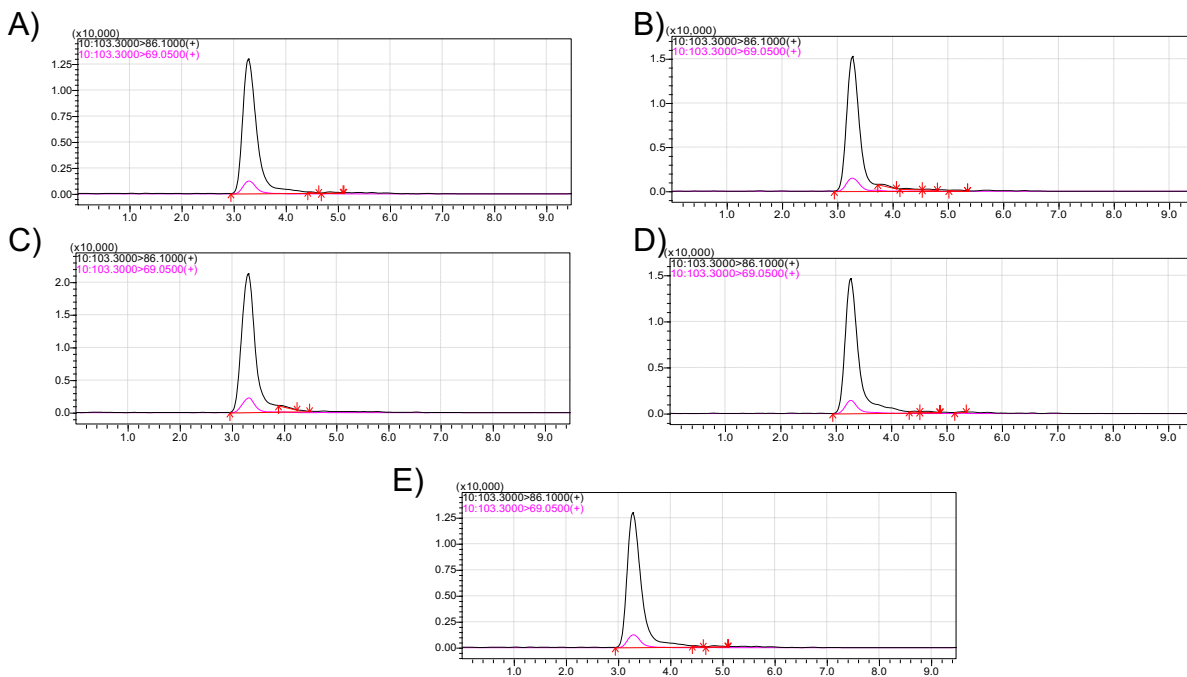
Supplementary figure 5.6: Chromatograms of 400 ng/mL T1AM in (A) solvent, (B) brain, (C) urine, (D) plasma and (E) gastrointestinal tissue eluting at 4.91 minutes. Intensity (cps) is reported on the y-axis and retention time (min) on the x-axis.



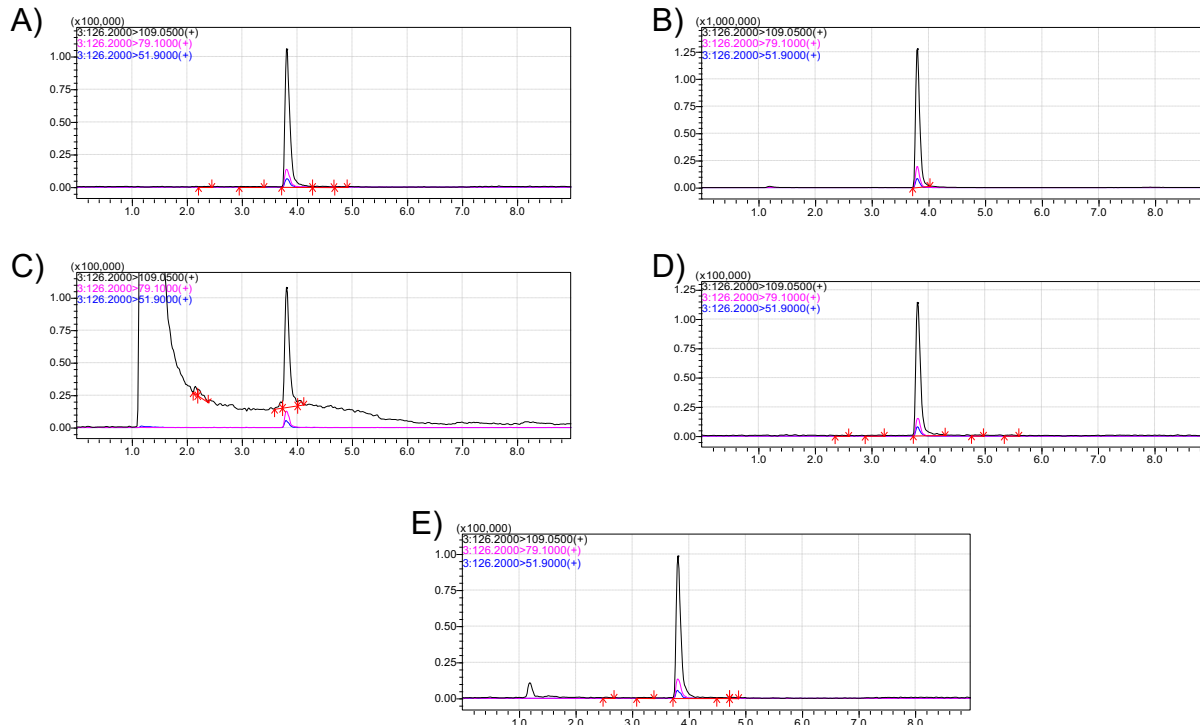
Supplementary figure 5.7: Chromatograms of 400 ng/mL AGM in (A) solvent, (B) brain, (C) urine, (D) plasma and (E) gastrointestinal tissue eluting at 3.30 minutes. Intensity (cps) is reported on the y-axis and retention time (min) on the x-axis.



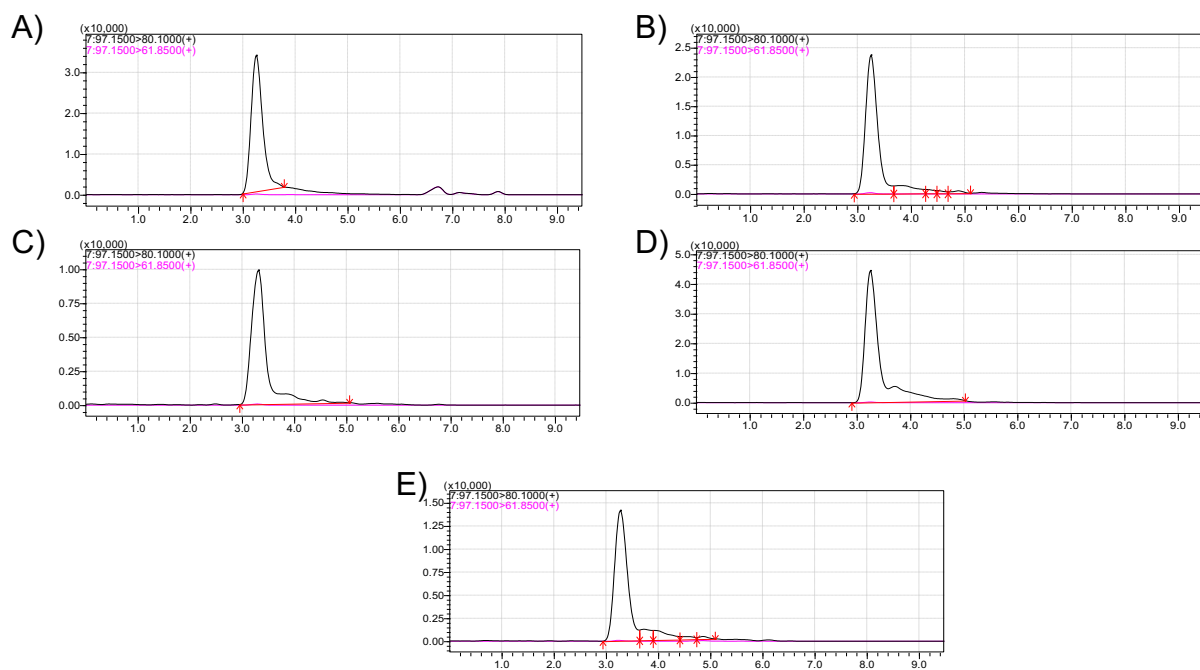
Supplementary figure 5.8: Chromatograms of 400 ng/mL PUT in (A) solvent, (B) brain, (C) urine, (D) plasma and (E) gastrointestinal tissue eluting at 3.26 minutes. Intensity (cps) is reported on the y-axis and retention time (min) on the x-axis.



Supplementary figure 5.9: Chromatograms of 400 ng/mL CAD in (A) solvent, (B) brain, (C) urine, (D) plasma and (E) gastrointestinal tissue eluting at 3.28 minutes. Intensity (cps) is reported on the y-axis and retention time (min) on the x-axis.



Supplementary figure 5.10: Chromatograms of 100 ng/mL PEA-d4 in (A) solvent, (B) brain, (C) urine, (D) plasma and (E) gastrointestinal tissue eluting at 3.81 minutes. Intensity (cps) is reported on the y-axis and retention time (min) on the x-axis.



Supplementary figure 5.11: Chromatograms of 400 ng/mL PUT-d4 in (A) solvent, (B) brain, (C) urine, (D) plasma and (E) gastrointestinal tissue eluting at 3.26 minutes. Intensity (cps) is reported on the y-axis and retention time (min) on the x-axis.